

Utah State University

DigitalCommons@USU

---

All Graduate Theses and Dissertations, Spring  
1920 to Summer 2023

Graduate Studies

---

5-2013

## A Middle to Late Holocene Record of Arroyo Cut-Fill Events in Kitchen Corral Wash, Southern Utah

William M. Huff  
*Utah State University*

Follow this and additional works at: <https://digitalcommons.usu.edu/etd>



Part of the [Geology Commons](#)

---

### Recommended Citation

Huff, William M., "A Middle to Late Holocene Record of Arroyo Cut-Fill Events in Kitchen Corral Wash, Southern Utah" (2013). *All Graduate Theses and Dissertations, Spring 1920 to Summer 2023*. 6742.  
<https://digitalcommons.usu.edu/etd/6742>

This Thesis is brought to you for free and open access by the Graduate Studies at DigitalCommons@USU. It has been accepted for inclusion in All Graduate Theses and Dissertations, Spring 1920 to Summer 2023 by an authorized administrator of DigitalCommons@USU. For more information, please contact [digitalcommons@usu.edu](mailto:digitalcommons@usu.edu).



A MIDDLE TO LATE HOLOCENE RECORD OF ARROYO CUT-FILL EVENTS  
IN KITCHEN CORRAL WASH, SOUTHERN UTAH

by

William M. Huff

A thesis submitted in partial fulfillment  
of the requirements for the degree

of

MASTER OF SCIENCE

in

Geology

Approved:

UTAH STATE UNIVERSITY  
Logan, Utah

2013

Copyright © William M. Huff 2013

All Rights Reserved

## ABSTRACT

A Middle to Late Holocene Record of Arroyo Cut-Fill Events in

Kitchen Corral Wash, Southern Utah

by

William M. Huff, Master of Science

Utah State University, 2013

Major Professor: Dr. Tammy M. Rittenour  
Department: Geology

This study examines middle to late Holocene episodes of arroyo incision and aggradation in the Kitchen Corral Wash (KCW), a tributary of the Paria River in southern Utah. Arroyos are entrenched channels in valley-fill alluvium, and are capable of capturing decadal- to centennial-scale fluctuations in watershed hydrology as evidenced by the Holocene cut-fill stratigraphy recorded within near-vertical arroyo-channel walls. KCW has experienced both historic (ca. 1880-1920 AD) and prehistoric (Holocene) episodes of arroyo cutting and filling. The near-synchronous timing of arroyo cut-fill events between the Paria River and regional drainages over the last ~1 have led some researchers to argue that arroyo development is climatically driven. However, the influence of allogenic (climate-related) or autogenic (geomorphic threshold) forcings on arroyo dynamics are less clear.

Uncertainty in influence of the controlling mechanisms of arroyo cutting and filling is partly due to the limited or poorly dated alluvial chronologies. This study tests the applicability of AMS radiocarbon and optically stimulated luminescence (OSL) dating to reconstruct alluvial chronologies in dryland fluvial systems, such as the KCW arroyo. Results from 12 arroyo-wall study sites in KCW indicate that 24 of the 39 analyzed AMS radiocarbon samples and

preliminary results from 12 of the 14 OSL samples returned stratigraphically consistent ages. Applying a combination of these two dating techniques allowed for increased sampling opportunities and cross-checking of ages to determine aberrant age results.

By using detailed stratigraphic panels, sedimentologic descriptions, and the age control from AMS radiocarbon and OSL dating, this study produces a new chronostratigraphy that suggests at least five arroyo cut-fill cycles during the middle to late Holocene with periods of aggradation at:  $\sim 4.35 - 3.4$  ka (Qf1),  $\sim 3.2 - 2.25$  ka (Qf2),  $\sim 2.15 - 1.45$  ka (Qf3),  $\sim 1.3 - 0.8$  ka (Qf4),  $\sim 0.7 - 0.12$  ka (Qf5), and an older period of aggradation from  $\sim 7.3 - 4.85$  ka identified in an earlier study. This newly developed KCW cut-fill chronostratigraphy is compared to regional alluvial and paleoclimate records to test hypotheses regarding allogenic or autogenic forcings. Regional alluvial chronologies do not show coherent patterns of arroyo cut-fill dynamics, but instead appear to be affected by both allogenic and autogenic influences.

(194 pages)

## PUBLIC ABSTRACT

A Middle to Late Holocene Record of Arroyo Cut-Fill Events in  
Kitchen Corral Wash, Southern Utah

by

William M. Huff, Master of Science

Utah State University, 2013

Major Professor: Dr. Tammy M. Rittenour  
Department: Geology

Arroyos are steeply entrenched channels that form by incision into weakly consolidated valley-fill alluvium. This study attempts to offers clues into the processes behind their formation by dating arroyo sediments using luminescence and radiocarbon techniques. The importance of understanding arroyo formation is due to a possible linkage with decadal to centennial-scale climate fluctuations. In the late 1800s and early 1900s, many of the shallow, perennial streams throughout southern Utah that used for a variety of agricultural and domestic uses were incised up to ~30 m into their alluvium by frequent and high-magnitude flood events. The economical and ecological effects of these floods were substantial, and a possible link to changes in climate could provide insight to future implications.

To better understand the possible influence of climate change to arroyo formation over the last ~7,500 years, field and lab work focused on identifying, describing, and dating sediments from arroyo outcrops in Kitchen Corral Wash, southern Utah. Arroyo outcrops were identified based on cross-cutting relationships in the stratigraphy. Using luminescence and radiocarbon dating to obtain the age of arroyo sediments allows us to reconstruct the alluvial history of Kitchen Corral Wash. To estimate the possible effects of climate change, this study compared the

alluvial history of Kitchen Corral Wash with other regional arroyos in southern Utah to identify similarities and differences in the timing of sediment deposition or flood-related incision.

A similar timing in deposition and incision might suggest a stronger climate effect, whereas a different timing in these processes might suggest a geologic threshold within each regional arroyo. Findings in this study indicate that climate effects and geologic thresholds both play an important role in the processes of arroyo formation. Funding for this project was obtained from the National Science Foundation grant (NSF-EAR 1057192), a research grant from the Colorado Scientific Society Memorial Funds, and awards from the Utah State University Department of Geology.

William M. Huff

## ACKNOWLEDGMENTS

I would first like to thank my wife, Elizabeth, for her unwavering love and encouragement. You have been overly supportive in my pursuit of an advanced degree in geology, and for that I will always be grateful. I am indebted to the constructive advice and time given by my committee members, Dr. Joel Pederson and Dr. Patrick Belmont, throughout this research project. I tremendously appreciate the assistance and company of Ben Lariviere in the field and the infinite support of Michelle Nelson at the Utah State Luminescence Laboratory. I would like to acknowledge my appreciation to the National Science Foundation, the Colorado Scientific Society, and the USU Department of Geology for their generous financial support of this research and as a teaching assistant.

I would like to thank my family for their love and continued interest in my research. Special thanks go out to USU geomorph graduate students, who were always there to lend a hand or give a laugh when it was needed. Finally, I wish to give my utmost thanks my advisor, Dr. Tammy Rittenour, for giving me the opportunity to work on an exceptional project in such a beautiful setting. I must express my gratitude to you for being a mentor, colleague, and friend. Your guidance throughout this project has been essential to my success and your geomorphological and geochronological acumen has strengthened my development as a geologist.

Will Huff

## CONTENTS

	Page
ABSTRACT.....	iii
PUBLIC ABSTRACT .....	v
ACKNOWLEDGMENTS .....	vii
LIST OF TABLES.....	x
LIST OF FIGURES .....	xi
CHAPTER	
1. INTRODUCTION .....	1
REFERENCES .....	2
2. ASSESSING THE USE OF AMS RADIOCARBON AND SINGLE-GRAIN LUMINESCENCE DATING TECHNIQUES ON ARROYO SEDIMENTS: A CASE STUDY FROM KITCHEN CORRAL WASH, SOUTHERN UTAH.....	3
ABSTRACT .....	3
2.1 Introduction.....	4
2.2 Background.....	6
2.3 Methods .....	15
2.4 Results.....	34
2.5 Discussion.....	43
2.6 Conclusions.....	57
REFERENCES .....	59
3. EPISODIC ENTRENCHMENT AND AGGRADATION IN KITCHEN CORRAL WASH, SOUTHERN UTAH.....	64
ABSTRACT .....	64
3.1 Introduction.....	65
3.2 Background.....	70
3.3 Methods .....	82
3.4 Results.....	89
3.5 Discussion.....	121
3.6 Conclusions.....	143
REFERENCES .....	145

4.	FINAL CONCLUSIONS AND RECOMMENDATIONS FOR FUTURE WORK .....	152
	REFERENCES .....	158
	APPENDICES .....	160
	Appendix A – Optically Stimulated Luminescence Data .....	161
	Appendix B – Stratigraphic Columns and Sedimentologic Descriptions .....	167

## LIST OF TABLES

Table		Page
2.1	KCW facies codes.....	18
2.2	Summary of radiocarbon ages .....	23
2.3	Summary of radiocarbon ages and sample characteristics.....	24
2.4	Dose rate chemistry data for analyzed KCW OSL samples .....	28
2.5	Preliminary single-grain age information and partial bleaching statistics .....	33
3.1	Arroyo cut-fill competing hypotheses and expected results .....	67
3.2	Summary of radiocarbon sample information and ages.....	84
3.3	Preliminary single-grain quartz OSL ages .....	88

## LIST OF FIGURES

Figure	Page	
2.1	Location map of the KCW drainage in southern Utah: (a) Physiographic map of displaying the KCW catchment, drainage, and study area (in green) (b) aerial photo from Park Wash looking south (c) ground photo of Deer Spring Wash with a 5 m scale looking north.....	7
2.2	Representation of (a) charcoal-rich lens in a ripple crossbedded (Sr) sand deposit from which sample 14C-11 was collected (Table 2.3) and (b) isolated angular charcoal in a massive (Sm) sand deposit. Note the charcoal in (a) is "floating" near the top of the Sr sand bed .....	10
2.3	Krotovina commonly seen in sand beds. These are representative of potential bioturbation or post-depositional mixing processes that can contribute to anomalous OSL ages if sampled: (a) desiccated, clay-filled krotovina in a trough crossbedded (St) deposit and (b) silty-sand filled krotovina in a low-angle crossbedded (St) deposit.....	14
2.4	Location map of key study exposures within KCW of (a) 5 m DEM and locations of all 12 study sites and (b) Google Earth aerial photo with arroyo outcrop sites discussed in this study (highlighted in red).....	16
2.5	Common lithofacies in KCW alluvial fills (see Table 2.1 for descriptions). Scale bar represents 10 cm and facies codes are represented at base of photographs .....	19
2.6	OSL sample extraction from the KCW study area: (a) Example of a >40 cm thick, very pale brown, low-angle crossbedded sand deposit prior to extraction, (b) hammering an opaque metal tube into a targeted sand bed, (c) end result of hammering that is followed by extraction of an OSL sample (USU-1026) and analysis at the USU Luminescence Laboratory.....	26
2.7	(a) Results from a preheat-plateau thermal-transfer (PP-TT) test on samples USU-1026 and USU-1101: Equivalent dose values increase significantly when preheat temperatures surpass 240°C. Recycling ratios for measurements are also shown. A preheat temperature of 220°C (outlined in green) was used for all SG measurements in this study. (b) Inherent overdispersion SG test results for naturally bleached and beta-dosed USU-1101 and USU-1103 .....	31
2.8	Fluvial architecture and geochronology of KCW-B. (a) Bold lines represent unconformable boundaries and thin lines represent fluvial sequences. OSL (circles) and <sup>14</sup> C (triangles) samples are indicated within alluvial beds and have been used to constrain the timing of arroyo-cut-fill cycles. (b) Facies textures identified and used to help select <sup>14</sup> C and OSL samples, and older and younger alluvial fill packages identified using detailed stratigraphic mapping and ages from both geochronometers.....	36

- 2.9 Fluvial architecture and geochronology of KCW-E. (a) Bold lines represent unconformable boundaries and thin lines represent fluvial sequences. OSL (circles) and  $^{14}\text{C}$  (triangles) samples are indicated within alluvial beds and have been used to constrain the timing of arroyo-cut-fill cycles. (b) Facies textures identified and used to help select  $^{14}\text{C}$  and OSL samples, and older and younger alluvial fill packages identified using detailed stratigraphic mapping and ages from both geochronometers..... 38
- 2.10 Fluvial architecture and geochronology of KCW-H. (a) Bold lines represent unconformable boundaries and thin lines represent fluvial sequences. OSL (circles) and  $^{14}\text{C}$  (triangles) samples are indicated within alluvial beds and have been used to constrain the timing of arroyo-cut-fill cycles. (b) Facies textures identified and used to help select  $^{14}\text{C}$  and OSL samples, and older, intermediate, and younger alluvial fill packages identified using detailed stratigraphic mapping and ages from both geochronometers.... 40
- 2.11 Fluvial architecture and geochronology of KCW-J. (a,b) Bold lines represent unconformable boundaries and thin lines represent fluvial sequences. OSL (circles) and  $^{14}\text{C}$  (triangles) samples are indicated within alluvial beds and have been used to constrain the timing of arroyo-cut-fill cycles. (c,d) Facies textures identified and used to help select  $^{14}\text{C}$  and OSL samples, and older, intermediate, and younger alluvial fill packages identified using detailed stratigraphic mapping and ages from both geochronometers.... 42
- 2.12 Apparent density difference between charcoal and coal: (a) charcoal fragments from radiocarbon sample 14C-26 remains suspended during AMS pretreatment and returned a stratigraphically agreeable age (b) coal fragment from radiocarbon sample 14C-14 immediately sunk during pretreatment and returned an age overestimation ..... 46
- 2.13 Overdispersion and facies comparison showing preliminary individual (diamond) and mean (square) overdispersion values. Triangle represent mean facies overdispersion values from Summa-Nelson and Rittenour (2012), where massive sand (Sm) facies are averaged small-aliquot overdispersion values and all other facies are averaged small-aliquot and single-grain overdispersion values. In KCW, USU-1194 and USU-1101 have overdispersion values below 35% (the single-grain threshold for adequate bleaching). Green line represents 30% overdispersion value. Samples with an overdispersion value greater than 30% are considered partially bleached based on suggestions from Arnold et al. (2007)..... 50
- 2.14 Overdispersion and bed thickness comparison showing preliminary individual (diamond) and mean (square) overdispersion values. Although overdispersion values roughly decrease with relative to bed thickness, no clear decreasing trend in overdispersion is apparent. Green line represents 30% overdispersion value. Samples with an overdispersion value greater than 30% are considered partially bleached based on suggestions from Arnold et al. (2007) ..... 52
- 2.15 Overdispersion and study site distance downstream comparison showing individual (diamond) and mean (square) overdispersion values. Unlike observations from Summa-

	Nelson and Rittenour (2012), a downstream decrease in preliminary overdispersion values was not observed. Green line represents 30% overdispersion value. Samples with an overdispersion value greater than 30% are considered partially bleached based on suggestions from Arnold et al. (2007) .....	54
2.16	Overdispersion and samples collected from different sediment sources comparison showing preliminary individual (diamond) and mean (square) overdispersion values. Overdispersion values show a clear decreasing trend from local (red, poorly sorted, silty-clay and very-fine grained sand) to upstream (very pale brown, well-sorted, fine- to medium-grained, frosted quartz sand) sediments, suggesting that targeting sediments based on their original sediment source (sedimentary bedrock lithology in KCW) is a better way to avoid problems with partial bleaching. Green line represents 30% overdispersion value. Samples with an overdispersion value greater than 30% are considered partially bleached based on suggestions from Arnold et al. (2007).....	56
3.1	Kitchen Corral Wash (KCW) is a tributary of the Para River in southern Utah that heads in the Paunsaugunt Plateau and. In this study, KCW encompasses Deer Springs Wash and Park Wash tributaries to the intersection of Kaibab Gulch at Highway-89 .....	71
3.2	Longitudinal profile of KCW from the headwaters of Park Wash to the intersection of Kaibab Gulch (A-A') and from the Headwaters of Deer Springs Wash to the confluence with the main KCW trunk stream (B-B'). KCW heads in Tertiary Claron Fm and ends in Triassic Moenkopi Fm. Three bedrock knickpoints are evident in KCW and range from 6-10 m in height.....	73
3.3	Geomorphic map of KCW displaying underlying Jurassic and Triassic bedrock and overlying Pleistocene terrace gravels and Quaternary alluvial sediments .....	76
3.4	.(a) Mean daily discharge at the Lee's Ferry Paria River Gage from 1923-2013. Data suggest a bimodal precipitation regime with the largest flows occurring during the early spring and summer seasons. (b) Mean daily precipitation from the Bryce Canyon COOP and Paria RS COOP .....	77
3.5	a) Adapted figure from Hereford (2002) correlating historic and prehistoric arroyo cut-fill events between regional drainages and (b) existing KCW chronologies reconstructed from Hereford (2002) and Harvey et al. (2011).....	79
3.6	Study site KCW-A showing a 7.5 m tall arroyo wall with evidence of two aggradation phases (Qf3, Qf5) separated by an incision event with (a) radiocarbon and OSL age results and (b) stratigraphic facies and depositional facies associations. See Fig. B-1 in Appendix B for detailed sedimentary descriptions and stratigraphic columns from each fill.....	93

- 3.7 Study site KCW-B showing a 9 m tall arroyo wall displaying two alluvial packages (Qf4, Qf5) separated by an erosional surface with (a) radiocarbon and OSL age results and (b) stratigraphic facies and depositional facies associations. See Fig B-2 in Appendix B for detailed sedimentary descriptions and stratigraphic columns..... 96
- 3.8 Study site KCW-C showing a 10.5 m tall arroyo wall displaying two alluvial packages (Qf2, Qf4) separated by an erosional surface with (a) radiocarbon and OSL age results and (b) stratigraphic facies and depositional facies associations. See Fig B-3 in Appendix B for detailed sedimentary descriptions and stratigraphic columns..... 98
- 3.9 Study site KCW-D showing a 10.8 m tall arroyo wall displaying two alluvial packages (Qf2, Qf4) separated by an erosional surface with (a) radiocarbon and OSL age results and (b) stratigraphic facies and depositional facies associations. See Fig B-4 in Appendix B for detailed sedimentary descriptions and stratigraphic columns..... 100
- 3.10 Study site KCW-E showing a 6.9 m tall arroyo wall with two alluvial packages (Qf4, Qf5) separated by an erosional surface with (a) radiocarbon and OSL age results and (b) stratigraphic facies and depositional facies associations. See Fig B-5 in Appendix B for detailed sedimentary descriptions and stratigraphic column ..... 103
- 3.11 Study site KCW-F showing a 8.5 m tall arroyo wall with two alluvial packages (Qf2, Qf5) separated by an erosional surface with (a) radiocarbon and OSL age results and (b) stratigraphic facies and depositional facies associations. See Fig B-6 in Appendix B for detailed sedimentary descriptions and stratigraphic columns ..... 106
- 3.12 Study site KCW-G showing a 5 m tall arroyo wall with three alluvial packages (Qf1, Qf4, Qf5) separated by two erosional surfaces with (a) radiocarbon and OSL age results and (b) stratigraphic facies and depositional facies associations. See Fig B-7 in Appendix B for detailed sedimentary descriptions and stratigraphic columns ..... 108
- 3.13 Study site KCW-H showing a 10.7 m tall arroyo will with three alluvial packages (Qf1, Qf4, Qf5) separated by erosional surfaces with (a) radiocarbon and OSL age results and (b) stratigraphic facies and depositional facies associations. See Fig B-8 in Appendix B for detailed sedimentary descriptions and stratigraphic columns ..... 111
- 3.14 Study site KCW-I showing a 9 m tall arroyo wall displaying four alluvial packages (Qf2, Qf3, Qf4, Qf5) separated by erosional surfaces with (a) radiocarbon and OSL age results and (b) stratigraphic facies and depositional facies associations. This site was previously visited by Harvey et al. (2011) and has been reinterpreted in this study. See Fig B-9 in Appendix B for detailed sedimentary descriptions and stratigraphic columns..... 113
- 3.15 Study site KCW-J showing a 5 to 6.6 m tall arroyo will displaying three alluvial packages (Qf3, Qf4, Qf5/Qf5') separated by erosional surfaces with (a) radiocarbon and OSL age results and (b) stratigraphic facies and depositional facies associations. See Fig B-10 in Appendix B for detailed sedimentary descriptions and stratigraphic columns..... 116

3.16	Study site KCW-K showing a 2.9 m tall arroyo wall with two alluvial packages (Qf4, Qf5) separated by erosional surfaces and showing (a) radiocarbon and OSL age results and (b) stratigraphic facies and depositional facies associations. See Fig B-11 in Appendix B for detailed sedimentary descriptions and stratigraphic columns.....	118
3.17	Study site KCW-L showing a 2.2 m tall arroyo will with two alluvial packages (Qf4?, Qf5?) separated by erosional surfaces .....	120
3.18	Chronology of Aggradation and Incision events at KCW derived from detailed stratigraphic mapping, AMS radiocarbon (triangles) and OSL (circles) dating. Green = Qf5 fill, orange = Qf4 fill, blue = Qf3 fill, yellow = Qf2 fill, purple = Qf1 fill .....	123
3.19	Comparison of existing KCW chronologies from KCW (e.g. Hereford, 2002; Harvey, 2009; Harvey et al., 2011) with the newly developed chronology from this study .....	124
3.20	(a) Modern stream profile and preserved arroyo-wall heights of KCW alluvial fills showing a relative increase over time. (b) Hypothetical time-transgressive aggradation of an irregular KCW stream profile to a more convex (prehistoric) stream profile .....	127
3.21	Schematic chronostratigraphy of KCW .....	130
3.22	Regional correlation of alluvial chronologies and the chronology derived from KCW in this study. Modern alluvium ages from KCW (Hereford, 2002), Kanab Creek (Webb et al., 1991), and the upper Escalante River (Webb, 1985) are reported .....	133
3.23	Holocene paleoclimate records correlated with alluvial chronologies from this study and regional drainages .....	137
3.24	Select Holocene paleoclimate records compared to chronologies of KCW and regional drainages over the last ~2.5 ka.....	140
A-1	Single-grain $D_e$ distribution for select OSL samples (USU-1026, USU-1027, USU-1028) as indicated on probability distribution functions (left) and radial plots (right) .....	162
A-2	Single-grain $D_e$ distribution for select OSL samples (USU-1029, USU-1101, USU-1103) as indicated on probability distribution functions (left) and radial plots (right) .....	163
A-3	Single-grain $D_e$ distribution for select OSL samples (USU-11176, USU-11177, USU-11178) as indicated on probability distribution functions (left) and radial plots (right)...	164
A-4	Single-grain $D_e$ distribution for select OSL samples (USU-1181, USU-1187, USU-1189) as indicated on probability distribution functions (left) and radial plots (right) .....	165
A-5	Single-grain $D_e$ distribution for select OSL samples (USU-1192, USU-1194) indicated on probability distribution functions (left) and radial plots (right) .....	166
B-1	Stratigraphic columns and sedimentologic descriptions of KCW-A. ....	168

B-2	Stratigraphic columns and sedimentologic descriptions of KCW-B .....	169
B-3	Stratigraphic column and sedimentologic descriptions of KCW-C .....	170
B-4	Stratigraphic column and sedimentologic descriptions of KCW-D.....	171
B-5	Stratigraphic columns and sedimentologic descriptions of KCW-E.....	172
B-6	Stratigraphic column and sedimentologic descriptions of KCW-F .....	173
B-7	Stratigraphic columns and sedimentologic descriptions of KCW-G .....	174
B-8	Stratigraphic columns and sedimentologic descriptions of KCW-H .....	175
B-9	Stratigraphic columns and sedimentologic descriptions of KCW-I.....	176
B-10	Stratigraphic columns and sedimentologic descriptions of KCW-J .....	177
B-11	Stratigraphic columns and sedimentologic descriptions of KCW-K .....	178

## CHAPTER 1

### INTRODUCTION

Fluvial systems in the semi-arid southwestern United States have the potential to capture decadal- to centennial-scale fluctuations in watershed hydrology, which is evident in the historic and prehistoric (Holocene) cut-fill stratigraphy within the walls of arroyo drainage systems. Arroyos are entrenched, steep-walled and often ephemeral drainages that form after a stream has incised into valley-fill alluvium. Episodes of arroyo incision and aggradation in the southwestern U.S. have been considered some of the most significant geomorphic events over the past century (Graf, 1983). Accordingly, the dynamic nature of these systems has initiated the study of arroyo systems and spurred the ongoing debate of the triggering mechanisms necessary for arroyo incision. Thesis research focuses on cut-fill events in Kitchen Corral Wash (KCW), a tributary of the Paria River in southern Utah, in an attempt to temporally constrain how Holocene climate perturbations (allogenic controls) and intrinsic geomorphic thresholds (autogenic controls) drive arroyo incision and aggradation.

The near-synchronous nature of arroyo cutting and filling events within KCW and other regional drainages has led to the proposal that climate may be the pivotal triggering mechanism (Hereford, 2002). However, previous attempts to constrain the timing of cut-fill events in KCW have resulted in poor temporal resolution (Hereford, 2002; Harvey et al., 2011) and have limited the ability to determine if arroyo dynamics are synchronous between regional drainages. The main project goal of this study is to update and expand the arroyo cut-fill chronology from KCW by building a detailed chronostratigraphic framework, which will better aide in answering questions related to dynamic processes of arroyo formation and the possible linkages to climate.

The second chapter of this thesis (Chapter 2) will offer procedural suggestions for the use of accelerator mass spectrometry (AMS) radiocarbon and optically stimulated luminescence (OSL) methods to date alluvial deposits in arroyo systems. The advantages and shortcomings of

field and laboratory applications of both geochronologic dating techniques and previously recommended strategies for improving the reliability of each technique will be discussed. The implementation of both techniques and results from KCW will then be presented and examined in an effort to assess the effectiveness of each strategy. This chapter will be revised for submittal to the journal *Quaternary Geochronology*.

Chapter 3 will discuss the methods used in creating stratigraphic panels and stratigraphic columns from the arroyo walls and will examine age results drawn from alluvial deposits using AMS and OSL dating. Results from the newly developed chronostratigraphic framework of KCW will be correlated to chronologies derived from regional drainages of similar size and paleoclimate records to test the hypotheses related to the timing of arroyo formation and possible connections to changes in climate. Chapter 3 will be revised for submittal to the journal *Quaternary Science Reviews*.

Lastly, Chapter 4 will summarize the implications of this research and will offer considerations for future studies. Details of the OSL and AMS results will be presented in an Appendix along with any figures not presented in the text.

## REFERENCES

- Graf, W.L., 1983. The arroyo problem – Paleohydrology and paleohydraulics in the short term. In: Gregory, K.G. (Ed.), *Background to Paleohydrology*. John Wiley and Sons, New York, 297-302.
- Harvey, J.E., Pederson, J.L., Rittenour, T.M., 2011. Exploring relations between arroyo cycles and canyon paleoflood records in Buckskin Wash, Utah: Reconciling scientific paradigms. *Geological Society of America Bulletin*, v. 123, 2266-2276.
- Hereford, R., 2002. Valley-fill alluviation during the Little Ice Age (ca. A.D. 1400–1880), Paria River basin and southern Colorado Plateau, United States. *Geological Society of America Bulletin* 114 (12), 1550-1563.

## CHAPTER 2

ASSESSING THE USE OF AMS RADIOCARBON AND SINGLE-GRAIN LUMINESCENCE  
DATING TECHNIQUES ON ARROYO SEDIMENTS: A CASE STUDY FROM  
KITCHEN CORRAL WASH, SOUTHERN UTAH**ABSTRACT**

Arroyo systems throughout the southwestern United States preserve alluvial deposits and stratigraphic sequences that record periods of incision separated by prolonged periods of aggradation. In southern Utah, sediments preserved in arroyo walls provide an important archive of these cut-fill responses to Holocene climate change or other internal controls. Testing hypotheses related to the forcing mechanisms that have influenced the fluvial dynamics of these arroyo systems requires sufficient age control. Previous studies have focused on dating and correlating arroyo events between regional drainages using accelerator mass spectrometry (AMS) radiocarbon and optically stimulated luminescence (OSL) dating techniques. However, poor age control due to problems or limitations with each technique has made arroyo sediments difficult to date. Whereas radiocarbon dating may have problems due to redeposition of charcoal or limited material for dating, drawbacks with OSL dating can arise from incomplete bleaching, either of which can preclude a meaningful regional correlation of arroyo dynamics. Using Kitchen Corral Wash (KCW) as an example, this study addresses these and other problems, and recommends new considerations to dating arroyo sediments when using AMS radiocarbon and OSL dating techniques.

Collectively, 39 AMS radiocarbon and 29 OSL samples were sampled to update and expand an existing alluvial chronology of KCW. Results indicate that 24 of the 39 radiocarbon samples returned accurate ages based on their stratigraphic context within identified Holocene alluvial fills. In comparison, all OSL samples showed significant signs of limited solar exposure

and required the application of the single-grain analyses and analyses using the minimum-age-model (MAM) to attenuate the effects of partial bleaching. However, 12 of the 14 single-grain OSL samples that were analyzed produced stratigraphically consistent results once partial bleaching was taken into account. Samples collected from deposits whose sediments were sourced upstream of the study area, presumably having a longer transportation distance and transport mechanism conducive to solar exposure, showed the least amount of partial bleaching. Additionally, four of the most well-dated arroyo-wall outcrops from KCW indicate that OSL dating can be used to identify anomalous AMS radiocarbon ages. Accordingly, this study provides evidence that applying a combination of dating techniques to alluvial deposits and cross-checking the results can yield the accurate chronostratigraphies needed to develop millennial-scale arroyo cut-fill chronologies.

## **2.1 Introduction**

Fluvial systems in the semiarid southwestern United States have the potential to capture decadal- to centennial-scale hydrologic fluctuations as indicated by Holocene cut-fill sequences recorded within the stratigraphy of arroyo drainage systems. Arroyos are steep-walled channels entrenched into fine-grained valley alluvium (e.g. Bryan, 1925; Bull, 1997). The arroyos currently expressed in the southern Utah landscape and throughout much of the southwestern U.S. developed throughout a period of region-wide entrenchment events during the late 1800s to early 1900s, which left former floodplains behind as terraces (see reviews by Cooke and Reeves, 1976; Webb et al., 1991; Hereford, 2002). Historic observations suggest that periods of frequent, high-magnitude flood events promote rapid entrenchment and headward migration of arroyos. However, no unifying hydrologic or climatic conditions needed for arroyo entrenchment have been proposed. Current hypotheses for the cause of arroyo cutting include land mismanagement and overgrazing following pioneer settlement (Bailey, 1935; Thornthwaite et al., 1942; Antevs, 1952; Patton and Boison, 1986), autogenic geomorphic adjustments (Schumm and Hadley, 1957;

Patton and Schumm, 1981; Patton and Boison, 1986; Tucker et al., 2006), and climate change to wetter or drier conditions (Antevs, 1952; Karlstrom, 1988; Hereford, 2002; Mann and Meltzer, 2007).

Reliable ages from alluvial deposits stored in arroyo drainages or other dryland fluvial systems are needed to test competing arroyo hypotheses and determine the hydrologic conditions needed for incision and aggradation. Researchers have applied a number of dating techniques to help determine the age of channel alluvium in efforts to resolve the timing and processes of incision and aggradation, which include repeat photography (Graf, 1983; Webb and Leake, 2006), tree-ring records from partially buried trees (Patton and Boison, 1986; Karlstrom, 1988; Hereford, 2002), and stratigraphic relationships of archaeological sites or artifacts (Hall, 1977; Hereford, 2002; Harvey et al., 2011). Currently, two of the most commonly applied techniques include accelerator mass spectrometry (AMS) radiocarbon and, to a lesser extent, optically stimulated luminescence (OSL) dating. However, obtaining accurate ages for alluvial sediments has often been difficult due to inherited limitations of each dating technique in fluvial settings.

For example, although radiocarbon dating is perhaps the most widely applied technique for dating alluvial deposits and has been recently used in a number of studies involving southwestern arroyo systems (e.g. Hereford, 2002; Mann and Meltzer, 2007; Jones et al., 2010), its use may be limited if organic material is scarce or is sourced from old wood or redeposited material. On the other hand, OSL dating is a relatively new technique that can be used to date fine-grained sediments. However, problems with applying OSL dating in fluvial environments can arise due to the presence of grains that were not exposed to sufficient sunlight needed to reset their luminescence signal, termed partial bleaching (e.g. Olley et al., 1999; Jain et al., 2004; Rittenour, 2008). While both techniques have clear problems and limitations, often resulting in age over-estimations, they have also had considerable success. Additionally, both techniques are currently the basis of most Holocene alluvial chronologies and are noteworthy for their

application to dating arroyo sediments (e.g. Arnold et al., 2007; Summa-Nelson and Rittenour, 2012).

The purpose of this paper is to test the use of AMS radiocarbon and OSL dating in tandem to date alluvial sediments in dryland fluvial systems, specifically those currently occupied by arroyos, by addressing and attempting to resolve some of the primary problems and limitations of each technique. This study uses Kitchen Corral Wash (KCW), an arroyo system in southern Utah, to show that the combination of both dating techniques not only allows for greater sampling opportunities in the field, but also provides a means for cross-checking to help eliminate anomalous ages. Further, an overview of the AMS radiocarbon and OSL field sampling techniques, analyses, and results from KCW provides noteworthy considerations and guidelines that can be used to construct a high-resolution dryland alluvial chronology. Accordingly, the radiocarbon and OSL ages obtained using these guidelines have updated and improved the existing chronology of KCW. This chronology is used in Chapter 3 to construct a complete chronostratigraphic framework of KCW in order to help to test competing hypotheses related to the timing and climate implications of Holocene arroyo cutting and filling in southern Utah.

## **2.2 Background**

### *2.2.1 Geographic Setting and Previous Chronologies*

Kitchen Corral Wash is a tributary of the Paria River located in Kane County, Utah approximately 45km east of the town of Kanab (Fig. 2.1). It is the main trunk stream of a drainage that assumes several names from its headwaters to its confluence with the Paria River (e.g. Park Wash, Deer Springs Wash, Kitchen Corral Wash, Kaibab Gulch, and Buckskin Gulch). However, for the purpose of this study the name Kitchen Corral Wash will encompass the Park Wash and Deer Spring Wash reaches from the base of the White Cliffs and the main Kitchen Corral Wash alluvial valley that extends from the base of the Vermillion Cliffs to the head of Kaibab Gulch (Fig. 2.1). The total drainage area of the KCW catchment upstream of Kaibab

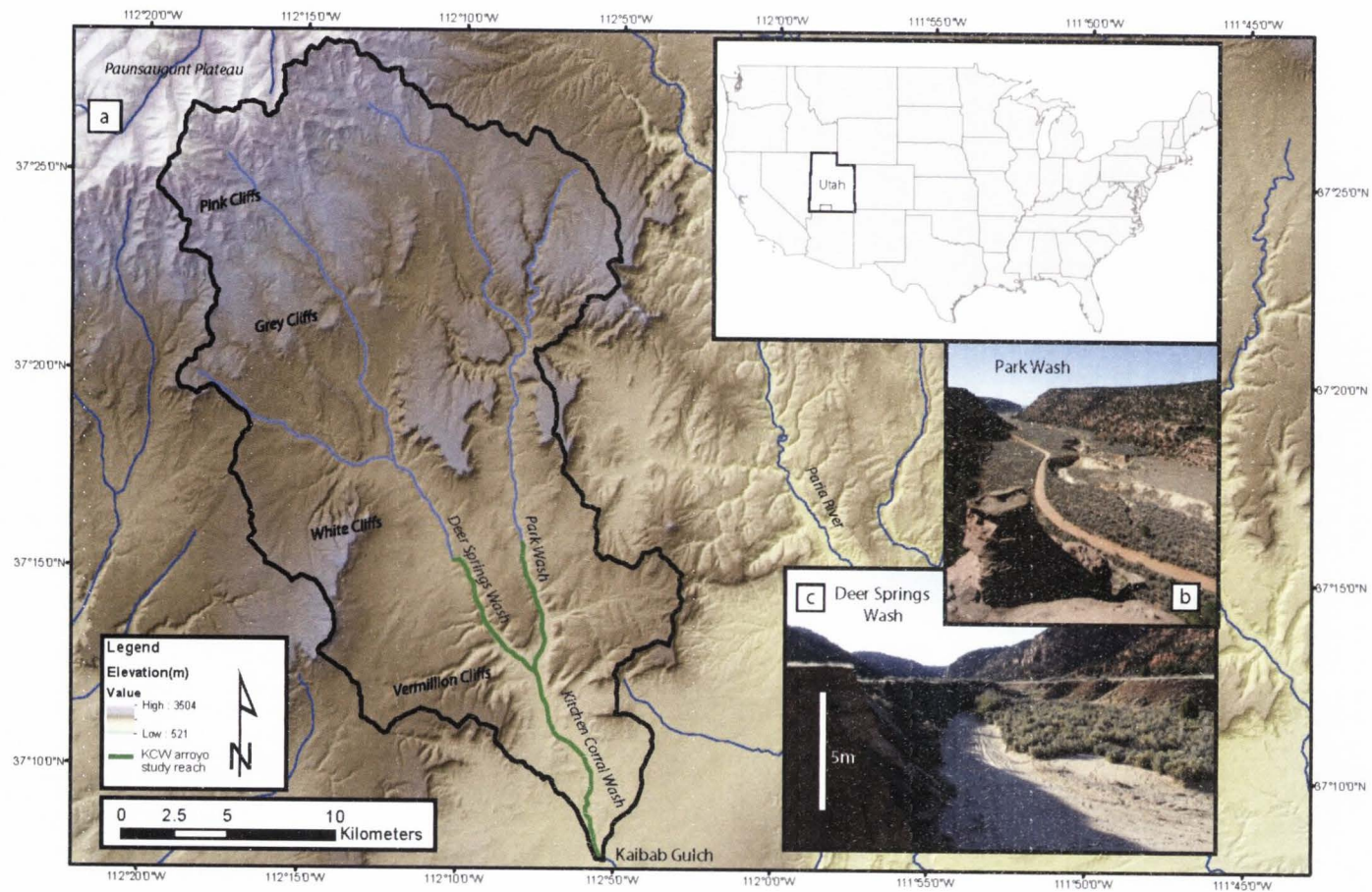


Fig. 2.1. Location map of the KCW drainage in southern Utah: (a) Physiographic map of displaying the KCW catchment, drainage, and study area (in green) (b) aerial photo from Park Wash looking south (c) ground photo of Deer Spring Wash with a 5 m scale looking north.

Gulch is 511 km<sup>2</sup> and ranges in elevation from ~2500m asl to just below 1800m asl. KCW flows approximately north to south and is currently entrenched with steep, mostly vertical wall

Original alluvial chronologies from KCW were partly derived from three unconformity-bound valley-fill alluvial packages described by Hereford (2002), and were correlated to similarly aged fills in regional drainages to test for near-synchronous and climate-induced arroyo incision and aggradation. However, only four radiocarbon ages from two separate sites were used to help build this alluvial chronology in KCW. Later, Harvey et al. (2011) used a combination of AMS radiocarbon and OSL dating techniques to date one arroyo exposure that contained four valley-fill alluvial packages. Results from Harvey's study indicate a temporal offset in arroyo incision and aggradation when compared to those identified by Hereford (2002).

#### 2.2.2 *AMS Radiocarbon Dating in Arroyos*

Radiocarbon dating is the most widely applied dating technique for alluvial deposits in general and for arroyo systems in particular. It relies on the measurement of the remaining concentration of radioactive carbon (<sup>14</sup>C) that originally accumulated in an organism and began to decay since its death (Libby et al., 1949). In general, the age of organic material (e.g. the time since death) can be calculated by comparing the concentration of <sup>14</sup>C remaining in a sample to standardized pre-1950 <sup>14</sup>C concentrations and taking into account the decay rate for <sup>14</sup>C (e.g. Stuiver and Polach, 1977; Cook and Van der Plicht, 2007). Radiocarbon dating is generally limited to estimating the age of organic materials that are less than ~50 ka BP and has problems dating materials less than 300 years BP because of high rates of natural variability in <sup>14</sup>C production and anthropogenic changes in atmospheric and biogenic <sup>14</sup>C concentrations due to nuclear weapons testing (Reimer et al., 2009). Production rate variability of <sup>14</sup>C can be reconciled by calibrating radiocarbon ages using a tree-ring based data series such as the IntCal09 dataset of Reimer et al. (2009). Radiocarbon dating has been previously applied to arroyo sediments KCW (Hereford, 2002; Harvey et al., 2011) and regional southwestern drainages (Ely,

1997; Delong and Arnold, 2007; Summa-Nelson and Rittenour, 2011). While each study had its own successes with radiocarbon dating charcoal samples, they also encountered age overestimations and stratigraphic age reversals most commonly due to problems caused by fluvial redeposition or the presence of coal.

The potential for redeposition of older organic material is an important concern in arroyos and other semiarid fluvial systems where charcoal, wood and other organic materials can be stored in hillslopes or alluvial deposits prior to being eroded and redeposited downstream (Baker, 1987; Gillespie et al., 1992). Accordingly, an analysis of isolated or mixed materials that were redeposited will only represent a maximum age for an alluvial deposit. Post-depositional processes, such as pedoturbation or bioturbation, may also cause downward movement and repositioning of organic material within a deposit. Percolation of young humic or fulvic acids through a deposit due to root penetration can also cause contamination by young carbon (Bird, 2007). These complications may also result in anomalously old ages if old material is brought up or age inversions if young material is shifted down.

Additional problems when using radiocarbon dating may arise when woody debris or charcoal from ancient trees on the semiarid landscape are transported and deposited into the system (McFadgen, 1982; Gavin, 2001). Also referred to as the "old wood" problem by Schiffer (1986), the radiocarbon age for a piece of charcoal or woody debris from the inner-rings of a tree will be significantly older than the outer and more recent ring growths. Limestone from surrounding sedimentary bedrock in the study area (e.g. Triassic Moenkopi Fm) can also cause problems because of its hard-water effect, in which dissolution of non-atmospherically equilibrated or geologically old carbonate can interact and deplete  $^{14}\text{C}$  levels in organic material (Taylor, 1987).

Prioritized field sampling can be employed to help reduce age discrepancies. *In situ* burned horizons or annually to semi-annually produced plant litter (e.g. twigs, leaves, and seeds) are optimal over samples from heartwood because their radiocarbon age will more closely

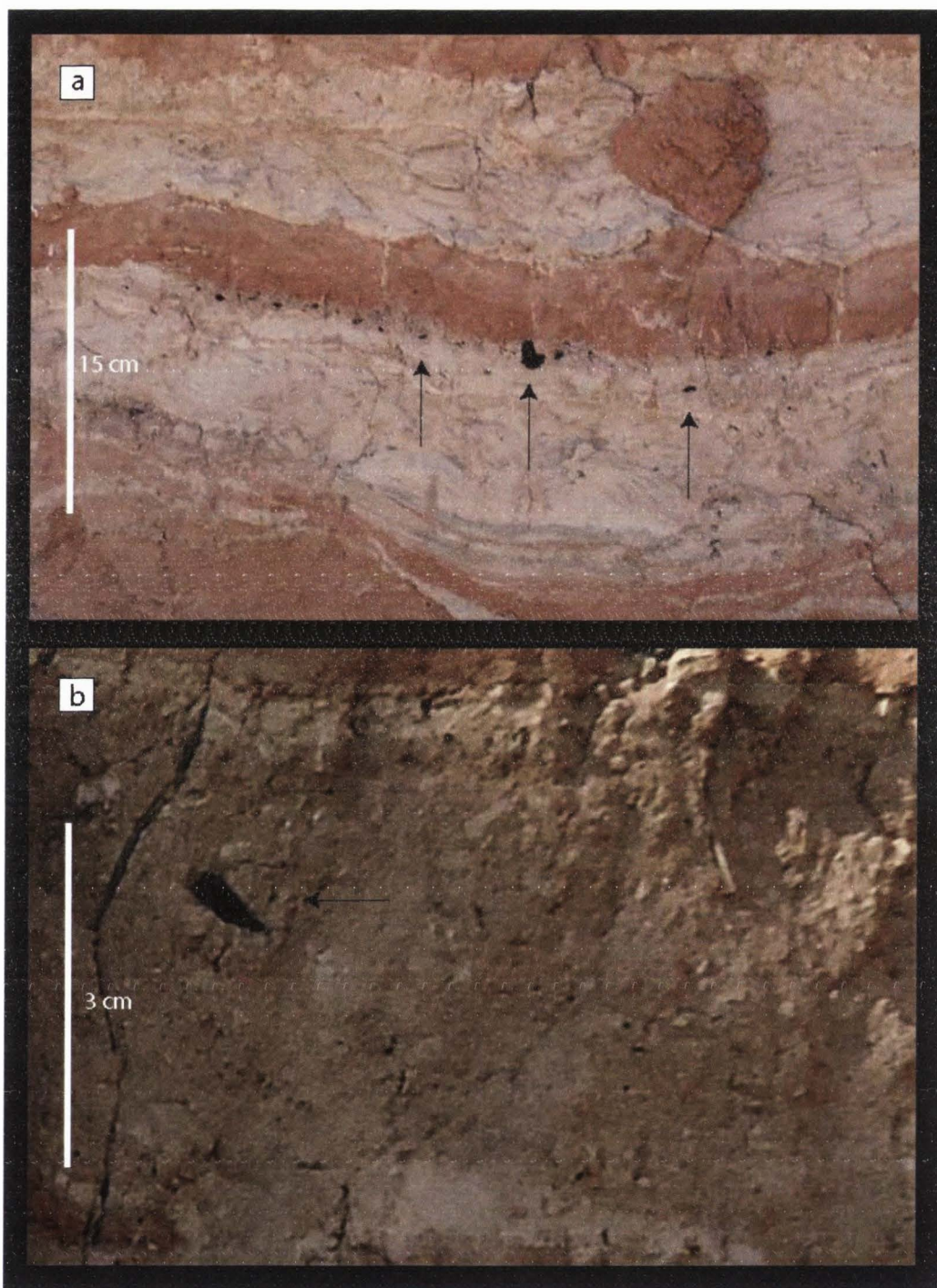


Fig. 2.2. Representation of (a) charcoal-rich lens in a ripple crossbedded (Sr) sand deposit from which sample 14C-11 was collected (Table 2.3) and (b) isolated angular charcoal in a massive (Sm) sand deposit. Note the charcoal in (a) is “floating” near the top of the Sr sand bed.

represent the time of deposition due to their fragile nature a short residence times on the landscape (McFadgen, 1982; Baker, 1987). In absence of these materials, concentrated lenses of angular charcoal likely represent minimal transport and original deposition following a fire-related event (Fig. 2.2). If only isolated charcoal fragments are available, large (>1mg) and angular pieces should be prioritized to reduce the possibility of redeposition. To avoid bioturbation, organic material should be collected from beds with intact sedimentary structures devoid of evidence for burrows or roots.

The presence of local coal-bearing geologic rock units can also complicate radiocarbon dating, wherein erosion of these rock units can lead to the deposition of coal within alluvial deposits. When analyzed, coal samples will produce anomalously old or infinite radiocarbon ages. Harvey (2009) and Hereford (2002) both indicated the presence of coal within alluvial deposits at or near KCW, which were likely derived from the coal-bearing strata of the local Cretaceous Dakota Sandstone and Straight Cliffs Formation. While it is difficult to identify charcoal and coal in the field, magnification of a sample using a hand lens or microscope can help distinguish the carbonized rings in charcoal from the homogeneous structure of coal. Additionally, charcoal has a lower density and specific gravity and can be easily discerned from coal based on these properties.

### 2.2.3 *OSL Dating in Arroyo Systems*

While AMS radiocarbon dating is a mainstay of alluvial dating techniques because of its numerous benefits, not all settings or deposits of interest contain sufficient or stratigraphically relevant material for dating. In these cases, or where charcoal redeposition and contamination are common, OSL dating can enhance age control. OSL dating provides an age estimate of the last time a grain of quartz or feldspar was exposed to sunlight (or heat). More specifically, it estimates the amount of time since the luminescence signal of a grain was reset (bleached) due to the release of electron charges from light sensitive mineralogical defects (traps) (Huntley et al.,

1985; Aitken, 1998). Following deposition, the luminescence signal grows over time as empty crystal lattice defects accumulate electrons produced by exposure to ionizing radiation from surrounding sediments (e.g. radioisotopes of K, Rb, Th, U) and from cosmic rays. The environmental dose rate can be measured by techniques such as beta-counting, a portable gamma spectrometer, or high-resolution gamma spectrometry and ICP-MS (this study). The rate at which energy is absorbed from the radiation (dose rate) can be determined from elemental concentrations using conversion factors (Aitken, 1998; Guerin et al., 2011). The contribution of cosmic-rays can be estimated as a function of depth, elevation above sea level, and geomagnetic latitude (Prescott and Hutton, 1994). Electrons trapped within the quartz grains will produce a natural luminescence signal when stimulated by light (or heat). OSL ages are calculated by dividing the equivalent dose ( $D_e$ ), which is the radiation required to produce a luminescence signal equal to the natural signal measured in grays (Gy), by the dose rate (Aitken, 1998) as indicated by equation 1:

$$\text{Age (ka)} = \frac{\text{Equivalent Dose (Gy)}}{\text{Dose Rate } \left(\frac{\text{Gy}}{\text{ka}}\right)} \quad (1)$$

OSL dating is complementary to  $^{14}\text{C}$  dating because samples can be collected from sand-rich deposits where radiocarbon material may be scarce. Unlike  $^{14}\text{C}$  dating, OSL provides a direct estimation of the time of deposition, and so sediments (quartz grains) within arroyo allostratigraphic sequences can be dated to constrain the timing in which alluviation initiated or was interrupted by an incision event.

Problems with OSL dating in semiarid drainages are related to the amount of sunlight exposure prior to deposition, post-depositional mixing, and microdosimetric effects. Ephemeral, semiarid systems, such as KCW, are dominated by flashy flows and high sediment loads that promote rapid deposition and limit sunlight exposure prior to burial (Wallinga, 2002; Jain et al.,

2004; Rittenour, 2008). Additionally, sediment sourced from highly erodible bedrock, local hillslopes, small tributaries, and slope-bank collapse may also be subject to limited solar exposure and incomplete resetting (Summa-Nelson and Rittenour, 2012), and residual luminescence signals acquired during a previous deposition will be measured during analysis. This is of particular concern for younger (Holocene) fluvial sediments where residual signals of only a few grays can lead to large age overestimations (Wallinga et al., 2001; Murray and Olley, 2002). Anomalously old  $D_e$  measurements can be objectively identified and reduced in weight when calculating ages by applying the minimum-age-model (MAM) of Galbraith et al. (1999). The MAM truncates a  $D_e$  distribution in order to statistically isolate a population of grains with the lowest equivalent doses, which are assumed to have been fully bleached at deposition. The central-age-model (CAM) is used for samples with limited evidence for partial bleaching and calculates the weighted mean of all  $D_e$  values.

Post-depositional mixing is also problematic throughout southwestern drainages because of bioturbation (Fig. 2.3). Root penetration and animal burrows (e.g. krotovina) can cause the mixing of older and younger grains to produce a mixed OSL signal that can result in erroneous OSL results (Bateman et al., 2003). Hence, deposits containing evidence of incipient soil formation should be identified and avoided prior to sampling, and deposits with recent insect burrows from the arroyo-wall surface should either be avoided or cleared beyond the depth of their penetration to evade mixed or recently exposed sand grains.

Other sources of error in OSL dating include broad variations in dosing due to microdosimetry (e.g. heterogeneous dosing at grain-scale). For example, a feldspar-rich sand bed can cause a localized increase of beta dosing from  $^{40}\text{K}$  decay and significantly alter the dose rate (Vandenberghé et al., 2003) or a deposit with variable grain sizes can be heterogeneously dosed due to radiation shielding by larger grains. Additionally, *in situ* water content affects the dose rate because water in pore spaces absorbs energy and attenuates some of the natural dose radiation. It is important to make an estimation of the average wetness of a sample over its burial

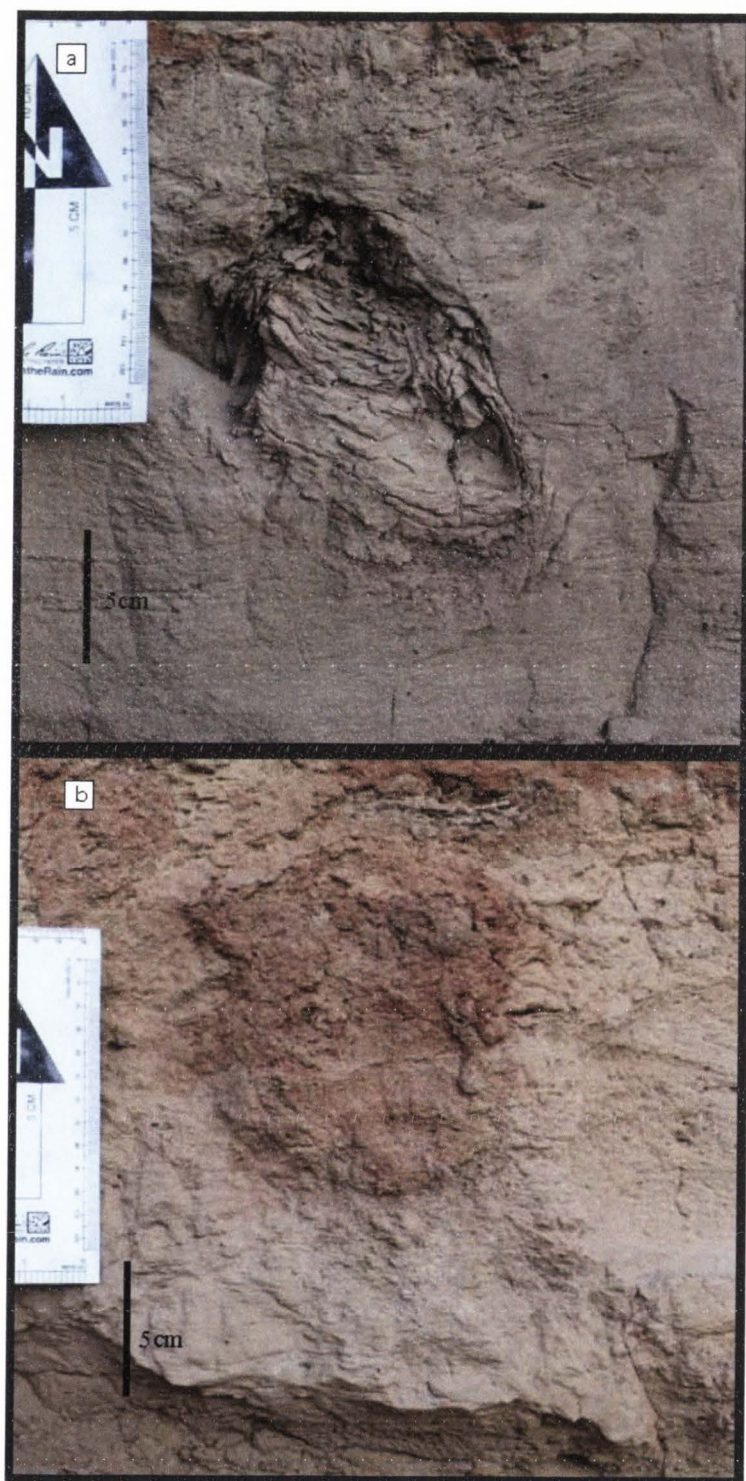


Fig. 2.3. Krotovina commonly seen in sand beds. These are representative of potential bioturbation or post-depositional mixing processes that can contribute to anomalous OSL ages if sampled: (a) desiccated, clay-filled krotovina in a trough crossbedded (St) deposit and (b) silty-sand filled krotovina in a low-angle crossbedded (St) deposit.

period to correct for this attenuation, which can be done by calculating the weight differences in samples before and after they were dried in an oven. In this study, an assumed value for the moisture content was used because all samples were dry at collection.

### 2.3 Methods

In order to test the applicability of AMS radiocarbon and single-grain OSL dating, twelve outcrops (A-L) were identified and examined in detail in the KCW study area (Figure 2.4a). Alluvial fill packages at each site were largely identified by prominent arroyo cut-fill characteristics which included buttress unconformities and buried soil horizons separating at least two alluvial fills. Prior to sampling, sites were described and surveyed using a GPS, and the alluvial stratigraphic and arroyo cut-fill architecture was sketched. Descriptions are based on the alluvial stratigraphy and sedimentology in each fill and specifically focused on facies assemblages and interpretations of depositional environments (see Chapter 3). A total of thirty-seven radiocarbon ( $^{14}\text{C}$ ) and 29 OSL samples were collected from the study area for AMS and single-grain OSL analyses. In addition, two AMS radiocarbon and two small-aliquot OSL ages from Harvey (2009) were used to help reconstruct the alluvial chronology.

#### 2.3.1 *Depositional Facies and Sedimentology*

Detailed stratigraphic and sedimentologic descriptions were made at each arroyo-wall exposure prior to radiocarbon and OSL field sampling. These descriptions were used to extract and compile a list of the most frequently observed depositional facies comprising KCW alluvial fills (Fig. 2.5). Descriptions were made in order to test for relationships between levels of partial bleaching or occurrences of redeposited charcoal and facies type. A total of 10 depositional facies (Table 2.1) have been identified within beds of the 12 arroyo study sites in KCW and have been given a facies code primarily based upon grain size and sedimentary textures or structures closely following those described in Miall (2000).

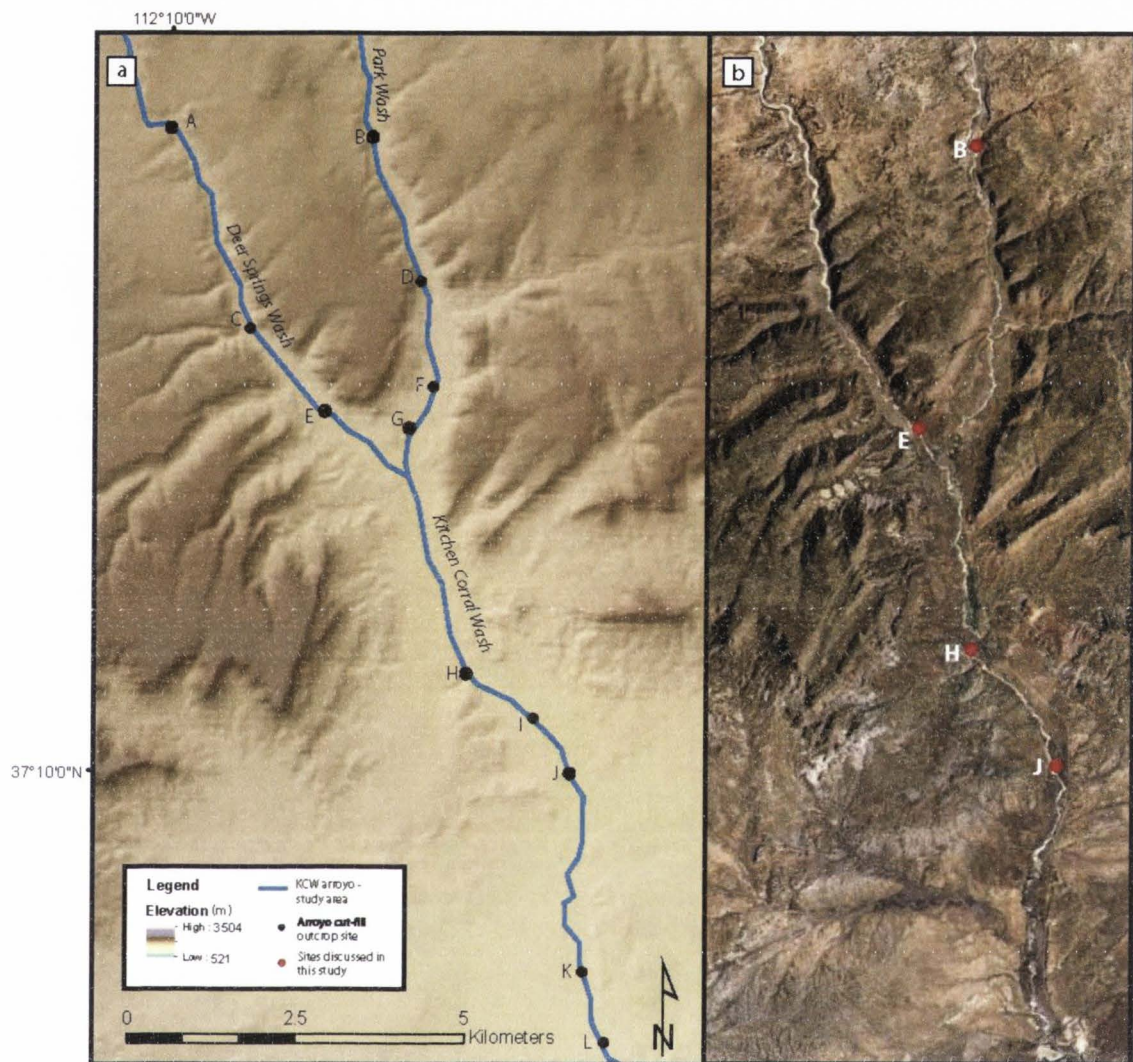


Fig. 2.4. Location map of key study exposures within KCW of (a) 5 m DEM and locations of all 12 study sites and (b) Google Earth aerial photo with arroyo outcrop sites discussed in this study (highlighted in red).

Alluvial sediments throughout KCW are primarily sourced from bedrock lithologies, Pleistocene terrace deposits, other Quaternary surficial deposits, and modern channel deposits. Accordingly, the stratigraphy of KCW is distinguished by alternating beds of sediment from the upstream or local sediment sources. In general, sediments from upstream sources are derived from Jurassic Navajo Sandstone bedrock and consist of very pale brown (10YR 8/3, 7/4), fine- to coarse-grained, sub- to well-rounded, well sorted, frosted, quartz-rich sand grains. Sediments derived from local sources are generally darker in color ranging from reddish yellow (5YR 6/6), light red (2.5YR 6/6), and red (2.5YR 4/6), sub-angular to sub-rounded, poorly to moderately sorted, very fine- to fine-grained sands containing variable amounts of silts and clays. These sediments are likely derived from Jurassic Kayenta and Moenave bedrock (sandstones), Triassic Chinle Fm (sandstone, siltstone, claystone), or heterogeneous mixtures of sand, silt, and clay from local hillslopes and tributaries. Upstream and local sediments were subjectively identified in the field and lab based on a visual assessment using the characteristics described above.

The most common facies in KCW primarily consist of trough crossbedded (St) or ripple crossbedded (Sr), very fine to medium-grained sands. In addition, low-angle ( $<15^\circ$ ) crossbedded sand (SI) that represents lower to upper flow regimes and horizontally or planar bedded deposits representative of upper flow regimes are also common in the arroyo-wall exposures studied. Deposits with these facies are generally ~20 to 50 cm thick and display tabular or broadly lenticular geometries. This facies assemblage is most often representative of a medium to low energy channel-margin (CM) depositional environment (see Ch. 3) and indicative of relatively modest unidirectional flow events.

The second most common facies assemblage throughout KCW alluvial fills is represented by very fine- to coarse-grained, massive, structureless sands, which often have variable amounts of clays and silts. These sand units range from a few centimeters to tens of centimeters thick that are broadly tabular and fall into three sedimentary facies classifications: massive sands (Sm), thinly laminated or desiccated clays and silty-sands (FI), variegated clay,

Table 2.1  
KCW facies codes

<b>Facies Code<sup>a</sup></b>	<b>Sedimentary Structures</b>	<b>Sedimentology</b>	<b>Flow Regime</b>	<b>Depositional Interpretation</b>
Sl	Low-angle crossbeds	Sand, very fine to coarse with variable amounts of gravels and pebbles	Lower-Upper	Scour-fill, transverse or linguoid bedforms
St	Trough crossbeds	Sand, very fine to coarse with variable amounts of gravels and pebbles	Lower-Upper	Bedform migration
Sh	Horizontally/Planar bedded	Sand, very fine to coarse with variable amounts of gravels and pebbles	Upper	Plane bed flow
Sr	Ripple crossbeds	Sand, very fine to coarse with variable amounts of gravels and pebbles	Lower	Supercritical climbing ripples
Sm	Massive	Sand, very fine to coarse with variable amounts of gravels and pebbles	Upper	Inner channel flood, overbank flood, levee deposit
Fl	Isolated , thinnly laminated or dessicated beds	Clay, Silt	Lower	Overbank or waning flood deposit
Fsmv	Interbedded massive and thin laminations	Variogated clay, silt, very fine sand	Lower	Backswamp, marsh deposit
P	Incipient soil, bioturbation	Clay, silt, very fine sand often containing roots and burrows		Soil formation along a stable surface
Gh	Horizontally bedded or massive	Clast or matrix supported gravels and pebbles	Upper	Lag deposits
Gt	Crossbedded	Clast or matrix supported gravels and pebbles	Upper	Channel Fills

<sup>a</sup>List of the most common sedimentary facies evident within the KCW study area. Facies codes closely follow those described in Miall (2000). OSL and radiocarbon samples were primarily targeted within the lithofacies highlighted in gray.

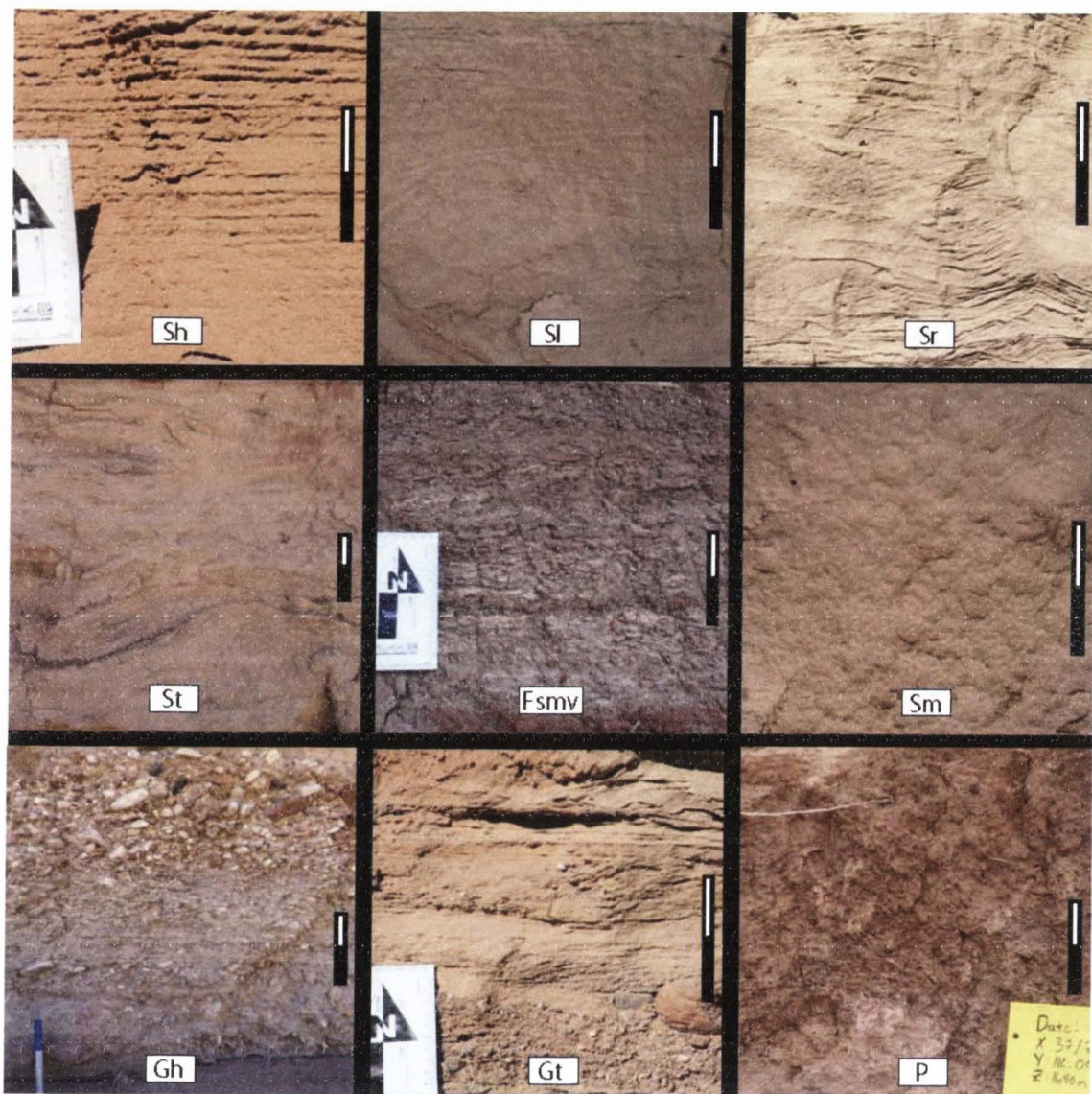


Fig. 2.5. Common lithofacies in KCW alluvial fills (see Table 2.1 for descriptions). Scale bar represents 10 cm and facies codes are represented at base of photographs.

silt, and very-fine sand interbeds (Fsmv). Massive sands (Sm) are typified by moderately to well sorted, fine to coarse grained sands likely deposited during high energy and high sediment yield events (upper flow regimes) and are most often interpreted to be channel-margin (CM) deposits (see Ch. 3). Individual beds of thinly laminated (<10cm) or dessicated clays and silty-sands (FI) are often interbedded with very very fine- to coarse-sand facies (Sh, St, Sr, Sl) and are deposited as a high flow event begins to wane within the channel. Thinly bedded (<5cm), commonly variegated, clayey-silt to very fine-grained and laminated sands (Fsmv) deposits are typically over 30cm thick, and are one of the most recognizable facies throughout KCW. Fsmv facies deposits are often laterally traceable for tens of meters, and were likely deposited in slackwater settings. In this study, incipient soil horizons are grouped separately even though they have developed within other sedimentary facies and therefore may share a similar grain size distribution (clay, silt, very-fine sand). Incipient soils are given the facies designation (P) and are commonly distinguishable as highly bioturbated or buried entisols or inceptisols that are typically part of the valley surface. The profacies of an incipient soil may be one of any previously mentioned facies textures (e.g. Sl, St, Sm, Fsmv).

The least common facies assemblage includes matrix- or clast-supported gravels and pebbles that are horizontally bedded or imbricated (Gh) or crossbedded (Gt). These facies are most commonly seen in basal deposits that generally occur as lenticular beds extending only a few meters. They are commonly seen within or underlying other lenticular deposits of Sh, St, Sl, Sr, or Sm and. Because of the grain size and bedding of these deposits, Gh and Gt facies are interpreted to have been deposited in channel-bottom (CB) depositional environments (see Ch. 3).

### 2.3.2 Radiocarbon Collection

Techniques for radiocarbon sampling closely followed the suggestions described in the previous section. Although preference would have been given to *in situ* burned horizons or annual plant material, samples were collected based on their availability and stratigraphic context.

Consequently, target material typically consisted of large concentrations of charcoal or thin lenses of charcoal separating sedimentary beds near the base or top of an alluvial fill. In a few instances, isolated charcoal fragments were sampled where opportunities for OSL dating were limited and no other sources of charcoal or woody debris were available. However, isolated charcoal was avoided in the presence of a highly bioturbated bed or beds indicating incipient soil formation. Once a charcoal rich lens or isolated charcoal fragment was targeted for collection, attention was paid to the size and angularity of individual pieces in order to reduce the odds of collecting a redeposited sample.

Prior to collection, the stratigraphic context of each sample was noted and sample locations were photo-documented. Charcoal and woody debris samples were collected using a steel trowel and immediately preserved in aluminum foil and stored in a plastic sample bag. If large, concentrated charcoal lenses were present, several fragments of charcoal may have been sampled as these were assumed to be sourced from the same fire event. However, only one charcoal fragment from each sample collected was typically analyzed in order to avoid averaging different radiocarbon ages. After collection, charcoal samples were extracted from the aluminum foil, examined under a microscope to check for annual rings and ensure coal was not sampled, weighed, and stored in 20 ml glass vials marked with unique numbers until being processed and analyzed. Additionally, samples containing more than the required amount of charcoal for analysis were separated and archived.

### *2.3.3 Radiocarbon Preparation and Analysis*

Sixteen of the 37 samples collected were sent to the UC Irvine Keck AMS Laboratory for processing and AMS analysis. An additional 17 samples were pretreated and combusted by the author at the University of Arizona (UA) NSF AMS Laboratory and later analyzed by the AMS lab staff. Two samples collected by Harvey (2009) are also used in this study and were sent to Beta Analytic Inc. for AMS analysis. Each sample was subject to a carbonate, fulvic acid and

humic acid removal pretreatment using a standardized acid-base-acid wash and rinsed with deionized water. Following pretreatment, approximately 1.5-3mg of each sample was packed with CuO and combusted ( $\sim 1000^{\circ}\text{C}$ ) in order to convert and isolate  $\text{CO}_2$  in gas form. A mixture of the  $\text{CO}_2$  gas and Fe powder was then reduced to a graphite target for AMS measurements. Resulting  $^{14}\text{C}$  ages were converted into radiocarbon years, calibrated using Calib 6.0 and the Intcal09 dataset of Reimer et al. (2009), and are reported in  $\text{BP}_{2010}$  as a maximum probability age and asymmetric 2-sigma error (Telford et al., 2004) (Table 2.2). Reporting as cal. kyr  $\text{BP}_{2010}$  allows for a direct correlation to ages derived from OSL dating.

#### 2.3.4 OSL Collection

OSL samples were collected concurrent with the collection of organic material for radiocarbon dating. In general, OSL samples were extracted where charcoal was scarce or where sandy alluvium was optimal for sampling. Where possible, samples were collected near the base or top of alluvial fills. A total of 29 (two from Harvey, 2009) OSL samples were collected from 12 alluvial outcrops displaying context for arroyo cut-fill events. Sample collection was performed following the guidelines provided by the Utah State University Luminescence Laboratory (<http://www.usu.edu/geo/luminlab/>).

As described above, varying levels of partially reset (bleached) sediments were expected in the alluvial deposits, so special attention was paid to the sedimentology and stratigraphy of targeted alluvium prior to sampling, wherein sedimentologic facies and stratigraphic context were observed and noted. Deposits displaying signs of soil formation, burrows, or roots were avoided (i.e. P beds) because of potential age inaccuracies resulting from broad equivalent dose values (e.g. Bateman et al., 2003). In general, sampling preference was given to beds under 40 cm thick with a ripple cross-laminated facies (Sr), indicated by Summa-Nelson and Rittenour (2012) to have been more likely exposed to adequate sunlight due to their deposition during a low flow

Table 2.2  
Summary of radiocarbon ages

Sample Number	Lab ID	Drainage Basin/Profile Site	<sup>14</sup> C Age	Error ±	2σ Calibrated Age Range (yr BP <sub>2010</sub> ) <sup>a</sup>	2σ Total Calibrated Age Range (rounded yr BP <sub>2010</sub> )	2σ Median Age (rounded cal yr BP <sub>2010</sub> )	Error ±	2σ Weighted Mean cal yr BP <sub>2010</sub> (rounded) <sup>b</sup>	Error +/- (rounded)
14C-1	113985	A	2015	15	1964-1966 (0.005), 1984-2058 (0.995)	1960-2060	2010	50	2020	40/60
14C-2	113986	A	365	15	385-436 (0.357), 488-556 (0.643)	390-560	470	90	480	80/160
14C-3	113981	B	500	15	571-598 (1)	570-600	590	10	580	20/10
14C-4	113989	B	1235	15	1142-1174 (0.107), 1180-1247 (0.447), 1261-1319 (0.446)	1140-1320	1230	90	1240	80/130
14C-5	X24136	C	2460	40	2421-2679 (0.742), 2692-2767 (0.258)	2420-2770	2590	170	2600	170/180
14C-6	X24137	C	49,400	4000					49,400	4000
14C-7	X24132	D	1488	38	1363-1478 (0.924), 1525-1571 (0.076)	1360-1570	1470	100	1440	130/80
14C-8	X24133	D	466	37	526-526 (1)	530-630	580	50	570	60/40
14C-9	X24135	D	1208	38	1073-1085 (0.016), 1115-1250 (0.811), 1257-1322 (0.173)	1070-1320	1200	130	1200	120/130
14C-10		D	not analyzed						not analyzed	
14C-11	113987	E	1420	15	1357-1404 (1)	1360-1400	1380	20	1380	20/20
14C-12	X24138	E	879	38	759-761 (0.003), 773-776 (0.004), 785-974 (0.993)	760-970	870	110	870	100/110
14C-13	113988	E	140	15	57-95 (0.208), 130-177 (0.228), 191-221 (0.122), 223-289 (0.279), 321-335 (0.163)	60-340	200	140	200	140/140
14C-14	X24139	F	42600	1600					42,600	1600
14C-15	X24140	F	609	37	603-717 (1)	600-7720	660	60	660	60/60
14C-16	X24141	F	>45700						>45,700	
14C-17	X24134	G	1194	38	1049-1053 (0.003), 1057-1092 (0.062), 1111-1245 (0.842), 1262-1304 (0.083), 1307-1316 (0.01)	1050-1320	1180	130	1180	140/130
14C-18	113982	G	665	15	624-648 (0.451), 703-728 (0.549)	620-730	680	50	680	50/60
14C-19		G	not analyzed				0	0	not analyzed	
14C-20		G	not analyzed				0	0	not analyzed	
14C-21	113984	G	3420	15	3692-3765 (0.993), 3767-3773 (0.007)	3690-3770	3730	40	3730	40/40
14C-22	105792	H	3480	30	3756-3841 (0.633), 3846-3888 (0.367)	3760-3890	3820	70	3820	70/60
14C-23		H	not analyzed						not analyzed	
14C-24	105793	H	1115	30	1034-1118 (1)	1030-1120	1080	40	1080	40/50
14C-25	105794	H	2200	40	2069-2079 (0.01), 2100-2404 (0.99)	2070-2400	2240	170	2280	120/210
14C-26	113983	H	3735	15	4053-4099 (0.31), 4135-4209 (0.69)	4050-4210	4130	80	4140	70/90
14C-27	X24142	H	849	40	743-862 (0.843), 870-889 (0.038), 818-964 (0.119)	740-960	850	110	830	130/90
14C-28	105788	I	1755	30	1674-1772 (1)	1670-1770	1720	50	1720	50/50
14C-29	X24144	I	46600	2700					46,600	2700
14C-30	105789	J	>31700						>31,700	
14C-31	105790	J	1730	30	1629-1644 (0.059), 1653-1759 (0.941)	1630-1760	1690	70	1700	60/70
14C-32	105791	J	1860	30	1789-1892 (0.858), 1898-1925 (0.142)	1790-1930	1860	70	1850	80/60
14C-33	X24143	J	2395	40	2400-2567 (0.829), 2587-2599 (0.009), 2653-2674 (0.032), 2697-	2400-2760	2580	160	2520	240/120
14C-34	X24129	K	993	46	849-1039 (0.993), 1099-1005 (0.007)	850-1110	980	130	950	160/100
14C-35	X24130	K	2002	40	1929-2120 (0.996), 2150-2152 (0.004)	1930-2150	2040	110	2010	140/80
14C-36	X24131	K	368	37	376-469 (0.473), 481-563 (0.527)	380-563	470	60	470	90/90
14C-37	X24145	L	46700	2800						
14C-38 <sup>c</sup>	Beta-256838	I	610	40	600-730 (1)	600-730	660	60	660	60/80
14C-39 <sup>c</sup>	Beta-256840	I	2220	40	2210-2400 (1)	2210-2400	2300	90	2300	60/90

<sup>a</sup>2-sigma calibrated age range calculated as a relative probability using Intcal09 calibration curve of Reimer et al. (2009)

<sup>b</sup>2-sigma calibrated ages (rounded to nearest 10) using Calib 6.0 and the Intcal09 dataset of Reimer et al. (2009), and are reported in BP<sub>2010</sub> as a maximum probability age and asymmetric 2-sigma error.

<sup>c</sup>Samples originally collected in Harvey (2009). Also used in Harvey et al. (2011) and this study. Samples analyzed by Beta Analytic.

Table 2.3  
Summary of radiocarbon ages and sample characteristics

Sample Number	Lab ID	Drainage Basin/Profile Site	Facies	<sup>14</sup> C Age	Error ±	2σ Weighted Mean cal yr BP <sub>2010</sub> (rounded)	Error +/- (rounded)	Targeted Sample <sup>a</sup>	Stratigraphic Agreement/Disagreement <sup>b</sup>
14C-1	113985	A	St	2015	15	2020	40/60	CRL	A
14C-2	113986	A	Sr	365	15	480	80/160	CRL	A
14C-3	113981	B	Sh	500	15	580	20/10	CRL	A
14C-4	113989	B	St	1235	15	1240	80/130	CRL	A
14C-5	X24136	C	Fsmv	2460	40	2600	170/180	IAC	A
14C-6 <sup>c</sup>	X24137	C	St	49,400	4000	49,400	4000	IAC	D (CC)
14C-7	X24132	D	Sl	1488	38	1440	130/80	CRL	A
14C-8	X24133	D	Fsmv	466	37	570	60/40	CRL	A
14C-9	X24135	D	St	1208	38	1200	120/130	IAC	D (RD)
14C-10		D	Sl	not analyzed		not analyzed		IBB	
14C-11	113987	E	St	1420	15	1380	20/20	CRL	A
14C-12	X24138	E	St	879	38	870	100/110	CRL	A
14C-13	113988	E	Sl	140	15	200	140/140	CRL	A
14C-14	X24139	F	St	42,600	1600	42,600	1600	CRL	D (CC)
14C-15	X24140	F	Sr	609	37	660	60/60	CRL	A
14C-16	X24141	F	St	>45,700		>45,700		IAC	D (CC)
14C-17	X24134	G	St	1194	38	1180	140/130	CRL	A
14C-18	113982	G	Fl	665	15	680	50/60	AWD	A
14C-19		G	Sm	not analyzed		not analyzed		IRL	
14C-20		G	St	not analyzed		not analyzed		CRL	
14C-21	113984	G	Sl	3420	15	3730	40/40	CRL	A
14C-22	105792	H	Sl	3480	30	3820	70/60	CRL	A
14C-23 <sup>e</sup>		H	Sm	not analyzed		not analyzed		IAC	
14C-24	105793	H	Sm	1115	30	1080	40/50	CRL	A
14C-25 <sup>c</sup>	105794	H	Sm	2200	40	2280	120/210	IRL	D (RD)
14C-26	113983	H	Sr	3735	15	4140	70/90	CRL	A
14C-27	X24142	H	St	849	40	830	130/90	IAC	A
14C-28	105788	I	Sl	1755	30	1720	50/50	CRL	A
14C-29	X24144	I	St	46,600	2700	46,600	2700	CRL	D (CC)
14C-30 <sup>f</sup>	105789	J	Sh	>31700		>31,700		CRL	D
14C-31	105790	J	Sl	1730	30	1700	60/70	CRL	A
14C-32	105791	J	Fsmv	1860	30	1850	80/60	IAC	A
14C-33	X24143	J	St	2395	40	2520	240/120	CRL	D (RD)
14C-34	X24129	K	Fsmv	993	46	950	160/100	CRL	A
14C-35 <sup>c</sup>	X24130	K	St	2002	40	2010	140/80	IAC	D (RD)
14C-36	X24131	K	St	368	37	470	90/90	CRL	A
14C-37	X24145	L	Sl	46,700	2800	46,700		CRL	D (CC)
14C-38 <sup>d</sup>	Beta-256838	I	Sl	610	40	660	60/80	AWD	A
14C-39 <sup>d</sup>	Beta-256840	I	St/Sl	2220	40	2300	60/90	CRL	A

<sup>a</sup> Targeted samples for AMS radiocarbon dating: CRL = Charcoal-rich Lens, IAC = Isolated Angular Charcoal, IBB = Isolate Burned Branch, IRL = Isolated Round Charcoal, AWD = Angular Woody Debris

<sup>b</sup> Notes if Weighted Mean calibrated radiocarbon age (BP<sub>2010</sub>) of each radiocarbon sample Agrees (A) or Disagrees (D) with stratigraphic relationships or OSL ages. Disagreement interpreted as CC = Cretaceous Coal, RD = Redeposited Sample.

<sup>c</sup> Samples Collected from within or near a colluvial deposit.

<sup>d</sup> Samples originally collected in Harvey (2009). Also used in Harvey et al. (2011) and this study.

<sup>e</sup> Sample did not undergo AMS measurement because it did not survive pretreatment chemistry

<sup>f</sup> Finely disseminated pieces of charcoal in deposit. Large uncertainty due to small sample size (0.056 mg) or possible mixing of Cretaceous coal.

regime. However, if this depositional facies was not present, secondary consideration was typically given to thin beds (<40 cm) with low to upper flow regime facies, such as trough crossbedded (St) or low-angle crossbedded (Sl) sand, or in some cases deposits that were horizontally bedded (Sh). Beds displaying thick (>1m) massive sand (Sm) devoid of sedimentary structures were avoided because of the possibility of rapid deposition and limited sunlight exposure during a high-magnitude flow event. Variegated clays and silty-sand (Fsmv) beds were not sampled for OSL because they contained a much larger fine-grained fraction and sand beds were generally <5 cm thick.

Opaque metal tubes were hammered into targeted alluvial deposits within the arroyo walls, and samples were collected at least one meter below the original ground surface in order to resolve the cosmic contribution to the dose rate and avoid problems with soils or bioturbation (Fig. 2.6). In addition, the longitude, latitude, elevation, and depth below the ground surface were recorded to calculate the cosmic dose contribution to the overall dose rate following Prescott and Hutton (1994). Samples were also collected at least one meter from an erosional contact or colluvial deposit in order to reduce the potential for partial bleaching due to erosion from an older fill or short sediment transport. After the OSL tube was extracted and packed securely to prevent mixing, a bulk representative sample of surrounding sediment was collected from a ~30 cm radius surrounding the sample location for environmental dose rate determination and a small sample (~50 g) was collected in an air-tight container for analysis of *in situ* water content.

### 2.3.5 OSL Preparation

Samples were processed in the Utah State University (USU) luminescence lab. Each sample was opened under dim amber light (590 nm) and the ends of each sample tube were removed because they may have been exposed to light during collection. The center of each sample was then excavated and wet sieved at grains-size fractions of 150-250  $\mu\text{m}$  or 180-250  $\mu\text{m}$ . Samples were then pretreated with 10% hydrochloric acid wash to dissolve carbonates followed

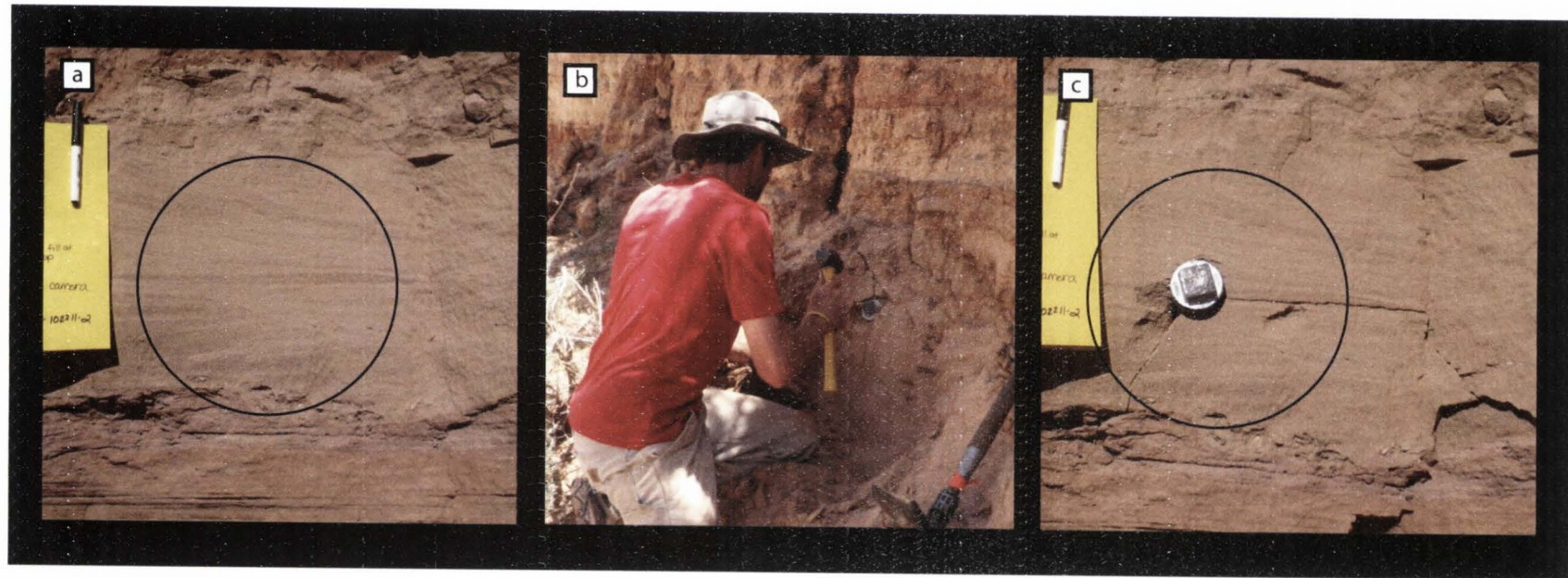


Fig. 2.6. OSL sample extraction from the KCW study area: (a) Example of a >40 cm thick, very pale brown, low-angle crossbedded sand deposit prior to extraction, (b) hammering an opaque metal tube into a targeted sand bed, (c) end result of hammering that is followed by extraction of an OSL sample (USU-1026) and analysis at the USU Luminescence Laboratory.

by household bleach to remove organics. Pretreated samples were then floated in sodium polytungstate ( $2.7 \text{ g/cm}^3$ ) to separate any heavy minerals from the quartz and feldspar fraction and then were subject to three 30 minute baths of concentrated (47%) HF to remove feldspars and etch the quartz grains, followed by one 30 minute bath of concentrated (37%) HCl to prevent the precipitation of fluorites. Subsequent to the HF treatment, samples were dried and resieved at  $75 \mu\text{m}$  to remove any partially dissolved feldspars. Sample purity was checked on all aliquots by monitoring response to infrared (IR) stimulation (e.g. Duller et al., 2003). A number of samples indicated a signal depletion response following IR exposure, suggesting feldspar contamination, and were re-treated with HF and re-sieved at  $75 \mu\text{m}$  to remove any partially dissolved feldspar until they no longer produced a luminescence response to IR stimulation.

Concurrent with sample processing, representative splits of the samples collected for dose rate determination were sent to ALS Chemex in Elko, NV for ICP-MS analysis of Rb, U, and Th content and ICP-AES analysis of K. Dose rate conversions followed Guerin (2010) and are presented in Table 2.4. Most of the samples collected from KCW had a moisture content  $<1\%$  and were generally dry upon collection because of semi-arid climate in southern Utah. Due to the expected variability of past ground-water levels and climate conditions, a moist value of  $3 \pm 3\%$  was used in age calculation.

### 2.3.6 OSL Analysis

Of the 29 OSL samples collected and processed, seventeen samples from KCW underwent quartz single-grain (SG) analyses using the single-aliquot regenerative (SAR) dose protocol from Murray and Wintle (2000). Optical measurements were performed on a Riso TL/OSL Model DA-20 reader and grains were stimulated using a focused green laser ( $532 \text{ nm}$ ) at 90% power ( $135 \text{ mW/cm}^2$ ) (Bøtter-Jensen et al., 2000) and at  $125^\circ\text{C}$  for 1 second over 60 channels with a 0.1 s pause before and after stimulation. Detection of the luminescence signal was achieved through a 7.5-mm UV filter (U-340) for 40 seconds at  $125^\circ\text{C}$ . The initial signal

Table 2.4  
Dose rate chemistry data for analyzed KCW OSL samples

USU Lab ID	Study Site	Latitude/Longitude	Elevation (m asl)	Depth (m)	K (%)	Rb (ppm)	Th (ppm)	U (ppm)	Cosmic Contribution (Gy/Ka)	Dose Rate (Gy/Ka)
USU-1189	A	N37.25507, W112.16564	1748	1.5	0.77 ± 0.02	29.4 ± 1.2	2 ± 0.20	0.8 ± 0.10	0.24 ± 0.02	1.28 ± 0.07
USU-1176	B	N37.25423, W112.13139	1721	1.5	1.77 ± 0.04	71.6 ± 2.9	6.2 ± 0.56	1.7 ± 0.12	0.24 ± 0.02	2.71 ± 0.14
USU-1177	B	N37.25423, W112.13139	1721	6	0.77 ± 0.02	29.4 ± 1.2	2 ± 0.20	0.7 ± 0.10	0.14 ± 0.01	1.15 ± 0.07
USU-1187	C	N37.22864, W112.15267	1726	5	0.92 ± 0.02	35 ± 1.4	2.6 ± 0.23	0.8 ± 0.10	0.16 ± 0.02	1.38 ± 0.08
USU-1178	D	N37.23512, W112.12296	1711	7.5	1.06 ± 0.03	41.2 ± 1.6	2.7 ± 0.24	0.9 ± 0.10	0.11 ± 0.01	1.50 ± 0.08
USU-1192	E	N37.21745, W112.13931	1705	4	0.96 ± 0.02	35.2 ± 1.4	2.1 ± 0.20	0.8 ± 0.10	0.18 ± 0.02	1.40 ± 0.08
USU-1194	F	N37.22137, W112.12116	1689	5	0.54 ± 0.01	20.8 ± 0.8	1.8 ± 0.20	0.7 ± 0.10	0.15 ± 0.02	0.94 ± 0.06
USU-1181	G	N37.21581, W112.12551	1686	1.5	0.46 ± 0.01	18.8 ± 0.8	2.1 ± 0.20	0.6 ± 0.10	0.24 ± 0.02	0.94 ± 0.06
USU-1101	H	N37.18361, W112.11550	1668	8.5	0.44 ± 0.01	14.9 ± 0.6	1.4 ± 0.20	0.5 ± 0.10	0.10 ± 0.01	0.73 ± 0.05
USU-1103	H	N37.18361, W112.11550	1668	7.5	1.2 ± 0.03	45.9 ± 1.8	3.2 ± 0.29	1 ± 0.10	0.11 ± 0.01	1.70 ± 0.09
USU-530 <sup>c</sup>	I	N37.17752, W112.10266	1653	8	1.04 ± 0.03	47.2 ± 1.3	3.2 ± 0.29	1 ± 0.10	0.11 ± 0.01	1.56 ± 0.07
USU-531 <sup>c</sup>	I	N37.17752, W112.10266	1653	4	1.39 ± 0.04	63 ± 1.7	5.8 ± 0.52	1.5 ± 0.11	0.17 ± 0.02	2.25 ± 0.10
USU-1026	J	N37.17012, W112.09731	1640	4	1.05 ± 0.03	44.5 ± 1.8	2.5 ± 0.25	0.9 ± 0.10	0.17 ± 0.02	1.54 ± 0.08
USU-1027	J	N37.17012, W112.09731	1640	4	0.99 ± 0.02	38.2 ± 1.5	2.5 ± 0.23	1 ± 0.10	0.17 ± 0.02	1.50 ± 0.08
USU-1028	J	N37.17012, W112.09731	1640	3	0.73 ± 0.02	26.5 ± 1.1	2.4 ± 0.22	0.7 ± 0.10	0.19 ± 0.02	1.20 ± 0.07
USU-1029	J	N37.17012, W112.09731	1640	1	1.02 ± 0.03	36.5 ± 1.5	2.1 ± 0.20	0.6 ± 0.10	0.25 ± 0.02	1.49 ± 0.08

<sup>a</sup> Latitude/Longitude: 37°N, 112°W; elevation: ~1.65 to 1.75 km asl, sediment density: 2 g/cm<sup>3</sup>, depth in table used for cosmic dose calculation. Dose rate calculations made using equations from Prescott and Hutton (1994) with an assumed 10% error.

<sup>b</sup> A 3±3 wt % H<sub>2</sub>O was used to represent moisture content during burial.

<sup>c</sup> Chemistry values from Harvey (2009). As in this study, split samples were sent to ALS Chemex in Elko, NV for ICP-MS analysis.

was calculated from 0.1 – 0.14 s of stimulation and the background signal was calculated from 0.7-0.9 seconds of stimulation.

#### *2.3.6.1 Preheat-Plateau Thermal-Transfer (PP-TT) Test*

Thermal transfer can cause unstable electrons to move to shallow electron traps and result in age overestimations in young samples. As samples from KCW were expected to be under 5ka years old, a preheat-plateau and thermal-transfer (PP-TT) test was given to samples USU-1026 and USU-1101 to determine the appropriate preheat temperature to use during analysis to remove unstable electrons from the shallow traps in quartz (e.g. Murray and Wintle, 2003) and reduce thermal transfer effects (e.g. Rhodes, 2000; Li and Li, 2006). Steps for this test closely followed those identified in Li and Li (2006). Initially, five small-aliquots (1-mm diameter) from samples USU-1026 and USU-1101, assumed to be representative of sediments in the study area, were subject two optical bleaching exposures at room temperature using 90% blue-green LED power (470 nm, 36 mW/cm<sup>2</sup>) for 40s to remove natural signals. Each exposure was followed by a 1000-s pause at room temperature to allow thermally transferred charges to thoroughly decay (Li and Li, 2006). After bleaching, the luminescence signal in both samples were assumed to have been fully reset ( $De = 0$  Gy) and the  $De$  was measured using the SAR protocol (160°C cut heat) following exposure to increasing preheat temperatures (20°C increments) from 180°C to 280°C for 10 seconds each. Optical measurements of small aliquots were then made at 125°C for 40 s at 90% LED power.

Based on results from the PP-TT test (Fig. 2.7a), measurements made at 240°C and below yielded the expected near-zero  $De$  measurements. However, the  $De$  values for both samples rose significantly after the preheat temperature exceeded 240°C, indicating a thermal-transfer affected measurement. Recycling ratios from repeated doses do not indicate a trend with increasing preheat temperatures and fall within error of one another (Fig. 2.7a). Accordingly, a preheat temperature of 220°C was selected for all KCW samples based on these PP-TT tests.

### 2.3.6.2 *Overdispersion Test*

To test for inherent overdispersion values of the  $D_e$  in KCW sediments not related to partial bleaching, an overdispersion test was conducted on two samples whose sediments were originally sourced from upstream (e.g. dominated by very pale brown, fine- to medium grained, frosted quartz sand) or local (e.g. dominated by red, silty-clay to very-fine grained sand) deposits. Subsamples from USU-1101 and USU-1103, both collected from site KCW-H (Fig. 2.4), were placed on four single-grain aliquots each and bleached in direct sunlight for 2 hours during early afternoon (e.g. 12-2 p.m.) to completely zero the luminescence signal. Aliquots were then given a known dose of 14Gy and analyzed using the SG SAR sequence with a 220°C preheat and 160°C cut-heat. One aliquot from sample USU-1103 was lost prior to being dosed. These analyses were conducted to see if there are differences in the inherent overdispersion of sediment sourced from upstream and local sediments. It is possible that the red-coloring of local sediments would increase grain opacity thereby limiting solar resetting and increasing inherent overdispersion.

Results from the overdispersion test indicate that the upstream sediment (USU-1101) had an inherent overdispersion of  $19 \pm 4.8\%$  while the local sediment (USU-1103) had an inherent overdispersion of  $17 \pm 4\%$  (Fig. 2.7b). The resulting ratios of given to recovered doses were 1.01 for USU-1101 and 0.98 for USU-1103 (Fig. 2.7b). Original assumptions were that the red-coloring of the local sediments would have affected their bleaching characteristics. However, this does not appear to be the case. These overdispersion values were used to assess best-case intrinsic overdispersion values for KCW sediments used for MAM calculations (see below).

### 2.3.6.3 *Equivalent Dose and Age Calculation*

Equivalent dose values were calculated from  $D_e$  distributions using the CAM, 3-parameter MAM (MAM-3), or 4-parameter MAM (MAM-4) of Galbraith et al. (1999) (Table 2.5). At least 75 accepted grains are preferred for CAM or MAM-4 calculation, but SG

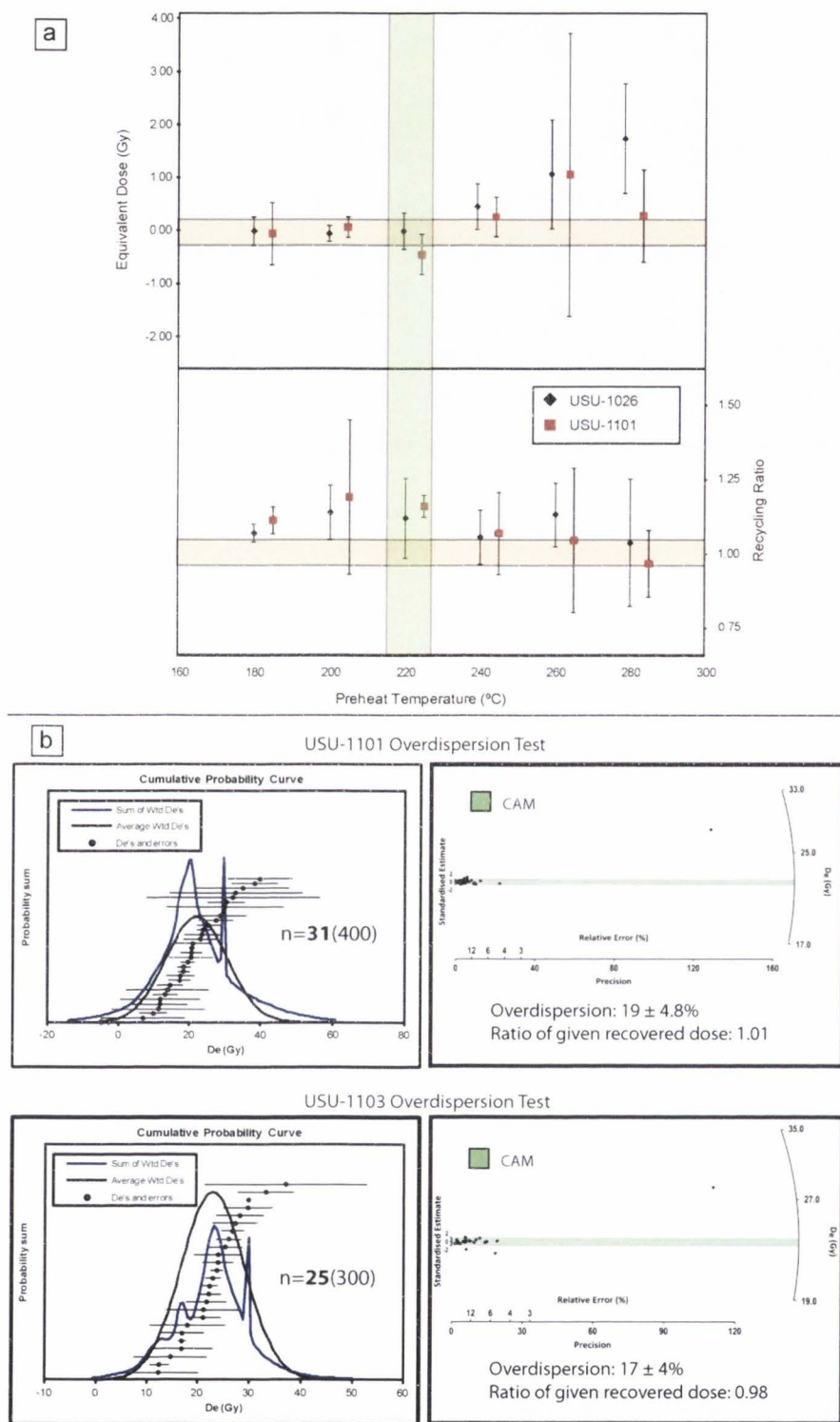


Fig. 2.7. (a) Results from a preheat-plateau thermal-transfer (PP-TT) test on samples USU-1026 and USU-1101: Equivalent dose values increase significantly when preheat temperatures surpass 240°C. Recycling ratios for measurements are also shown. A preheat temperature of 220°C (outlined in green) was used for all SG measurements in this study. (b) Inherent overdispersion SG test results for naturally bleached and beta-dosed USU-1101 and USU-1103

analyses are currently preliminary and more accepted grains will come from future analyses. Rejection criteria for single-grain data were similar to those described in Summa-Nelson and Rittenour (2012). First, quartz sand grains were rejected if they showed evidence of feldspar contamination, as indicated by an IR depletion ratio of  $>1.6$ , when OSL results with and without IR stimulation are compared (modified from Duller et al., 2003). Additionally, single-grain discs were exposed to IR diode stimulation prior to every OSL measurement. Grains were then rejected if they gave a low signal response (initial signal was less than 3 times the background) of all regenerative doses excluding the zero dose. If grains were sufficiently bright, they were rejected due to poor recycling ratios ( $<0.5$  or  $>1.5$ ) of repeated doses, equivalent doses greater than the highest regenerative dose, negative  $D_e$  values and a poor dose-response growth curve fit. Due to the young nature of these samples from KCW, the typical 30% cut-off for recuperation used by Summa-Nelson and Rittenour (2012) was not followed (similar to Feathers et al., 2006). Prior to age model application and age analysis, a 7% error was uniformly added to all single-grain  $D_e$  errors in order to account for uncertainties unrelated to luminescence intensities as described in Thomsen et al. (2005), which include differences in beta source activity, illumination variability from individual measurements, and general problems with instrument reproducibility.

The choice of statistical models used to calculate  $D_e$  for age calculation was dependent on a combination of partially bleached grains and the number of single-grain  $D_e$  values available for analysis. For this study, partial bleaching was indicated by high overdispersion values ( $>30\%$ ) or significant positive skew in  $D_e$  distribution. In these cases, a MAM was used because it statistically selects the lowest  $D_e$  values in a sample that were most likely to have been zeroed prior to deposition (Galbraith et al., 1999). In contrast, the CAM was used on samples whose  $D_e$  values did not show significant overdispersion or skewness. Additionally, the usage of MAM-3 and MAM-4 statistical models in this study was generally based on criteria set forth in a study by Arnold et al. (2007). However, the MAM-4 was most commonly used for single-grain  $D_e$  values (Table 2.5).

Table 2.5  
Preliminary single-grain OSL ages and partial bleaching statistics

USU Lab ID	Study Site	# Grains Accepted (Analyzed)	Facies <sup>a</sup>	Primary Sediment Source <sup>b</sup>	Approximate Bed Thickness (cm)	Skew <sup>c</sup>	Kurtosis <sup>c</sup>	Overdispersion (%) <sup>c</sup>	Mean/median <sup>c</sup>	CAM/MAM <sup>c</sup>	OSL age (cal ka)	Age Model <sup>d</sup>
USU-1189	A	25 (700)	Sl	Mixed	40	0.95 ± 0.49	<b>-0.27 ± 0.98</b>	<b>54.6 ± 16.0</b>	<b>1.43</b>	<b>1.87</b>	<b>1.38 ± 0.64</b>	MAM-4
USU-1176	B	22 (600)	Sh	Local	55	<b>2.67 ± 0.52</b>	<b>6.30 ± 1.04</b>	<b>87.6 ± 20.2</b>	<b>2.15</b>	<b>1.50</b>	<b>0.74 ± 0.19</b>	MAM-4
USU-1177 <sup>f</sup>	B	16(500)	Sh	Local	20	<b>1.83 ± 0.61</b>	<b>3.14 ± 1.22</b>	<b>50.1 ± 25.6</b>	<b>1.25</b>	<b>1.54</b>	<b>2.02 ± 1.09</b>	MAM-4
USU-1187	C	25(700)	St	Mixed	40	<b>2.11 ± 0.49</b>	<b>3.78 ± 0.98</b>	<b>63.1 ± 20.5</b>	<b>1.41</b>	<b>1.88</b>	<b>1.14 ± 0.36</b>	MAM-3
USU-1178	D	26 (700)	Sr	Upstream	50	<b>3.33 ± 0.48</b>	<b>13.07 ± 0.96</b>	<b>59.5 ± 14.3</b>	<b>1.4</b>	<b>1.25</b>	<b>1.77 ± 0.31</b>	MAM-4
USU-1192	E	29 (800)	St	Local	45	<b>1.76 ± 0.45</b>	1.75 ± 0.91	<b>75.2 ± 17.8</b>	<b>1.93</b>	<b>2.59</b>	<b>0.92 ± 0.20</b>	MAM-4
USU-1194	F	28 (700)	St	Upstream	55	0.86 ± 0.46	0.35 ± 0.93	26.4 ± 11.6	1.15	<b>1.36</b>	<b>2.97 ± 0.70</b>	CAM
USU-1181	G	36 (1300)	Sl	Mixed	45	<b>1.54 ± 0.41</b>	<b>2.42 ± 0.82</b>	<b>58.8 ± 13.8</b>	<b>1.38</b>	<b>2.14</b>	<b>1.47 ± 1.08</b>	MAM-4
USU-1101	H	41 (1300)	Sl	Upstream	50	<b>0.82 ± 0.38</b>	<b>1.48 ± 0.77</b>	<b>36.4 ± 8.4</b>	<b>1.1</b>	<b>1.34</b>	<b>4.21 ± 1.46</b>	MAM-4
USU-1103	H	38 (1000)	Sh	Local	40	<b>2.19 ± 0.40</b>	<b>5.24 ± 0.79</b>	<b>42.3 ± 9.3</b>	<b>1.31</b>	<b>1.32</b>	<b>1.56 ± 0.37</b>	MAM-4
USU-530 <sup>e</sup>	I	29 (45)	Sl	Upstream	25	<b>0.98 ± 0.45</b>	<b>0.41 ± 0.91</b>	<b>36.7 ± 7.4</b>	<b>1.14</b>	<b>1.66</b>	<b>2.25 ± 0.85</b>	CAM
USU-531 <sup>e</sup>	I	33 (41)	St	Upstream	45	<b>1.93 ± 0.43</b>	<b>3.31 ± 0.85</b>	<b>48.9 ± 7.2</b>	<b>1.42</b>	<b>1.48</b>	<b>2.82 ± 0.32</b>	CAM
USU-1026	J	45 (1500)	Sl	Mixed	40	<b>1.27 ± 0.37</b>	<b>0.82 ± 0.73</b>	<b>62.4 ± 10.3</b>	<b>1.55</b>	<b>2.02</b>	<b>1.29 ± 0.37</b>	MAM-4
USU-1027	J	52 (1300)	Sl	Mixed	35	<b>1.17 ± 0.34</b>	<b>0.74 ± 0.64</b>	<b>50.7 ± 9.3</b>	<b>1.29</b>	<b>1.86</b>	<b>1.58 ± 0.30</b>	MAM-4
USU-1028	J	25 (600)	Sl	Upstream	40	<b>2.92 ± 0.49</b>	<b>10.66 ± 0.98</b>	<b>48.5 ± 12.5</b>	<b>1.37</b>	<b>1.76</b>	<b>1.52 ± 0.74</b>	MAM-4
USU-1029 <sup>f</sup>	J	25 (600)	Sm	Local	60	<b>2.59 ± 0.49</b>	<b>8.20 ± 0.98</b>	<b>70.4 ± 14.7</b>	<b>1.79</b>	<b>1.68</b>	<b>1.67 ± 0.35</b>	MAM-4

<sup>a</sup> Facies used for OSL sample collection. See Table 2.1 for descriptions.

<sup>b</sup> Primary sediment source based on sedimentologic characteristics of each sample deposit. See text for details.

<sup>c</sup> Statistics (e.g. Skew, Kurtosis, Overdispersion, Mean/Median, and CAM/MAM) used to identify partially bleached samples and used to suggest appropriate age model for De calculation.

Bold text indicates significant partial bleaching characteristics based on statistics and suggestions from Arnold et al. (2007). Highlighted samples (USU-1177 and USU-1029)

indicate age overestimations based on preliminary results. In this study, overdispersion was primarily used as an indicator of partial bleaching and was compared to results from Summa-Nelson and Rittenour (2012).

<sup>d</sup> De calculated using the central-age model (CAM) or minimum-age model (MAM) of Galbraith et al. (1999).

<sup>e</sup> OSL samples originally analyzed in Harvey (2009). Samples were re-analyzed in this study using the small-aliquot SAR sequence of Murray and Wintle (2000).

<sup>f</sup> Preliminary results suggest age overestimations based on stratigraphic position and related to other age control. All results may change with further analyses.

## 2.4 Results

The objective of this study was to test the applicability of AMS radiocarbon and OSL dating to semiarid fluvial deposits to discuss the best practices for developing an alluvial chronology. In total, 35 of the 39 radiocarbon samples and 17 of the 29 OSL samples collected were analyzed using AMS and single-grain dating techniques respectively (Tables 2.2 and 2.5). One unanalyzed sample (14C-23) did not survive the chemistry pretreatment and three additional radiocarbon samples were deemed unnecessary for analysis because of their stratigraphic location (Table 2.2). During a subsequent trip to the study area, the approximate location in which the sample lost during pretreatment was re-sampled and analyzed. Nearly all of the radiocarbon samples analyzed returned stratigraphically consistent ages. However, five samples returned ages that were significantly older than expected ( $>42$  ka) and are suspected to be Cretaceous coal. Additionally, four other sample ages were determined to be out of stratigraphic context and are considered to have been redeposited older charcoal (Table 2.3). Results for radiocarbon samples, calibrated to BP<sub>2010</sub>, are shown in Tables 2.2 and 2.3, and displayed on arroyo-wall stratigraphic panels where sampled.

As expected, nearly every OSL sample was partially bleached, requiring the use of single-grain dating. Partial bleaching is evident based on the equivalent doses for each sample plotted as a probability density function (i.e. the cumulative frequency plot of De distribution) and radial plots (see Appendix A for all KCW De distributions). Table 2.5 contains results from 16 OSL samples that underwent single-grain dating analyses and displays OSL ages as calendar years ka with 2-sigma error. The total number of grains used for SG analysis and the number of accepted grains used in age calculation (~50-100 grains preferred) are indicated in Table 2.5 along with the chosen age models (e.g. MAM-3 or MAM-4) for De calculation. In general, the level of De rejection was relatively high, largely due to non-luminescent grains.

The four study sites containing the most temporally constrained alluvial fills from AMS radiocarbon and OSL dating are presented to help evaluate the utility of the sample collection and

analysis techniques employed for both geochronometers (Fig. 2.4). In general, results indicate that the sampling techniques and dating analyses resolved many of the conventional problems and limitations, effectively generating stratigraphically consistent ages. However, three of the four study sites (KCW-B, KCW-H, and KCW-J) show that erroneous ages or age inversions were still encountered. These sites are discussed here.

#### 2.4.1 *KCW-B*

KCW-B is a 9 m tall, west-facing arroyo cut-fill exposure located in the Park Wash (PW) reach of the KCW study area approximately 16km upstream of Kaibab Gulch (Figs. 2.4 and 2.13). Cut-fill stratigraphic evidence and age results helped identify two distinct alluvial fill packages that are mostly composed of 20-50cm thick, tabular beds of very fine- to medium-grained sand. The older alluvial fill is dominantly characterized by the presence of low-angle (SI) and trough (St) crossbedded sands that are separated or capped by massive (Sm) or variegated clay, silt, and very-fine sand (Fsmv) deposits that show evidence of incipient soil formation (Fig. 2.8). A radiocarbon sample (14C-4) that yields an age of  $1.24^{+0.08}_{-0.13}$  cal ka BP<sub>2010</sub> (Table 2.5) was collected from a charcoal rich lens in a basal St sand bed ~2m from the channel bottom and ~1 m upstream of the incision unconformity. An OSL sample (USU-1175) was collected ~1 m above this radiocarbon sample in a SI bed but was not analyzed. A stratigraphically higher OSL sample (USU-1176) collected from a 50cm thick, very pale brown, fine- to medium-grained, horizontally bedded (Sh) sand deposit nearly 6.5m above 14C-4. Using the MAM-4 statistical analysis, this sample yielded a preliminary age of  $0.74 \pm 0.19$  ka (Table 2.5).

Similar to the older fill, the younger fill is typified by the presence of SI and St sand beds, but also contains significant number of ripple crossbeds (Sr) and thinly laminated or desiccated silty-clay sand beds (FI). To constrain the age of this deposit, one OSL sample was collected near the base of the deposit and a radiocarbon sample was collected ~3 m higher. The OSL sample (USU-1177) was extracted from a 20cm thick, very pale brown, fine- to medium-grained Sh

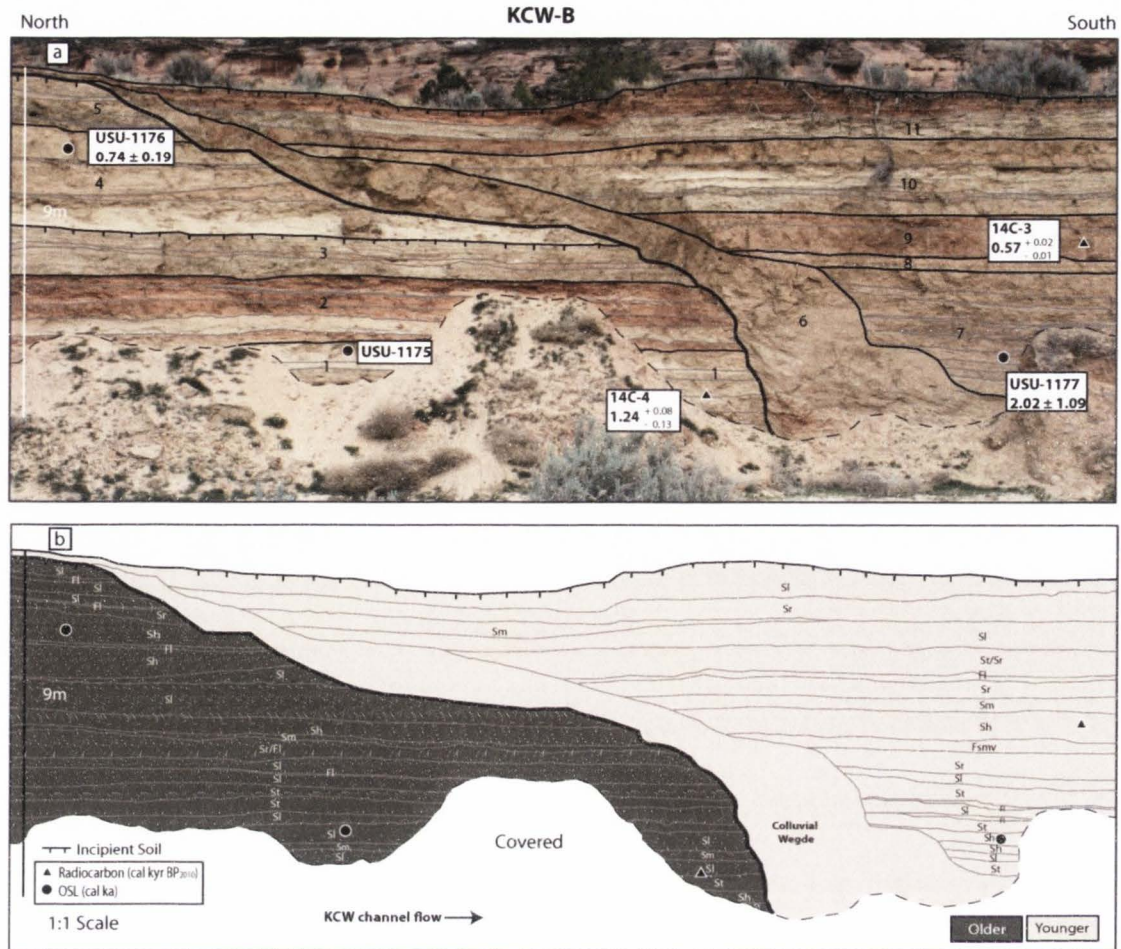


Fig. 2.8. Fluvial architecture and geochronology of KCW-B. (a) Bold lines represent unconformable boundaries and thin lines represent fluvial sequences. OSL (circles) and  $^{14}\text{C}$  (triangles) samples are indicated within alluvial beds and have been used to constrain the timing of arroyo-cut-fill cycles. (b) Facies textures identified and used to help select  $^{14}\text{C}$  and OSL samples, and older and younger alluvial fill packages identified using detailed stratigraphic mapping and ages from both geochronometers.

deposit located ~1.5 m downstream from the toe of a colluvial wedge (Fig. 2.8). This sample yields a preliminary OSL age of  $2.02 \pm 1.09$  ka using MAM-4 statistical analyses (Table 2.5). The stratigraphically higher radiocarbon sample (14C-3) was collected from a light red, SI sand deposit and has a calibrated age of  $0.57^{+0.02}_{-0.01}$  cal kyr BP<sub>2010</sub> (Fig. 2.8; Table 2.2).

#### 2.4.2 KCW-E

KCW-E is a 6.9 m tall, north-facing arroyo cut-fill exposure located in the Deer Springs Wash (DSW) tributary of the main KCW trunk stream approximately 12 km upstream from Kaibab Gulch (Figs. 2.4 and 2.14). A buttress unconformity truncating alluvial beds and evidence of a long-lived stable surface with significant bioturbation and incipient soil formation were used to help identify two distinct alluvial fill packages. The oldest alluvial fill is ~4m thick and mainly consists of St, Sh, and Sr beds that are commonly interbedded with thinly laminated silty sand beds (Fl). This fill is capped by a massive sand (Sm) showing evidence of soil formation. A radiocarbon sample (14C-11) was collected from a concentrated lens of charcoal within a 10 cm thick St bed and yields an age of  $1.38 \pm 0.02$  cal kyr BP<sub>2010</sub> (Table 2.2). An OSL sample (USU-1192) was collected ~2.5 m above 14C-11 in the lower half of a 40 cm thick, very pale brown, fine- to coarse-grained St bed that showed very faint evidence of incipient soil formation in the upper 10 cm of the deposit (Fig. 2.9). USU-1192 returned a preliminary single-grain OSL age of  $0.92 \pm 0.20$  ka using the MAM-4 statistical analysis (Table 2.5).

The youngest alluvial fill is at least 5 m thick and is also dominated by St, SI, and Sr beds that contain several interbeds of thinly laminated or desiccated clays and silty-sands (Fl). A radiocarbon sample (14C-12) was collected from a charcoal rich lens in a trough crossbedded deposit approximately 1.75 m upstream of a thick colluvial wedge (Fig. 2.9). This sample has a calibrated age of  $0.87^{+0.10}_{-0.11}$  cal kyr BP<sub>2010</sub> (Table 2.2). In a very pale brown, fine- to medium-grained SI sand bed nearly 2.3 m above 14C-12, OSL sample USU-1191 was extracted but was not age-measured. A younger deposit caps both alluvial fills as indicated by a radiocarbon

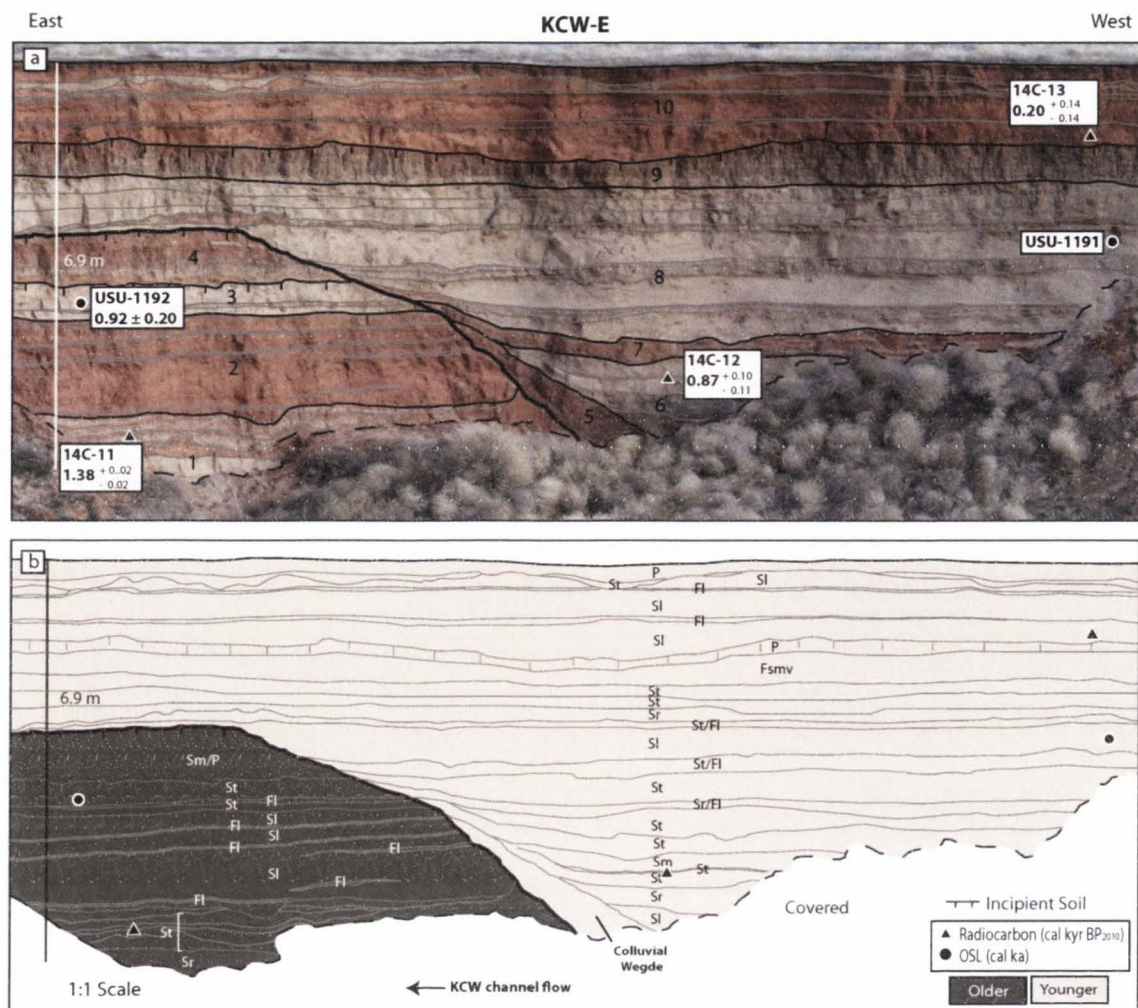


Fig. 2.9. Fluvial architecture and geochronology of KCW-E. (a) Bold lines represent unconformable boundaries and thin lines represent fluvial sequences. OSL (circles) and  $^{14}\text{C}$  (triangles) samples are indicated within alluvial beds and have been used to constrain the timing of arroyo-cut-fill cycles. (b) Facies textures identified and used to help select  $^{14}\text{C}$  and OSL samples, and older and younger alluvial fill packages identified using detailed stratigraphic mapping and ages from both geochronometers.

sample (14C-13) that was extracted from a charcoal rich lens in a light red SI deposited that has an age of  $0.2 \pm 0.14$  cal kyr BP<sub>2010</sub> (Table 2.2).

#### 2.4.3 *KCW-H*

KCW-H is 10.7 m tall cut-fill exposure with sediments underlying the axial terrace at a meander bend in the main trunk stream of KCW. This study site is located approximately 7.5 km upstream of Kaibab Gulch (Fig. 2.4). At least three alluvial fill packages are separated by unconformably bounding surfaces (Fig. 2.10). The oldest fill, is at least 9 m thick and primarily contains a mixture of SI, St, Sr, Sh, and Sm facies sourced from both upstream and local sources. The stratigraphically lowest radiocarbon sample (14C-26) was collected ~1 m above the modern channel bottom from a charcoal rich lens in an Sr bed and yields an age of  $4.14^{+0.07}_{-0.09}$  cal kyr BP<sub>2010</sub> (Table 2.2). Less than a meter above 14C-26, an OSL sample (USU-1101) was collected from an 80 cm thick, very pale brown, fine- to medium-grained SI bed. Using the MAM-4 statistical model, USU-1101 gives a preliminary age of  $4.21 \pm 1.46$  ka (Table 2.5). The stratigraphically highest radiocarbon sample (14C-22) collected and analyzed from the oldest alluvial fill yields an age of  $3.82^{+0.07}_{-0.06}$  cal kyr BP<sub>2010</sub> (Table 2.2). This sample was collected 4.5 m above the channel floor in a charcoal rich SI deposit. A piece of isolated, angular charcoal was collected 7.5 m above the channel floor in a massive, very fine- to fine-grained sand deposit but was not measured.

Buttressed against the oldest fill, an intermediate aged alluvial fill is dominantly composed of basal gravels (Gh) and overlying sandy, lenticular beds of SI, Sm, and St (Fig. 2.10). Within a younger channel migration deposit of this fill, an OSL sample (USU-1102) was collected from a 40 cm thick, light red, very fine- to fine-grained sand SI bed, but was not analyzed. At 4.5 m above the channel floor, a stratigraphically higher charcoal sample (14C-24) was collected from a charcoal rich lens in a massive sand (Sm) deposit and returned an age of  $1.08^{+0.04}_{-0.05}$  cal kyr BP<sub>2010</sub> (Fig. 2.10; Table 2.2). In a thicker (~8 m) and apparently younger fill ,

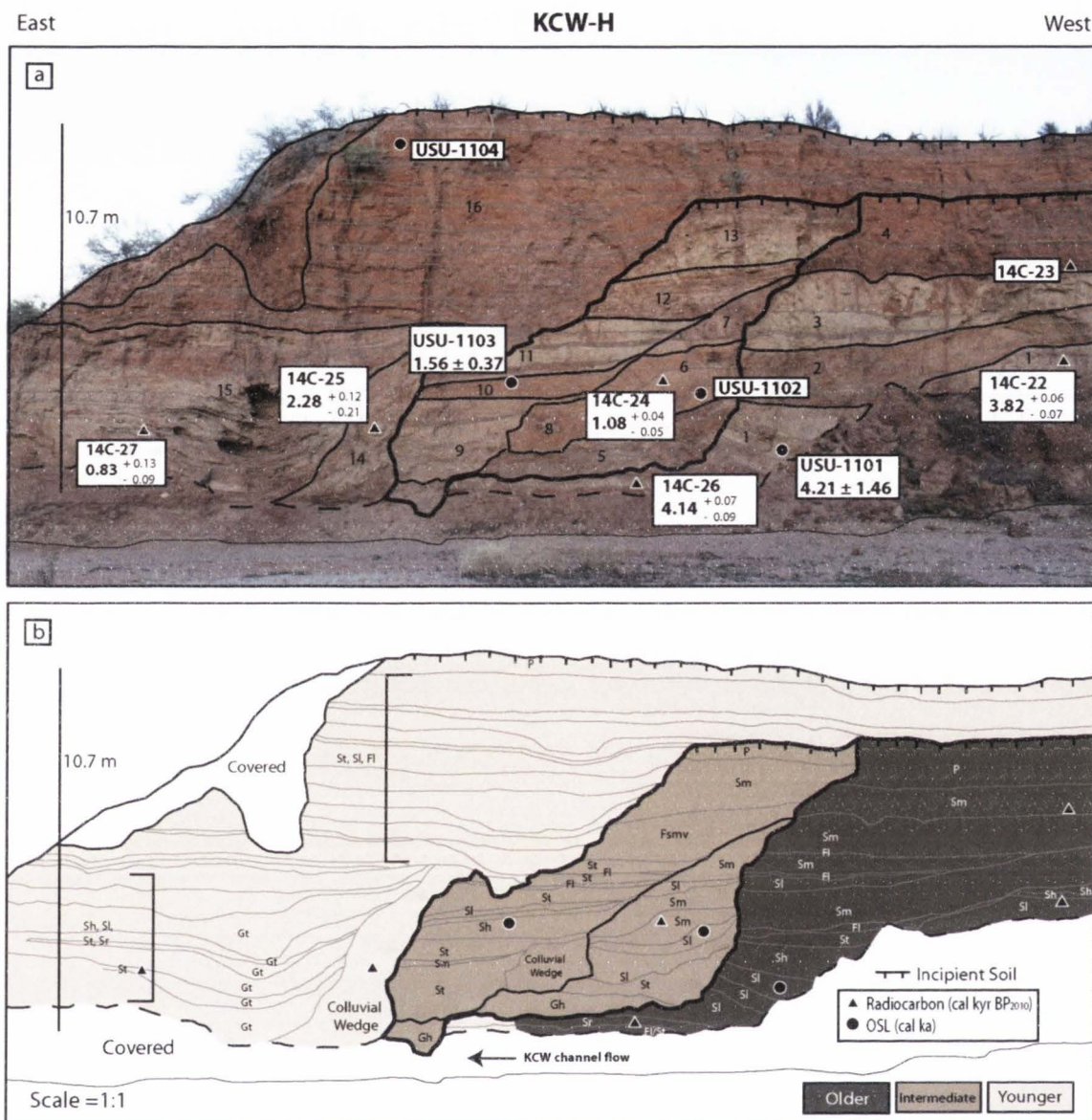


Fig. 2.10. Fluvial architecture and geochronology of KCW-H. (a) Bold lines represent unconformable boundaries and thin lines represent fluvial sequences. OSL (circles) and  $^{14}\text{C}$  (triangles) samples are indicated within alluvial beds and have been used to constrain the timing of arroyo-cut-fill cycles. (b) Facies textures identified and used to help select  $^{14}\text{C}$  and OSL samples, and older, intermediate, and younger alluvial fill packages identified using detailed stratigraphic mapping and ages from both geochronometers.

an OSL sample (USU-1103) was collected from a 45cm thick, light red, very fine- to medium-grained, horizontally bedded (Sh) sand deposit. Single-grain analyses and use of the MAM-4 model gives this sample a preliminary age of  $1.56 \pm 0.37$  ka (Table 2.5). Within the youngest alluvial fill, two radiocarbon samples were analyzed. One isolated, sub-rounded charcoal sample (14C-25) was collected from a deposit identified as a colluvial wedge. This sample yielded an age of  $2.28^{+0.12}_{-0.12}$  cal kyr BP<sub>2010</sub> (Table 2.2) and produces an apparent age inversion when compared with results of the intermediate fill (Fig. 2.10). Additionally, 14C-25 shows an inverted age when compared to a radiocarbon sample (14C-27) from a charcoal-rich, stratigraphically lower S1 sand bed in the youngest fill and yields a radiocarbon age of 14C-27 is  $0.83^{+0.13}_{-0.09}$  cal kyr BP<sub>2010</sub> (Table 2.2). An OSL sample (USU-1104) was also collected near the top of the youngest alluvial fill but was not analyzed (Fig. 2.10).

#### 2.4.4 KCW-J

KCW-J ranges from 5 to 6.6 m in height above the modern channel bottom, is west-facing, and is located ~4.5 km upstream from Kaibab Gulch (Fig s. 2.4 and 2.16). This exposure contains three alluvial fill packages that were originally identified based on unconformable buttresses and bounding surfaces. The oldest alluvial package is dominantly characterized by the presence of 30 cm to 1 m thick, lenticular or broadly tabular, low angle crossbeds of sand. An OSL sample (USU-1028) was collected from a 40cm thick, very pale brown, fine- to medium-grained S1 bed (Fig. 2.11). Using the MAM-4 statistical model, this OSL sample gives a preliminary age of  $1.52 \pm 0.74$  ka (Table 2.5). This fill appears to contain a younger scour-fill deposit primarily composed of St and S1 beds that is capped by a ~1.5 m thick, broadly tabular interbeds of variegated clay and silty-sands (Fsmv). An OSL (USU-1027) and radiocarbon (14C-31) sample were collected from the same 40 cm thick, very pale brown, sandy S1 bed approximately 1.25 m above the modern channel floor. The stratigraphically lower 14C-31 was collected from a charcoal rich lens and yields an age of  $1.70^{+0.06}_{-0.07}$  cal kyr BP<sub>2010</sub> (Table 2.2)

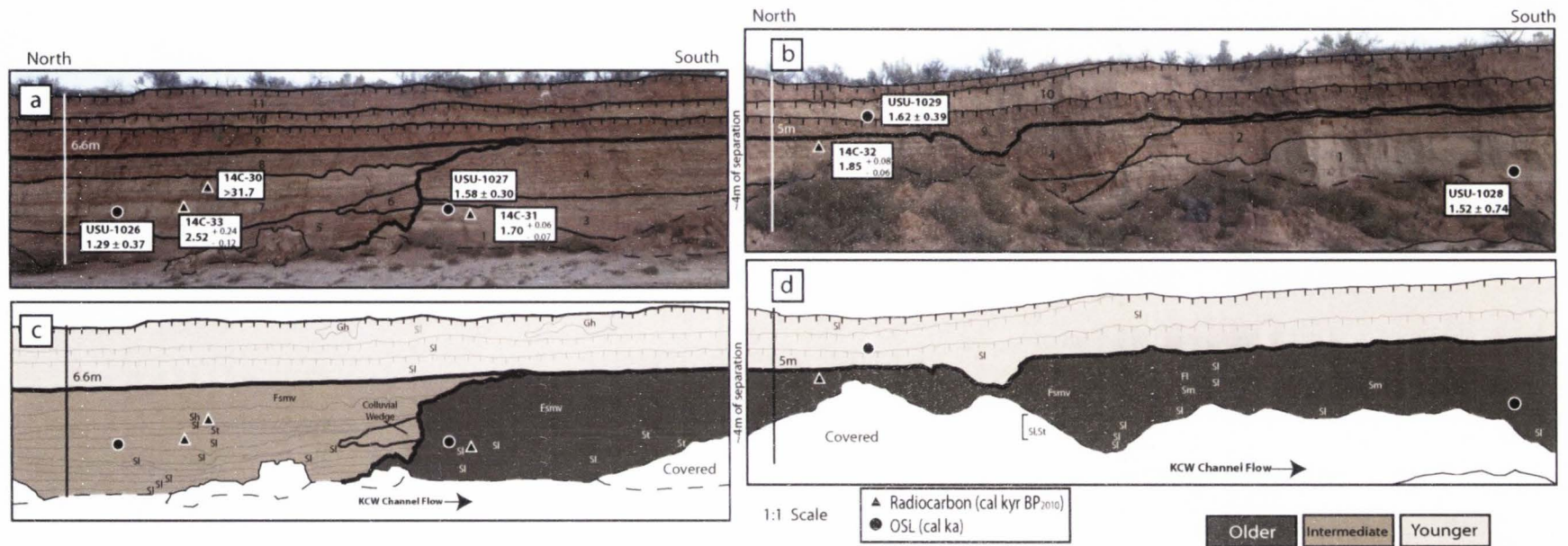


Fig. 2.11. Fluvial architecture and geochronology of KCW-J. (a,b) Bold lines represent unconformable boundaries and thin lines represent fluvial sequences. OSL (circles) and  $^{14}\text{C}$  (triangles) samples are indicated within alluvial beds and have been used to constrain the timing of arroyo-cut-fill cycles. (c,d) Facies textures identified and used to help select  $^{14}\text{C}$  and OSL samples, and older, intermediate, and younger alluvial fill packages identified using detailed stratigraphic mapping and ages from both geochronometers.

while USU-1027 (20 cm higher) produces a preliminary age of  $1.58 \pm 0.30$  ka (Table 2.5). In the capping Fsmv deposit, an additional angular charcoal sample (14C-32) collected from a charcoal rich lens ~2 m above 14C-31 yield a slightly inverted age of  $1.85^{+0.08}_{-0.06}$  cal kyr BP<sub>2010</sub> (Table 2.2).

Inset into the oldest fill, the strata of the intermediate fill are also primarily composed of low-angle crossbedded sand (SI) deposits that are capped by a ~1 m thick Fsmv bed (Fig. 2.11). All geochronologic samples from this fill were collected from two lenticular beds in a ~15 m wide channel swale. An OSL sample (USU-1026) was collected in the stratigraphically lower, very pale brown, fine- to medium-grained SI sand bed and an isolated, angular piece of charcoal was collected from a stratigraphically higher (~1m) Sh deposit. Using the MAM-4 model, USU-1026 yields a preliminary age of  $1.29 \pm 0.37$  ka (Table 2.5). However, sample 14C-30 was contaminated by coal. On a subsequent trip to KCW-J, an additional charcoal sample (14C-33) was collected from a charcoal rich lens within the same bed as USU-1026. However, it produced an inverted age of  $2.52^{+0.24}_{-0.12}$  cal kyr BP<sub>2010</sub> (Table 2.2) when compared to USU-1026 and samples from stratigraphically older deposits in the same outcrop (Fig. 2.11). A final OSL sample (USU-1029) was collected from a 60 cm thick, very pale brown SI bed within the youngest and uppermost alluvial fill. Using the MAM-3 statistical, USU-1029 yields a preliminary age estimate of  $1.62 \pm 0.39$  ka (Fig 2.16; Table 2.5).

## 2.5 Discussion

### 2.5.1 Comparison of Radiocarbon and OSL Ages

Chronostratigraphies from dynamic arroyo systems in the semiarid southwestern United States can be used to infer landscape response to climate change or other hydrologic and geomorphic conditions. In KCW, the unique cut-fill stratigraphy and sedimentary facies preserved in the mostly fine-grained sand exposures allowed previous studies to identify 3 to 4 incision and aggradation events (e.g. Hereford, 2002; Harvey, 2009; Harvey et al., 2011). However, temporally constraining the timing of each cut-fill event has been problematic due to

the lack of age control. Hence, this study used a combination of radiocarbon and OSL dating techniques in order to expand the existing chronology at KCW. The use of OSL dating alongside radiocarbon dating not only allowed for expanded sampling opportunities, as previously mentioned, but has also provided the opportunity to directly compare ages and evaluate the effectiveness of both geochronometers on dating arroyo sediments. Radiocarbon and OSL ages of alluvial deposits from twelve study sites throughout KCW suggest that both dating methods generally work well. Along with stratigraphic descriptions, ages from these techniques provide evidence for six episodes of alluviation and incision in KCW throughout the late Holocene.

#### *2.5.2 Evaluation of Radiocarbon Dating*

Results from this study indicate that 26 of the 37 AMS radiocarbon ages were in stratigraphic agreement when compared to one another and to OSL ages from similarly aged deposits. As expected, the least problematic radiocarbon ages came from charcoal that was sampled from charcoal rich lenses or annual plant litter (Table 2.3). In general, isolated charcoal pieces, though rarely sampled or analyzed, were only problematic if they were noticeably rounded (e.g. 14C-25). Although an age bias could not be discerned between radiocarbon sampling sediment derived from upstream or local sediment sources, samples extracted from trough crossbedded (St), ripple crossbedded (Sr), low-angle crossbedded (Sl) sand and variegated clay and silt interbeds (Fsmv) generally returned stratigraphically consistent ages (Table 2.3). It is possible that the mostly low flow regimes from each associated facies allowed charcoal to undergo relatively minimal transport and rapid deposition. For example, samples 14C-11, -12, and -13 from study site KCW-E were collected from charcoal rich lenses in low flow regime facies and yielded stratigraphically consistent calibrated radiocarbon ages.

While most radiocarbon samples show stratigraphic agreement, three inherit problems of radiocarbon dating in southwestern dryland systems are the most likely cause of age disagreement: (1) collection of coal (2) redeposited charcoal and (3) sample size. The majority

(5) of the stratigraphically inconsistent radiocarbon ages produced age results consistent with analyses of coal (Table 2.3). Study site KCW-F is a good example of the age-overestimation problems that can be encountered if Cretaceous coal is analyzed despite strategic sampling (see Table 2.3). Samples 14C-14 and 14C-16 were both collected from ideal facies (St) and while 14C-16 was isolated, it was suitable for sampling because of its location and angularity. Even though both samples were carefully examined under 40x magnification prior to analysis, it appears that fragments of Cretaceous coal were still analyzed. Accordingly, while microscopic examination of samples may be somewhat beneficial when trying to separate charcoal from coal, it may be necessary to set forth other sampling strategies to avoid these types of erroneous ages.

Comparison of stratigraphically consistent radiocarbon ages with field and photo evidence of charcoal-rich sand deposits in KCW reveal that a number of the least problematic radiocarbon samples were collected near the top of a deposit most likely because the low density of charcoal causes it to float (Fig. 2.2). Moreover, when 17 of the samples were pretreated at the University of Arizona AMS facility, it was noted that samples where radiocarbon material either stayed suspended or floated to the top of a test tube returned stratigraphically agreeable ages (Fig. 2.12). By comparison, nearly every sample which some or all of the radiocarbon material sunk returned severe age overestimations (e.g. >42ka). Moreover, when Cretaceous coal ages were compared to the weight of samples submitted, following AMS measurements, it was found that weight-to-size ratio of the coal-bearing radiocarbon material was significantly higher. Accordingly, sinking and relative weight properties can be explained because of differences in specific gravity between charcoal (~0.4) and coal (~1.2). Hence, it is suggested here that considering the apparent specific gravity of coal and charcoal in the field or lab can be a useful preventative for sampling or analyzing Cretaceous: (a) strategically sampling charcoal lenses deposited near or at the top of a sand bed, (b) closely examining whether radiocarbon material sinks or floats during pretreatment protocols and (c) noting the relative size-to-weight ratio when weighing material for radiocarbon analysis.

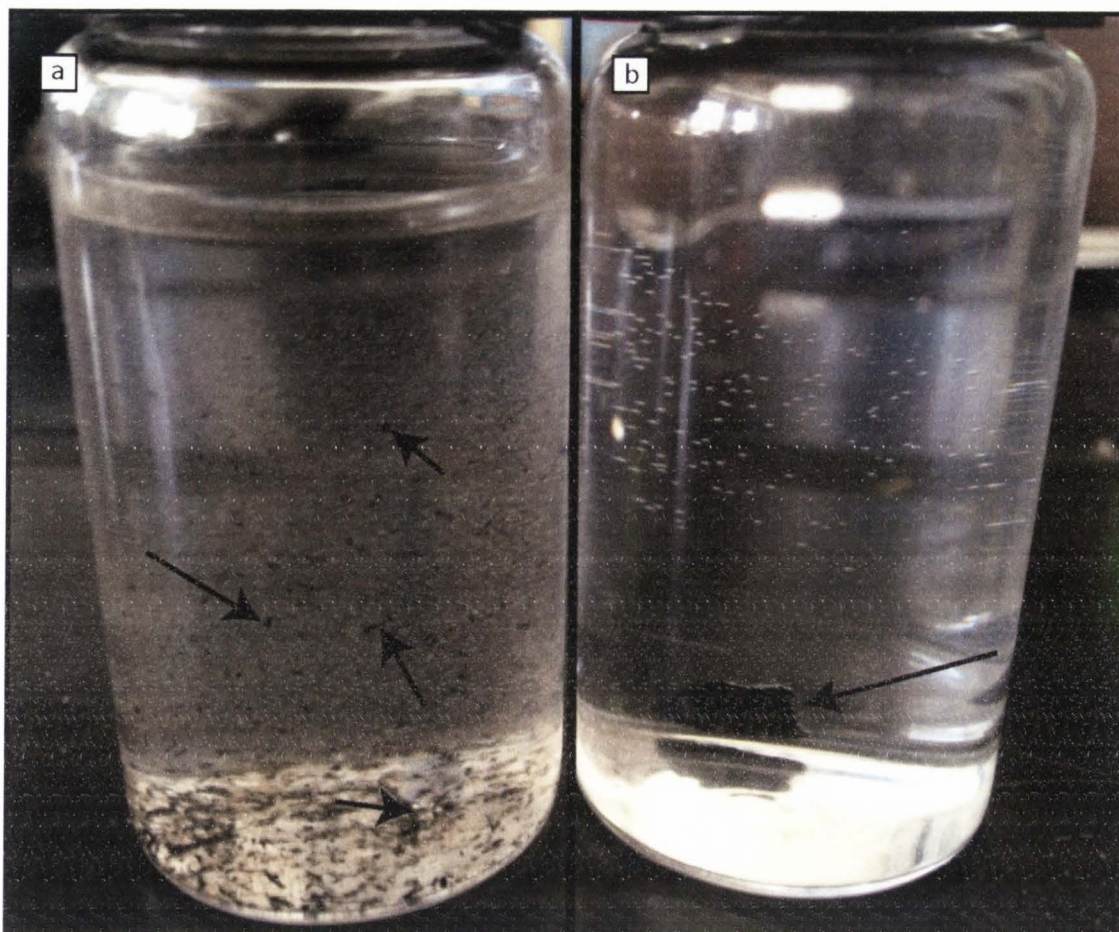


Fig 2.12. Apparent density difference between charcoal and coal: (a) charcoal fragments from radiocarbon sample 14C-26 remains suspended during AMS pretreatment and returned a stratigraphically agreeable age (b) coal fragment from radiocarbon sample 14C-14 immediately sunk during pretreatment and returned an age overestimation.

Compared to Cretaceous coal, redeposited charcoal also appears to have played a large role in the overall radiocarbon age discrepancies of this study, affecting four samples (Table 2.3). While sampling strategies applied to prevent collecting charcoal with a considerably longer residence times were generally effective, a few redeposited samples were still collected. As indicated from sample 14C-25 at KCW-H (Fig. 2.10; Table 2.3) and 14C-35 from KCW-K (see Ch. 3), sample collection at or near colluvial deposits were problematic. While sample 14C-25 was collected from a deposit that was later identified as a colluvial wedge (Fig. 2.10), sample 14C-35 was an angular piece of charcoal collected from a basal St sand bed to help constrain the age of an aggradation event. Nonetheless, the apparent age inversion of 14C-35 can be explained because of its proximity (~30cm) to a colluvial wedge and disconformable surface (see Fig. 3.16 in Ch. 3). Based on their age, other isolated angular pieces of charcoal collected away from these locations did not indicate redeposition (Table 2.3). However, because of the sample location, it is more likely that 14C-35 was derived from the exposed and unstable surface of a previously deposited fill. Hence, both samples provide support for why sample collection at or near a colluvial wedge deposit should be avoided, and indicates a strong likelihood that radiocarbon material will be sourced from older deposits and will be prone to overestimating the age of younger alluvium.

A final source of error in radiocarbon ages was the amount of sample collected for analysis. Although a primary advantage to using AMS radiocarbon dating is the ability to date relatively small samples, problems arose in this study because an inadequate sample volume was collected from a few study sites. In particular, radiocarbon material for sample 14C-30 was collected from a smaller lens of finely disseminated charcoal fragments in an Sh bed at study site KCW-J and returned an calibrated age of >31.7 kyr BP (Fig. 2.11). While this kind of overestimation is similar to that seen from Cretaceous coal, the error involved in this sample was partly due to the large age uncertainty caused by the dearth of charcoal material analyzed (0.056 mg) following pretreatment of ~4 mg of material. Alternatively, this age overestimation might be

due to sample mixing prior to analysis. As individual fragments of radiocarbon material collected from the charcoal rich lens weighed less than ~2 mg, several pieces of charcoal from 14C-30 were needed to closely meet the minimum weight criteria (5 mg) for pretreatment procedures and AMS measurement. Hence, it is possible that fine-grained pieces of coal may have contaminated the charcoal. Additionally, since only 0.056 mg of material was measured, results indicate that sample 14C-30 had radiocarbon activity very close to zero after background subtraction, and so its original radiocarbon age was quoted as a 2-sigma lower limit. However, while age-error uncertainty for this sample was high, sample contamination from coal is the most likely cause for the severely overestimated >31.7 cal kyr BP age. Other studies have noted that combining smaller sized fractions of organic material for AMS analysis have resulted in severe age overestimations caused by coal and redeposited organic material contamination (Baker et al., 1983; Nelson et al., 1988). Therefore, findings from this study confirm that only one piece of charcoal material large enough to withstand pretreatment be used for AMS analysis in order reduce averaging effects from material of different ages.

### 2.5.3 *Evaluation of Single-grain OSL Dating*

Results for single-grain dating suggest that high amounts of partially bleached grains are present within alluvial fills at each study site in KCW. As suggested earlier, this was to be expected given results from similar studies that used OSL dating in dryland fluvial systems (e.g. Arnold et al., 2007; Harvey et al., 2011; Summa-Nelson and Rittenour, 2012). As complete zeroing of the luminescence signal is directly related to the time and intensity of solar exposure prior to deposition, understanding of the fluvial processes controlling sediment transport and deposition were used as a proxy to help identify deposits that likely contained grains that were sufficiently bleached. Indeed, previous studies have used similar approaches with measurable success and have helped recommend sampling strategies for luminescence dating in different fluvial environments (e.g. Fuchs et al., 2005, 2007; Thrasher et al., 2009). Specifically, a recent

study by Summa-Nelson and Rittenour (2012) recommended a number of sampling considerations for OSL dating arroyo systems based on small-aliquot and single-grain ages from Kanab Creek, southern Utah. Primary considerations from this study not only suggest that relatively thin (< 40 cm) beds with ripple-laminated facies are most suitable for OSL dating, mentioned earlier, but also that grains from the downstream reaches in an arroyo system are more significantly bleached. Moreover, this study indicated that the sediment-laden flows and transport mechanisms associated with Sm, Sl, and Sh (>20 cm) facies are not conducive to solar resetting. These sediment facies and transportation distance bleaching considerations were based on SG and SA overdispersion values and CAM to MAM ratios respectively. However, SG results from KCW sediments indicate that other recommendations for identifying well-bleached sediments may be more useful. Hence, the following section will both build on suggestions offered by Summa-Nelson and Rittenour (2012) and will offer additional recommendations for OSL sampling in dryland fluvial systems.

The alluvial stratigraphy and sedimentary facies preserved in the arroyo walls of KCW suggest that previous fluvial conditions were most conducive to depositing laterally continuous, <30 cm thick, low-angle crossbedded (Sl), trough crossbedded (St), and horizontally bedded (Sh) sands. Consequently, these bedforms were most commonly sampled for OSL dating and only one 50 cm thick ripple crossbedded (Sr) deposit (USU-1178) from study site KCW-D (see Ch. 3) was sampled (Table 2.5). In general, lower overdispersion values from De distributions of samples collected from low-angle crossbedded (Sl) and ripple crossbedded (Sr) deposits may have a bleaching history more suitable for luminescence dating (Fig. 2.13; Table 2.5). In contrast, sedimentary beds with horizontally bedded (Sh), massive (Sm), or trough crossbedded (St) facies have some of the highest overdispersion values (Fig. 2.13; Table 2.5). Additionally, a look at sample De overdispersion values and the original bed thickness for each sample also reveals that as bed thickness decreases, overdispersion typically decreases (Fig. 2.14). Similarly, Summa-Nelson and Rittenour (2012) also suggested that beds <40cm thick were most adequately

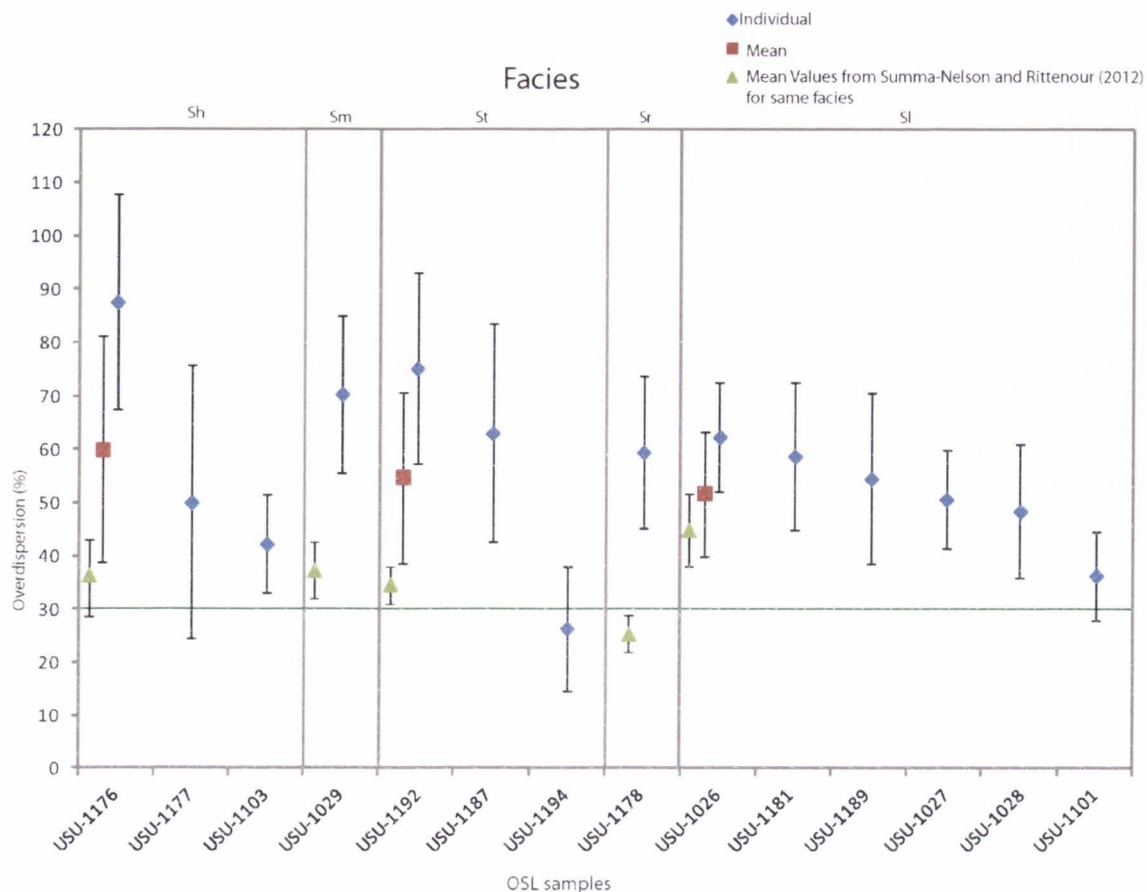


Fig. 2.13. Overdispersion and facies comparison showing preliminary individual (diamond) and mean (square) overdispersion values. Triangle represent mean facies overdispersion values from Summa-Nelson and Rittenour (2012), where massive sand (Sm) facies are averaged small-aliquot overdispersion values and all other facies are averaged small-aliquot and single-grain overdispersion values. In KCW, USU-1194 and USU-1101 have overdispersion values below 35% (the single-grain threshold for adequate bleaching). Green line represents 30% overdispersion value. Samples with an overdispersion value greater than 30% are considered partially bleached based on suggestions from Arnold et al. (2007).

bleached. However, while some of the results from this study agree with those from Summa-Nelson and Rittenour (2012), depositional environment and sedimentation differences between the KCW and Kanab Creek drainages may have resulted in different overdispersion values. For example, USU-1176 was collected from a 55 cm thick, horizontally bedded sand deposit and has one of the highest overdispersion values (Table 2.5). Based on recommendations from Summa-Nelson and Rittenour (2012), this was to be expected and sampling this deposit should have been avoided. However, whereas relatively thick (>40cm) low-angle crossbedded deposits from Kanab Creek typically returned high single-grain overdispersion values (e.g. 40-80%), two of the lowest overdispersion values in KCW came from a 50 cm thick (USU-1101) and a 40 cm thick (USU-1028) S1 facies deposit (Fig. 2.14; Table 2.5). Accordingly, sedimentary facies and bed thickness can be initially used to suggest three things from KCW: (a) sediment-laden flows in mostly upper flow regimes will deposit thick (>50cm) deposits with Sh or Sm facies, and will usually have the highest potential for partial bleaching, (b) low-angle and ripple crossbedded sands in KCW are not always the most well-bleached and (c) an additional environmental factor controlling the bleaching potential for sediments must be in play.

Sediment transport distance has often been attributed as a significant control of bleaching in fluvial environments because other problems associated with water-lain sediments, including transport mechanism and light attenuation, often result in insufficiently exposure to sunlight (e.g. Wallinga, 2003; Olley et al., 2004; Rittenour, 2008). In general, it can be assumed that transport distance is proportional to sunlight exposure, so partial bleaching should be less problematic in sediments deposited downstream. In their study, Summa-Nelson and Rittenour (2012) found that samples collected from downstream reaches in Kanab Creek were more adequately bleached based on a comparison of small-aliquot and single-grain MAM ratios and CAM to MAM ratios, and overdispersion values. A similar approach was taken here by comparing overdispersion values from upstream to downstream study sites, starting at KCW-A and ending at KCW-J (Fig. 2.15). The distance between these two sites is approximately 12km. Results indicated that

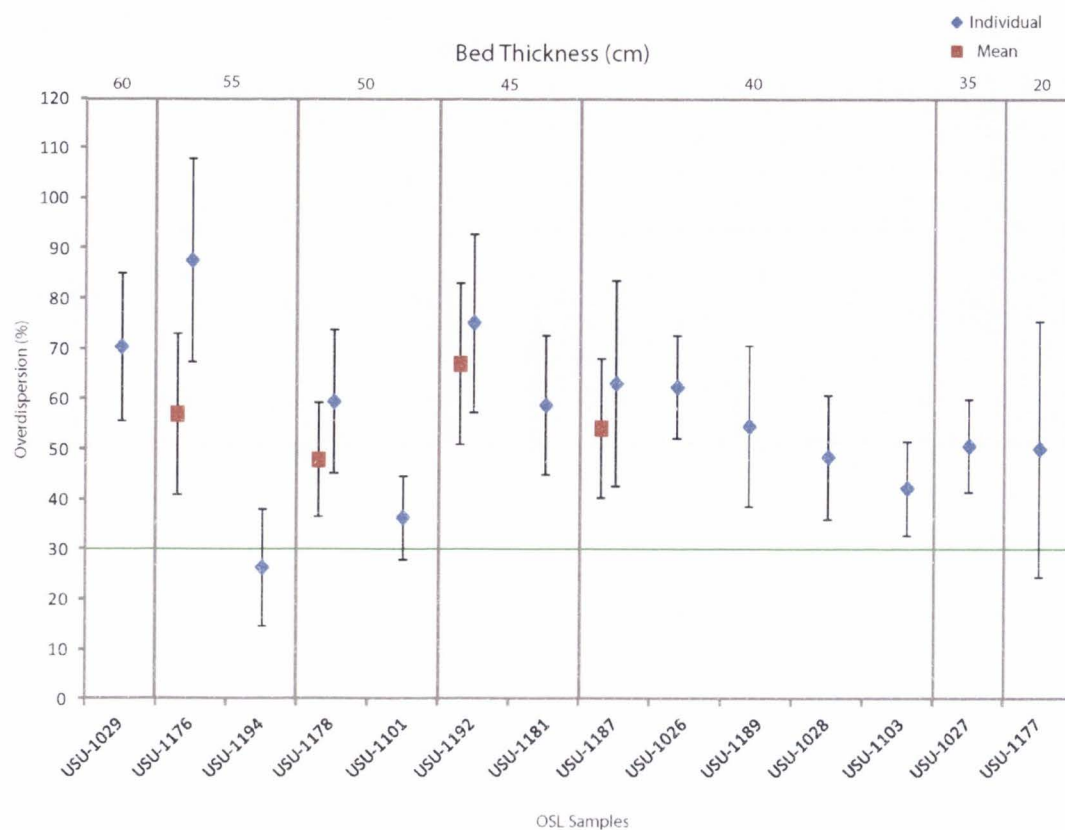


Fig. 2.14. Overdispersion and bed thickness comparison showing preliminary individual (diamond) and mean (square) overdispersion values. Although overdispersion values roughly decrease with relative to bed thickness, no clear decreasing trend in overdispersion is apparent. Green line represents 30% overdispersion value. Samples with an overdispersion value greater than 30% are considered partially bleached based on suggestions from Arnold et al. (2007).

although the highest overdispersion value was obtained from study site KCW-B (USU-1176) and one of the lowest overdispersion values was obtained from study site KCW-J (e.g. USU-1028), a clear decreasing trend in overdispersion with distance downstream is not expressed. High overdispersion values might be a reflection of the temporary storage of sediments in arroyo settings. If storage is minimal, it is likely that sediments collected downstream will have been adequately bleached. However, when the timing of sediment storage increases, it is likely that partial bleaching will become problematic. Consequently, targeting sediments solely based on their downstream distance in KCW may not necessarily result in a better-bleached population of grains.

In an overview of OSL dating of fluvial sediments, Rittenour (2008) noted that the direct input of non-zeroed sediment from the erosion of older deposits happens frequently in fluvial environments and can result in De scatter and anomalous ages. As implied earlier, the flashy flow and high-sediment discharge events that create the >30cm thick and often high-energy bedforms (e.g. Sl, Sm, St, Sh) suggest this kind of rapid deposition occurs throughout all reaches of KCW and is another reason why both upstream and downstream sediments can show significant signs of partial bleaching. In KCW, a significant fraction of sediment input is derived from regional bedrock lithologies, and so a better understanding of the sediment source could help elucidate bleaching history. Upstream sources of sediment are primarily derived from Jurassic Navajo sandstone while local sediments are derived from various tributary sediments and bedrock lithologies (e.g. Jurassic Kayenta, Triassic Chinle, and others) surrounding the KCW study area. As described above, sediments from each lithology have diagnostic characteristics and, upon visual inspection, were able to be discerned.

Accordingly, as an additional way to detect partial bleaching, sediment source was compared against overdispersion values (Fig. 2.16). Beds dominantly derived from upstream sediments were expected to be more sufficiently bleached because of their increased transport distance and coarser grain size while sediments from local bedrock, tributary, and hillslope

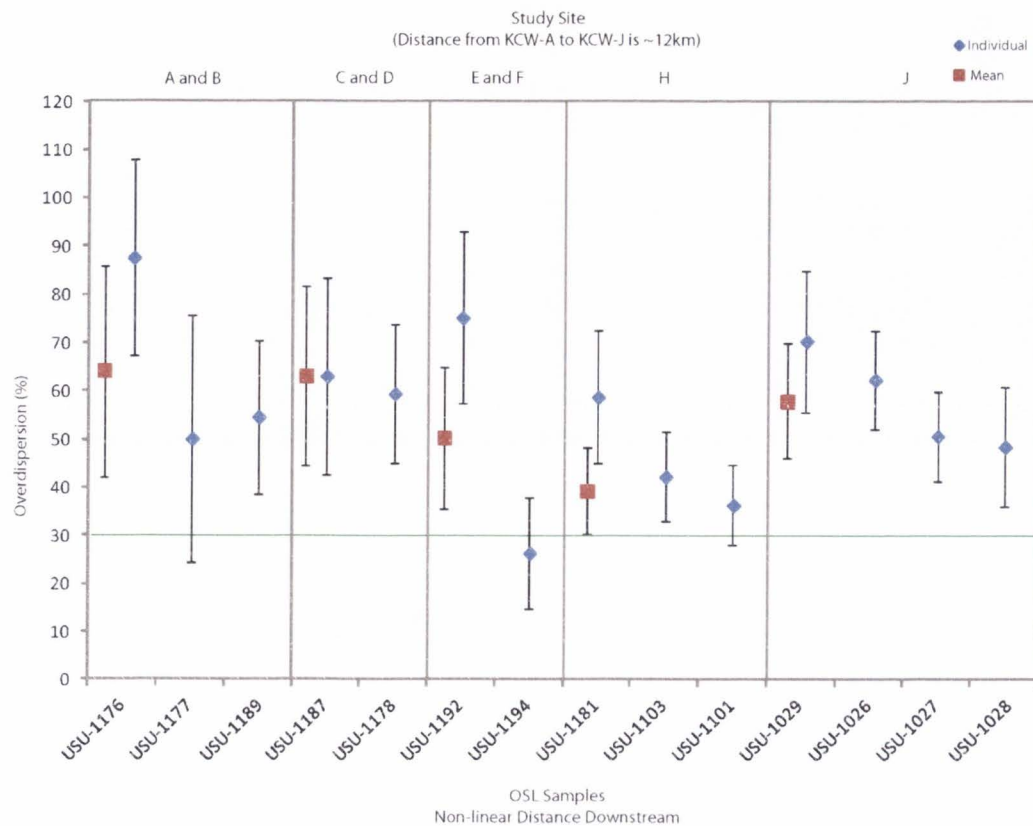


Fig. 2.15. Overdispersion and study site distance downstream comparison showing individual (diamond) and mean (square) overdispersion values. Unlike observations from Summa-Nelson and Rittenour (2012), a downstream decrease in preliminary overdispersion values was not observed. Green line represents 30% overdispersion value. Samples with an overdispersion value greater than 30% are considered partially bleached based on suggestions from Arnold et al. (2007).

sources were expected to be poorly bleached because of a shorter transport distance and a dominantly silt, clay and fine-grained sand composition. Additionally, the transport mechanisms of upstream and local sediments were expected to play a role in bleaching characteristics. Given their location, upstream sediments were likely deposited in less turbid, low-flow regimes from events such as snow-melt and regional precipitation events. Conversely, the silty and clay-rich local sediments that are dominantly sourced from downstream bedrock and tributaries were more likely to have been deposited as hyper-concentrated flows with increased turbidity during local high-magnitude flow events such as with monsoon-related precipitation. Evidence of mixed sediment deposits suggests increased flow in the main KCW channel during input of the locally sourced sediment.

Not surprisingly, single-grain overdispersion values were significantly lower (21-38.1%) in samples containing a larger population of upstream-sourced sand grains, making these deposits more suitable for single-grain dating (Fig. 2.16). It is also evident that these low values may not be contingent on the sedimentary facies or thickness of the deposit sampled. For example, USU-1194 was collected from a 55 cm thick trough-crossbedded (St) sand deposit at study site KCW-F (proposed by Summa-Nelson and Rittenour (2012) to have high overdispersion values), but its single-grain  $D_e$  distribution shows one of the lowest overdispersion values (26.4%). An outlier (USU-1178) with a slightly higher overdispersion value was collected from a thicker Sr bed at KCW-D. However, a calculated single-grain CAM to MAM ratio of 1.25 (Table 2.5) indicates that the sample was better-bleached because of its transportation distance (e.g. ratios < 1.3; Summa-Nelson and Rittenour, 2012). In contrast, deposits containing a large portion of locally derived sediments returned single-grain  $D_e$  measurements with the highest overdispersion (70.4-87.6%). Two outlying samples (USU-1177 and USU-1103) returned relatively modest overdispersion values of ~50.1% and ~42.3% respectively. However, the CAM to MAM ratio for USU-1177 was 1.54 and for USU-1103 was 1.32 (Table 2.5), which indicates a larger proportion of non-zeroed grains. These results imply that samples collected with nearly equal proportions of

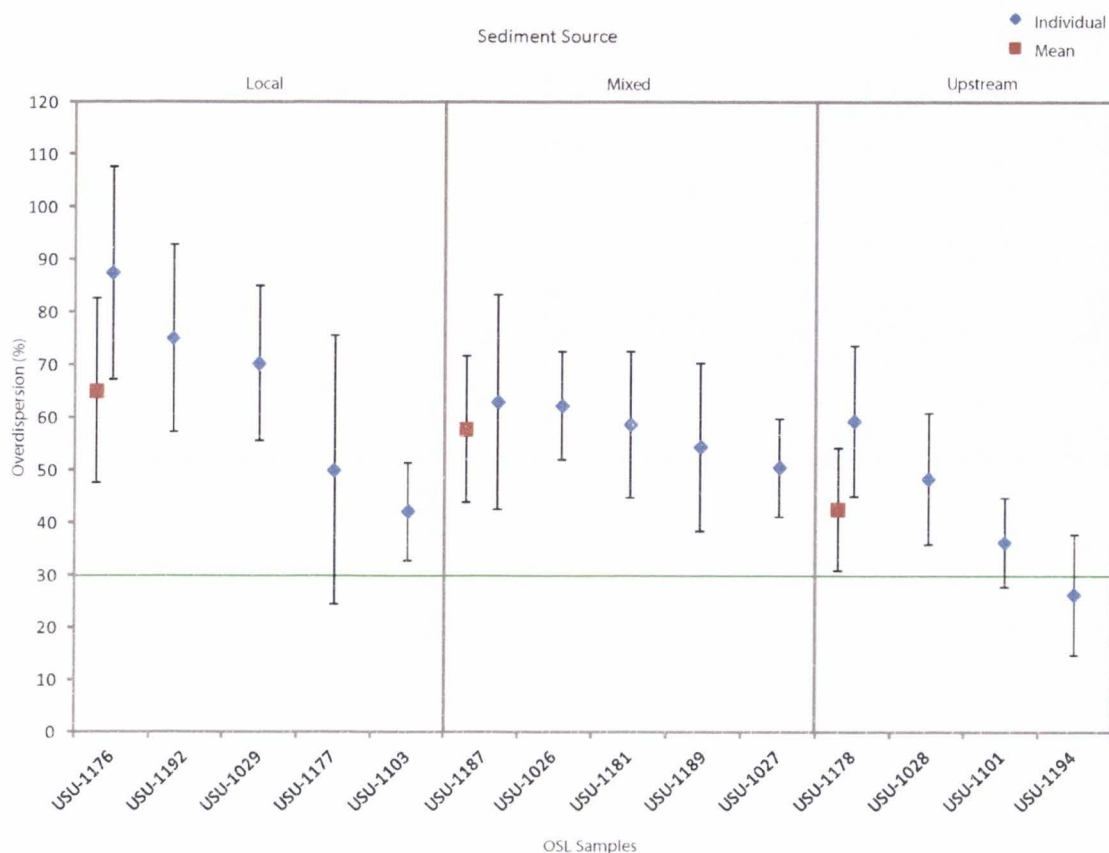


Fig. 2.16. Overdispersion and samples collected from different sediment sources comparison showing preliminary individual (diamond) and mean (square) overdispersion values. Overdispersion values show a clear decreasing trend from local (red, poorly sorted, silty-clay and very-fine grained sand) to upstream (very pale brown, well-sorted, fine- to medium-grained, frosted quartz sand) sediments, suggesting that targeting sediments based on their original sediment source (sedimentary bedrock lithology in KCW) is a better way to avoid problems with partial bleaching. Green line represents 30% overdispersion value. Samples with an overdispersion value greater than 30% are considered partially bleached based on suggestions from Arnold et al. (2007).

upstream and locally sourced grains should return intermediate overdispersion values. Indeed, samples with this mix returned overdispersion values ranging from ~51-63.1% (Fig. 2.16; Table 2.5).

As indicated earlier, no significant differences were found in the inherent overdispersion values of upstream and locally derived sediments. Accordingly, the clear decrease in single-grain overdispersion values from local to upstream sediment sources suggests that sediment source in dryland fluvial systems may be a good indicator of bleaching history. At the time of this writing, all OSL ages and therefore overdispersion values and CAM to MAM ratios are preliminary. Hence, relationships between facies, bed thickness, distance downstream, and sediment source may become more lucid with continued single-grain analyses and more accepted grains.

## **2.6 Conclusions**

A comparison of stratigraphic relationships and age results from four of the most well-constrained arroyo cut-fill exposures in KCW illustrates the benefits of using a combination of radiocarbon and OSL dating to construct an alluvial chronology in semiarid fluvial systems. This approach and a careful consideration of sample selection can help mitigate the common limitations of each dating technique. Radiocarbon age inaccuracies can arise when Cretaceous coal or redeposited charcoal fragments are analyzed. While identifying the carbonized rings of charcoal under a microscope may be difficult, observations from this study suggest that density and specific gravity differences between charcoal and coal can also be used to distinguish these materials. Additionally, it was determined that charcoal should be collected from low energy facies (e.g. Sr, St, Sl, Fsmv) in a charcoal-rich lens located several meters away from colluvial wedges and erosional unconformities. Finally, large pieces of angular charcoal (>5 mg each) should be collected from each charcoal-rich lens so that only one piece of charcoal will be necessary for volume and weight requirements for AMS analysis.

OSL samples were expected to show signs of partial bleaching based on the flashy-flow and high sediment discharge conditions interpreted from the stratigraphy and sedimentology of each deposit and because the most common facies assemblages (Sl, St, Sh) in KCW did not allow all strategies from Summa-Nelson and Rittenour (2012) to be closely followed. However, preliminary SG overdispersion values and a few CAM to MAM ratios from KCW samples suggested that not every strategy recommended by Summa-Nelson and Rittenour (2012) applied to KCW. For example, some observations from this study do support earlier suggestions that relatively thick (45 cm to meter-scale) deposits with facies from upper flow regimes (e.g. Sh, St, Sm) are more likely to be partially bleached and should be avoided when sampling. However, preliminary overdispersion values from KCW samples do not suggest better-bleached sediments with increasing downstream distance. Rather, preliminary results found that in addition to strategies by Summa-Nelson and Rittenour (2012), specific emphasis should be placed on the original sediment source. For example, sediments identified as being sourced from upstream sandstone bedrock likely had a longer transport and were deposited less rapidly in the KCW system, which allowed for more adequate bleaching. In contrast, sediments input from local bedrock or tributaries were more likely to have been redeposited quickly and contain larger amounts of silts and clays, potentially decreasing the total amount of solar exposure. Hence, sample selection using a combination of facies, bed thickness, and sediment source analyses should be used to aid in sample collection and can help attenuate some problems with partial bleaching. Regardless of the methods applied, partial bleaching will still remain a problem for some sediment. Accordingly, a minimum-age-model combined with single-grain dating should be applied to mitigate age overestimations due to partial bleaching.

Ultimately, the alluvial chronology built in this study has updated and filled in temporal gaps from existing KCW alluvial chronologies (e.g. Hereford, 2002; Harvey, 2009; Harvey et al., 2011). The accomplishments of this study were largely dependent on merging both techniques,

which allowed for increased sampling opportunities and cross-checking of results to determine age inaccuracies.

## REFERENCES

- Aitken, M.J., 1998. *An Introduction to Optical Dating*. Oxford University Press, Oxford.
- Antevs, E., 1952. Arroyo-cutting and filling. *Journal of Geology* 60, 375-385.
- Arnold, L.J., Bailey, R.M., Tucker, G.E., 2007. Statistical treatment of fluvial dose distributions from southern Colorado arroyo deposits. *Quaternary Geochronology* 2, 162-167.
- Bailey, R.W., 1935. Epicycles of erosion in the valleys of the Colorado Plateau province. *Journal of Geology* 43, 337-355.
- Bailey, R.M., Arnold, L.J., 2006. Statistical modeling of single grain quartz De distributions and an assessment of procedures for estimating burial dose. *Quaternary Science Reviews* 25, 2475-2502.
- Baker, V., 1987. Paleoflood hydrology and extraordinary flood events. *Journal of Hydrology* 96, 79-99.
- Baker, V.R., Pickup, G., Polach, H.A., 1983. Desert palaeofloods in central Australia. *Nature (London)* 301, 502-504.
- Bateman, M.D., Frederick, C.D., Jaiswal, M.K., Singhvi, A.K., 2003. Investigations into the potential effects of pedoturbation on luminescence dating. *Quaternary Science Reviews* 22, 1169-1176.
- Bird, M.I., 2007. Radiocarbon dating: charcoal. In: Elias, S. (Eds.), *Encyclopedia of Quaternary Sciences*, Elsevier, Oxford, 2950-2958.
- Bøtter-Jensen, L., Bulur, E., Duller, G.A.T., Murray, A.S., 2000. Advances in luminescence instrument systems. *Radiation Measurements* 32, 523-528.
- Bryan, K., 1925. Date of channel trenching (arroyo-cutting) in the arid southwest. *Science* 62, 338-344.
- Bull, W.B., 1997. Discontinuous ephemeral streams. *Geomorphology* 19, 227-276.
- Cook, G.T., van der Plicht, J., 2007. Radiocarbon dating: conventional method. *Encyclopedia of Quaternary Science*. Amsterdam: Elsevier, 2899-2911.
- Cooke, R.U., Reeves, R.W., 1976. *Arroyos and Environmental Change in the American Southwest*. Clarendon Press, Oxford.

- Duller, G.A.T., Bøtter-Jensen, L., Murray, A.S., 2003. Combining infrared- and green-laser stimulation sources in single-grain luminescence measurements of feldspar and quartz. *Radiation Measurements* 32, 435-457.
- Ely, L.L., 1997. Response of extreme floods in the south-western United States to climatic variations in the late Holocene. *Geomorphology* 19, 175-201.
- Feathers, J.K., Holliday, V.T., Melzter, D.J., 2006. Optically stimulated luminescence dating of Southern High Plains archaeological sites. *Journal of Archaeological Science* 33, 1651-1665.
- Fuchs, M., Straub, J., Zoller, L., 2005. Residual luminescence signals of recent river flood sediments: A comparison between quartz and feldspar of fine- and coarse-grain sediments. *Ancient TL* 23, 25-30.
- Fuchs, M., Woda, C., Bürkert, A., 2007. Chronostratigraphy of a sediment record from the hajar mountain range in north Oman: implications for optical dating of insufficiently bleached sediments. *Quaternary Geochronology* 2, 202-207.
- Galbraith, R.F., Roberts, R.G., Laslett, G.M., Yoshida, H., Olley, J.M., 1999. Optical dating of single and multiple grains of quartz from Jinmium rock shelter, northern Australia. Part I. *Archaeometry* 41 (2), 339-364.
- Gavin, D.G., 2001. Estimation of inbuilt age in radiocarbon ages of soil charcoal from fire history studies. *Radiocarbon* 43 (2), 27-44.
- Gillespie, R., Prosser, I.P., Dlugokencky, E., Sparks, R.J., Wallace, G., Chappel, J.M.A., 1992. AMS dating of alluvial sediments on the southern tablelands of New-South-Wales, Australia. *Radiocarbon* 34 (1), 29-36.
- Graf, W.L., 1983. The arroyo problem – Paleohydrology and paleohydraulics in the short term. In: Gregory, K.G. (Eds.), *Background to Paleohydrology*. John Wiley and Sons, New York, 297-302.
- Guerin, G., Mercier, N., Adamiec, G., 2011. Dose-rate conversion factors: update. *Ancient TL* 29, 231-238.
- Hall, S.A., 1977. Late Quaternary Sedimentation and Paleoecologic History of Chaco Canyon, New Mexico. *Geological Society of America Bulletin*, vol. 88, pp. 1593-1618.
- Harvey, J.L., 2009. Reconciling Holocene Alluvial Records in Buckskin Wash, Southern Utah. M.S. Thesis, Utah State University, unpublished.
- Harvey, J.E., Pederson, J.L., Rittenour, T.M., 2011. Exploring relations between arroyo cycles and canyon paleoflood records in Buckskin Wash, Utah: Reconciling scientific paradigms. *Geological Society of America Bulletin*, v. 123, 2266-2276.

- Hereford, R., 2002. Valley-fill alluviation during the Little Ice Age (ca. A.D. 1400–1880), Paria River basin and southern Colorado Plateau, United States. *Geological Society of America Bulletin* 114 (12), 1550-1563.
- Huntley, D.J., Godfrey-smith, D.I., Thewalt, M.L.W., 1985. Optical dating of sediments. *Nature* 313, 105-107.
- Jain, M., Murray, A.S., Bøtter-Jensen, L., 2004. Optically stimulated luminescence dating: How significant is incomplete light exposure in fluvial environments? *Quaternaire*, 15 (1-2), 143-157.
- Jones, L.S., Ronseburg, M., del Mar Figueroa, M., McKee, K., Haravitch, B., Hunter, J., 2010. Holocene valley-floor deposition and incision in a small drainage basin in western Colorado, USA. *Quaternary Research* 74, 199-206.
- Karlstrom, T.N.V., 1988. Alluvial chronology and hydrologic change of Black Mesa and nearby regions. In: Bumerman, G.J. (Ed), *The Anasazi in a Changing Environment*. Cambridge, Cambridge University Press, pp. 45-91.
- Li, B., Li, S., 2006. Correcting for thermal transfer in OSL measurements of young sediment samples. *Radiation Measurements* 41, 855-861.
- Libby, W.F., Anderson, E.C., Arnold, J.R., 1949. Age determination by radiocarbon content: world-wide assay of natural radiocarbon. *Science* 4, 227-228.
- Mann, D.H., Meltzer, D.J., 2007. Millennial-scale dynamics of valley fills over the past 12,000 <sup>14</sup>C in northeastern New Mexico, USA. *Geological Society of America Bulletin* 119, 1433-1448.
- Miall, A.D., 2000, *Principles of sedimentary basin analysis*, 3<sup>rd</sup> ed. Springer, New York.
- Mcfadgen, B.G., 1982. Dating New Zealand archaeology by radiocarbon. *New Zealand Journal of Science* 25, 379-392.
- Murray, A.S., Olley, J.M., 2002, Precision and accuracy in the optically stimulated luminescence dating of sedimentary quartz: a status review. *Geochronometria* 21, 1-16.
- Murray, A.S., Wintle, A.G., 2000. Luminescence dating of quartz using an improved single-aliquot regenerative-dose protocol. *Radiation Measurements* 32, 57-73.
- Murray, A.S., Wintle, A.G., 2003. The single aliquot regenerative dose protocol: potential for improvements in reliability. *Radiation Measurements* 37, 377-381.
- Nelson, R.G., Carter, L.D., Robinson, S.W., 1988. Anomalous radiocarbon ages form a Holocene detrital organic lens in Alaska and their implications for radiocarbon dating and paleoenvironmental reconstructions in the Arctic. *Quaternary Research* 29, 66-71.
- Olley, J.M., Pietsch, T., Roberts, R.G., 2004. Optical dating of Holocene sediments from a variety of geomorphic settings using single grains of quartz. *Geomorphology* 60, 337-358.

- Olley, J.M., Caitcheon, G.G., Roberts, R.G., 1999. The origin of dose distributions in fluvial sediments, and the prospect of dating single grains from fluvial deposits using optically stimulated luminescence. *Radiation Measurements* 30, 207-217.
- Patton, P.C., Schumm, S.A., 1981. Ephemeral-stream processes: implications for studies of Quaternary valley fills. *Quaternary Research* 15, 24-43.
- Patton, P.C., Boison, P.J., 1986. Processes and rates of formation of Holocene alluvial terraces in Harris Wash, Escalante River basin, south-central Utah. *GSA Bulletin* 97, 369-378.
- Prescott, J.R., Hutton, J.T., 1994. Cosmic ray contributions to dose rates for luminescence and ESR dating: large depths and long-term time variations. *Radiation Measurements* 23, 497-500.
- Reimer, P.J., M G L Baillie, M.G.L., Bard, E., Bayliss, A., Beck, J.W., Blackwell, P.G., Bronk Ramsey, C., Buck, C.E., Burr, G.S., Edwards, R.L., Friedrich, M., Grootes, P.M., Guilderson, T.P., Hajdas, I., Heaton, T.J., Hogg, A.G., Hughen, K.A., Kaiser, K.F., Kromer, B., McCormac, F.G., Manning, S.W., Reimer, R.W., Richards, D.A., Southon, J.R., Talamo, S., Turney, C.S.M., van der Plicht, J., Weyhenmeyer, C.E., 2009. Intcal09 and Marine09 radiocarbon age calibration curves, 0-50,000 years cal BP. *Radiocarbon* 51 (4), 1111-1150.
- Rhodes, E.J., 2000. Observation of thermal transfer OSL signals in glacial quartz. *Radiation Measurements* 32, 595-602.
- Rittenour, T.M., 2008. Luminescence dating of fluvial deposits: applications to geomorphic, palaeoseismic, and archaeological research. *Boreas* 37, 613-635.
- Schiffer, M.B., 1986. Radiocarbon dating and the "old wood" problem: the case of the Hohokan chronology. *Journal of Archaeological Sciences* 13, 13-30.
- Schumm, S.A., Hadley, R.F., 1957. Arroyos and the semiarid cycle of erosion. *American Journal of Science* 255, 161-172.
- Stuiver, M., Polach, H.A., 1977. Discussion: Reporting of  $^{14}\text{C}$  data. *Radiocarbon* 19, 355-363.
- Summa-Nelson, M.C., Rittenour, T.M., 2012. Application of OSL dating to middle to late Holocene arroyo sediments in Kanab Creek, southern Utah, USA. *Quaternary Geochronology* 10, 167-174.
- Taylor, R.E., 1987. *Radiocarbon Dating: An Archeological Perspective*. Academic Press, Orlando.
- Telford, R.J., Heegaard, E., Birks, H.J.B., 2004. The intercept is a poor estimate of a calibrated radiocarbon age. *The Holocene* 14, 296-298.
- Thomsen, K.J., Murray, A.S., Bøtter-Jensen, L., 2005. Sources of variability in OSL dose measurements using single grains of quartz. *Radiation Measurements* 39, 47-61.

- Thornthwaite, C.W., Sharpe, C.F.S, Dosch, E.F., 1942. Climate and accelerated erosion in the arid and semi-arid Southwest with special reference to the Polacca Wash drainage basin, Arizona. U.S. Dep. Agric. Tech. Bull. 808, 134 pp.
- Thrasher, I.M., Mauz, B., Chiverrell, R.C., Lang, A., Thomas, G.S.P, 2009. Testing an approach to OSL dating of Late Devensian glaciofluvial sediments of the British Isles. *Journal of Quaternary Science* 24, 785-801.
- Tucker, G.E., Arnold, L., Bras, R.L., Flores, H., Istanbuloglu, E., Solyon, P., 2006. Headwater channel dynamics in semiarid rangelands, Colorado high plains, USA. *Geological Society of America Bulletin* 118, 959-974.
- Vandenbergh, D., Hossain, S.M., De Corte, F., Van den haute, P., 2003. Investigations on the origin of the equivalent dose distribution in a Dutch coversand. *Radiation Measurements* 37, 433-439.
- Wallinga, J., 2002. Optically stimulated dating of fluvial deposits: a review. *Boreas* 31, 303-322.
- Wallinga, J., 2003. On the detection of OSL age overestimation using single-aliquot techniques. *Geochronometica* 21, 17-26.
- Wallinga, J., Murray, A.S., Duller, G.A.T., Tørnqvist, T.E., 2001. Testing optically stimulated luminescence dating of sand-sized quartz and feldspar from fluvial deposits. *Earth and Planetary Science Letters* 193, 617-630.
- Webb, R.H., Smith, S.S., McCord, V.A., 1991. Historic Channel Change of Kanab Creek, Southern Utah and Northern Arizona. Grand Canyon Natural History Association Monograph.
- Webb, R.H., Leake, S.A., 2006, Ground-water surface-water interactions and long-term change in riverine riparian vegetation in the southwestern United States. *Journal of Hydrology* 320, 302-32

## CHAPTER 3

EPISODIC ENTRENCHMENT AND AGGRADATION IN KITCHEN CORRAL WASH,  
SOUTHERN UTAH**ABSTRACT**

Fluvial systems in the semiarid southwestern United States are sensitive to Holocene climate perturbations, evident from the entrenched, steep-walled arroyo channels throughout the region. Kitchen Corral Wash (KCW), a tributary of the Paria River in southern Utah, has experienced both historic and pre-historic (Holocene) episodes of arroyo cutting and filling. During the most recent arroyo-cutting event (~1880-1920 AD), KCW and other regional drainages were entrenched up to 30 m into their fine-grained alluvial fills, leaving former floodplains perched above new channel bottoms. Although arroyo entrenchment and aggradation sequences have been studied for over a century, exact causes of arroyo cutting are still not fully understood. Hereford (2002) argued that arroyo dynamics over the last ~1 ka are climatically driven based on near-synchronous timing of arroyo cutting in drainages from southern Utah and the surrounding region. However, recent results from KCW and nearby drainages suggest a more complex pattern of aggradation and incision.

While previous studies have attempted to constrain the timing of arroyo cut-fill events in KCW, poor age control has limited the results. In order to better understand the timing of arroyo cutting events, this study updates and improves the arroyo cut-fill chronology from KCW by using alluvial stratigraphic descriptions and age control from optically stimulated luminescence (OSL) and accelerator mass spectrometry (AMS) radiocarbon dating. Results are based on twelve study sites, each exposing a number of cut-fill cycles in the arroyo-wall stratigraphy, and suggest at least six arroyo cycles over the last ~7.3 ka. These chronostratigraphic results are also used to test hypotheses related to climatic forcing of arroyo dynamics by comparing the

chronology from KCW to recently updated alluvial chronologies from nearby arroyo systems and to paleoclimate records. Results indicate temporally complex regional alluvial chronologies, suggesting a combination of allogenic and autogenic influences.

### 3.1 Introduction

For over a century, researchers and land managers have been interested in understanding the fluvial dynamics of semi-arid environments, which are often characterized by the presence of arroyos in the southwestern United States. Arroyos are an end-member geomorphic state typical of high sediment yield fluvial systems, and are characterized by steep-walled channels entrenched into fine-grained valley-fill alluvium (e.g. Bryan, 1925; Bull, 1997). Evidence for past cut-fill events exposed in arroyo walls suggests that entrenchment is triggered by stream disequilibrium. Arroyo wall stratigraphy suggests that incision into an alluvial fill is followed by channel widening and sediment deposition that promotes aggradation towards the original stream profile (Bull, 1997; Gellis and Elliot, 2001). Region-wide flood events ca. 1880-1920 AD in southern Utah caused shallow, perennial streams to entrench tens of meters into thick valley fills, leaving former floodplains behind as terraces. This historic period of was witnessed in many southwestern United States drainages (e.g. Bryan, 1925; Hack, 1942; Webb et al., 1991; Hereford, 2002).

Prior to this historic arroyo cutting event, early pioneers settled in areas throughout the southwestern U.S. where shallow, marshy perennial streams provided surface water for a variety of domestic and agricultural uses (Webb et al., 1991). However, widespread and nearly synchronous historical arroyo cutting resulted in severe property damage and the abandonment of many settlements in the region (Cooke and Reeves, 1976; Webb et al., 1991). Moreover, arroyo formation proved to be ecologically costly by disrupting riparian ecosystems and wildlife habitat due to rapid lowering of the groundwater table, increased flooding hazards, and increased downstream sedimentation from lateral channel migration and headward incision (Webb and

Leake, 2006; DeLong et al., 2011). The detrimental effect and the apparent regionally contemporaneous timing of these incision events spurred the study of arroyo systems and hypotheses regarding the causes of valley-fill entrenchment (e.g. Cooke and Reeves, 1976; Webb et al., 1991). In fact, the near synchronous nature of historic arroyo cutting is thought to be one of the most significant geomorphic events of the past century in the southwestern United States (Bryan, 1925; Hack, 1942).

Research has largely focused on identifying possible triggering mechanisms for arroyo evolution as a way to support or dispute the possibility of region-wide, nearly contemporaneous incision or aggradation events (e.g. Antevs, 1952; Schumm and Hadley, 1957; Cooke and Reeves, 1976; Hereford, 2002; and others ). Hypotheses related to the causes of arroyo incision range from land mismanagement or overgrazing during pioneer settlement (Bailey, 1935; Thornthwaite et al., 1942; Antevs, 1952), autogenic geomorphic controls (Schumm and Hadley, 1957; Patton and Schumm, 1981; Patton and Boison, 1986; Tucker et al., 2006), and climate changes related to sediment supply, stream discharge, or both (Bryan, 1941, Antevs, 1952; Karlstrom, 1988; Hereford, 2002; Mann and Meltzer, 2007). Hence, these competing arroyo cut-fill hypotheses can be grouped according to their possible triggering mechanism (autogenic or allogenic) or regional response to arroyo evolution (nearly synchronous and asynchronous) as seen in Table 3.1

Early workers suggested that near-synchronous historic arroyo cutting events resulted from poor land management related to livestock overgrazing, soil compaction and desertification of the land which may have decreased soil infiltration capacity (e.g. Bryan, 1925; Bailey, 1935; Antevs, 1952; Cooke and Reeves, 1976). Other studies have suggested that the creation of cattle paths or ditches by early settlers would enhance runoff and increase stream power, resulting in channel incision (Webb et al., 1991; Bull, 1997). Additionally, some studies have found geoarchaeological evidence for irrigation canals created in discontinuous gullies that were likely used for floodwater farming by Puebloan settlements in southwestern Colorado and New Mexico between ~600 and 1300 A.D. (e.g. Huckleberry and Billman, 1998; Huckleberry and Duff, 2008)

Table 3.1  
Arroyo cut-fill competing hypotheses and expected results

Possible Triggering Mechanisms and Controls for Arroyo Formation	Possible Cause	Controlling Effect	Expected Regional Response	References
<b>Allogenic (Climate Dependent)</b>				
Periods of regionally drier conditions	Weak and Infrequent ENSO or Weakend North American Monsoon	Reduced effective moisture and lowered groundwater tables would result in vegetation reduction and would lower a channel's hydraulic roughness. These conditions generally promote regional alluviation but can cause channels to become more susceptible to downcutting by enhancing peak runoff discharge. Channel downcutting could continue to lower groundwater table and enhance degradation.	Synchronous channel incision.	(Bryan, 1925; Antevs, 1952; Euler et al., 1979; Bull, 1997; Waters and Haynes, 2001; Webb and Leake, 2006; Mann and Meltzer, 2007)
		Following a period of channel downcutting. Vegetation reduces along axial terraces and hillslopes and increases potential sediment load. Groundwater table elevates and woody riparian vegetation is established within channel, promoting aggradation during small floods (Huntington, 1914; Webb and Hereford, 2001; Webb and Leake, 2006).	Synchronous channel aggradation	(Huntington, 1914; Webb and Hereford, 2001; Webb and Leake, 2006).
Periods of regionally wetter conditions	Increased Frequency and Intensity of ENSO wet events or Strengthening of the North American Monsoon	Increased regional precipitation and substantial increase in effective moisture lead to enhanced runoff resulting in larger and more frequent flood events causing channel entrenchment.	Synchronous channel incision	(Huntington, 1914; Graf, 1983; Waters and Haynes, 2001; Webb and Hereford, 2001; Hereford, 2002; Mann and Meltzer, 2007).
<b>Autogenic (Independent of Climate)</b>				
Land Use	Overgrazing and trampling caused by a significant rise in livestock or land modification from human practices	Reduced vegeation and enhanced soil compaction coupled with the formation of canals, trenches, or ditches by Anglo or Pueblan settlement. These conditions reduced infiltration of rainfall, resulting in enhanced and/or channelized runoff and increased stream power necessary for incision. This is able to account for the historic arroyo cutting events, but evidence of paleoarroyos indicates cut-fill events pre-dating anglo settlement. Some authors also note that Pueblan settlements were abandoned prior to the most recent prehistoric arroyo cutting event. Additionally, time constraints between settlement and incision are not enough for an overgrazing effect. (Bryan, 1925; Bailey, 1935; Antevs, 1952; Hastings, 1952; Cooke and Reeves, 1976; Webb et al., 1991)	Possibility of synchronous channel incision if widespread or non-synchronous, catchment specific channel incision	(Bryan, 1925; Bailey, 1935; Hack, 1942; Antevs, 1952; Cooke and Reeves, 1976; Webb et al., 1991; Webb and Hereford, 2001; Huckleberry and Duff, 2008)
Lithology	Highly erodible bedrock	Channels flowing through highly erodible bedrock or alluvial fill have high sediment yields that can overwhelm stream power and inhibit sediment removal. This may result in downstream aggradation.	Non-synchronous, catchment specific channel aggradation	(Mcfadden and McAuliffe, 1997; Jones et al., 2010).
	Resistant bedrock	Channels flowing over or through resistant bedrock or alluvial fills enhance runoff, increase stream power, and may cause downstream incision.	Non-synchronous, catchment specific channel incision	(Balling and Wells, 1990; Jones et al., 2010).
Intrinsic Channel Processes	Complex Response	High sediment yields in semiarid drainages cause stream gradients to oversteepen, which induces channel incision followed by widening, and subsequent reaggradation. Channels continue to follow this feedback mechanism in a temporally complex manner.	Non-synchronous, catchment specific channle incision or aggradation	(Schumm and Hadley, 1957; Schumm, 1973; Patton and Schumm, 1981; Bull, 1997; Tucker et al., 2006; Daniels, 2008; Jones et al., 2010)

It is possible that these canals could have channelized run-off during periods of increased precipitation (following periods of drought) and initiated one of the prehistoric episodes of downcutting and channel-widening. Entrenchment and arroyo formation are thought to have lowered the groundwater table (e.g. Webb and Leake, 2006), which could have possibly lead to the abandonment of Puebloan settlements (Miller and Kochel, 1999). However, there is limited evidence for large prehistoric cultural populations or intensified aggradation practices proximal to southern Utah drainages before the penultimate incision event at ~1200 A.D.

Other studies have suggested that autogenic thresholds within drainages may drive arroyo cutting and filling (Schumm and Hadley, 1975; Patton and Schumm, 1981; Tucker et al., 2006). For example, field and lab analyses conducted on southwestern arroyos have suggested that arroyo cutting and filling is a fundamental fluvial response to knickpoint formation and recession, stream gradient fluctuations, and internal changes in sediment yield that are not driven by allogenic forcings (Schumm and Hadley, 1957; Patton and Schumm, 1981). Rather, it has been suggested that internal mechanisms controlling arroyo formation are merely perturbed by changes in climate (Patton and Schumm, 1981).

A final mechanism, climate change, has received the most attention because it offers the best explanation for a regionally near-synchronous response (e.g. Knox, 1983; Karlstrom, 1988; Hereford and Webb, 1992; Hereford, 2002). For example, in a period of regionally drier conditions, reduced effective moisture and a lowered groundwater table could increase potential sediment load in upstream regional catchments and could promote regionally near-synchronous channel aggradation (e.g. Huntington, 1914; Webb and Leake, 2006). Conversely, during period of regionally wetter climate conditions, increased precipitation and effective moisture could lead to enhanced run-off and the potential for more regionally erosive floods that could cause near-synchronous incision (e.g. Hereford and Webb, 1992). Hereford (2002) originally suggested that regionally synchronous arroyo cut-fill events over the past ~1000 years were due to regional climate shifts related to the Little Ice Age and Medieval Climate Anomaly. However, while it is

obvious the climate plays a role in arroyo dynamics, the exact climate conditions needed to initiate historic and prehistoric arroyo cutting and filling remain unresolved. Additionally, climate-related incision and aggradation events primarily have been explored independent of other possible forcing mechanisms. It is quite possible that a combination of triggering mechanisms, such as catchment specific geomorphic thresholds, have contributed to the formation and timing of historic and prehistoric arroyo cutting and filling.

This study examines the arroyo cut-fill chronology of Kitchen Corral Wash (KCW), a tributary of the Paria River in southern Utah. KCW is currently in an incised state. Stratigraphic evidence indicates that it has experienced prehistoric arroyo entrenchment and aggradation. As with many regional arroyo systems, KCW provides an archive of fluvial response to previous geomorphic and climate conditions. While Hereford (2002) suggested a climatically driven near-synchronous response, chronologies derived from the near-by drainages of Kanab Creek (Summa-Nelson and Rittenour, 2012; personal communication with Summa-Nelson) and the upper Escalante River (Hayden, 2011) indicate prehistoric arroyo cutting and filling events may be more temporally complex. Moreover, Harvey et al. (2011) identified four valley-fill alluvial packages in KCW that suggest a different arroyo cut-fill chronology than Hereford's (2002) study. However, the ages of these four alluvial packages are poorly constrained. Hence, the current chronology from KCW precludes the ability to determine if arroyo dynamics between regional drainages are contemporaneous and therefore related to climate change.

The purpose of this study is to construct a detailed chronostratigraphy of KCW by expanding and updating the skeletal alluvial chronologies developed by Hereford (2002) and Harvey et al. (2011). This is achieved by combining detailed sedimentologic descriptions and stratigraphic panels at twelve study sites with age control derived from accelerator mass spectrometry (AMS) radiocarbon and optically stimulated luminescence (OSL) dating techniques. Ultimately, results from this study are used to better understand the complex timing of arroyo aggradation and incision episodes. Evidence for temporally similar aggradation and

entrenchment episodes would suggest a more dominant allogenic control, such as regional climate forcing. Alternatively, catchment specific chronologies would suggest an autogenic control, such as internal geomorphic thresholds. A strong correlation between cut-fill cycles and paleoclimate records might also support a dominant climate forcing.

## 3.2 Background

### 3.2.1 Physiographic Setting of KCW

Kitchen Corral Wash is a tributary of the Paria River located in Kane County, Utah approximately 45km east of the town of Kanab. It is the main trunk stream of a drainage that assumes several names from its headwaters to its confluence with the Paria River (e.g. Park Wash, Deer Springs Wash, Kitchen Corral Wash, Kaibab Gulch, and Buckskin Gulch). However, for the purpose of this study the name Kitchen Corral Wash will encompass the Park Wash (PW) and Deer Spring Wash (DSW) reaches from the base of the White Cliffs and the main Kitchen Corral Wash alluvial valley that extends from the base of the Vermillion Cliffs to the intersection with Kaibab Gulch at U.S. Highway-89 (Fig. 3.1). From its headwaters in the Pausaugunt Plateau to the head of Kaibab Gulch, the total drainage area of KCW is 511 km<sup>2</sup> and ranges in elevation from ~2500 m asl to just below 1800 m asl. KCW flows approximately north to south and occupies a continuous arroyo that is entrenched ~2-12 m within its fine-grained alluvial valley fill. The total reach-length of the study area (combining PW, DSW, and KCW) is ~28 km.

Kitchen Corral Wash heads in Tertiary (upper Paleocene to middle Eocene) Claron Formation (T<sub>cp</sub> and T<sub>cw</sub>) sandstones, siltstones, and mudstone of the Paunsaugunt Plateau (Fig. 3.2). The Claron Formation forms the Pink Cliffs that are exposed as the uppermost unit of the Grand Staircase (GS) geomorphic province of the Colorado Plateau. From here the drainages continue incising through Cretaceous Kaiparowits Formation (K<sub>k</sub>), Wahweap Formation (K<sub>w</sub>), and Straight Cliffs Formation (K<sub>s</sub>) sediments as the lower Pink Cliffs change to the upper Gray

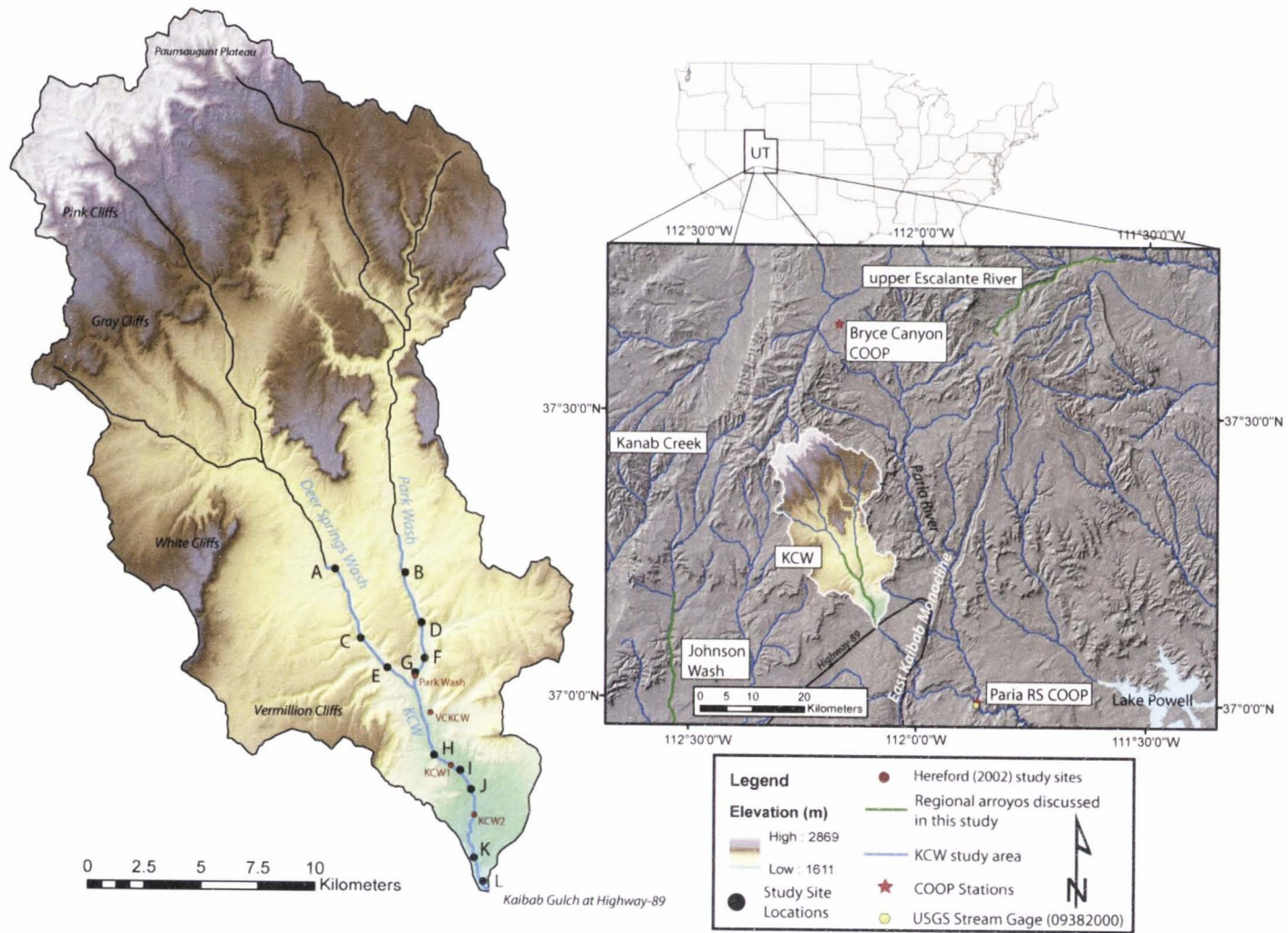


Fig. 3.1. Kitchen Corral Wash (KCW) is a tributary of the Para River in southern Utah that heads in the Paunsaugunt Plateau and. In this study, KCW encompasses Deer Springs Wash and Park Wash tributaries to the intersection of Kaibab Gulch at Highway-89.

Cliffs. The Kaiparowits Formation lies unconformably beneath the Claron Formation and is composed of subarkose sandstone. The interbedded mudstone to sandstone of the Wahweap Formation overlies the Straight Cliffs Formation, which is made of cliff-forming sandstones, and slope-forming mudstones and coal interbeds (Doelling et al., 2000). The drainages continue through resistant Dakota Formation (Kd) sandstone at the base of the Gray Cliffs until transitioning into Late and Middle Jurassic Entrada Sandstone (Je) and Carmel Formation (Jc) sediments. Below these two sedimentary units, the Jurassic Navajo Formation (Jn) sandstone composes the White Cliffs, and has high-angle cross-bedding because of its eolian origin and is primarily composed of white to tan-colored fine and medium grained sand (Doelling et al., 2000). Exiting the White Cliffs, the drainages headwaters converge into Park Wash and Deer Springs Wash and incise through Jurassic Kayenta Formation (Jk) and upper Vermillion Cliffs. The confluence of Park Wash and Deer Springs Wash form the main channel of Kitchen Corral Wash, which exits through the Moenave Formation (Jmo) at the base of the Vermillion Cliffs and then cross Triassic Chinle (Trc) and Moenkopi (Trm) Formations. The Chinle Formation is primarily composed of interbedded mudstones, sandstone, and conglomerates, and also contains fossilized wood of the Petrified Forest Member. Finally, after exiting the disconformity-bounded Moenkopi Formation, KCW is renamed Buckskin Gulch as it narrows and becomes entrenched within Permian limestones and sandstones of the Kaibab Formation.

The modern channel of KCW is typified by steep, vertical arroyo walls ranging from 12 to <5 m in height, which were produced by the most recent arroyo cutting event between 1880 and 1920 AD (Hereford, 2002). The active channel is 20 to 100 m wide and is inset into Holocene alluvium which lies within a broad (>1 km wide) Quaternary-aged alluvial valley bound by Pleistocene-aged terraces tens of meters high that are mantled with cobble to gravel sized alluvium (Fig. 3.3). Although mainly an alluvial channel, in places KCW narrows to several meters and is surrounded by bedrock outcrops where it transitions from weak lithologic

## KCW Longitudinal Profile

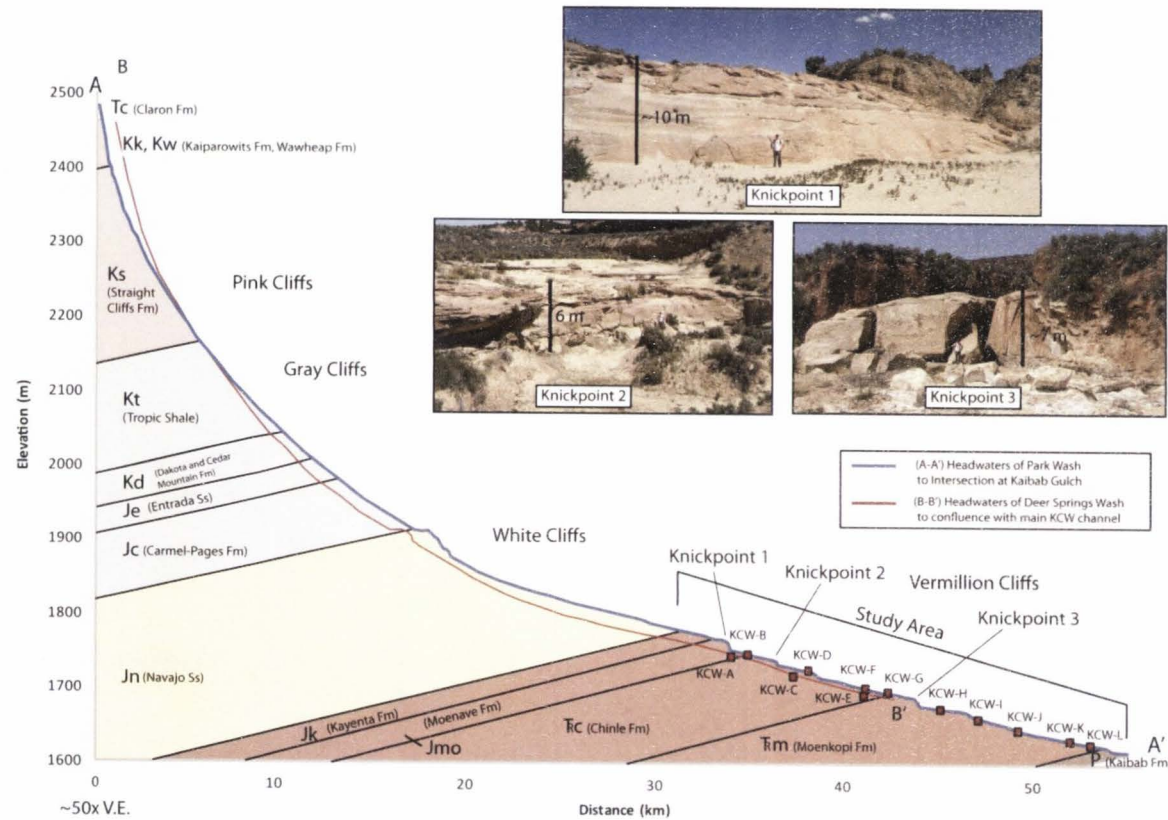


Fig. 3.2. Longitudinal profile of KCW from the headwaters of Park Wash to the intersection of Kaibab Gulch (A-A') and from the Headwaters of Deer Springs Wash to the confluence with the main KCW trunk stream (B-B'). KCW heads in Tertiary Claron Fm and ends in Triassic Moenkopi Fm. Three bedrock knickpoints are evident in KCW and range from 6-10 m in height.

formations (e.g. Jc) to a more resistant lithology (e.g. Jn) and exposes >6 m tall knickpoints (Fig. 3.2).

Structural features within and surrounding the KCW catchment include folds initiating from the Sevier orogeny, early-Tertiary faults formed during the Laramide Orogeny, and continued faulting following basin and range extension starting around 15Ma (Doelling et al., 2000). The most significant features include the Paunsaugunt Fault and East Kaibab monocline. The Paunsaugunt Fault is a high-angle normal fault that extends from northern Arizona through central Utah (Doelling et al., 2000) and crosses KCW near the channel head of DSW. The East Kaibab monocline, expressed as the Cockscomb near KCW, is a prominent, northeast trending feature that is locally faulted. Neither of these features crosses the project study area (Fig. 3.3) and no Quaternary activity has been reported along the several small-scale faults that exist within the catchment of the KCW.

Climate within the region is semi-arid and two Cooperative Observation Program (COOP) weather stations upstream and downstream within the Paria River drainage indicate mean maximum and minimum annual temperatures (ca. 2001-2012) ranging from 22.3°C to 5.5°C (Paria RS COOP) and 13.7°C to -4.2°C (Bryce Canyon Nat'l Park COOP) at 1341 m and 2413 m elevation respectively. Additionally, differences in mean annual precipitation for these same sites are indicative of an orographic influence (Paria RS COOP = 198.1mm, Bryce Canyon Nat'l Park COOP = 364.7mm). Climate in the region is also typified by a bimodal precipitation regime with the majority of precipitation falling primarily during the winter and late summer to fall (Fig. 3.4). Discharge records from the Paria River gage at Lee's Ferry (USGS 09382000), downstream of KCW, indicate early spring and late summer peaks in discharge (Fig. 3.4). Moisture within the region is generated from North Pacific frontal storms during the winter (Dec-March), convective thunderstorms during the late summer (July-Sept), and cut-off tropical storms and/or monsoons during the fall (Sept-Nov). Variations in climate throughout the region are a function of fluctuations in sea-surface temperature (SST), atmospheric pressure, and atmospheric

circulation patterns and operate on short, seasonal (El Niño, La Niña, North American Monsoon, tropical cyclones) and multi-decadal (Pacific Decadal Oscillation) timescales (Hereford , 2002; Sheppard et al., 2002).

Interannual fluctuations in sea-surface temperatures and pressures in the tropical Pacific, related to ENSO (El Niño-Southern Oscillation), produce interannual shifts in precipitation in southern Utah and surrounding regions (Hereford et al., 2002; Sheppard et al., 2002). A warming of Pacific SST (El Niño) tends to bring wet winters the southwest and an increase in streamflow whereas a cooling of Pacific SST (La Nina) typically accounts for drier winters (Cayan et al., 1999). However, the strength and timing of ENSO activity within this region are often variable (Sheppard et al., 2002). The Pacific Decadal Oscillation (PDO) can also account for multi-decadal precipitation variability across the Colorado Plateau (Hereford et al., 2002). Specifically, PDO and ENSO climate patterns are related both temporally and spatially such that positive and negative phases of the PDO (warmer or cooler NPO) can influence the effect of El Niño-related activity in the southwestern U.S. (Sheppard et al., 2002).

One of the main climatic features of warm-season precipitation in the southwestern United States is the North American Monsoon (NAM). Although it is most noticeable throughout Arizona and New Mexico, the effects of the NAM are evident throughout the entire southwest and include the central region of the Colorado Plateau, which includes the KCW drainage area (Sheppard et al., 2002). By mid-July, repositioning of the Intertropical Convergence Zone (ITCZ) into the northern hemisphere allows prevailing winds to transport moisture from the Gulf of Mexico and/or the Gulf of California over the plateau (Poore et al., 2005). Additionally, during the late summer and early fall, tropical cyclones are capable of penetrating the southwest and delivering extreme amounts of precipitation over the plateau (Sheppard et al., 2002).

Vegetation is sparse along the KCW system and primarily consists of spruce and pine in the higher elevations and sagebrush, pinyon pine, and juniper across the broad alluvial valley that spans the study area. Riparian vegetation is typically lacking becomes very dense within several

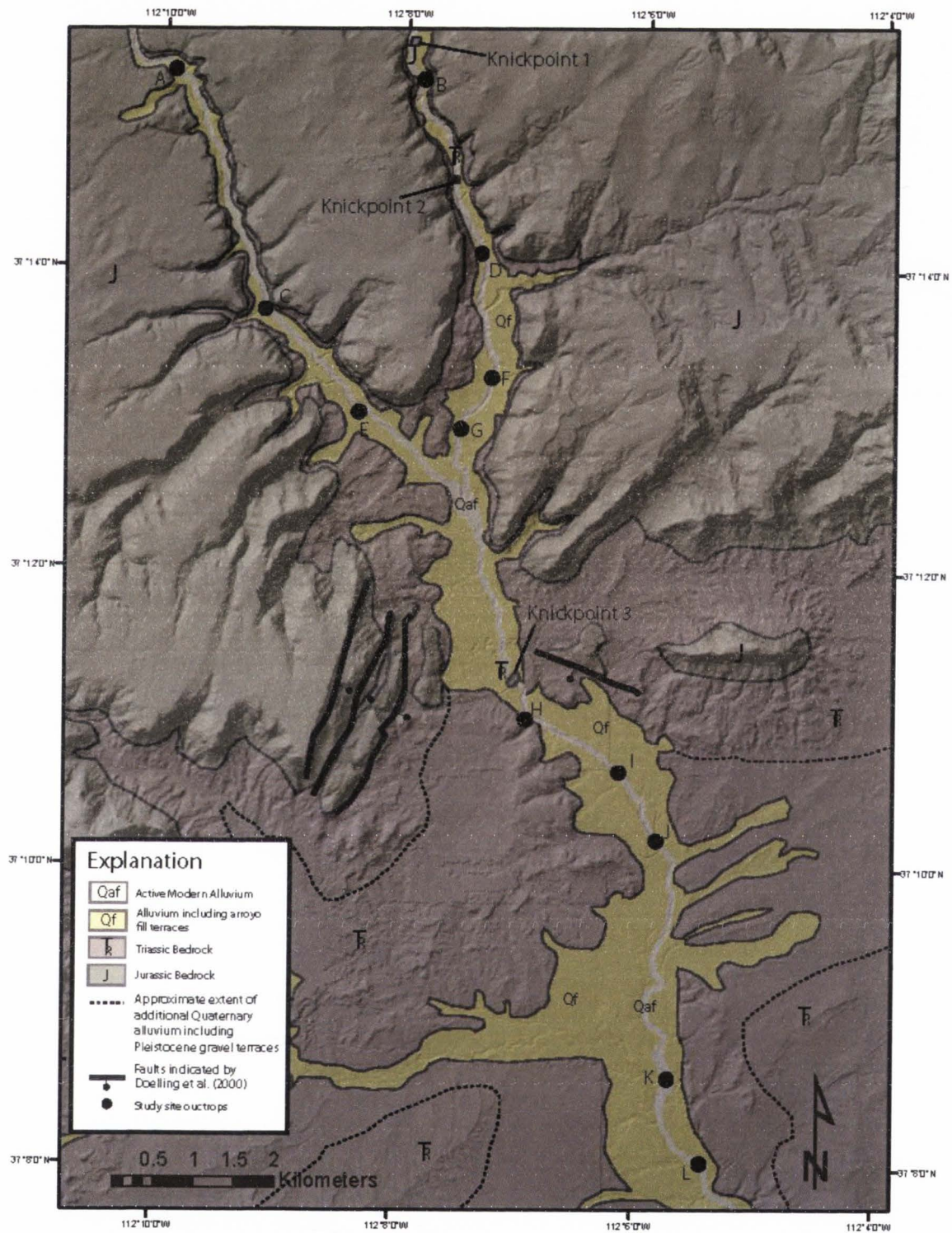


Fig. 3.3. Geomorphic map of KCW displaying underlying Jurassic and Triassic bedrock and overlying Pleistocene terrace gravels and Quaternary alluvial sediments.

## Daily Discharge, Lee's Ferry Paria River Gage (1923-2013)

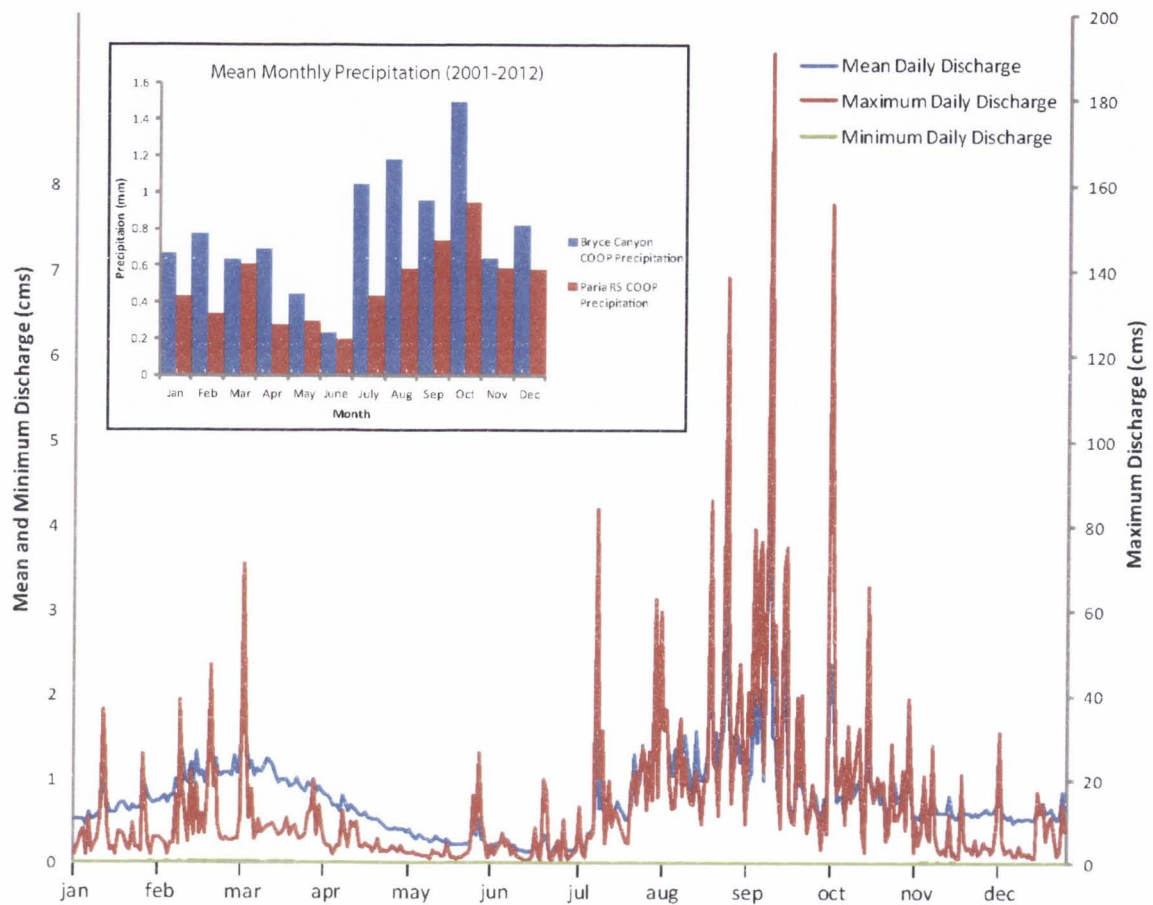


Fig. 3.4.(a) Mean daily discharge at the Lee's Ferry Paria River Gage from 1923-2013. Data suggest a bimodal precipitation regime with the largest flows occurring during the early spring and summer seasons. (b) Mean daily precipitation from the Bryce Canyon COOP and Paria RS COOP.

meander bends beginning at the confluence of Deer Springs Wash and Park Wash, and along smaller tributaries at the south end of the study area.

The ongoing arroyo cut-fill activity in KCW has limited the effect of soil-formation processes within alluvial deposits resulting in widespread, but discernible entisols. Within the KCW study area, these soils may occur on top of the youngest alluvial terraces or as buried soils inset between alluvial deposits. Since these incipient soils have formed in valley-fill alluvium, they can be used as stratigraphic markers of a hiatus in sedimentation.

### *3.2.2 Previous Work in KCW and Regional Drainages*

Past research in Kitchen Corral Wash and surrounding regional drainages has focused on constructing alluvial histories to help test hypotheses of the mechanisms leading to arroyo cutting and filling. As mentioned earlier, Hereford (2002) examined the stratigraphic and geomorphic relationships between valley-fill packages exposed within arroyo walls in the Paria River basin, including KCW, to constrain the timing of reach-wide alluviation and degradation events. Using a combination of tree-ring chronologies from partially buried juniper trees, Kayenta Anasazi potsherds, and radiocarbon dating of charcoal deposits within alluvium, Hereford (2002) constrained the ages of three alluvial packages within KCW (termed younger, intermediate and older alluvium) on the basis of their stratigraphic relationships. Hereford (2002) recognized that the youngest valley-fill alluvium (ca. A.D. 1400-1880) was correlative with Holocene alluvium observed and dated elsewhere on the Colorado Plateau (Fig. 3.5a), such as the "Naha alluvium" in the Black Mesa region (Hack, 1942) and post-Bonito alluvium in Chaco Canyon (Hall, 1977). Moreover, Hereford (2002) recognized that the timing of this regional aggradational episode was nearly coincident with the Little Ice Age (LIA) climate anomaly, a regionally cooler period interpreted to have decreased high flow events and increased sediment yield from hillslopes due to below normal precipitation. In addition to this period of aggradation, Hereford (2002) provided evidence for region-wide prehistoric (ca. A.D. 1200-1400) and historic (post-1880)



arroyo cutting, which he attributed to increased flooding events during the Medieval Climate Anomaly (MCA) and increased ENSO activity at the end of the LIA.

Harvey et al. (2011) revisited KCW and identified four episodes of Holocene aggradation and incision based on stratigraphic mapping from two study sites and ages derived from alluvial deposits using AMS radiocarbon and OSL dating methods. The youngest alluvial package (package IV) was deposited between  $\sim 0.7$ - $0.15$  ka and correlates with Hereford's "younger" alluvium as well as other regional fills of the same age (e.g. post-Bonito, Naha alluvium, and others). The next oldest fill (package III) was not dated, the age of package II ( $\sim 1.2$ - $2.0$  ka) is not tightly constrained, and the oldest fill (package I) has an age range of  $2.8$ - $2.15$  ka based on a combination of AMS radiocarbon and OSL samples. A meaningful correlation could not be made between packages III-I from Harvey et al. (2011) and the "intermediate" or "older" alluvium described by Hereford (2002) (Fig. 3.5b).

Another alluvial deposit, comprising the "settlement terrace and alluvium," was identified along the upper alluvial valley of the Virgin River in Zion National Park (Hereford et al., 1996a), and is correlative to the youngest valley-fill alluvium of Hereford (2002). In this study, Hereford et al. (1996a) linked natural variability in stream flow and sediment discharge to the geomorphic history of the Virgin River. Using repeat photography, historic records, and dendrochronology, Hereford et al. (1996a) identified three primary terrace deposits (prehistoric, settlement, and modern) whose deposition was interrupted by two periods of incision, similar to those identified by Hereford (2002) within the Paria River basin. In addition, estimations of annual stream flow, measured from tree-ring growth and modern streamflow, linked periods of anomalously high stream flow with incision and periods of low stream flow with aggradation.

Previous work on the near-by Escalante River and its tributaries, northeast of KCW, has also focused on reconstructing the timing of arroyo incision and aggradation events (e.g. Patton and Boison, 1986; Webb and Baker, 1987; Webb and Hasbargen, 1997; Hayden, 2011). Webb and Hasbargen (1997) suggest four episodes of prehistoric arroyo entrenchment at approximately

2ka, 1.5ka, 1ka, and 0.5  $^{14}\text{C}$  ka BP (1950) in the upper Escalante River. By identifying burned charcoal horizons, fossil mollusk shells, and alluvial pollen in the stratigraphy, the authors suggest that these prehistoric arroyo incision events often initiated during periods of low precipitation and relatively low groundwater tables. Studies of preserved alluvial terraces in tributaries of the lower Escalante River have produced mixed age results due to sediment increases from mass wasting (Coyote Gulch) or other intrabasinal controls such as land-use changes and local changes in bedrock erodibility (Patton and Boison, 1986). Most recently, Hayden (2011) reconstructed the timing of arroyo cut-fill cycles in the upper Escalante River using AMS radiocarbon and OSL methods and detailed sedimentary and stratigraphic descriptions. She recognized at least six arroyo cutting events since the middle Holocene, with incision occurring at  $\sim 4.4\text{-}4.2$  ka,  $\sim 2.6\text{-}2.4$  ka,  $\sim 1.8\text{-}1.5$  ka,  $\sim 1.0\text{-}0.9$  ka,  $\sim 0.5\text{-}0.4$  ka and during historic arroyo cutting in 1909 AD.

Nearly 40 km to the west of KCW, Kanab Creek, a tributary of the Colorado River, has also been recognized and studied for its historic and prehistoric arroyo cut-fill stratigraphy (e.g. Smith, 1990; Webb et al., 1991). Webb et al. (1991) provide one of the most comprehensive overviews of the historic channel cutting in the Kanab Creek arroyo, which he attributed to large-magnitude flood events. Historic and prehistoric arroyo cutting and filling events in the canyon reach of Kanab Creek have more recently been investigated by Summa (2009) and Summa-Nelson and Rittenour (2012). In these studies, four alluvial fills along the Kanab Creek drainage were identified, with periods of entrenchment at  $\sim 3.5$  ka,  $\sim 2.2$  ka,  $\sim 1$  ka and post-1882 AD.

Ely (1997) reconstructed century-scale paleoflood records from multiple southwestern U.S. drainages, including Kanab Creek, the Paria River, and the Escalante River, which indicate a clustering of floods throughout the Holocene (Ely, 1997). These records show a sharp increase in flooding events around A.D. 1400 that is broadly coincident with a prehistoric period of arroyo cutting (Ely, 1997; Hereford, 2002). Similar to Hereford (2002), Ely (1997) also suggests that periods of increased flood frequency might occur near the transition from one climate regime to

another, such as MCA to LIA, and could be linked to the frequency and intensity of ENSO activity. However, Harvey et al. (2011) suggest that paleoflood records from Ely (1997) are disparate and may not be correlative to the records found in arroyo systems, such as KCW.

### **3.3 Methods**

#### *3.3.1 Stratigraphy and Sedimentologic Descriptions*

In order to test if episodic arroyo cutting and filling has been regionally near-synchronous, this research explores the stratigraphic cut-fill relationships, sedimentology, and ages of KCW arroyo-wall outcrops. Approximately 28 km of the KCW alluvial channel, starting at the intersection of U.S. Highway-89 and including Park Wash and Deer Springs Wash, was traversed in 2011 and 2012 in order to identify outcrops with the best expressed arroyo cut-fill architecture. Aside from well-expressed stratigraphy, each outcrop chosen for sampling and detailed description was >2m in height and displayed at least on near-vertical buttress unconformity with a colluvial wedge at the base. These criteria were chosen in order to reduce the chances of selecting a channel migration deposit. A total of 12 study sites were identified, which included three arroyo outcrops located in Deer Springs Wash (KCW-A, KCW-C, and KCW-E), four arroyo outcrops located in Park Wash (KCW-B, KCW-D, KCW-F, and KCW-G), and five arroyo outcrops located in the main-stem KCW stream (KCW-H, KCW-I, KCW-J, KCW-K, and KCW-L) (Fig. 3.1; 3.3).

The alluvial stratigraphy and sedimentology within each arroyo outcrop was extensively delineated and described. Outcrops were photographed with a high-resolution camera and locations were marked using a high-precision hand-held GPS. Each outcrop exposure was then sketched in detail and/or photographs were annotated. Field drawing and annotated photos were used to create detailed stratigraphic panels of each outcrop. Additionally, the arroyo-wall stratigraphy was separated into stratigraphic units. These stratigraphic units were initially selected in the field were used to more easily delineate and describe the outcrops. Stratigraphic

units were selected based on similar packages of sediment (e.g. sediment source and thickness) or distinct erosional surfaces.

Sedimentologic descriptions of alluvial fills from each outcrop were compiled by noting bed thickness and geometry, Munsell color, grain size and sedimentary structures, grading and sorting, bioturbation or evidence of soil development, and character of the basal contact. Key depositional facies and facies associations were then identified and a list of the most frequently encountered depositional facies was compiled (see Chapter 2). Additionally, interpretations of depositional environments for beds within each alluvial-fill package were made using bed geometry and facies analyses. Finally, the stream profile of KCW (Fig. 3.2) from its headwaters in Park Wash to its intersection at Kaibab Gulch and from the headwaters of Deer Springs Wash to the confluence with the main KCW channel was interpolated using an autocorrelated 5 m digital elevation model. The stream line used for profile interpolation was based on an identification of the active channel as defined by a flow accumulation dataset created in ArcGIS 10.1.

### 3.3.2 *Geochronology*

Age control for KCW alluvial deposits was obtained using AMS radiocarbon and optically stimulated luminescence (OSL) dating. Using these dating techniques in tandem not only allowed for greater sampling opportunities in the field, but has also provided a means for comparing the ages of alluvial deposits and reconciling aberrant results. In general, samples were collected from near the base or top of unconformity-bound alluvial fills.

### 3.3.3 *AMS Radiocarbon Dating*

Thirty-seven samples for radiocarbon dating were collected from KCW. Two additional radiocarbon samples used in this study were collected by Harvey et al. (2011) and three were collected by Hereford (2002). Charcoal was targeted for sampling because of its abundance

Table 3.2  
Summary of radiocarbon sample information and ages

Sample Number	Sample ID	Drainage Basin/Profile Site	Facies	<sup>14</sup> C Age	Error ±	Weighted Mean cal yr BP <sub>2010</sub> (rounded)	Error +/- (rounded)	Targeted Sample <sup>a</sup>	Stratigraphic Agreement/Disagreement <sup>b</sup>
14C-1	113985	A	St	2015	15	2020	40/60	CRL	A
14C-2	113986	A	Sr	365	15	480	80/160	CRL	A
14C-3	113981	B	Sh	500	15	580	20/10	CRL	A
14C-4	113989	B	St	1235	15	1240	80/130	CRL	A
14C-5	X24136	C	Fsmv	2460	40	2600	170/180	IAC	A
14C-6 <sup>c</sup>	X24137	C	St	49,400	4000	49,400	4000	IAC	D (CC)
14C-7	X24132	D	Sl	1488	38	1440	130/80	CRL	A
14C-8	X24133	D	Fsmv	466	37	570	60/40	CRL	A
14C-9	X24135	D	St	1208	38	1200	120/130	IAC	D (RD)
14C-10		D	Sl	not analyzed		not analyzed		IBB	
14C-11	113987	E	St	1420	15	1380	20/20	CRL	A
14C-12	X24138	E	St	879	38	870	100/110	CRL	A
14C-13	113988	E	Sl	140	15	200	140/140	CRL	A
14C-14	X24139	F	St	42,600	1600	42,600	1600	CRL	D (CC)
14C-15	X24140	F	Sr	609	37	660	60/60	CRL	A
14C-16	X24141	F	St	>45,700		>45,700		IAC	D (CC)
14C-17	X24134	G	St	1194	38	1180	140/130	CRL	A
14C-18	113982	G	Fl	665	15	680	50/60	AWD	A
14C-19		G	Sm	not analyzed		not analyzed		IRL	
14C-20		G	St	not analyzed		not analyzed		CRL	
14C-21	113984	G	Sl	3420	15	3730	40/40	CRL	A
14C-22	105792	H	Sl	3480	30	3820	70/60	CRL	A
14C-23 <sup>f</sup>		H	Sm	not analyzed		not analyzed		IAC	
14C-24	105793	H	Sm	1115	30	1080	40/50	CRL	A
14C-25 <sup>c</sup>	105794	H	Sm	2200	40	2280	120/210	IRL	D (RD)
14C-26	113983	H	Sr	3735	15	4140	70/90	CRL	A
14C-27	X24142	H	St	849	40	830	130/90	IAC	A
14C-28	105788	I	Sl	1755	30	1720	50/50	CRL	A
14C-29	X24144	I	St	46,600	2700	46,600	2700	CRL	D (CC)
14C-30 <sup>g</sup>	105789	J	Sh	>31700		>31,700		CRL	D
14C-31	105790	J	Sl	1730	30	1700	60/70	CRL	A
14C-32	105791	J	Fsmv	1860	30	1850	80/60	IAC	A
14C-33	X24143	J	St	2395	40	2520	240/120	CRL	D (RD)
14C-34	X24129	K	Fsmv	993	46	950	160/100	CRL	A
14C-35 <sup>c</sup>	X24130	K	St	2002	40	2010	140/80	IAC	D (RD)
14C-36	X24131	K	St	368	37	470	90/90	CRL	A
14C-37	X24145	L	Sl	46,700	2800	46,700		CRL	D (CC)
14C-38 <sup>d</sup>	Beta-256838	I	Sl	610	40	660	60/80	AWD	A
14C-39 <sup>d</sup>	Beta-256840	I	St/Sl	2220	40	2300	60/90	CRL	A
14C-40 <sup>e</sup>		Park Wash		4330	40	5000	250/380		
14C-41 <sup>e</sup>		Park Wash		5650	35	6490	70/110		
14C-42 <sup>e</sup>		Park Wash		6320	80	7300	180/220		

<sup>a</sup> Targeted samples for AMS radiocarbon dating: CRL = Charcoal-rich Lens, IAC = Isolated Angular Charcoal, IBB = Isolated Burned Branch, IRL = Isolated Round Charcoal, AWD = Angular Woody Debris

<sup>b</sup> Notes if Weighted Mean calibrated radiocarbon age (BP<sub>2010</sub>) of each radiocarbon sample Agrees (A) or Disagrees (D) with stratigraphic relationships or OSL ages. Disagreement interpreted as CC = Cretaceous Coal, RD = Redeposited Sample.

<sup>c</sup> Samples Collected from within or near a colluvial deposit.

<sup>d</sup> Samples originally collected in Harvey (2009). Also used in Harvey et al. (2011) and this study.

<sup>e</sup> Samples collected from Hereford (2002) in years BP and calibrated with the IntCal dataset (Reimer et al., 2009).

<sup>f</sup> Sample did not undergo AMS measurement because it did not survive pretreatment chemistry

<sup>g</sup> Finely disseminated pieces of charcoal in deposit. Large uncertainty due to small sample size (0.056 mg) or possible mixing of Cretaceous coal.

within each of the aggradational fill packages, allowing for selective instead of opportunistic sampling. Due to potential age inaccuracies from charcoal redeposition, and other sources of error detailed in Chapter 2, sampling targeted material typically consisted of large concentrations of charcoal or thin lenses of charcoal separating alluvial deposits. In a few instances, isolated (detrital) charcoal fragments were targeted where sediment for OSL dating was poor and no other sources of charcoal or woody debris were available. However, detrital charcoal was avoided if present in massive deposits and only collected if sedimentary structures were evident. Once a charcoal-rich layer was targeted, attention was paid to the size and angularity of the charcoal in order to reduce the odds of collecting redeposited material.

Sixteen of the 37 samples collected were sent to the UC Irvine Keck AMS Laboratory analysis and an additional seventeen samples were pretreated by the author at the University of Arizona NSF AMS Laboratory in Tucson and later analyzed by the AMS lab staff. One of the 37 radiocarbon samples was not analyzed because it did not survive pretreatment chemistry and three other samples were deemed unnecessary for analysis. Excess radiocarbon samples were archived in labeled, glass vials and are available for further analysis if necessary. Sample ages were converted from radiocarbon years to calendar years  $BP_{2010}$  using Calib 6.0 and the IntCal09 dataset (Reimer et al., 2009). Results are reported in  $BP_{2010}$  as a maximum probability age and asymmetric 2-sigma error (Table 3.2). Reporting as cal. kyr  $BP_{2010}$  allows for a direct correlation to ages derived from OSL dating.

#### 3.3.4 *Optically Stimulated Luminescence (OSL) Dating*

Optically stimulated luminescence (OSL) dating provides an age-estimate of the last time sediment was exposed to light prior to burial (Huntley et al., 1985). During transport, quartz or feldspar grains are exposed to sunlight (or heat) and their luminescence signal is reset (bleached) when electron charges stored in mineral defects are released (Aitken, 1998). Following deposition, defects in the crystal lattice begin to accumulate electrons produced by ionizing

radiation from surrounding sediments and from cosmic rays, which cause the luminescence signal to grow over time. The dose-rate environment can be measured by using multiple techniques, such as high-resolution gamma spectrometry or ICP-MS (this study), and the rate at which energy is absorbed from the radiation (dose rate) can be determined through a set of conversion factors (Aitken, 1998; Guerin et al., 2011). The natural OSL signal of a sample is compared with an OSL signal that is derived from given doses of artificial laboratory radiation in order to determine the equivalent dose ( $D_e$ ), which is the radiation required to produce a luminescence signal equal to the natural signal. The mean or other statistical analyses of the  $D_e$  obtained from many aliquots or individual grains, measured in grays (Gy), is then divided by the dose rate (Gy/ka) in order to obtain the age of a sample (Aitken, 1998).

OSL dating is used in concert with AMS radiocarbon dating in this study because samples can be collected from any sandy arroyo deposit not otherwise containing charcoal or organic materials. However, as with radiocarbon dating, OSL dating has its own set of problems that can lead to erroneous ages. In fluvial environments, such as KCW, the most challenging problem to overcome is the potential for incomplete resetting of the luminescence signal, commonly referred to as partial bleaching (see reviews by Wallinga, 2002; Rittenour, 2008). Partially bleaching may occur for a number of reasons in dryland fluvial systems, such as KCW, due to flashy flow and high-magnitude discharge events, light attenuation through the water column, and/or rapid deposition (see Chapter 2). In fact, a previous study from KCW (Harvey et al., 2011) and studies in nearby drainages (Hayden, 2011; Summa-Nelson and Rittenour, 2012) have identified partial bleaching as a significant problem. Partial bleaching can lead to significant overdispersion and high positive skew of equivalent dose values and might contribute to significant age overestimations (e.g. Wallinga et al., 2001; Murray and Olley, 2002; Rittenour, 2008).

The possibility of partially bleached sediments in KCW necessitated preferential collection of OSL samples based on guidelines set forth in Chapter 2 and from an earlier study by

Summa-Nelson and Rittenour (2012). Special attention was paid to the sedimentology and stratigraphy of alluvial fills targeted for sample collection. First, sampling preference was given to thin (>0.4m) ripple-cross laminated sand beds, which were indicated by Summa-Nelson and Rittenour (2012) to have more likely been exposed to adequate sunlight. Beds displaying sedimentary structures indicative of rapid deposition and/or high sediment concentrations were avoided because they likely had limited sunlight exposure prior to burial. Additionally, bioturbated beds and soils were avoided because of the possibility of sediment mixing.

Twenty-nine OSL samples (two from Harvey et al., 2011) were collected from the 12 arroyo cut-fill outcrops in KCW and processed at the USU Luminescence Lab (Table 3.3). Samples were wet sieved to specific grains size fractions (150-250  $\mu\text{m}$  or 180-250  $\mu\text{m}$ ), and pretreated with 10% hydrochloric acid to dissolve carbonates and a base wash (bleach) to remove organics. Heavy minerals were separated using sodium polytungstate (2.7  $\text{g}/\text{cm}^3$ ), and then treated with concentrated HF for 90 minutes to remove feldspars and etch quartz grains and re-sieved at 75 $\mu\text{m}$  to remove partially dissolved feldspars.

Of the 29 OSL samples collected, seventeen were chosen for age-determination. The two samples from Harvey et al. (2011) were analyzed using the small-aliquot single-aliquot regenerative (SAR) technique of Murray and Wintle (2000). All other samples were analyzed using the single-grain SAR protocol. Single-grain (SG) analysis has been widely applied to partially bleached sediments because it allows grains with different bleaching histories to be identified (Duller, 2008). In addition to SG dating, the minimum-age-model (MAM) statistical analysis of Galbraith et al. (1999) was applied to SG  $D_e$  distributions with significant overdispersion values and positive skew to help accurately isolate the population of grains that were bleached prior to deposition. Those samples without significant overdispersion or positive skewness were analyzed using the central-age-model (CAM) of Galbraith et al. (1999). SG OSL analysis and age data are presented in Table 3.3.

Table 3.3  
Preliminary single-grain quartz OSL ages

USU Lab ID	Study Site	Fill	Facies <sup>a</sup>	OSL age (cal ka)			Age Model
USU-1176	B	Qf4	Sh	<b>0.74</b>	±	<b>0.19</b>	MAM-4
USU-1192	E	Qf4	St	<b>0.92</b>	±	<b>0.20</b>	MAM-4
USU-1187	C	Qf4	St	<b>1.14</b>	±	<b>0.36</b>	MAM-3
USU-1026	J	Qf4	Sl	<b>1.29</b>	±	<b>0.37</b>	MAM-4
USU-1189	A	Qf3	Sl	<b>1.38</b>	±	<b>0.64</b>	MAM-4
USU-1181	G	Qf4	Sl	<b>1.47</b>	±	<b>1.08</b>	MAM-4
USU-1028	J	Qf3	Sl	<b>1.52</b>	±	<b>0.74</b>	MAM-4
USU-1103	H	Qf4	Sh	<b>1.56</b>	±	<b>0.37</b>	MAM-4
USU-1027	J	Qf3	Sl	<b>1.58</b>	±	<b>0.30</b>	MAM-4
USU-1029	J	Qf5/Qf5 <sup>1</sup>	Sm	<b>1.67</b>	±	<b>0.35</b>	MAM-4
USU-1178	D	Qf3	Sr	<b>1.77</b>	±	<b>0.31</b>	MAM-4
USU-1177	B	Qf5	Sh	<b>2.02</b>	±	<b>1.09</b>	MAM-4
USU-530 <sup>b</sup>	I	Qf3	Sl	<b>2.25</b>	±	<b>0.85</b>	CAM
USU-531 <sup>b</sup>	I	Qf2	St	<b>2.82</b>	±	<b>0.32</b>	CAM
USU-1194	F	Qf2	St	<b>2.97</b>	±	<b>0.70</b>	CAM
USU-1101	H	Qf1	Sl	<b>4.21</b>	±	<b>1.46</b>	MAM-4

<sup>a</sup> Facies based on descriptions from Miall (2000). See Table 2.1 in Chapter 2 for descriptions.

<sup>b</sup> Small aliquot ages from samples collected by Harvey (2009).

### 3.4 Results

#### 3.4.1 *Stratigraphy and Sedimentology of KCW*

The alluvial stratigraphy of KCW is characterized by very fine- to coarse-grained sand deposited as either broadly tabular or lenticular beds. Colors are primarily 10YR (yellowish-brown), 2.5YR (red), and 5R (reddish-brown). These distinct colors are a result of sediment being derived from upstream sources versus more local bedrock surrounding the study reaches and allowed individual beds and units to be more easily distinguished. The yellowish-brown sand units are fine- to medium-grained, well-sorted, sub- to well-rounded, and composed of frosted quartz grains predominately derived from the Navajo Sandstone Fm upstream of the field area (Fig. 3.2). The red to reddish-brown sand units are poorly to moderately sorted and composed of very fine- to medium-grained, sub-angular to sub-rounded sands with variable amounts of clay and silt. These are predominately derived from bedrock lithologies proximal to the study area including the Moenave, Chinle, and Moenkopi Formations. In agreement with Harvey (2009), the yellowish-brown beds are considered mainstem sediments because of their upstream source whereas the red and reddish-brown sand were likely sourced from smaller tributaries of the mainstem.

Arroyo-wall exposures vary in height. Those located directly downstream of a knickpoint are the tallest (~8-12m), and sites located directly upstream of a knickpoint and in the downstream reach of KCW are the shortest (~2-5m). Consequently, the tallest arroyo-wall exposures were the most helpful in reconstructing the arroyo cut-fill stratigraphy of KCW and identifying the sedimentary facies in alluvial fills.

A total of ten sedimentary facies were identified in KCW and are primarily defined by their grain size and sedimentary structures, which are explicitly described in Chapter 2. In this chapter, three depositional facies associations that are similar those described by Harvey et al. (2011) have been identified and include channel-bottom (CB), channel-margin (CM), and valley-surface (VS). Additionally, two new subsets of these depositional facies associations were also

identified and include channel-margin slackwater (CMs) and valley-surface colluvial wedges (VSc).

Channel-bottom (CB) deposits are commonly associated with the basal stratum and include thalweg or other axial channel deposits. These deposits are relatively coarse and include matrix or clast-supported pebble-gravel and medium- to coarse-grained sand that are often horizontally bedded (Gh) or crossbedded (Gt). They usually have a lenticular geometry and, because they are deposited during high-energy scour-fill events in the active channel, may be imbricated.

The channel-margin (CM) facies association is the most abundant in the arroyo-wall stratigraphy and are primarily composed of tabular to broadly lenticular, laterally extensive, very fine- to coarse grained sand that are deposited adjacent to the main channel thalweg or as overbank sheet-flows. Upper flow regime sediments may be deposited as trough cross-bedded (St), ripple cross-bedded (Sr) or as massive sand (Sm) deposits whereas low flow regime sediments may be low-angle crossbedded (Sl) or horizontally bedded (Sh) sand. Massive sand deposits are generally very fine- to medium-grained sands, but may also contain variable amounts of clay, silt, or even coarse-grained sands depending on the source of the alluvium. In addition, thick sand deposits may be capped with thinly bedded silty sand (Fl) that was deposited during a waning flow. Because these channel-margin deposits are usually associated with vertical accretion, they tend to display broadly tabular bedding geometries with thicknesses that most often range from thin (>20cm) to sub-meter scale.

Within the channel-margin but distal to the axial channel, deposits may be composed of thin, very fine-grained laminated sands and variegated clay beds (Fsmv) or as very fine to fine-grained massive sands (Sm). These beds are interpreted to have been deposited in quite water settings and are generally identifiable as floodplain slackwater deposits (CMs). CMs deposits also display a broadly tabular geometry that may be continuous for tens of meters. As CMs deposits are not part of the active channel, they are often subject to bioturbation or soil formation

and may sometimes appear as structureless massive sand deposits (Sm) or contain incipient soils (P) that include roots and organics.

The valley-surface (VS) facies association is identifiable as either hillslope or eolian sediments that were deposited outside of the channel-margin or, more commonly, as incipient soils where the valley floodplain was stable for an extended period. Incipient soils are devoid of sedimentary structures due to considerable bioturbation, and are composed of variable amount of clays, silts, and sands. Hillslope are generally massive sand (Sm) resulting from scour-fill deposition at the valley surface, while eolian sediments are primarily fine-grained and typically cap older incipient soils.

The valley-surface facies association has been subdivided to identify colluvial wedge (VSc) deposition at the base of a buttress unconformity. These deposits are primarily composed of clays, silts, and very fine- to coarse-grained sands that have no sedimentary structures and contain gravel- to cobble-sized rip-up clasts and blocks of cohesive older sediment. These deposits are commonly identified as colluvial wedges that are generally derived from valley surface alluvium and deposited at the toe of paleoarroyo walls following incision. These deposits are similar to a modern mass failure deposits at the base of arroyo-wall exposures. The presence of these VSc deposits at the toe of an arroyo is a good indication that the arroyo surface was stable for a significant period. This helps discern true arroyo exposures from channel migration deposits.

#### 3.4.2 *Geochronology*

Thirty-five AMS radiocarbon (plus two compiled from Harvey et al., 2011 and 4 from Hereford, 2002) and 17 OSL ages were produced for this study. Nearly all of the radiocarbon samples returned ages that are stratigraphically consistent (Table 3.2). However, nine radiocarbon ages revealed evidence of charcoal reworking or the analysis of Cretaceous coal (see Ch.2). Additionally, every OSL sample showed evidence of partial bleaching, which necessitated using

the SG dating technique for analyses of all samples and largely relied on the MAM statistical analysis of Galbraith et al. (1999) to calculate De values (Table 3.3). In general, radiocarbon and OSL ages suggest the KCW cut-fill sequences are middle to late Holocene in age, ranging from ~7.3 to 0.2 ka.

### 3.4.3 *Chronostratigraphic Observations and Interpretations*

Identification of alluvial fill packages was primarily based on cross-cutting relationships and the presence of buried soils, and secondarily based on stratigraphically consistent ages from AMS radiocarbon and OSL results. Five Holocene-aged aggradational fill packages from this study and one older unit dated and described by Hereford (2002) have been identified in the KCW study area. This is more than the three aggradational packages identified by Hereford (2002) and the four aggradational packages identified by Harvey et al. (2011). Based on a recalibrated radiocarbon age from Hereford (2002), the oldest fill package began to aggrade prior to  $7.30^{+0.18}_{-0.20}$  cal kyr BP<sub>2010</sub>, whereas the youngest fill package stopped aggrading prior to the ~1880-1920 AD arroyo entrenchment. The following sections describe the key stratigraphic and sedimentologic observations and deposit ages at each of the 12 described arroyo outcrops. Additionally, stratigraphic columns and sedimentary descriptions are found in Appendix B. The GPS location of each study site is indicated in Table 2.4 of Chapter 2.

### 3.4.4 *KCW-A Observations*

Outcrop KCW-A is a north-facing arroyo wall located ~18km upstream from Kaibab Gulch in the Deer Springs Wash tributary of KCW and ranges from 7.5 to 5.2 m in height (Figs. 3.1 and 3.6). The lower ~2.5 m of the outcrop is obscured by unconsolidated sediment and a relatively shallow-dipping buttress unconformity separates two alluvial fill packages. The oldest alluvial fill is located upstream of the unconformity while the youngest fill is located on the downstream side. Sediments deposited within each of these alluvial fills are primarily hues of

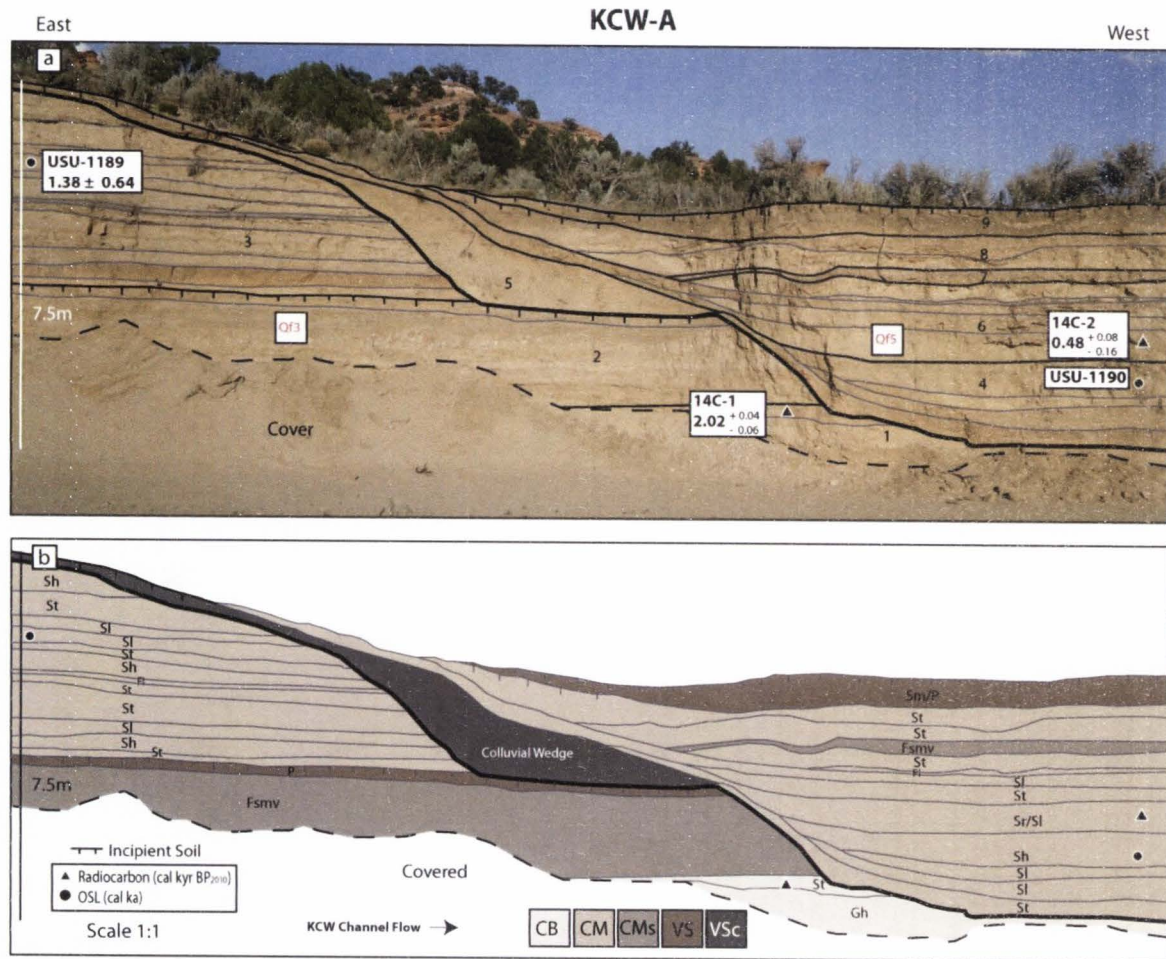


Fig. 3.6. Study site KCW-A showing a 7.5 m tall arroyo wall with evidence of two aggradation phases (Qf3, Qf5) separated by an incision event with (a) radiocarbon and OSL age results and (b) stratigraphic facies and depositional facies associations. See Fig. B-1 in Appendix B for detailed sedimentary descriptions and stratigraphic columns from each fill.

10YR, range from very fine- to medium-grained sand with few thin silt and clay beds (Fig. B-1), and are interpreted to be derived from upstream Jn sandstone and from minor amounts of local bedrock units (e.g. Jk, Jmo). The base of the oldest alluvial fill consists of gravelly channel-bottom (CB) and channel-margin (CM) deposits capped by channel-margin slackwater (CMs) deposits (Fig. 3.6). The upper 3.7 m contains 12 thin, broadly tabular beds of low-angle crossbedded (Sl), horizontally bedded (Sh), and trough crossbedded (St) sand that contain a minor presence of bioturbation and roots upsection without clear evidence of soil formation. A 14C sample collected at the base of this older unit produced an age of  $2.02^{+0.04}_{-0.06}$  cal kyr BP<sub>2010</sub>, while an OSL sample (USU-1189) collected near the top of the fill yields a preliminary age of  $1.38 \pm 0.64$  ka (Tables 3.2 and 3.3).

The inset younger alluvial package is a ~5.2 m thick and is composed of channel-margin, broadly tabular, fine- to medium-grained, St, Sl, or Sh sands. A number of these beds onlap a small colluvial wedge that drapes the buttress unconformity, and the uppermost bed in this deposit shows evidence of incipient soil formation. An OSL sample (USU-1190) was collected at the base of the fill but was not analyzed, and a radiocarbon sample (14C-2) collected ~3 m below top of the arroyo-wall surface yields an age of  $0.48^{+0.08}_{-0.16}$  cal kyr BP<sub>2010</sub> (Table 3.2).

#### 3.4.5 *KCW-A Interpretations*

Study site KCW-A shows stratigraphic evidence for two episodes of aggradation interrupted by a period of arroyo incision (Figs. 3.6 and B-1). Based on radiocarbon sample 14C-1, it appears that this section of the DSW reach was incised down to or near the modern channel and the older alluvial fill began to aggrade around  $2.02^{+0.04}_{-0.06}$  cal kyr BP<sub>2010</sub> and continued until after  $\sim 1.38 \pm 0.64$  ka. A buttress unconformity indicates at least 5 m of entrenchment sometime prior to  $0.48^{+0.08}_{-0.16}$  cal kyr BP<sub>2010</sub>, and subsequent deposition of the younger alluvium. The end of youngest aggradation is indicated by the presence of a massive sand deposit with evidence of incipient soil formation (Fig. 3.6).

### 3.4.6 *KCW-B Observations*

Site KCW-B is a 9 m tall arroyo wall located in the Park Wash (PW) tributary of the main KCW trunk stream (Fig. 3.7). This west-facing arroyo wall study site is located approximately 16 km upstream of Kaibab Gulch and less than 1 km downstream from a 7.5 m tall bedrock knickpoint (Figs. 3.1 and 3.2). It displays two alluvial fill packages that primarily contain broadly tabular beds composed of 10YR and 2.5YR hued, very fine- to medium-grained sand (Fig. B-2). The older alluvial fill contains broadly tabular, Sl, St, and Sh sands (Fig. 3.7). A radiocarbon sample (14C-4) was collected from at the base of the fill and yields an age of  $1.24^{+0.08}_{-0.13}$  cal kyr BP<sub>2010</sub> (Table 3.2), and an OSL sample was collected ~1 m above this but was not analyzed. Additionally, an OSL sample (USU-1176) was collected ~1.5 m below the valley surface gives a preliminary age of  $0.74 \pm 0.19$  ka (Fig. 3.7; Table 3.3).

The buttress unconformity that separates the older alluvial fill from the younger alluvial fill is completely covered with a thick (~4.5 m) colluvial wedge (VSc) containing an abundance of clay rip-up clasts and organic material. The younger alluvial fill onlaps this colluvial wedge and contains broadly tabular finely-laminated sands (Fl) and ripple crossbedded sand (Sr) interbedded within St, Sl, Sh, beds and a CMs deposit of variegated clay, silt and sand (Fsmv) (Figs. 3.7 and B-2). An OSL sample (USU-1177) extracted near the base of this fill yields a preliminary age of  $2.02 \pm 1.09$  ka, and a radiocarbon sample (14C-3) collected at ~3.9 m depth returns an age of  $0.57 \pm 0.06$  cal kyr BP<sub>2010</sub> (Tables 3.2 and 3.3).

### 3.4.7 *KCW-B Interpretations*

The stratigraphy in KCW-B indicates two periods of alluviation interrupted by an episode of incision. Unlike KCW-A, the variable grains sizes and mixed population of red-colored sediments at this study site indicates a greater local and tributary source contribution. Based on radiocarbon and OSL age results, it appears that KCW had incised down to or below its current level prior to  $1.24^{+0.08}_{-0.13}$  cal kyr BP<sub>2010</sub> at this location (Fig. 3.7; Table 3.2). Channel-margin



aggradation followed this incision event and was nearly continuous until shortly after  $\sim 0.74 \pm 0.19$  ka. Between  $\sim 0.74 \pm 0.19$  ka and  $0.57 \pm 0.06$  cal kyr BP<sub>2010</sub> (Tables 3.2 and 3.3), an incision event lowered the channel back to near its current depth until aggradation resumed once again. The OSL sample (USU-1177) collected from the base of the youngest fill is stratigraphically inconsistent and is assumed to be an age overestimation due to partial bleaching. Further analysis is expected to refine this preliminary estimate.

#### 3.4.8 *KCW-C Observations*

Study site KCW-C is a 10.5 m tall, north-facing arroyo wall that is located in DSW approximately 14.5 km upstream from Highway-89 and Kaibab Gulch (Figs. 3.1 and 3.8). The cut-fill architecture of KCW-C shows two alluvial fill packages whose sediments are 10YR and 2.5YR hues. The older alluvial fill is  $\sim 5$  m thick and composed of CB, CM, CMs and VS deposits. These deposits contain basal lenticular beds of horizontally-bedded gravel (Gh), massive sand (Sm), Sl and St, and overlying broadly tabular interbeds of St, Sl, Sm, Fl, and Fsmv (Figs. 3.8 and B-3). Bioturbation, roots, and a loss of sedimentary structures give evidence of soil formation near the top of this deposit and may reflect a former land surface. A radiocarbon sample (14C-5) was collected near the base of this fill yields an age of  $2.60^{+0.17}_{-0.18}$  cal kyr BP<sub>2010</sub>, and an OSL sample (USU-1188) was collected near the top of this older fill but was not analyzed (Tables 3.2 and 3.3).

The younger inset alluvial fill is separated from the older fill by a buttress unconformity draped with a colluvial wedge (Fig. 3.8). This fill predominately consists of basal, lenticular, Gh, St, and Sl beds comprising the channel-bottom facies association. These are overlain by broadly tabular, CM and CMs deposits containing St, Sr, Fl, and Fsmv beds (Fig. B-3). At  $\sim 3$  m depth, a slackwater (Fsmv) deposit shows evidence of soil formation and is capped by a thick channel-margin sheetflow deposit that also has evidence of an incipient soil at the top of the arroyo-wall surface. A radiocarbon sample collected at the base of the deposit and near the toe of the

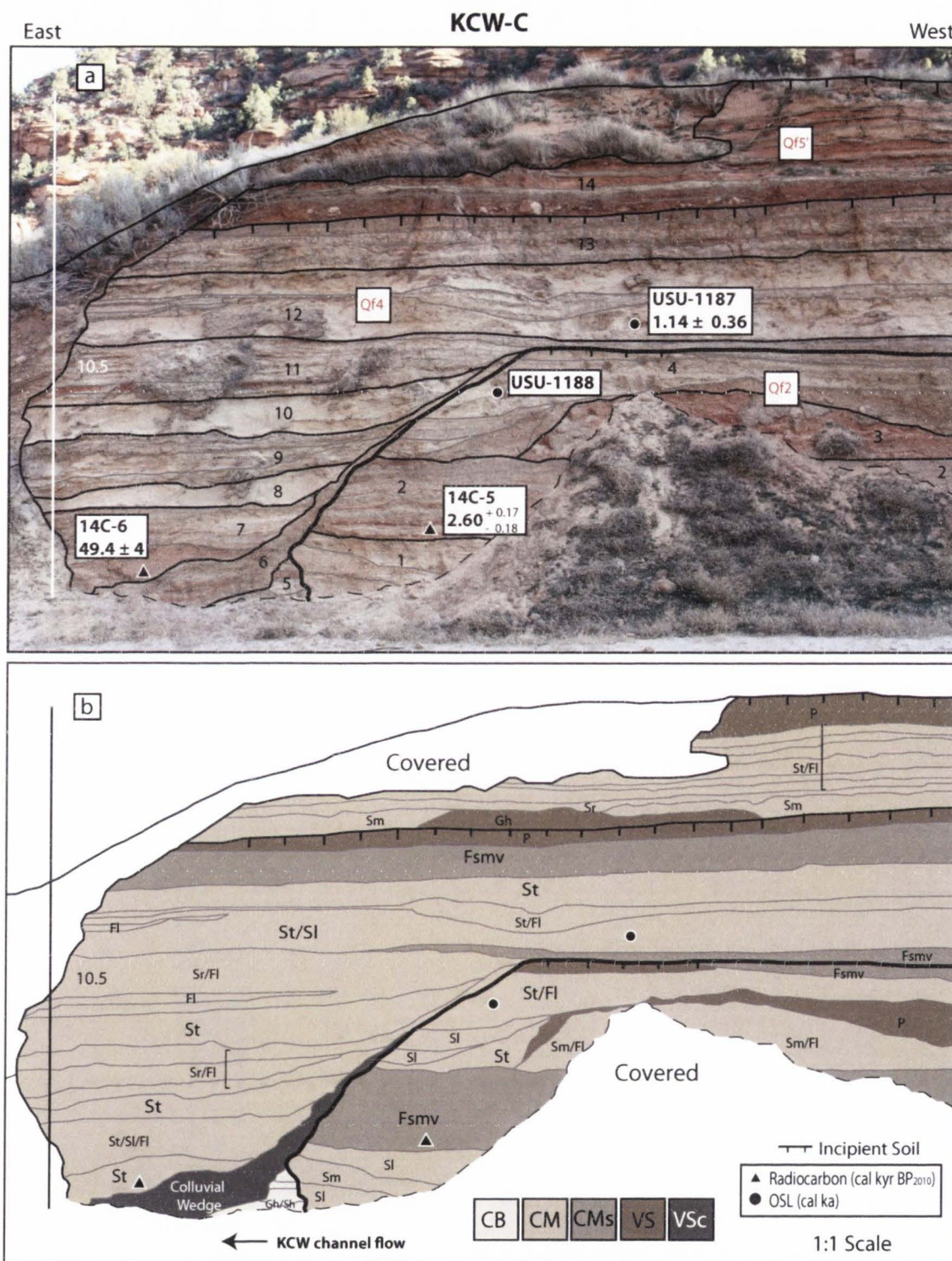


Fig. 3.8. Study site KCW-C showing a 10.5 m tall arroyo wall displaying two alluvial packages (Qf2, Qf4) separated by an erosional surface with (a) radiocarbon and OSL age results and (b) stratigraphic facies and depositional facies associations. See Fig B-3 in Appendix B for detailed sedimentary descriptions and stratigraphic columns.

colluvial wedge produced an age of  $49.4 \pm 4$  cal kyr BP<sub>2010</sub> and an OSL sample collected at ~5 m depth produce a preliminary age of  $1.14 \pm 0.36$  ka (Tables 3.2 and 3.3).

#### 3.4.9 *KCW-C Interpretations*

Site KCW-C records two episodes of aggradation separated by a period of incision. Prior to at least  $2.60^{+0.17}_{-0.18}$  cal kyr BP<sub>2010</sub>, KCW was incised at or below its modern grade and began to fill at least 5 m to create the older fill exposure (Fig. 3.8). Following some period of soil formation, KCW incised at least 5 m before re-aggrading at least 8 m to create the younger inset alluvial fill. Limited age control constrains this aggradation event to have occurred before  $1.14 \pm 0.36$  ka based on preliminary ages. Aggradation continued until reaching another hiatus in sedimentation as indicated by a buried soil at ~3 m depth. The upper 2.5-3 m of sheet-flood sediments overlying this buried soil are sourced from local sediments. The interpretation of these deposits will be discussed later in section 3.5.1.

#### 3.4.10 *KCW-D Observations*

Study site KCW-D contains a north-facing ~10.8 m tall arroyo wall along a meander bend in PW approximately 14 km upstream from Highway-89 and Kaibab Gulch (Fig. 3.9). Just upstream from this study site (~1.2 km), a 5 m tall knickpoint (knickpoint 2) of Triassic Chinle formation outcrops and arroyo wall heights immediately surrounding the knickpoint transition from ~10-12 m in height downstream to less than 6 m in height upstream (Fig 3.2). As indicated by the stratigraphy at this site, there are two alluvial fill packages separated by an unconformable surface. The older alluvial fill is ~6 m thick and dominantly composed of 10YR hued sediments that are broadly tabular, St, Sr, Sh, and Sl beds (Fig. B-4). An OSL sample (USU-1178) was collected ~4 m above the modern channel and returned a preliminary age of  $1.77 \pm 0.31$  ka and a stratigraphically higher radiocarbon sample (14C-7) was collected from the uppermost channel-

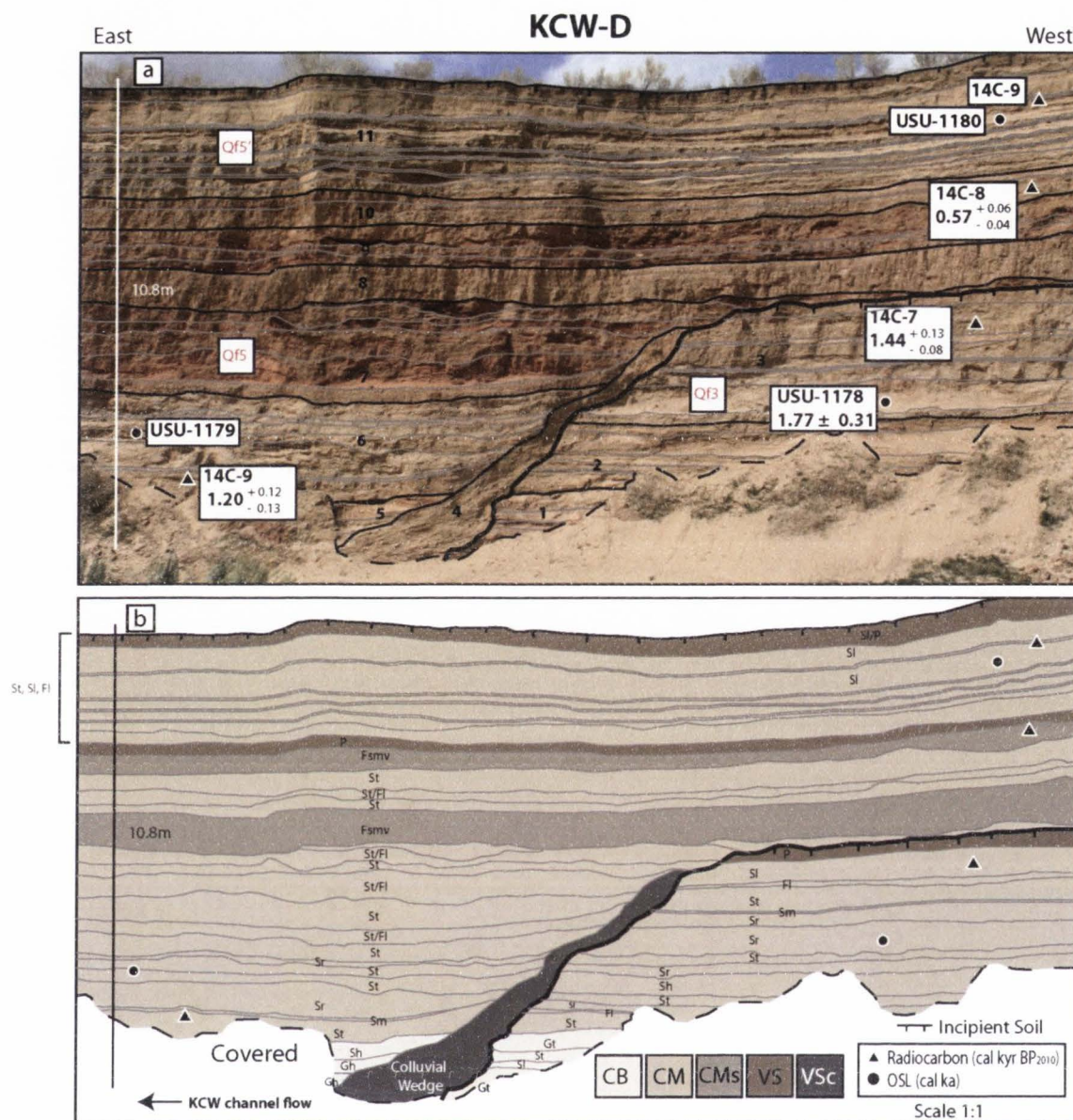


Fig. 3.9. Study site KCW-D showing a 10.8 m tall arroyo wall displaying two alluvial packages (Qf2, Qf4) separated by an erosional surface with (a) radiocarbon and OSL age results and (b) stratigraphic facies and depositional facies associations. See Fig B-4 in Appendix B for detailed sedimentary descriptions and stratigraphic columns.

margin bed in Qf3 and produced age of  $1.44^{+0.13}_{-0.08}$  cal kyr BP<sub>2010</sub> (Tables 3.2 and 3.3). This bed also showed minor evidence of soil formation. The younger inset fill is at least 10.8 m thick and contains a meter-scale colluvial wedge onlapping the buttress unconformity of the older alluvial fill and 10YR, 2.5YR, and 5YR hued sediments (Fig. B-4).

The younger fill contains basal, lenticular channel-bottom deposits (Gh) that are overlain by ~10-30 cm thick interbeds of broadly tabular and laterally extensive Sm, Sr, St, Fl channel-margin and two Fsmv slackwater deposits (Fig. 3.9). The uppermost Fsmv deposit has evidence of soil formation and is capped by 2-3 m of St, Sl, and Fl interbeds. A radiocarbon sample (14C-9) collected ~2 m above the modern channel produced an age of  $1.20^{+0.12}_{-0.13}$  cal kyr BP<sub>2010</sub> (Table 3.2), and an OSI sample (USU-1179) was collected from a stratigraphically higher deposit but was not analyzed. An additional radiocarbon sample (14C-8) was collected from the uppermost CMs deposit and yields an age of  $0.57^{+0.06}_{-0.04}$  cal kyr BP<sub>2010</sub> (Table 3.2).

#### 3.4.11 KCW-D Interpretations

KCW-D indicates two episodes of aggradation separated by an arroyo incision event (Fig. 3.9). The channel reach surrounding KCW-D began to incise near its modern grade prior to  $1.77 \pm 0.31$  ka and then began to aggrade until shortly after  $1.44^{+0.13}_{-0.08}$  cal kyr BP<sub>2010</sub>, creating the older fill. The presence of a buried soil at the top of the older fill indicates a hiatus in sedimentation, which was followed by at least 6 m of entrenchment sometime before  $1.20^{+0.12}_{-0.13}$  cal kyr BP<sub>2010</sub>. The younger fill began to aggrade after this period of entrenchment until sometime before  $0.57^{+0.06}_{-0.04}$  cal kyr BP<sub>2010</sub>. A buried soil near the top of this deposit suggests that the arroyo-wall surface was stable until large, sediment-laden sheet-flow events deposited ~2.3 m of sediment, which was followed by historic channel incision.

#### 3.4.12 KCW-E Observations

KCW-E is located in the Deer Springs Wash tributary of the main KCW study area

located along a meander bend approximately 9.5km upstream of Highway-89 and Kaibab Gulch (Fig. 3.2). This north-facing site is 6.9m tall, and its cut-fill architecture displays two alluvial fill packages that are separated by a buttress unconformity (Fig. 3.10). The older alluvial fill is at least ~4.5 m thick with basal channel-margin beds, and is composed of 2.5YR to 10YR colored, broadly lenticular and tabular, St, Sl, and Fl sands (Fig. B-5). An upper St bed shows evidence of soil formation and is capped with a ~1 m thick (Sm) bed that also shows evidence of an incipient soil. A radiocarbon sample (14C-11) collected near the base of this fill produced an age of  $1.38^{+0.02}_{-0.02}$  cal kyr BP<sub>2010</sub> and an OSL sample (USU-1192) collected ~1.1m below the surface produced a preliminary age of  $0.92 \pm 0.20$  ka (Fig. 3.10; Table 3.3).

The younger ~6.9 m thick inset fill contains a colluvial wedge draped across the buttress unconformity and channel-margin deposits that are 10-30 cm thick, basally lenticular transitioning to broadly tabular, Sr, Sl, St, and Fl bed. These are capped with a sub-meter thick slackwater (Fsmv) deposit showing evidence of soil formation (Fig. 3.10). An erosional surface extends across this Fsmv deposit and is overlain by the uppermost deposit of the younger fill. This deposit is ~2.5 m thick and contains broadly tabular interbeds of Sl, St, and Fl. A radiocarbon sample (14C-12) collected ~1.5 above the modern channel grade produced an age of  $0.87^{+0.10}_{-0.11}$  cal kyr BP<sub>2010</sub> and another <sup>14</sup>C sample from the base of the uppermost channel-margin deposit returned an age of  $0.2 \pm 0.14$  cal kyr BP<sub>2010</sub> (Table 3.2). An OSL sample (USU-1191) collected from the middle of the younger channel fill was not analyzed.

#### 3.4.13 KCW-E Interpretations

Age control and stratigraphic evidence at study site KCW-E suggest the presence of two alluvial fills, and indicates that the channel incised at or below its current grade prior to  $1.38^{+0.02}_{-0.02}$  cal kyr BP<sub>2010</sub> (Fig. 3.10). This was followed by aggradation until a brief hiatus in

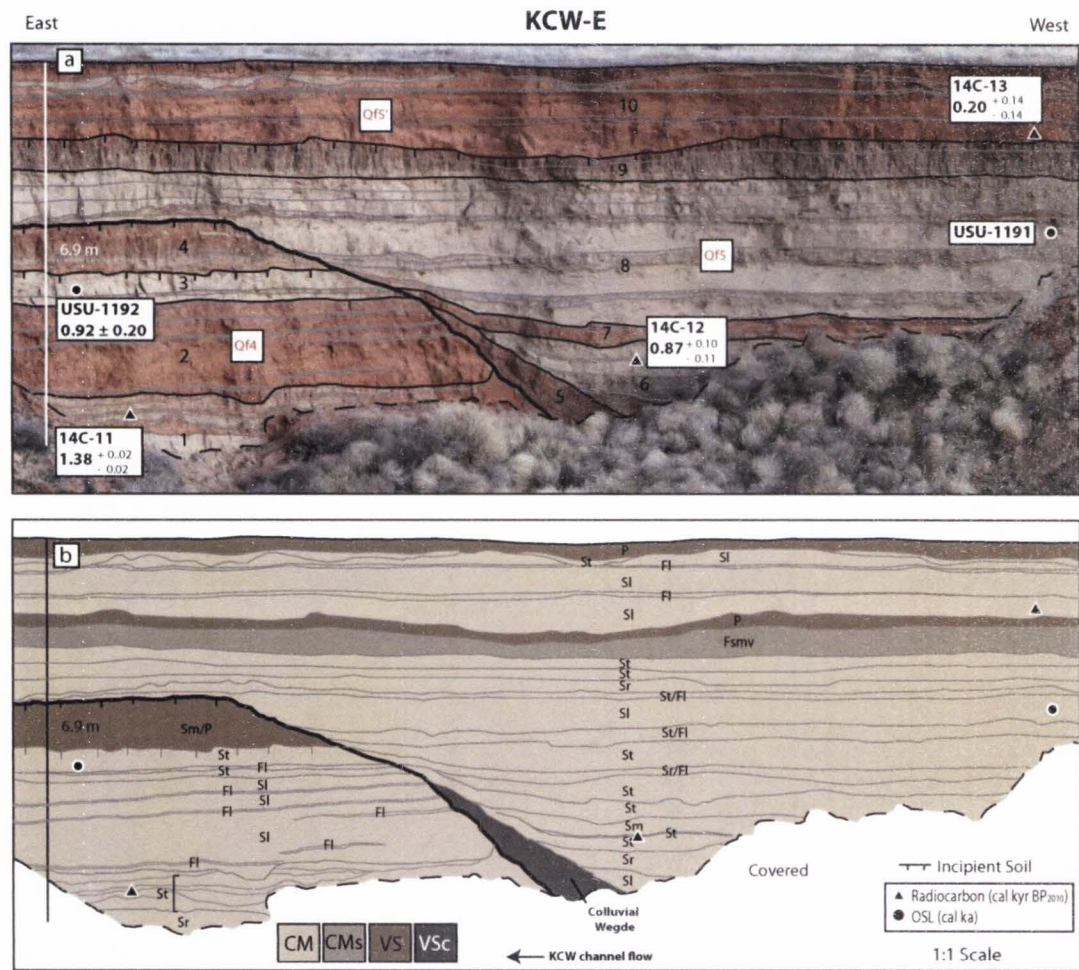


Fig. 3.10. Study site KCW-E showing a 6.9 m tall arroyo wall with two alluvial packages (Qf4, Qf5) separated by an erosional surface with (a) radiocarbon and OSL age results and (b) stratigraphic facies and depositional facies associations. See Fig B-5 in Appendix B for detailed sedimentary descriptions and stratigraphic column.

sedimentation shortly after  $0.92 \pm 0.20$  ka, as indicated by an OSL sample age and buried soil. Deposition resumed at this location for some amount of time until aggradation was interrupted by another episode of entrenchment prior to  $0.87^{+0.10}_{-0.11}$  cal kyr BP<sub>2010</sub>. Channel margin sedimentation of the younger alluvial fill persisted until at least 5 m of alluvium had been deposited, at which time CMs sedimentation ensued and soil formation followed prior to  $0.2 \pm 0.14$  cal kyr BP<sub>2010</sub>. This was followed by localized erosion and sheetflow deposition prior to historic channel cutting.

#### 3.4.14 KCW-F Observations

Approximately 1.5 km downstream from KCW-D in Park Wash, study site KCW-F contains a north-facing, 8.5 m tall arroyo wall (Figs. 3.2 and 3.11). The cut-fill stratigraphy of this site stretches along the length of a meander bed just south of a canyon tributary to PW, and shows evidence for two alluvial fill packages separated by a buttress unconformity with two thick colluvial wedges along this contact. The older alluvial fill is composed of 10YR hued sediments while the younger inset fill is dominated by 2.5YR and 7.5YR colored sediments (Fig. B-6). Basal units of both fills contain broadly lenticular, gravel and sand channel-bottom and channel-margin deposits (e.g. Gt, Gh, St, Fl, Fl, Sr) that are overlain by broadly tabular, ~10-50 cm thick, channel-margin beds (e.g. Sh, St, Sl, Sm, Sr, Fl). Both fills also have capping massive sand deposits that show evidence of incipient soil formation, and the younger fill has an additional incipient soil <1m below its upper erosional contact. Capping the younger fill is a ~1.9 m thick deposit of broadly tabular, 10-40 cm thick interbeds of Sm, Sl, and Fl with evidence of soil formation at the surface.

A radiocarbon sample (14C-14) was collected near the base of the older fill and produced a near infinite age of 42.6 cal kyr BP<sub>2010</sub> and a OSL sample (USU-1194) was collected ~3m above this and produced a preliminary age of  $2.97 \pm 0.70$  ka (Fig. 3.11; Tables 3.2 and 3.3). In the younger inset fill, a <sup>14</sup>C sample (14C-16) was collected ~2 m above the modern channel grade and returned an age of >45.7 cal kyr BP<sub>2010</sub> while another radiocarbon sample (14C-15) collected ~3

m below the valley surface produced an age of  $0.66^{+0.06}_{-0.06}$  cal cal kyr BP<sub>2010</sub> (Table 3.2). USU-1193 was collected at the base of the youngest fill but was not analyzed.

#### 3.4.15 *KCW-F Interpretations*

Stratigraphic evidence and age results indicate that study site at KCW-F had incised at or below its current grade and had begun to deposit the older alluvial for some amount of time prior to  $2.96 \pm 0.70$  ka (Fig. 3.11). Buried soils in the older alluvial fill suggest that hiatuses in sedimentation occurred near the top of this stacked fill package. Currently, the lack of reliable age data from the base of the younger fill makes it difficult to constrain the timing of the incision at this site prior to  $0.66^{+0.06}_{-0.06}$  cal kyr BP<sub>2010</sub>. Following this incision event, colluvial deposits onlapping the buttress unconformity suggest that the arroyo wall collapsed and caused material to be deposited at the channel-bottom. A buried incipient soil at ~1.5 m depth suggests a hiatus in channel-margin deposition, followed by a period of sheetflow deposition immediately prior to historic arroyo cutting (Fig. 3.11).

#### 3.4.15 *KCW-G Observations*

Study site KCW-G is located approximately 12 km upstream of Highway-89 and Kaibab Gulch, and nearly 3 km upstream of a 6 m tall bedrock knickpoint (knickpoint 3) (Fig. 3.2). This site is a 5 m high west-facing arroyo wall that shows evidence of two alluvial fill packages separated by an erosional unconformity (Fig. 3.12). The oldest fill is composed of tabular St and Sl beds overlain by a ~1 m thick Sm deposit, and a ~65 cm thick, red buried soil that is highly bioturbated and has no visible sedimentary structures (Fig. B-7). A <sup>14</sup>C sample (14C-21) was collected near the base of this fill and returned an age of  $3.73 \pm 0.04$  cal kyr BP<sub>2010</sub> (Table 3.2).

Overlying the oldest fill units is a tabular Sl bed and overlying variegated silts and sands (Fsmv) and Sm deposit with evidence of an incipient soil (Figs. 3.12 and B-7). An OSL sample (USU-1181) was collected from the Sl bed (unit 3) of this intermediate fill and produced a



preliminary age of  $1.47 \pm 1.08$  ka (Table 3.3). Onlapped against these beds is an intermediate fill composed of basal St and Sl interbeds and is capped by an 80 cm thick Fsmv deposit that also shows evidence of soil formation. Radiocarbon samples 14C-17 ( $1.18^{+0.14}_{-0.13}$  cal kyr BP<sub>2010</sub>) and 14C-20 (not analyzed) were collected from the base of unit 5 (Table 3.2).

Inset against a buttress unconformity covered with a thin colluvial wedge is the next youngest fill packages that is primarily composed of four units of alternating Sl, Sm, Sh, St and Fsmv beds and two interbedded units of Fsmv (Fig. B-7). A radiocarbon sample 14C-18 ( $0.68^{+0.05}_{-0.06}$  cal kyr BP<sub>2010</sub>) was collected from the base of this fill (Table 3.2) and an OSL sample (USU-1186) was collected from the middle of this package but was not analyzed. The uppermost slackwater (Fsmv) bed in the youngest fill indicates ~20 cm of soil formation across an erosional upper contact with an overlying valley-surface deposit (Fig. 3.12).

#### 3.4.16 KCW-G Interpretations

The stratigraphy at site KCW-G, suggests at least 3 alluvial fills with aggradation of the oldest fill beginning sometime after  $3.73^{+0.04}_{-0.04}$  cal kyr BP<sub>2010</sub>, following a period of entrenchment. Evidence of a massive buried soil suggest a long period of surface stability ~3 m above the modern channel-bottom that was eventually followed by an episode of aggradation that capped these older deposits by  $1.47 \pm 1.08$  ka (Fig. 3.12). Aggradation of this intermediate fill was interrupted by a hiatus in sedimentation and subsequent channel incision prior to  $1.18^{+0.14}_{-0.13}$  cal kyr BP<sub>2010</sub>. Aggradation of the intermediate fill continued with channel-margin and slackwater deposition until sometime prior  $0.68^{+0.05}_{-0.06}$  cal kyr BP<sub>2010</sub>, when aggradation ceased and the stream entrenched to its modern grade, producing a buttress unconformity (Fig. 3.12). Ensuing aggradation continually shifted from channel-margin to slackwater deposition until a final hiatus in sedimentation at ~4.9 m above the modern channel. This was followed by a period of soil formation and sheetflood deposition prior to historic arroyo cutting.

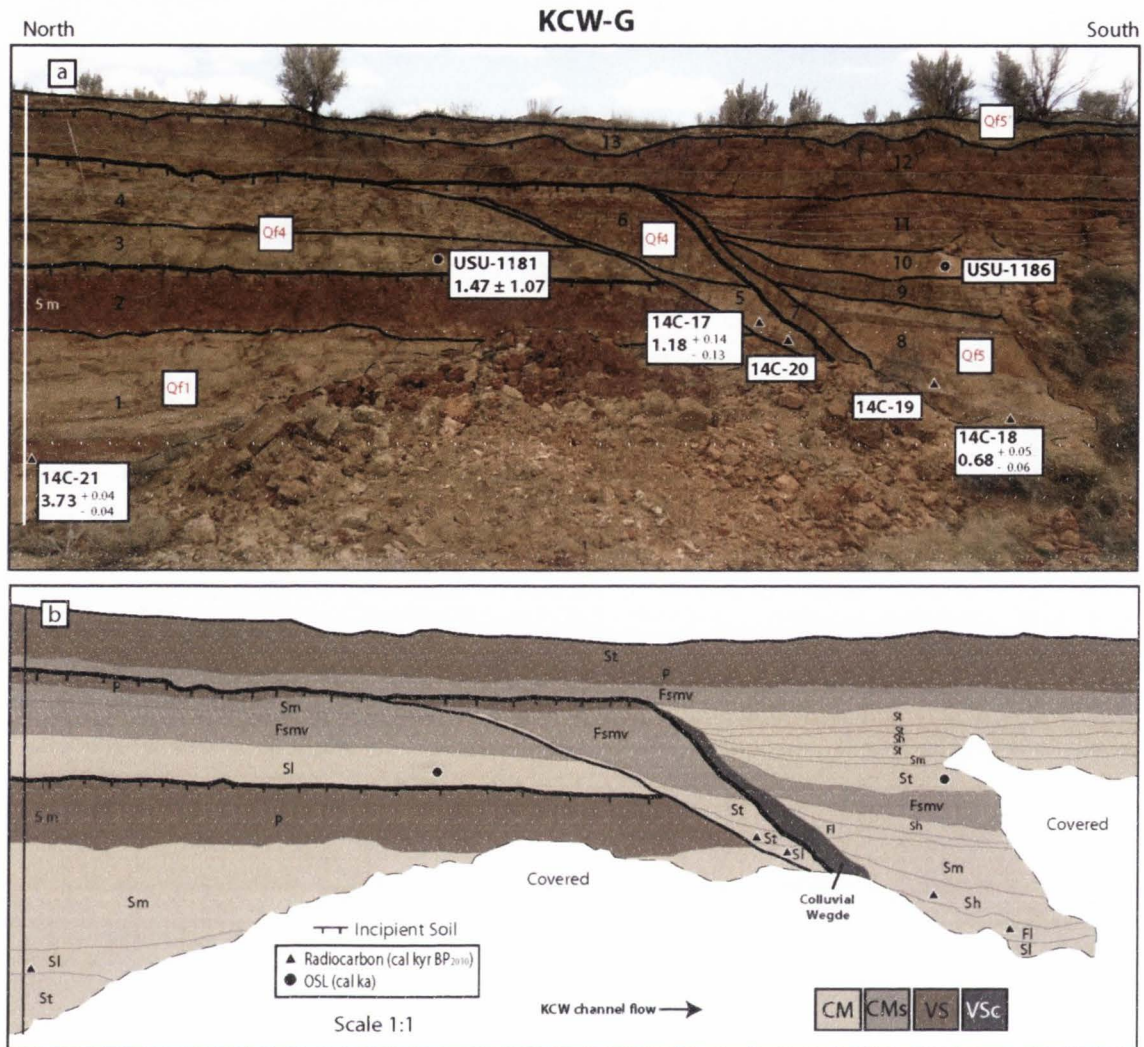


Fig. 3.12. Study site KCW-G showing a 5 m tall arroyo wall with three alluvial packages (Qf1, Qf4, Qf5) separated by two erosional surfaces with (a) radiocarbon and OSL ages and (b) stratigraphic facies and depositional facies associations. See Fig B-7 in Appendix B for detailed sedimentary descriptions and stratigraphic columns.

### 3.4.17 KCW-H Observations

The KCW-H study site is located approximately 7.5 km upstream of Kaibab Gulch and Highway-89, and less than 1 km downstream from knickpoint 3 in the main trunk channel of KCW (Figs. 3.1 and 3.2). It is a mostly north-facing, 10.7 m tall arroyo wall that wraps around a meander bend, and whose sediments have been partially deposited along outcropping bedrock of Triassic Chinle formation (Fig. 3.13). The arroyo-wall stratigraphy at KCW-H shows evidence of at least three alluvial fills that are separated by erosional unconformities. An additional 4 m tall fill between the oldest and intermediate appears to be a separate alluvial fill. However, it contains discontinuous, lenticular shaped beds and is considered to be part of the intermediate fill. This outcrop predominantly contains 10-50 cm thick beds that are composed of 10YR, 7.5YR, and 2.5YR hued sediments, suggesting a range of sediment sources (Fig. B-8). The oldest alluvial fill consists of several tabular alternating Sl, Sh, and Sm beds (Fig. 3.13). A radiocarbon sample (14C-26) from the base of this alluvial fill and yielded an age of  $4.14^{+0.07}_{-0.09}$  cal kyr BP<sub>2010</sub> (Table 3.2), and an OSL sample (USU-1101) was extracted ~1 m above this and produced a preliminary age of  $4.21 \pm 1.46$  ka (Table 3.3). Another radiocarbon sample (14C-22) was collected ~2 m above this OSL sample and yielded an age of  $3.82^{+0.07}_{-0.06}$  cal kyr BP<sub>2010</sub>. The uppermost portion of this oldest alluvial package is composed of a thick (~2.2 m) massive sand (Sm) that is now highly bioturbated and shows clear evidence of soil formation. This soil appears to be similar to that observed in the oldest fill at KCW-G.

An intermediate fill inset against the oldest fill package contains an erosional contact within the general stratigraphy (Fig. 3.13). Basal channel-bottom (CB) deposits upstream of the erosional contact contain lenticular Gh beds overlain by St and Sl beds and overlying 10-20 cm thick, Sl and Sm interbeds, of which radiocarbon sample 14C-24 ( $1.08^{+0.04}_{-0.05}$  cal kyr BP<sub>2010</sub>) and OSL sample USU-1102 (not analyzed) were collected. Downstream of the erosional surface is a ~5 m thick package of channel-margin St, Sm, Sh, and Sl interbeds that are overlain by a

slackwater Fsmv deposit and massive bioturbated sand (Fig. B-8). An OSL sample (USU-1103) was collected ~4 m above the modern channel grade and produced a preliminary age of  $1.56 \pm 0.37$  ka. Compared to the radiocarbon ages from the same fill, it appears that USU-1103 is producing an age overestimation.

Buttressed against this intermediate fill is a small colluvial wedge within the youngest fill that is overlapped by a sequence of channel deposits containing broadly lenticular beds Gt, Sh, Sl, St, and Sr, and Fl. A radiocarbon sample (14C-25) was collected from the colluvial wedge and yielded an age of  $2.28^{+0.18}_{-0.16}$  cal kyr BP<sub>2010</sub> while a <sup>14</sup>C sample (14C-27) collected outside of the colluvial wedge yielded an age of  $0.83^{+0.13}_{-0.09}$  cal kyr BP<sub>2010</sub> (Fig. 3.13; Tables 3.2 and 3.3). An OSL sample (USU-1104) was collected ~1 m below the valley surface but was not analyzed.

#### 3.4.18 KCW-H Interpretations

Stratigraphic evidence and age control suggests this outcrop exposes three alluvial fill packages (Fig. 3.13). Entrenchment at or below the modern channel grade occurred prior to  $4.14^{+0.07}_{-0.09}$  cal kyr BP<sub>2010</sub>, and was followed by aggradation in the channel until sometime after  $3.82^{+0.07}_{-0.06}$  cal kyr BP<sub>2010</sub>. A pause in sedimentation was caused by another incision event and allowed pedogenesis to occur along the stable surface of the older alluvial fill. The intermediate fill began aggrading prior to  $1.08^{+0.04}_{-0.05}$  cal kyr BP<sub>2010</sub>, and filled to a level similar in height as the older fill. A steep buttress unconformity suggests an arroyo cutting event lowered the channel near its modern depth prior to  $0.83^{+0.13}_{-0.09}$  cal kyr BP<sub>2010</sub> and was followed by at least 10.7 m of aggradation prior to historic arroyo cutting event.

#### 3.4.19 KCW-I Observations

Study site KCW-I contains a nearly 10 m tall arroyo wall that faces the west and is located just over 5.5 km upstream from Kaibab Gulch and Highway-89 (Fig. 3.1), and was previously studied by Harvey et al. (2011). Arroyo wall stratigraphy shows four alluvial fill



packages separated by three buttress unconformities (Fig. 3.14). Beds in this outcrop are generally 10-50 cm thick and mostly contain 10YR and 2.5YR hued sediments (Fig. B-9). The oldest fill is composed of tabular interbeds of Sm, St, and Sl that are capped by a thick Fsmv bed, which shows signs of soil formation. An OSL (USU-531) and radiocarbon (14C-39) samples were previously collected from this deposit by Harvey et al. (2011) and returned ages of  $2.82 \pm 0.32$  ka and  $2.3^{+0.06}_{-0.09}$  cal kyr BP, respectively (Fig. 3.14; Tables 3.2 and 3.3). The next younger alluvial fill is ~ 7 m thick and is composed of basal lenticular Gh and St beds that are overlain by broadly tabular Sh, St, Sm and Sl beds and capped by a thick, red massive sand (Sm) bed. This Sm bed shows evidence of incipient soil formation and has an erosional base in places (Fig. B-9). A radiocarbon sample (14C-29) was collected near the base of the fill and returned an age of  $>46$  cal kyr BP<sub>2010</sub> and an OSL sample (USU-530) collected by Harvey et al. (2011) from an inset channel-bottom deposit returned a small-aliquot age of  $2.25 \pm 0.85$  ka (Fig. 3.14; Table 3.3). Another OSL sample (USU-1025) was collected from a slightly higher position but was not analyzed.

Buttressed against the intermediate fill is a younger fill package composed of basal Gh beds overlain with tabular channel-margin (e.g. Sl, Fl, Sl, Sr, Sm) and slackwater (e.g. Fsmv) beds (Fig. 3.14). Capping this fill package is a ~1 m thick incipient soil (P). A radiocarbon sample near the base of this fill yields an age of  $1.72 \pm 0.05$  cal kyr BP<sub>2010</sub> (Table 3.2). The youngest alluvial fill is at least 9 m thick, overtops all other alluvial fills, and is composed of lens of Gh and tabular beds of Sl, Sh, and Fl. These beds onlap a thick colluvial wedge which drapes the buttress unconformity of the intermediate fill (Fig. 3.14). A radiocarbon sample (14C-38) was collected by Harvey et al. (2011) from the middle of this fill and yields an age of  $0.66^{+0.06}_{-0.08}$  cal kyr BP<sub>2010</sub> (Table 3.2). Additional observations of KCW-I are described in Harvey et al. (2011) under the name KCW-A.

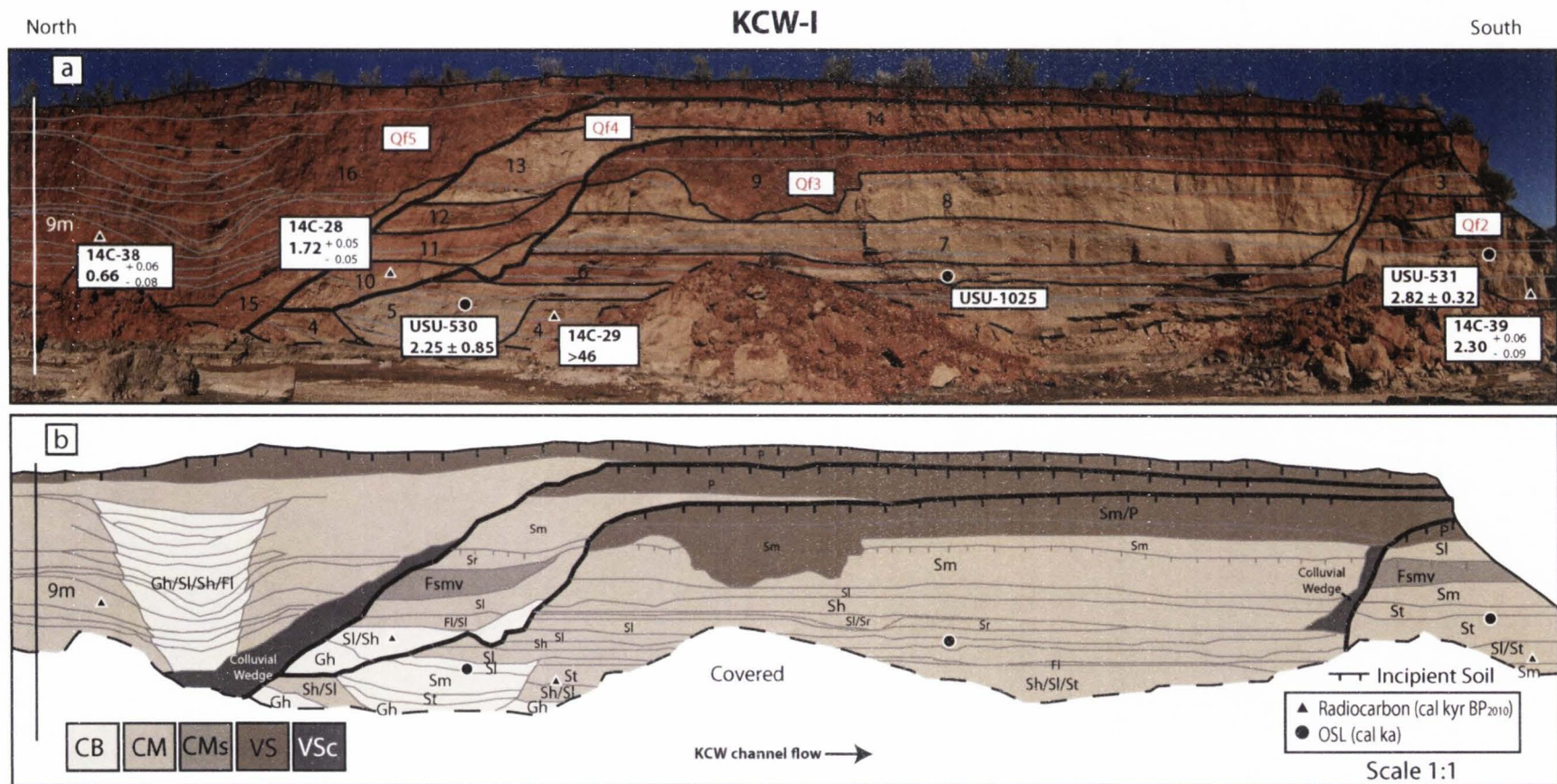


Fig. 3.14. Study site KCW-I showing a 9 m tall arroyo wall displaying four alluvial packages (Qf2, Qf3, Qf4, Qf5) separated by erosional surfaces with (a) radiocarbon and OSL ages and (b) stratigraphic facies and depositional facies associations. This site was previously visited by Harvey et al. (2011) and has been reinterpreted in this study. See Fig B-9 in Appendix B for detailed sedimentary descriptions and stratigraphic columns.

### 3.4.20 *KCW-I Interpretations*

Based on stratigraphic relationships, and OSL and radiocarbon results, four alluvial packages identified are present in KCW-I (Fig 3.14). It appears that entrenchment at this site to or below its modern depth occurred prior to  $2.30^{+0.06}_{-0.09}$  cal kyr BP<sub>2010</sub>. Ensuing aggradation of the oldest alluvial fill was briefly interrupted by a hiatus in sedimentation as indicated by a buried soil (Fig. 3.14). A second episode of entrenchment prior to  $2.25 \pm 0.85$  ka is identified by a buttress unconformity, and was followed by deposition of the second oldest alluvial fill and incipient soil formation. Following a third prehistoric incision event, the second youngest fill started to aggrade prior to  $1.72^{+0.05}_{-0.05}$  cal kyr BP<sub>2010</sub> and continued until overtopping the second youngest fill at 7.5 m above the modern channel grade. A buried soil at the top of this fill suggests another long hiatus in sedimentation until a final prehistoric arroyo cutting event prior to  $0.66^{+0.06}_{-0.08}$  cal kyr BP<sub>2010</sub>, which was followed by the vertical accretion of the youngest fill and historic arroyo cutting event.

### 3.4.21 *KCW-J Observations*

Site KCW-J is located approximately 5 km upstream from Highway-89 and Kaibab Gulch, and has an exposed arroyo wall rising between 5m and 6.6m above the modern alluvial channel (Figs. 3.1 and 3.15). As one of the widest exposures in this study, the cut-fill architecture of KCW-J expands well over 50 m of a meander bend in a north-south direction, and unconformable bounding buttresses suggest three aggradational fill packages (Fig. 3.15). The oldest alluvial fill contains channel-margin deposits that are primarily composed of 10YR and 2.5YR hues, and broadly tabular St, Sl, and Sm sands that are capped by a thick Fsmv deposit (Fig. B-10). A massive sand deposit filled with 30-50 cm thick, blocky and tabular pebbles and cobbles with no evidence of sorting is inset below the Fsmv deposit and does not conform to the surrounding facies (Fig. B-10). OSL and radiocarbon samples (Tables 3.2 and 3.3) were collected near the base of this fill and yield preliminary single-grain ages of  $1.52 \pm 0.74$  ka (USU-

1028) and  $1.58 \pm 0.30$  ka (USU-1027), and a calibrated  $^{14}\text{C}$  age of  $1.70^{+0.06}_{-0.07}$  kyr BP<sub>2010</sub> (14C-31). Additionally, a radiocarbon sample from the upper Fsmv deposit produced an age of  $1.85^{+0.08}_{-0.06}$  cal kyr BP<sub>2010</sub>. The next younger inset alluvial fill contains four units (5-8) consists of both broadly tabular and lenticular Sl, St, and Sh beds that are capped by a 0.8 m thick slackwater Fsmv deposit (Figs. 3.15 and B-10). An OSL sample (USU-1026) and two radiocarbon samples (14C-30, 14C-33) were collected from this middle of this alluvial fill and returned ages of  $1.29 \pm 0.37$  ka (preliminary),  $>31.7$  cal kyr, and  $2.52^{+0.24}_{-0.12}$  cal kyr BP<sub>2010</sub> respectively (Tables 3.2 and 3.3). The youngest alluvial deposit is erosionally inset in places but largely drapes over the two older fill packages and is characterized by three highly bioturbated, tabular beds with incipient soils. All beds show some evidence of low-angle cross-bedding (Sl) at their base but are primarily structureless due to bioturbation. An OSL sample was collected from  $\sim 1.5$  m below the valley surface and yields a preliminary age of  $1.62 \pm 0.39$  ka (Table 3.3).

#### 3.4.22 KCW-J Interpretations

The stratigraphy and age control from site KCW-J suggests that three Holocene alluvial fills separated by buttress unconformities are preserved at this site. Prior to  $1.52 \pm 0.74$  ka, KCW was at a grade similar to the modern channel. Aggradation of the oldest fill began proximal to the channel until the thalweg of the channel migrated past this site and left an inset channel scour that was later infilled by overbank and slackwater deposits. The tabular pebbles and cobbles in the Sm deposit are far from any bedrock source and may have been placed due to anthropogenic practices. Alternative interpretations of the stratigraphy in the oldest fill package may suggest two individually aged alluvial packages, but current age control suggest deposits on either side of the channel scour are contemporaneous. Age control from the next younger alluvial fill suggests aggradation was underway by  $1.29 \pm 0.37$  ka. Sometime after  $1.29 \pm 0.37$  ka the channel began to deposit tabular sheetflood beds at this site, with several lapses in sedimentation is indicated by presence of a buried soils (Fig. 3.15). Age control for these upper capping deposits is limited due

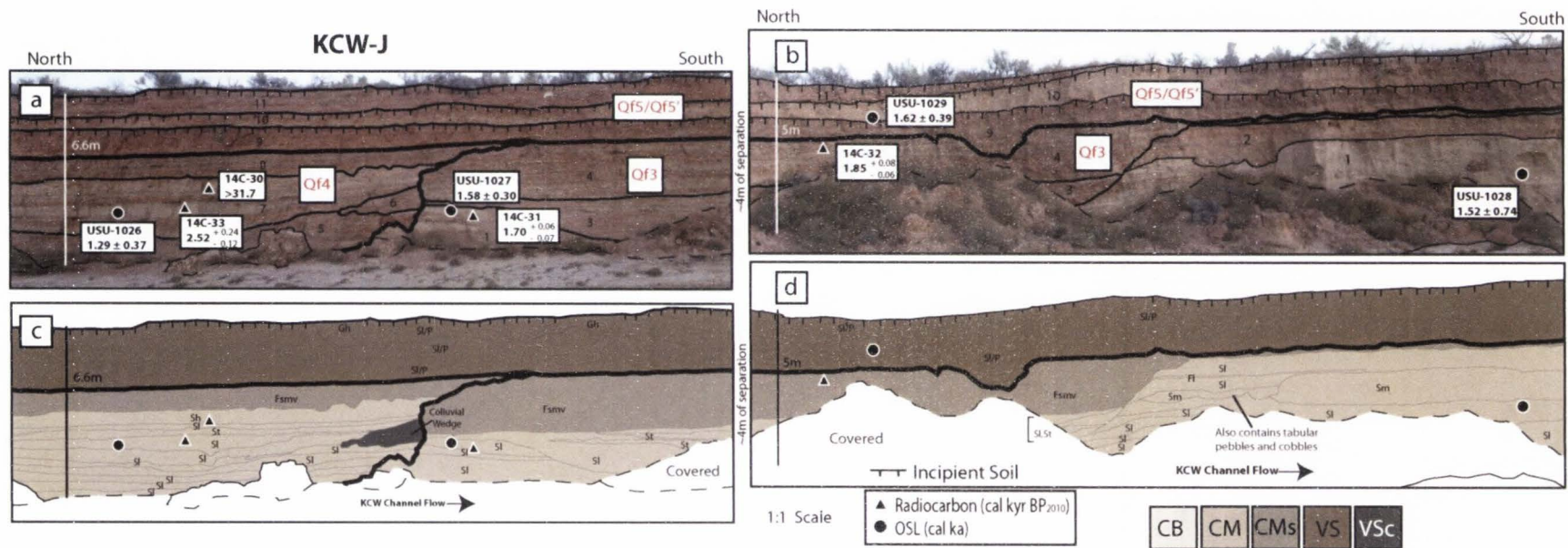


Fig. 3.15. Study site KCW-J showing a 5 to 6.6 m tall arroyo will displaying three alluvial packages (Qf3, Qf4, Qf5/Qf5') separated by erosional surfaces with (a) radiocarbon and OSL age results and (b) stratigraphic facies and depositional facies associations. See Fig B-10 in Appendix B for detailed sedimentary descriptions and stratigraphic columns.

to a stratigraphically inconsistent OSL age (USU-1029), but their stratigraphic position suggests they are some of the youngest alluvium and were deposited prior to historic arroyo cutting.

#### 3.4.23 *KCW-K Observations*

Study site KCW-K contains a ~2.9 m tall arroyo wall that is located in the main KCW trunk stream just over 1 km north of Highway-89 and Kaibab Gulch (Fig. 3.1). At this location, the modern KCW channel is nearly 100 m wide and its sandy alluvial floor is covered in vegetation on its channel bars. Arroyo wall stratigraphy and sedimentology at KCW-K show two aggradational packages separated by an unconformable bounding surface that are dominantly composed of broadly tabular, reddish brown and light red sand beds (Fig. 3.16). The oldest fill is composed of St and Fl interbeds capped by an Fsmv deposit (Fig. B-11). An OSL sample (USU-1106) was collected from the basal deposit but was not analyzed and a radiocarbon sample (14C-34) was collected from the Fsmv deposit and returned an age of  $0.95^{+0.16}_{-0.10}$  cal kyr BP<sub>2010</sub> (Fig. 3.15; Table 3.3). Two separate inset deposits of the younger alluvial fill are separated by an erosional surface and either buttress against or overtop this older fill. These two deposits are composed of tabular St, Sl, Sh, and Fsmv beds that are capped by separate thick Sm deposits, each showing evidence of soil formation (Figs. 3.16 and B-11). A radiocarbon sample (14C-35) was collected from the base of the deposit and returned an age of  $2.01^{+0.14}_{-0.08}$  cal kyr BP<sub>2010</sub>, and ~50 cm above this an OSL sample (USU-1107) was collected but was not analyzed. An upper Sm deposit with evidence of soil formation is truncated by a shallowly dipping erosional surface to the south and overlain by broadly lenticular channel-margin beds. Radiocarbon (14C-36) and OSL (USU-1108) samples were collected downstream of the erosional surface in this younger alluvial fill. The radiocarbon yielded an age of  $0.47^{+0.09}_{-0.09}$  cal kyr BP<sub>2010</sub> (Table 3.2) and the OSL sample was not analyzed.

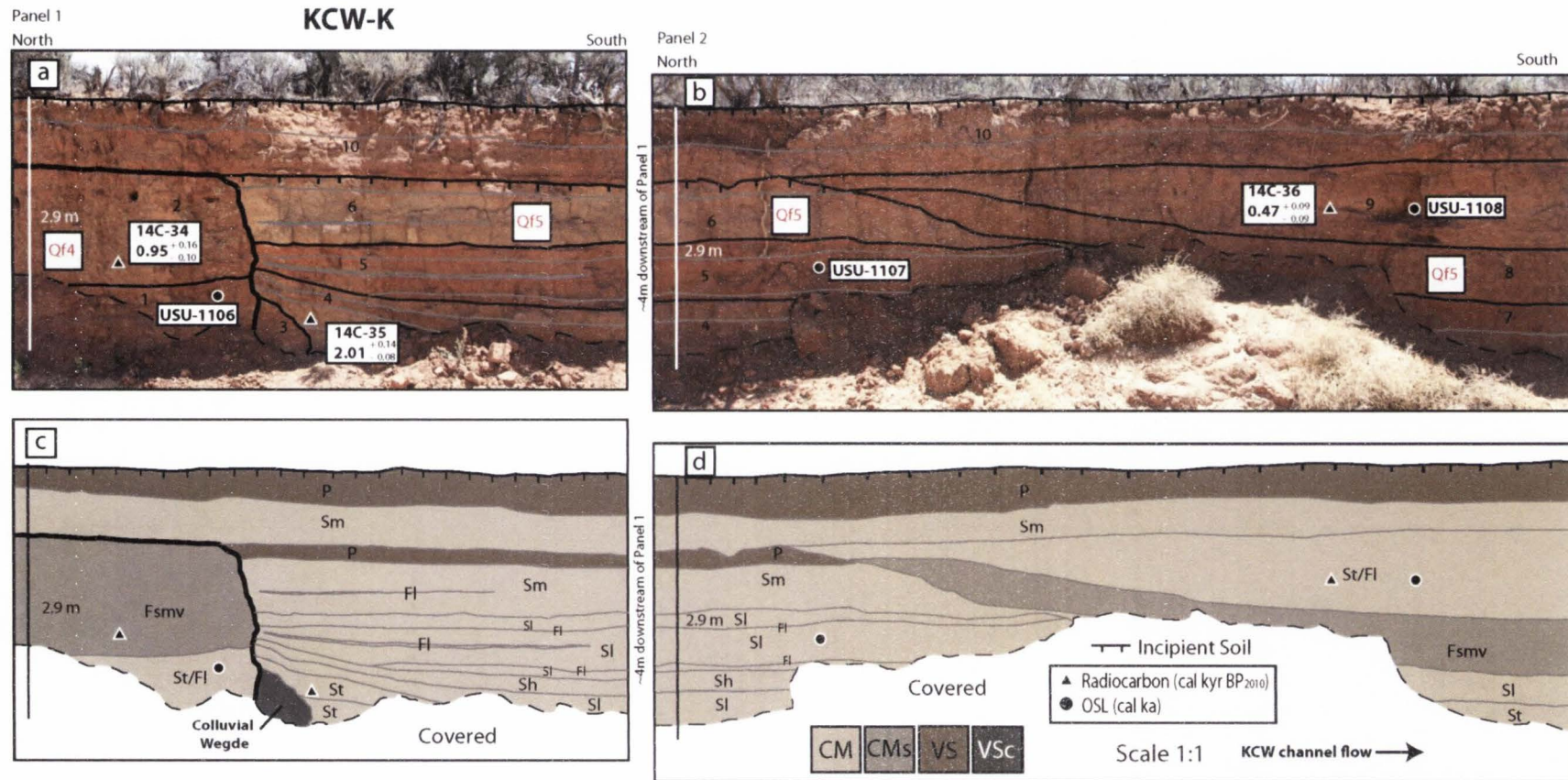


Fig. 3.16. Study site KCW-K showing a 2.9 m tall arroyo wall with two alluvial packages (Qf4, Qf5) separated by erosional surfaces and showing (a) radiocarbon and OSL age results and (b) stratigraphic facies and depositional facies associations. See Fig B-11 in Appendix B for detailed sedimentary descriptions and stratigraphic columns.

#### 3.4.24 *KCW-K Interpretations*

Combined radiocarbon ages with stratal units and erosional surfaces at the KCW-K site indicate the two alluvial fills at this site (Fig. 3.16). Based on age control, it is evident that the channel floor at this site was incised prior to  $0.95^{+0.16}_{-0.10}$  cal kyr BP. The broad geometry of the modern channel at this location and presence of mid-channel bars suggests that this incision event may have lowered KCW well below its modern depth. Aggradation of the older fill was followed by a subsequent entrenchment event that occurred sometime after  $0.95^{+0.16}_{-0.10}$  cal kyr BP<sub>2010</sub>. This event is hard to temporally constrain because the age of 14C-35 ( $2.01^{+0.14}_{-0.08}$  cal kyr BP<sub>2010</sub>) suggests that this sample has been redeposited. Following the initial deposition of the younger fill, a hiatus in sedimentation occurred as the channel appears to have migrated and scoured into underlying deposits to an unidentifiable depth. Deposition of the younger fill resumed prior to  $0.47^{+0.09}_{-0.09}$  cal kyr BP<sub>2010</sub> and was followed by historic channel incision.

#### 3.4.25 *KCW-L Observations and Interpretations*

Study site KCW-L is located approximately 400 m from Kaibab Gulch and Highway-89, and contains a 2.2 m tall exposure containing two alluvial fill packages (Figs 3.1 and 3.17). OSL samples were collected from both the older and younger alluvial fill packages (USU-1183, USU-1184) but were not analyzed. A radiocarbon sample (14C-37) was collected from the younger fill but returned an age of ~46.7 kyr BP (Table 3.2), which is anomalously old and was likely a piece of Cretaceous coal. Unlike other arroyo wall exposures in KCW, KCW-L displays neither a characteristic colluvial wedge deposit between alluvial fill packages nor does it show an accretionary sequence of thinly bedded sediment deposition common in all other arroyo exposures. Additionally, given its position downstream and less than 3 m height, it is likely that KCW-L is representative of a scour-fill event or channel migration deposit rather than a larger scale arroyo cut-fill episode.

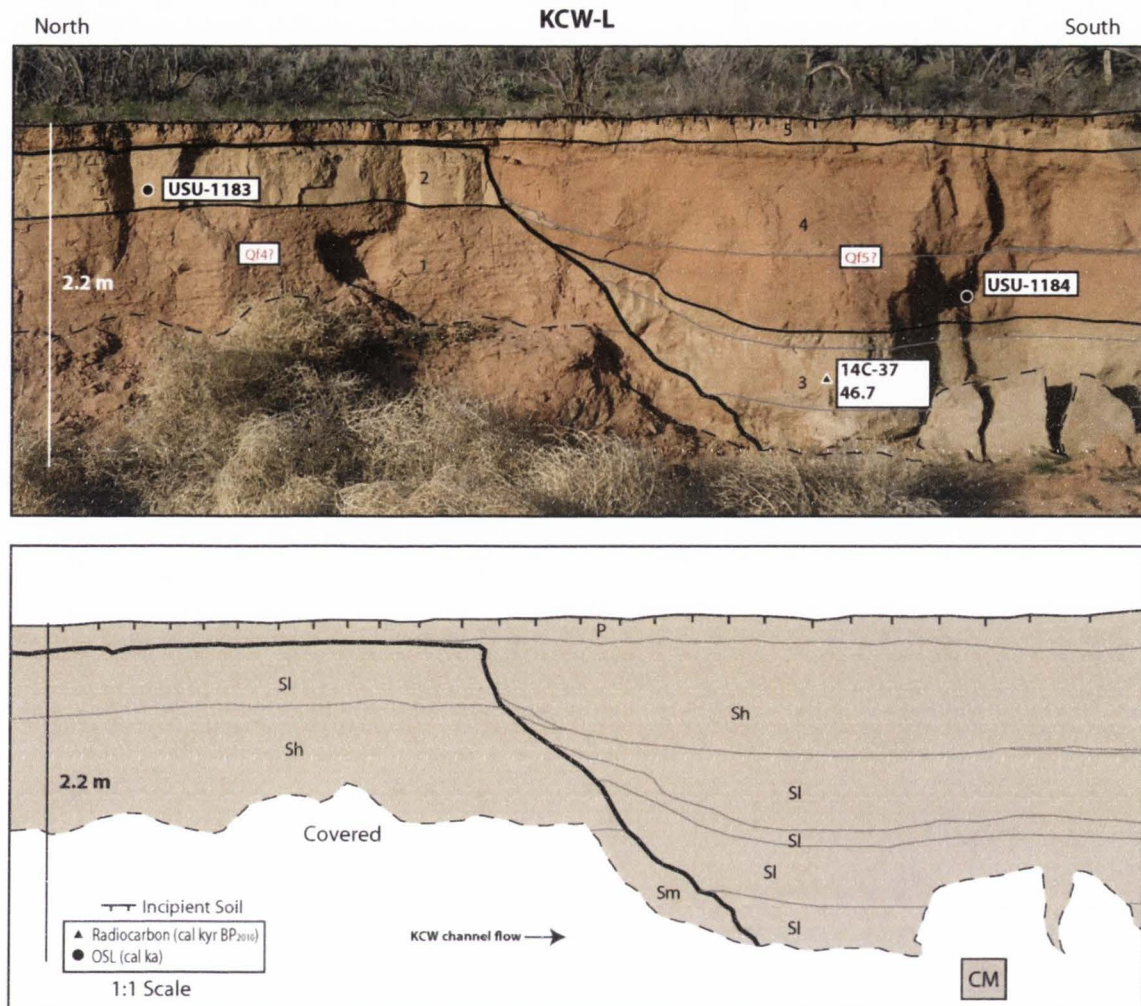


Fig. 3.17. Study site KCW-L showing a 2.2 m tall arroyo wall with two alluvial packages (Qf4?, Qf5?) separated by erosional surfaces.

### 3.5 Discussion

#### 3.5.1 *Development of Holocene Chronostratigraphy*

OSL and radiocarbon dates combined with arroyo-wall stratigraphic relationships at each study site in KCW indicate that at least six episodes of middle to late Holocene aggradation that repeatedly refilled the arroyo system to varying levels above the modern channel floor, following four episodes of prehistoric arroyo entrenchment (Fig. 3.18). The identification of these aggradation episodes was primarily based on stratigraphic evidence from the study sites and secondarily from  $^{14}\text{C}$  and OSL age control. From oldest to youngest, the six episodes of alluvial fill aggradation are: the older Hereford (2002) fill (~7.3 – 4.85 ka), Qf1, Qf2, Qf3, Qf4, and Qf5. The older fill of Hereford (2002) is not described in this study because the exposure was not seen during field research. This exposure was described by Hereford prior to 2002 and may no longer be preserved.

The oldest alluvial fill, Qf1, is evident at sites KCW-G and KCW-H and has an age range of ~4.35 to 3.4 ka. This alluvial fill package has a unique thick incipient red soil developed at its surface and is generally ~3 to 8.5 m above the modern channel floor. In this study, the older fill of Hereford (2002) has been identified as a separate aggradation episode from Qf1 because age results from these two fills do not appear to overlap (see Table 3.2 and 3.3). However, it is possible the Qf1 alluvial fill is representative of continued aggradation of the older fill of Hereford (2002). Alluvial fill Qf2 is located at sites KCW-C, KCW-F, and KCW-I and has an age range of ~3.2 to 2.25 ka. The preserved surface of the Qf2 ranges from ~5 to 7.5 m above the modern channel and is characterized by thinly developed soils. Alluvial fill Qf3 is located at sites KCW-A, KCW-D, KCW-I, and KCW-J and has an age ranges of ~2.15 to 1.45 ka. The preserved surface of this alluvial fill ranges from ~4.5 to 7.5 m above the modern channel. The Qf4 alluvial fill shows up at sites KCW-B, KCW-C, KCW-E, KCW-G, KCW-H, KCW-I, KCW-J, and KCW-K and has an age ranging from ~1.3 – 0.8 ka. Preserved surface heights of this alluvial fill package ranges from ~ 2 to 9 m above the modern channel. The youngest alluvial fill,

Qf5, is evident at every site in KCW and has an age range of ~0.7 to 0.12 ka. This alluvial fill is commonly the tallest or capping deposit in the study area and reaches a maximum height of ~11 m above the modern channel floor. Ultimately, this study successfully updated the existing chronology from the three Holocene episodes of aggradation as identified by Hereford (2002) and the four poorly constrained alluvial fills identified by Harvey et al. (2011) (Fig. 3.19).

Complications involved in determining the timing of incision and deposition events in KCW were primarily centered on each geochronologic dating technique. These problems are detailed in Chapter 2, but are briefly mentioned here because of their overall impact on the alluvial chronology. One of the primary problems with radiocarbon dating was mistakenly analyzing Cretaceous coal. Five radiocarbon samples returned near-infinite ages ranging from ~42.6 to 49.4 cal kyr BP (Fig. 3.18; Table 3.2). Redeposition of charcoal was equally problematic and accounted for four age reversals at study sites KCW-D (14C-9), KCW-H (14C-25), and KCW-J (14C-33), and KCW-K (14C-35). Hence, constraining the timing of aggradation at each of these sites relied on OSL ages or stratigraphically consistent radiocarbon ages. Moreover, a major assumption with radiocarbon dating in general is that sample deposition occurred shortly after the death of the organism dated. Hence, the radiocarbon ages only provide a maximum age of deposition.

Partial bleaching of alluvium was a particular concern for OSL dating. The flashy flow and high sediment-discharge events indicated in the alluvial stratigraphy suggest that most sand grains may not have been sufficiently exposed to light before being deposited. This was expected as indicated by previous OSL-related studies from dryland fluvial systems (e.g. Bailey and Arnold, 2006; Arnold et al., 2007; Summa-Nelson and Rittenour, 2012). Most of these problems were reduced by using single-grain (SG) dating and a minimum-age-model (MAM) (e.g. Galbraith et al., 1999) to calculate the equivalent dose for samples with high overdispersion or a significant positive skew in  $D_e$  distribution. Despite the use of SG and MAM, OSL samples USU-1177 (KCW-B) and USU-1029 (KCW-J) show preliminary age inversions when compared

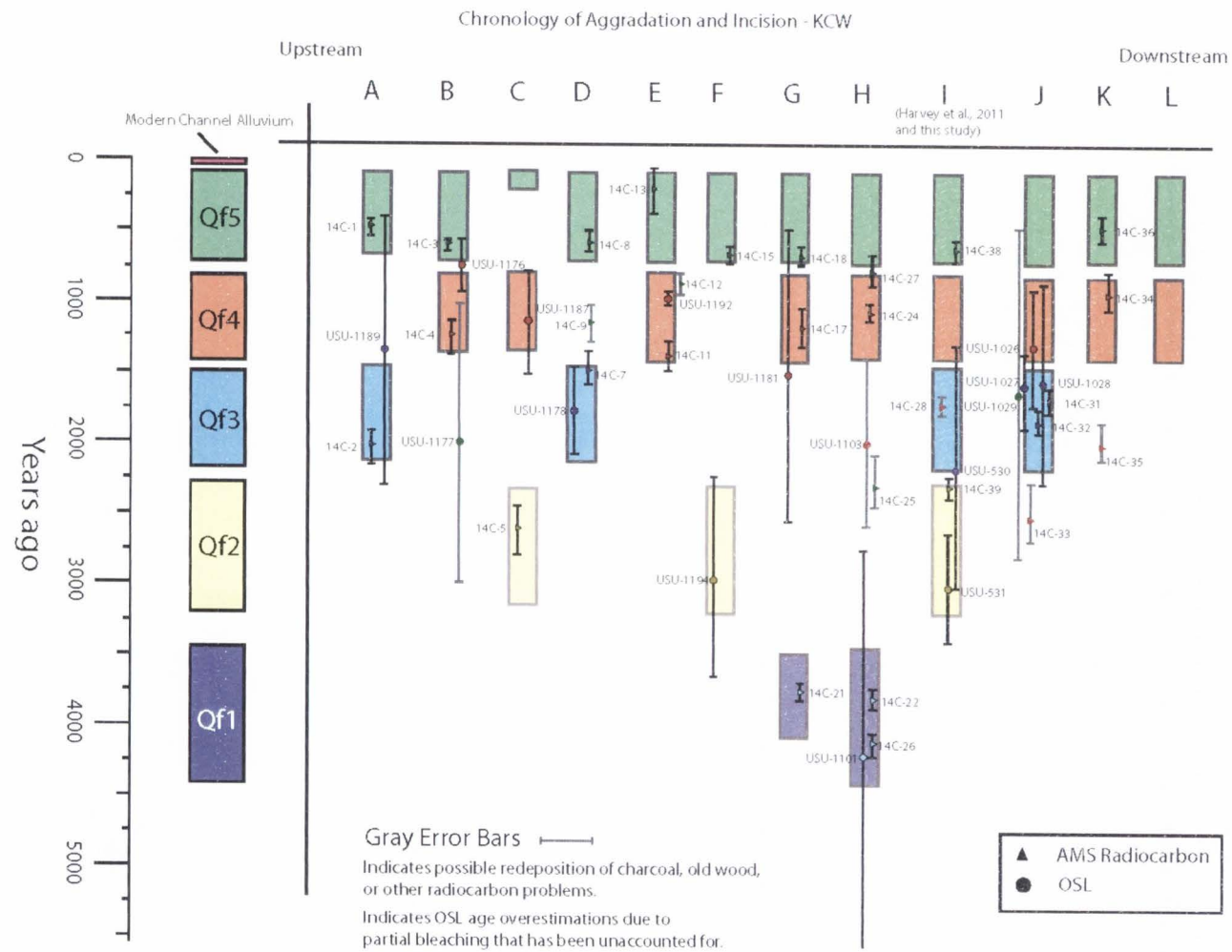


Fig. 3.18. Chronology of Aggradation and Incision events at KCW derived from detailed stratigraphic mapping, AMS radiocarbon (triangles) and OSL (circles) dating. Green = Qf5 fill, orange = Qf4 fill, blue = Qf3 fill, yellow = Qf2 fill, purple = Qf1 fill.

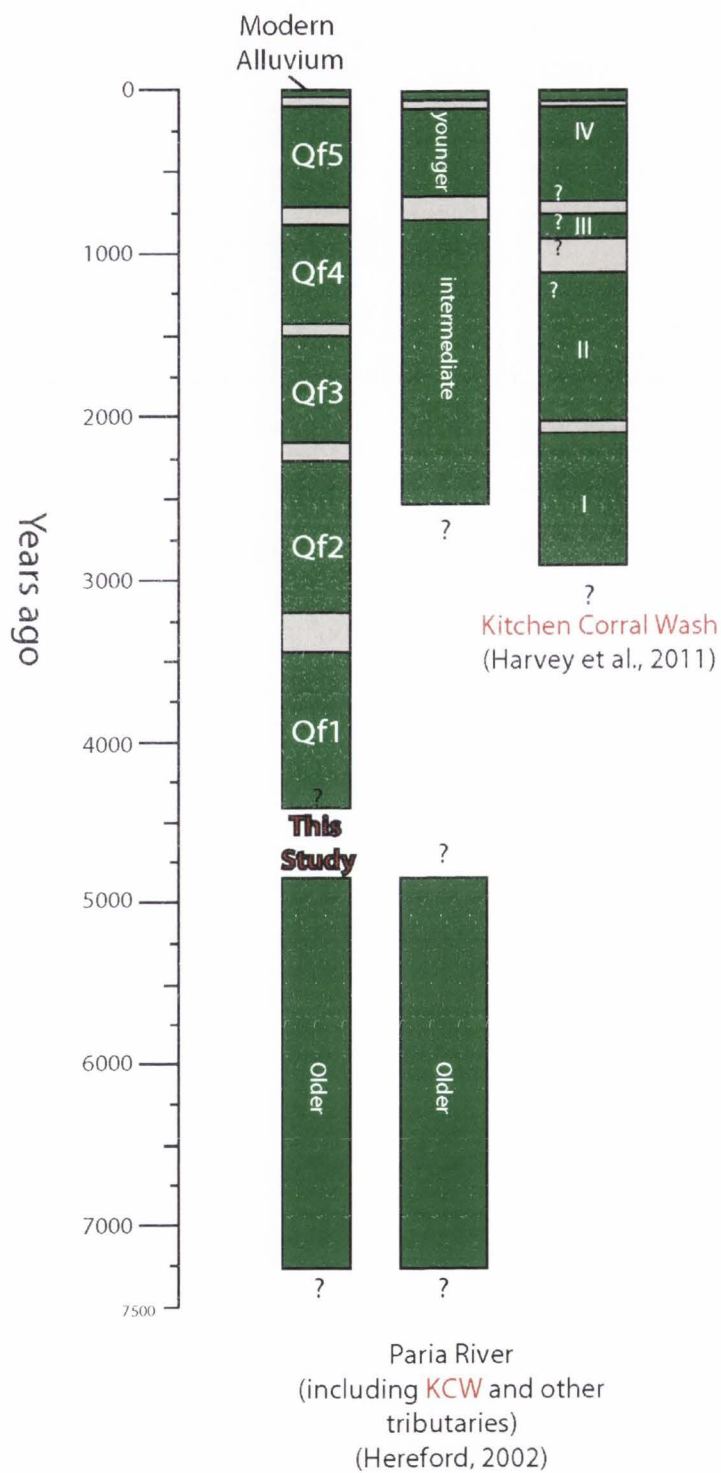


Fig. 3.19. Comparison of existing KCW chronologies from KCW (e.g. Hereford, 2002; Harvey, 2009; Harvey et al., 2011) with the newly developed chronology from this study.

to the arroyo-wall stratigraphy at each site (Fig. 3.18; Table 3.3), and other radiocarbon and OSL ages. However, further analyses of each sample may reconcile these aberrant ages.

Besides problems with geochronologic dating techniques, preservation of alluvial fill packages varied throughout KCW. Only three sites (KCW-G, KCW-H, KCW-J) showed evidence for at least three alluvial fills in their arroyo wall exposures, while only one site (KCW-I) showed evidence for at least four alluvial fills (Fig. 3.20). In general, the two youngest alluvial fill packages (Qf4, Qf5) were most commonly preserved and so age reconstruction on the aggradation of these fills is the best constrained. Unsurprisingly, the oldest alluvial fill packages (Qf1, Qf2, and Qf3) were preserved at fewer study sites and so age constraints of these fills, especially Qf1, are limited. Variability in preservation of alluvial fills at KCW was expected because of the dynamic nature of the arroyo system removes the sedimentary record over time and limits the preservation and exposure of older deposits. Importantly, identification of the oldest alluvial fill (Qf1) was largely aided by the presence of a thick (>65 cm) buried soil capping this fill (Figs. 3.12 and 3.13). At KCW-G, radiocarbon and OSL age control initially seemed to conflict in what seemed to be a continuous alluvial fill package. However, though only ~3 m of the Qf1 fill is exposed, the stratigraphy of tabular channel-margin deposits underlying a meter-scale thick, red buried soil was correlative to the better constrained Qf1 fill at study site KCW-H. Additionally, radiocarbon ages at each of these sites show good correspondence (Figs. 3.12 and 3.13).

### 3.5.2 *Potential Intrabasinal Influences*

The modern channel profile along the length of Park Wash to the main KCW channel has knickpoints that formed as a result of locally exposed bedrock (Figs. 3.2 and 3.20). Within the main KCW alluvial channel, a ~7 m tall sandstone outcrop of the Triassic Moenkopi formation forms a topographic high (knickpoint 3) between two tributary study sites (e.g. KCW-E and KCW-G) and a main-stem study site (KCW-H). If downcutting has recurred across this

knickpoint during every episode of historic and prehistoric arroyo incision, it is possible that this knickpoint prevented or delayed upstream migration of the of the arroyo headcut, thereby creating a critical threshold for upstream incision during episodes of arroyo cutting.

Collectively, Deer Springs Wash and Park Wash tributaries have every Holocene alluvial fill preserved in their arroyo wall exposures, which suggest that arroyo incision was never disconnected in the KCW study area (Fig. 3.20). Additionally, reconstructed relict arroyo-wall heights suggest that aggradation likely overtopped this knickpoint prior to any Holocene arroyo cutting event. In this case, incision would not have initially been perturbed by knickpoint 3 and therefore upstream migration of the channel headcut would have likely proceeded uninterrupted.

Finally, if it is assumed that incision occurred across this knickpoint during every entrenchment event, it must also be assumed that this knickpoint is laterally continuous across the alluvial valley. Currently, the only evidence for a continuous knickpoint is a bedrock outcrop of Triassic Moenkopi Fm exposed above the valley floor and located ~200 m to the east. However, bedrock outcrops at knickpoint 1 and knickpoint 2 located upstream in the Park Wash tributary are not evident in the Deer Springs Wash tributary (Fig. 3.3). This suggests that the knickpoints in the study area are localized and may not have been influential in prehistoric arroyo cutting unless incision continued over a fixed position.

Holocene alluvial fill heights above the modern channel also suggest that arroyo cutting of the KCW channel was most likely influenced by changes in the channel profile geometry. The modern channel in the study area has a gradient of ~0.008 and an irregular profile caused by the removal of valley fill alluvium during the historic arroyo cutting event. When overlain by the heights of relict alluvial fills, it is evident that the KCW stream profile changes to more convex (Fig. 3.20) because alluviation causes steepening of the channel gradient along reaches throughout KCW. These oversteepened alluvial reaches likely created a catchment-specific critical threshold resulting from processes such as localized tributary debris fan deposition or

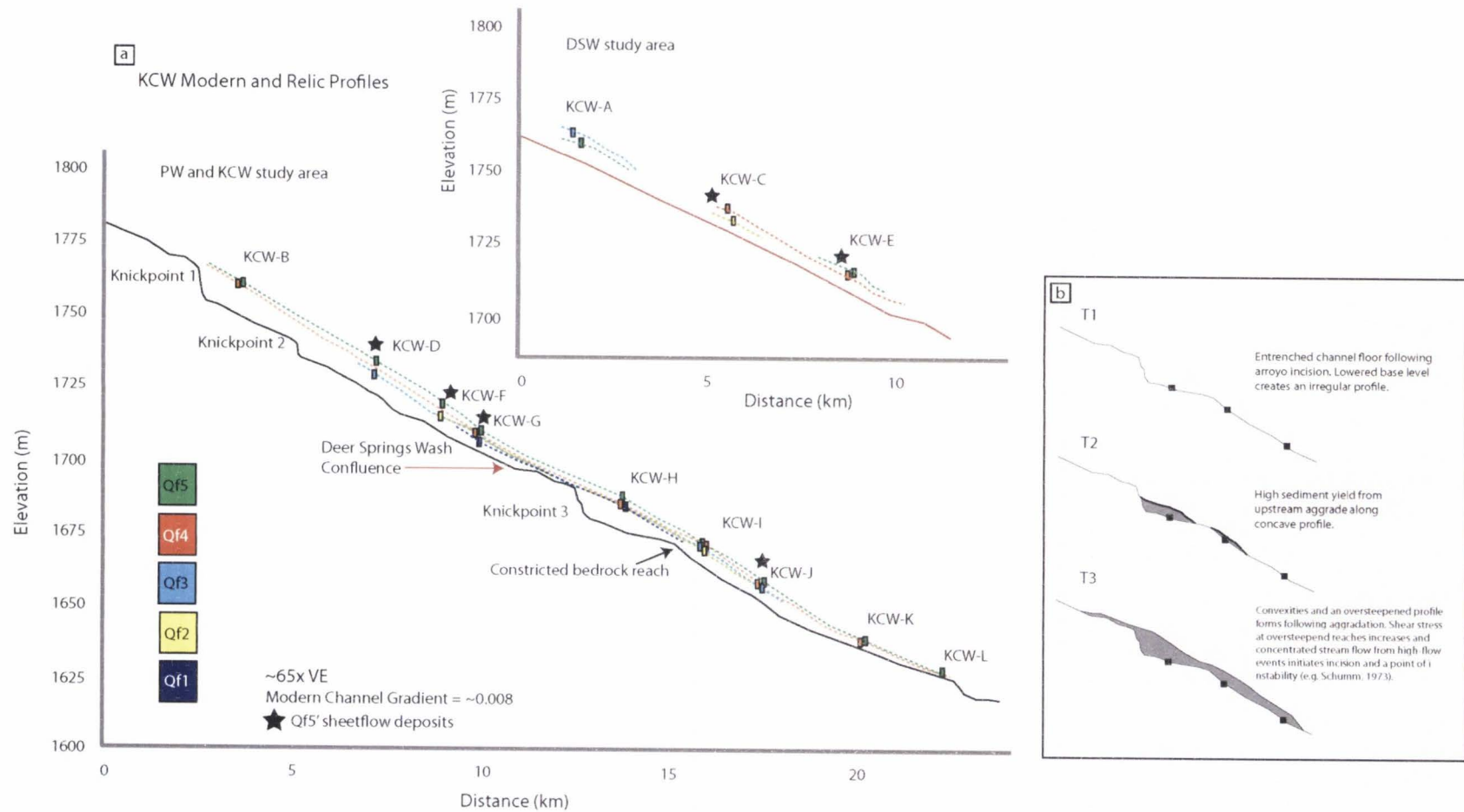


Fig. 3.20. (a) Modern stream profile and preserved arroyo-wall heights of KCW alluvial fills showing a relative increase over time. (b) Hypothetical time-transgressive aggradation of an irregular KCW stream profile to a more convex (prehistoric) stream profile.

deposition downstream from a loss of sediment transport capacity due to bed infiltration (e.g. Graf, 1983; Harvey and Pederson, 2011). When hit by high-magnitude flood events with enough stream power, arroyo incision could occur along a point of channel instability, as originally suggested by Schumm and Hadley (1957). Incision and subsequent channel widening would continue until some process (e.g. change in channel gradient, channel-wall failure, vegetation, or climate) began to promote reaggradation. In KCW, it appears that every episode of arroyo cutting significantly changed the channel geometry or was unable to lower the channel to its previous depth. In this case, reaggradation of the system may have needed to attain a greater height to approach a critical threshold for incision (see Fig. 3.20). However, this is based on the preserved arroyo-wall heights, which may or may not indicate the maximum height of arroyo paleosurfaces.

### 3.5.3 *Deposition of Qf5' alluvium*

A number of arroyo wall exposures in KCW are capped with ~1-3 m of channel-margin (CM) and valley-surface (VS), broadly tabular sheetflow deposits (e.g. St, Sl, Sm, Sr, Sh) that typically overlie a buried incipient soil. These deposits most commonly the capping units of alluvial fill Qf5, and are referred to as Qf5'. Downstream of knickpoint 1 in PW, Qf5' deposits are absent at KCW-B, thicken to ~2.3 m at KCW-D, thin to 1.9 m at KCW-F, and begin to pinch out at KCW-G (Figs. 3.7, 3.9, 3.11, and 3.12). In the DSW tributary, these sheet-flow deposits first appear as a ~2.4 m thick unit at KCW-C and thin to a 1.3 m thick deposit at KCW-E (Figs. 3.8 and 3.10). In the main trunk channel of KCW, Qf5' deposits are initially missing below knickpoint 3 at KCW-H and KCW-I, and then appear at KCW-J as a 50 cm thick low-angle crossbedded sand deposits. A radiocarbon sample (14C-8) collected ~40 cm below the Qf5' deposit at site KCW-D returned an age of  $0.57^{+0.11}_{-0.01}$  cal kyr BP<sub>2010</sub> while a radiocarbon sample (14C-20) collected above a buried soil in a Qf5' deposit at site KCW-E returned a near modern

age of  $0.2^{+0.19}_{-0.09}$  cal kyr BP<sub>2010</sub>, suggesting these deposits are considerably younger than the Qf5 alluvial fills they overlie.

The capping sheetflood deposits in this study are characteristically similar to the D3 deposits described by Delong et al. (2011) from the Cuyama River arroyo in west-central California. In their study, Delong et al. (2011) suggested that arroyo entrenchment and the deposition of inset fill terraces (e.g. D3) within downstream and upstream reaches of the Cuyama River was correlative with valley-floor sheetflow deposition of capping alluvium (e.g. D3) along unentrenched reaches. Their interpretations were largely based off of depositional facies, soil development, and radiocarbon ages. Currently, radiocarbon age results from the present study cannot confirm that the Qf5' deposits are temporally correlative with historic channel incision, and so may not have been deposited by processes described in Delong et al. (2011).

Alternatively, the near-modern radiocarbon ages from KCW suggest it is possible that a change in paleoflood hydrology along the Qf5 valley surface caused sheetflow deposition just before historic channel incision. Deposition of Qf5' may have resulted from an increase in overbank flow caused by an increase in the frequency and magnitude of flood events, or from overspilling at the valley surface as paleoarroyo channel was reaching its maximum fill. Additionally, buried soils that appear to be separating Qf5' alluvial deposits at KCW-J suggest sheetflood episodes may have been discontinuous (Fig. 3.15). Moreover, the alluvial fills in KCW appear to show a trend of increasing alluvial surface heights following aggradation (Figs. 3.20 and 3.21). Whatever the depositional mechanism, it appears that Qf5' is the highest fill deposit within the study area (Fig. 3.21).

#### 3.5.4 *Comparing and Understanding Regional Chronologies*

Initial comparisons of chronologies from KCW, the canyon reach of Kanab Creek (Summa, 2009; Summa-Nelson and Rittenour, 2012) and the upper Escalante River (Hayden, 2011) indicate a different number of cut-fill events throughout the Holocene that have been

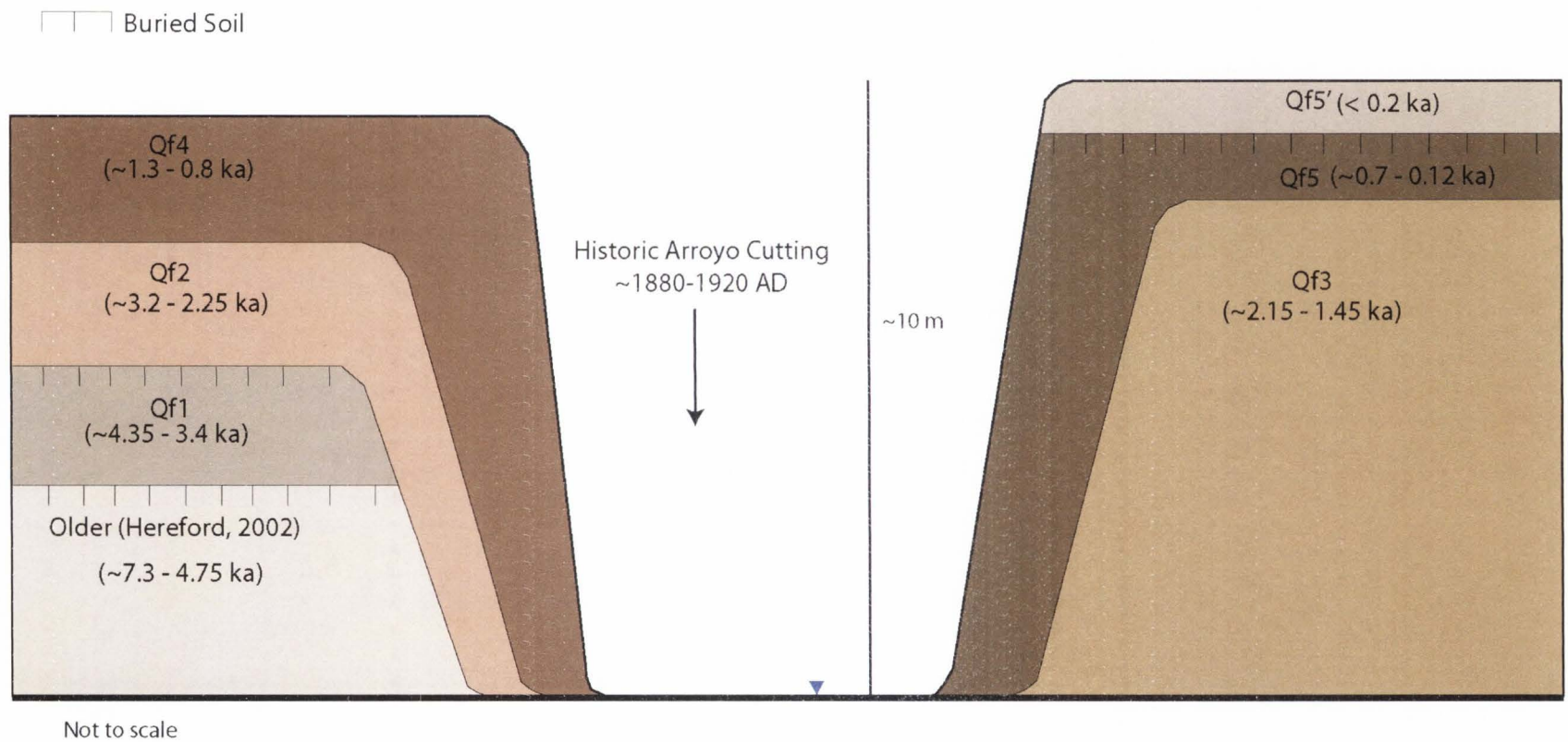


Fig. 3.21. Schematic chronostratigraphy of KCW.

inferred from stratigraphic relations, and radiocarbon and OSL ages of alluvial packages (Fig. 3.22). Whereas KCW indicates at least six cut-fill events, results from the upper Escalante River indicate a higher frequency of arroyo cut-fill events (six) while canyon reach of Kanab Creek reveals a lower frequency (four) over the last ~ 5 to 7 ka. However, uncertainties in the frequency of arroyo cutting and filling in all studies are limited to arroyo-wall preservation and accurate identification of arroyo stratigraphic cut-fill relations. Further, correlating regional chronologies to either allogenic or autogenic forcings is difficult due to the temporal complexity of arroyo cutting and filling, and the centennial-scale age resolution from radiocarbon and OSL dating techniques. Nonetheless, alluvial chronologies can be used to make some general statements regarding the balance between allogenic and autogenic forcings in regional arroyos.

When compared to the canyon reach of Kanab Creek (KC), the KCW chronology suggests that there are some similarities in the timing of arroyo aggradation and incision over the last ~1 ka (Fig. 3.22) as originally described by Hereford (2002). Although it appears that incision at KCW may have initiated slightly later (~0.8 ka) than the ~0.9 ka incision events at KC, the temporal resolution of the KCW radiocarbon and OSL ages are within error of this episode of incision. The start of this ~0.9 ka episode of incision is also evident when compared to the chronology of the upper Escalante River (ER). However, an intermediate cut-fill episode is indicated in the chronostratigraphy of Hayden (2011) which starts at ~0.5 ka and ends prior to the historic channel incision (~1903 – 1932 AD) identified by Webb and Baker (1987) (Fig. 3.22). This transitional cut-fill episode suggests that the upper Escalante River may have been more geomorphically sensitive to climatic or hydrologic perturbations over the past ~1 ka when compared to KCW and KC. It is also possible that flashy flow events during this time were much more variable within the contributing area of the upper Escalante River. This variability may be due to fluctuations in the frequency and intensity of climate-related events such as late summer tropical storms or the North American Monsoon. Conversely, results from Hayden (2011) indicate significant age-overlapping between the Unit VI alluvial fill and preceding alluvial fill

(Unit V). This overlap suggests that the ~0.5 to 0.12 ka cut-fill episode may have actually been continued aggradation of the Unit V fill from sheet-flood deposition caused by a change in the paleohydrology, similar to the Qf5' alluvial deposits in KCW. Additionally, Hayden (2011) does not indicate that a buttress unconformity separates Unit VI from Unit V that would otherwise support arroyo cutting.

Beyond the last ~1 ka, arroyo aggradation and incision episodes between each of these drainages are more temporally complex. For example, an episode of incision occurred between ~1.45 and 1.3 ka prior to the aggradation of alluvial fill Qf4 in KCW (Fig. 3.22). This episode of entrenchment is within error of incision at ER but overlaps with a period of aggradation (Qa3 fill) seen in KC records. Hence, this near-synchronous relationship between KCW and ER may be a result of characteristically similar catchment-specific geomorphic thresholds during an interval of flood intensive regional climate perturbations. On the other hand, aggradation of the Qa3 fill at KC might have been due to a less sensitive geomorphic threshold in the face of similar climate perturbations. This one scenario can be explained by differences in regional arroyo morphology. The channel geometry of KC may have reduced the overall sediment transport capacity, thereby only enabling continued deposition. Similarly, critical thresholds for incision in KCW and ER may have been approached more readily due to a smaller sediment transport capacity and rapid deposition derived from upstream, local tributary or hillslopes sediments.

Temporal offsets in arroyo dynamics also exist at ~3.5 ka, where KCW and KC indicate a near-synchronous episode of entrenchment but ER indicates a ~1.6 ka year episode of aggradation of the Unit II alluvial fill (Fig. 3.22). However, given the approximate <700 year time span for complete channel aggradation and incision during the late Holocene in ER, it is likely that deposition of the Unit II alluvial fill was interrupted by channel cutting events. Moreover, Hayden (2011) acknowledges that cut-fill relationships in ER were generally inferred from depositional breaks, not buttress unconformities, and so evidence of an incision event in ER

## Correlation of Regional Drainage Chronologies

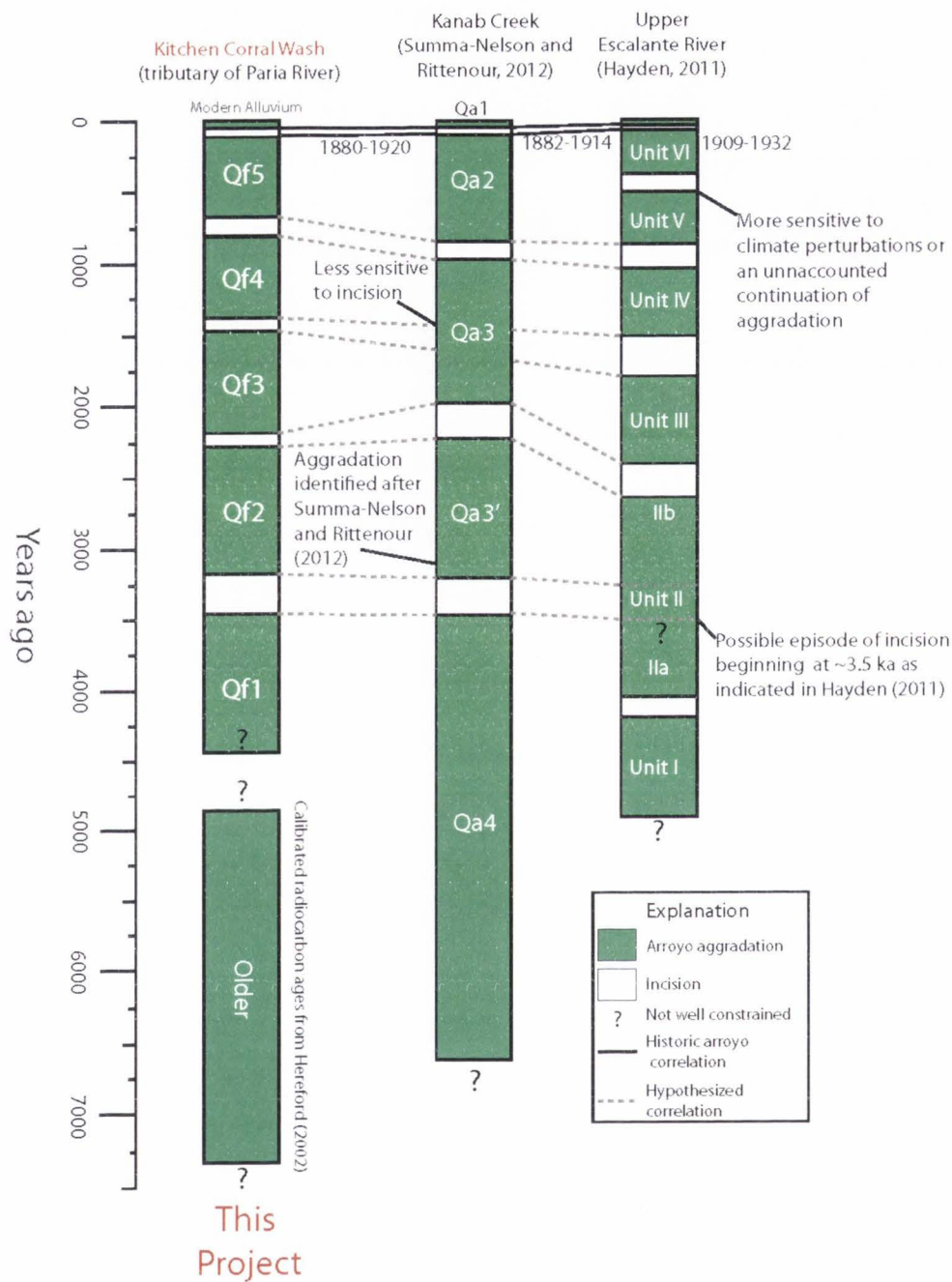


Fig. 3.22. Regional correlation of alluvial chronologies and the chronology derived from KCW in this study. Modern alluvium ages from KCW (Hereford, 2002), Kanab Creek (Webb et al., 1991), and the upper Escalante River (Webb and Baker, 1987) are reported.

generally relied on distinct separations in the chronologies an alluvial package. Hence, a gap in the timing of Unit II deposition identified by Hayden (2011) suggests that there may have been an episode of incision at  $\sim 3.5$  ka (Fig. 3.22). This would be temporally consistent with the timing of entrenchment events in KCW and KC and would suggest that incision at this interval was likely caused by an allogenic (climate-related) forcing. As the oldest alluvial fills from KCW (Qf1), KC (Qa4), and ER (Unit I) are poorly preserved and have limited age control, correlation between episodes of aggradation and incision is unclear. However, alluvial chronologies from regional drainages suggest an extensive period of aggradation was ongoing prior to  $\sim 4.35$  ka and may have started as early as  $\sim 7.3$  ka (e.g. Hereford, 2002).

When taking into account the uncertainties involved with age resolution, alluvial fill preservation, and arroyo-wall stratigraphic cut-fill interpretation, it is clear that a near-synchronous correlation between these three regional arroyo systems can be made. Comparing the regional alluvial chronologies from  $\sim 3.5$  ka to present suggests that an allogenic forcing (e.g. climate) was likely a driver of arroyo dynamics. The frequency of arroyo cut-fill events between drainages becomes more similar if the episode of incision between Unit V and Unit VI in ER (see Hayden, 2011) is actually continued deposition and if the 1.6 ka episode of aggradation in ER was interrupted by arroyo cutting events  $\sim 3.5$  ka. While uncertainties in ER exist, radiocarbon and OSL ages from each regional alluvial fill are within error of one another and the cut-fill episode between KCW and ER are strikingly similar, as would be expected from a dominantly allogenic forcing.

On the other hand, the Qa3 alluvial fill in KC suggests there may be an asynchronous relationship between regional drainages (Fig. 3.22). As mentioned earlier, this could be due to the difference in intrinsic geomorphic thresholds (autogenic controls) during the period from  $\sim 1.3$  to 1.8 ka. More importantly, historical documentation suggests a difference of  $\sim 30$  years between arroyo cutting between these three drainages (e.g. Webb and Baker, 1987; Webb et al., 1991; Webb and Hasbargen, 1997; Hereford, 2002). Hence, while climate played a role in historic

channel incision, it is also clear that catchment-specific thresholds (in addition to anthropogenic activity) may have contributed to the temporal offsets in incision or aggradation. Ultimately, the temporal complexity or arroyo dynamics makes it difficult to qualify the effect allogenic or autogenic forcings by only comparing regional alluvial chronologies. While a climate-related forcing may be more influential to arroyo dynamics, as suggested from a comparison of regional stratigraphy and age results, a qualitative comparison to paleoclimate records is needed to test this assertion.

### 3.5.5 *Comparison to Paleoclimate Records*

There is debate about the role of climate in driving episodes of arroyo cutting and filling, and a number of studies have attempted to resolve this by comparing alluvial chronologies to paleoclimate records (e.g. Hereford, 2002; Mann and Meltzer, 2007). Hereford (2002) compared his KCW and regional alluvial chronologies with dendroclimatic reconstructions of the southern oscillation index (SOI) from Stahle et al. (1998) and suggested that historic and Late Holocene arroyo cutting events in the southern Utah were caused by extreme flood events resulting from increases in the frequency and intensity of El Niño-Southern Oscillation (ENSO) activity. Later, Mann and Meltzer (2007) suggested that it would be unlikely for interannual or decadal-scale teleconnections, like ENSO, to drive century to millennial-scale incision and aggradation events. Rather, they suggested that decadal-scale teleconnections, such as ENSO, are imbedded and help modulate more influential and longer climatic perturbations, such as those associated with the North American Monsoon (NAM). They compared their alluvial records to isotopic  $\delta^{18}\text{O}$  and  $\delta^{13}\text{C}$  from snail shells and  $\delta^{15}\text{N}$  from bison bones (Meltzer, 2006) and regional paleoclimate records to propose that the strength of the NAM controls summer-wet (strengthened NAM) or summer-dry (weakened NAM) conditions respectively contribute to valley entrenchment or alluviation in northeastern New Mexico. The following sections will compare alternative ENSO,

NAM, and representative regional paleoclimate records of the past ~7.3 ka to the alluvial chronology from KCW to test for similar climatic forcings.

### 3.5.6 *Mid-Holocene Paleoclimate Records*

Paleoclimate records suggest conditions during aggradation of the oldest fill (~7.3 – 4.85 ka) from Hereford (2002) were some of the warmest and driest of the mid-Holocene and directly align with the Altithermal warm period from ~7 to 5 ka (Antevs, 1952; Thompson et al., 1993; Menking and Anderson, 2003). For example, Reheis et al. (2005) noted dune activity from ~8.5–6 ka in Canyonlands National Park, indicating a period of drought throughout the Colorado Plateau, and Ford et al. (2010) indicated a later period (~4 ka) of increased dune activity at Coral Pink Sand Dunes State Park in southern Utah which is attributed to reduced precipitation (Fig. 3.22). Moreover, winter precipitation in the southwestern United States is known to decrease during enhanced La Niñas in response to teleconnections with ENSO (Redmond and Koch, 1991) and periods of increased dune activity and dust emissions have often been linked to a weakened ENSO (Okin and Reheis, 2002; Reheis, 2006). Weakened ENSO and enhance La Niña conditions are also corroborated by atmospheric-oceanic teleconnections from the mid-Holocene in which high boreal summer insolation and strong austral winter insolation likely contributed to the warm and dry Altithermal conditions (Liu et al., 2000). Finally, data derived from decreased sedimentation in the Laguna Pallacocha (southern Ecuador) and the El Junco sand (Galapagos Islands) record proxies suggest a mostly weakened ENSO signal from ~7.5 to 3.5 ka (e.g. Moy et al., 2002; Conroy et al., 2008). This long and relatively dry Altithermal interval not only aligns with the deposition of Hereford's (2002) older fill (~7.3 – 4.85 ka) but also with the oldest fill in KC (Qa4, ~6.5 – 3.5 ka).

Alluviation of the Qf1 fill in KCW and Unit 1 fill in ER falls within the ~5 to 3.2 ka interval of the early Neoglacial, a period of glacial advancement and some periglacial activity

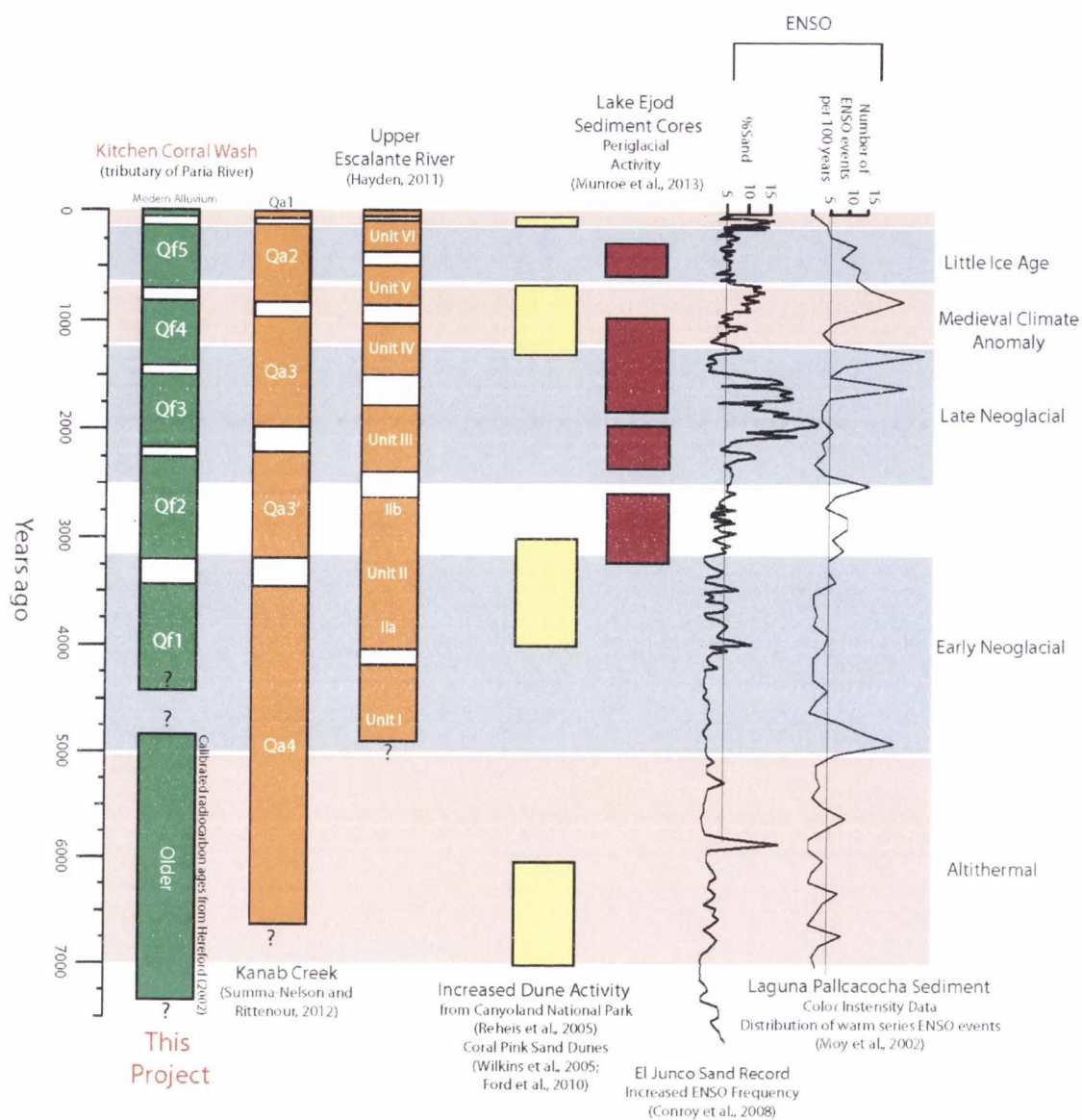


Fig. 3.23. Holocene paleoclimate records correlated with complete chronologies from this study and regional drainages.

characterized by regionally cooler temperatures and increased effective moisture (Denton and Karlen, 1973; Fall, 1997) (Fig. 3.23). Castiglia and Fawcett (2006) noted distinct episodes of increased precipitation within this period are distinguished by periodic lake level highstands throughout the Palomas basin system in northern Mexico from ~4.25 to 3.8 ka, which correlate with glacial advance records in northwestern New Mexico (Armour et al., 2002). Additionally, records derived from Laguna Pallcacocha (Moy et al., 2002) and El Junco sand (Conroy et al., 2008) suggest a slight increase in ENSO variability starting after ~5 ka and extending to ~3.5 ka. As suggested by Webb et al. (1991), increased effective moisture during this period may have increased sediment input regional systems due to physical and chemical weathering of bedrock and hillslope deposits, thereby promoting system aggradation. Additionally, it is possible that regional drainages would have aggraded to some critical geomorphic threshold during the length of the early Neoglacial, and the slight variability in ENSO strength may have contributed to arroyo episodes of arroyo incision up to ~3.2 ka (Fig. 3.23).

### 3.5.7 *Increased Climate Variability into the Late Holocene*

Following the end of the early Neoglacial at ~3.2 ka, paleoclimate records indicate a clear transition to a period of increased climate variability that extends through the late Neoglacial, Medieval Climate Anomaly (MCA) and the Little Ice Age (LIA) (Fig. 3.23; 3.24). It is also during this period that the frequency of episodic arroyo cutting and filling appears to increase. Hence, while a relatively stable climate from ~7 to 3.2 ka may have allowed for infrequent episodes of arroyo aggradation and incision, increased climate instability in the late Holocene may also directly correlate with an increase in the frequency of arroyo cutting and filling. However, there is no clear correlation between arroyo cut-fill events and specific climate events, such as drought or increased precipitation.

For example, the period of Qf2 (KCW) and Qa3' (KC) aggradation at ~3.2 - 2.25 ka overlaps with peak values of clastic sediments in lake cores from Lake Ejod in Uinta Mountains

of northern Utah (Monroe et al., 2013) (Fig. 3.23). This paleoclimate record is a proxy of periglacial activity and could be used as a good indication of the warm and dry intervals often associated with arroyo aggradation. However, this record of periglacial activity also overlaps an interval of increased ENSO-related activity, as indicated in the Laguna Pallacocha record of Moy et al. (2002). A similar scenario comparing these two paleoclimate records is evident during the ~2 - 1 ka aggradation of alluvial Qa3 at Kanab Creek but episodes of cutting and filling within the ER and KCW (Fig. 3.23).

A possible explanation for this discrepancy is that correlation does not always equate to causation. As indicated earlier, it is largely accepted that frequent high-magnitude discharge events promote incision while periods of infrequent, low-magnitude flow events promote aggradation (e.g. Leopold, 1951; Webb and Baker, 1987). However, because these high-flow events relate to particular weather phenomenon, it is difficult to separate their frequency and magnitude from temporally complex paleoclimate records. Hence, while the hydrologic conditions inferred from “wet” or “dry” paleoclimate records might imply an increase or reduction in floods, this may not always be the case.

Examples of this are also evident when comparing paleoclimate records to the historical channel cutting events. Webb et al. (1991) indicates that the first erosive floods of historical channel cutting in Kanab Creek occurred in August of 1882 and July of 1883 and were related to monsoonal events. Similarly, Webb and Baker (1987) indicated that large flood events in the Escalante River, starting in 1909 and ending in 1932, also occurred in the later summer and early fall, and were coincident with monsoonal rains. However, a period of intense drought reconstructed from summer-forming latewood tree-rings in southeastern Arizona related to negative standardized precipitation indices (decrease in monsoonal precipitation) from 1882 to 1904 (e.g. Griffin et al., 2013) overlap historic incision in KCW and KC, but an increase in monsoonal precipitation persisted from 1904 until the early 1920s. As discussed earlier, Hereford (2002) attributed historic channel cutting in KCW to wet, flood-related El Niño events with a 5-yr

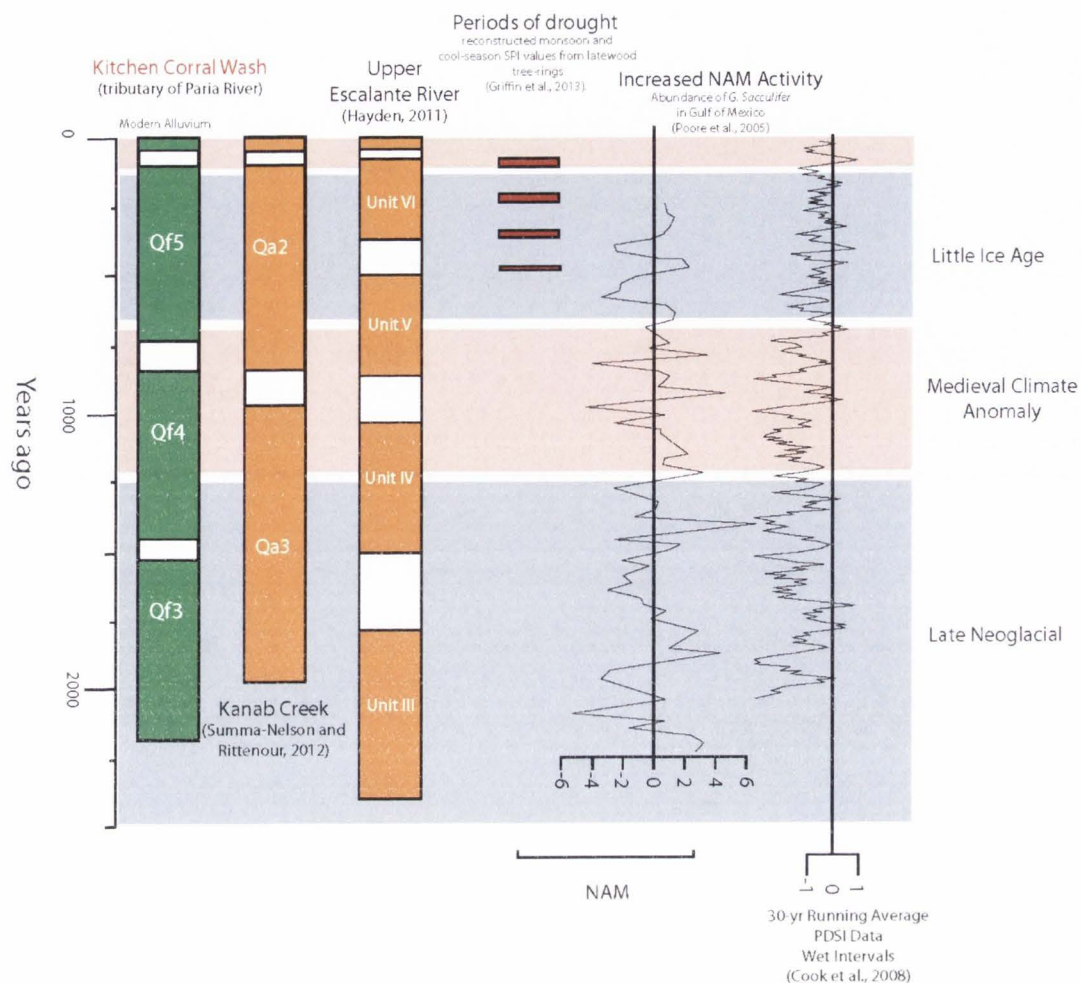


Fig. 3.24. Select Holocene paleoclimate records compared to chronologies of KCW and regional drainages over the last ~2.5 ka.

recurrence interval and Webb et al. (1991) indicate that heavy flooding from heavy snowmelt due to increased ENSO-related winter snowfall caused continued incision at Kanab Creek into the early 1900s. Indeed, the El Junco sand record (e.g. Conroy et al., 2008) clearly show this spike in ENSO activity during the late 1800s (Fig. 3.23). However, Laguna Pallacocha record (e.g. Moy et al., 2002) show a distinct decrease in ENSO activity (i.e. 2-8 year variance) starting at ~1.2 ka and extending to this time (Fig. 3.23). Hence, combining these records indicate that some of the major weather-related events which caused historic arroyo cutting are often imbedded in “warm and dry” paleoclimate records. For this reason, caution should be used when trying to directly correlate ENSO, NAM, or any other regional paleoclimate records to episodes of cutting and filling. Rather, it may be more accurate to relate the relative increase in climate variability to potential arroyo cutting and filling episodes.

For example, drought reconstructions of the southwestern United States from dendrochronologic proxies and the Palmer Drought Severity Index (PDSI) indicate oscillating dry and wet periods over the last ~2.1 ka (e.g. Cook et al., 2008; Fig. 3.24). Additionally, sub-millennial-scale fluctuations in *G. sacculifer* abundance in the Gulf of Mexico from ~2.3 ka to 0.5 ka is interpreted to correspond to precipitation variability due to increased or decreased monsoonal activity in the Colorado Plateau (Poore et al., 2005; Fig. 3.24). These records may not indicate individual flood events, but they do suggest that the variability in monsoonal activity throughout the late Holocene may have contributed to increased arroyo activity. Thus, the role of intrinsic geomorphic thresholds must also contribute to arroyo dynamics in the face of increased climate variability.

### 3.5.8 *Climate and Geomorphic Threshold Interactions*

As expressed earlier, Schumm and Hadley (1957) suggested that arroyos must meet some intrinsic critical threshold for incision to occur. Thus, increased climate variability could increase the timing at which a system will meet a critical threshold. For example, following entrenchment,

a centennial-scale period of dry and warm conditions may initially increase the amount of sediment stored in a drainage basin due to a reduction in stream power and a decline in vegetation along terraces and hillslopes. Intermittent low-magnitude flows imbedded within this period of drought may cause a system to slowly aggrade by depositing thin flood packages of sediment as woody riparian vegetation is established within the channel due to stabilization of the groundwater table at the channel bottom (e.g. Webb and Leake, 2006). Indeed, the common <30cm thick and low-flow regime facies deposits in KCW, KC, and ER indicate this kind of flood-related deposition has occurred. Moreover, at its current aggrading state, several reaches throughout KCW are overwhelmed with riparian vegetation.

A transition to a centennial-scale period of dominantly cooler and wetter climate conditions would likely to continue aggradation, where a vegetation-strengthened hydraulic roughness could allow larger magnitude flows to deposit thicker (>50cm) flood packages with high-flow regime facies. These characteristic deposits are also evident in KCW and other regionally drainages (e.g. thick, massive sand deposits). However, in a system already nearing its critical threshold, a high-magnitude flood event could initiate arroyo cutting. If the climatic, biologic, and geomorphic conditions described are similar within regional drainages, near-synchronous channel incision may occur. On the other hand, it is possible continued aggradation would occur in a system whose critical geomorphic, and biologic, threshold was in dissimilar to nearby drainages. Hence, if hydrologic conditions changed due to a transition back to a regionally warm and dry climate, aggradation would eventually increase the sensitivity of the dissimilar system toward a critical threshold. Accordingly, increased stream power from a series of flood events imbedded within regionally drier conditions would push a system past its critical threshold and trigger incision, but the timing of incision may be asynchronous to other regional drainages.

### 3.6 Conclusions

In this study, a detailed chronstratigraphy of KCW was built using stratigraphic relationships from arroyo-wall exposures and age results from AMS radiocarbon and OSL dating. While each dating method was subject to potential problems, combining the two methods allowed for increased sampling opportunities and cross-checking of results to eliminate aberrant ages. Ultimately, this newly developed chronostratigraphy has expanded and updated the previous KCW alluvial chronologies developed by Hereford (2002) and Harvey et al. (2011), and resulted in the identification of at least six episodes of Holocene aggradation from  $\sim 4.35 - 3.4$  ka,  $\sim 3.2 - 2.25$  ka,  $\sim 2.15 - 1.45$  ka,  $\sim 1.3 - 0.8$  ka, and  $\sim 0.7 - 0.12$  ka, plus an older fill ( $\sim 7.3 - 4.85$  ka) of Hereford (2002), that are interrupted by centennial-scale periods of incision.

Knickpoints identified in the active channel appear to cause local entrenchment depths to decrease immediately upstream of the knickpoints, but do not appear to affect the timing or development of arroyo entrenchment. Rather, the timing of arroyo cutting and filling in KCW may have been influenced by the transition from a shallower, irregular profile following entrenchment to a more convex and potentially more unstable profile during aggradation. Incision was likely induced along reaches with increase convexity during high-magnitude flood events which caused channel cutting to propagate upstream. Additionally, the identification of a young sheetflood deposit capping a number of alluvial fills may have been deposited concurrent with arroyo entrenchment or may have been deposited due to a change in channel paleohydrology immediately before channel incision.

When the alluvial chronology of KCW is compared to regional chronologies from the canyon reach of Kanab Creek and the upper Escalante River, it is evident that the difference in the timing and frequency of arroyo cut-fill episodes may be due to uncertainties in arroyo-wall preservation, stratigraphic cut-fill relationships, and age results. However, when all available uncertainties are taken into account, it seems that the timing and frequency of most regional cut-fill episodes are near-synchronous. This near-synchronous relationship may indicate a strong

climate-related forcing. Additionally, when these regional alluvial chronologies are compared to paleoclimate records, it is apparent that the frequency of arroyo cut-fill episodes responds to the temporal variability of climate change. This appears to support Hereford's (2002) suggestion that regionally contemporaneous aggradation and incision events over the last ~1 ka could be tied to regional shifts in climate related to the Little Ice Age and Medieval Climate Anomaly. However, it is not easy to directly correlate periods of dominantly "wet" or "dry" climate condition (e.g. ENSO or NAM-related) to arroyo cutting and filling chronologies. The reason for this difficulty is two-fold. To begin, it is difficult to separate climate-related changes in hydrologic conditions, either erosional or depositional, from paleoclimate records. Additionally, some catchment-specific geomorphic and biologic threshold must be met before incision can occur. It appears that this critical threshold makes it difficult to draw parallels between alluvial chronologies, causing disconnect between the timing of regional arroyo dynamics wherein arroyo aggradation and incision may not be contemporaneous.

Given the results of this study, more work is needed to bridge the gap that exists with correlation uncertainties between the chronostratigraphy of KCW, and the regional alluvial chronologies and paleoclimate records. This can be resolved in a multi-step approach. To begin, additional alluvial chronologies from characteristically similar drainages proximal and distal to KCW need to be developed for a more meaningful temporal correlation of arroyo cutting and filling. For example, Johnson Wash is an arroyo system located ~25 km to the west KCW that shares similar reach elevations (2800 to 1500 m asl) and arroyo wall heights (< 15 m), but an alluvial chronology for this drainage does not currently exist. In addition, local paleoclimate records (e.g. tree-rings) could be reconstructed from specific catchments to help better resolve some uncertainties with the frequency and strength of aggradational or erosional flood events, which may be a function of annual increases in precipitation.

## REFERENCES

- Aitken, M.J., 1998. *An Introduction to Optical Dating*. Oxford University Press, Oxford.
- Antevs, E., 1952. Arroyo-cutting and filling. *Journal of Geology* 60, 375-385.
- Armour, J., Fawcett, P.J., Geissman, J.W., 2002. 15 k.y. paleoclimate and glacial records from northern New Mexico. *Geology* 30, 723-726.
- Arnold, L.J., Bailey, R.M., Tucker, G.E., 2007. Statistical treatment of fluvial dose distributions from southern Colorado arroyo deposits. *Quaternary Geochronology* 2, 162-167.
- Bailey, R.W., 1935. Epicycles of erosion in the valleys of the Colorado Plateau province. *Journal of Geology* 43, 337-355.
- Baker, V., 1987. Paleoflood hydrology and extraordinary flood events. *Journal of Hydrology* 96, 79-99.
- Balling, R.C., Wells, S.G., 1990. Historical rainfall patterns and arroyo activity within the Zuni River Drainage Basin, New Mexico. *Annals of the Association of American Geographers* 80, 603-617.
- Bryan, K., 1925. Date of channel trenching (arroyo-cutting) in the arid southwest. *Science* 62, 338-344.
- Bull, W.B., 1997. Discontinuous ephemeral streams. *Geomorphology* 19, 227-276.
- Castiglia, P.J., Fawcett, P.J., 2006. Large Holocene lakes and climate change in the Chihuahuan Desert. *Geology* 34, 113-116.
- Cayan, D.R., Redmond, K.T., Riddle, L.G., 1999. ENSO and hydrologic extremes in the western United States. *Journal of Climate*, 2881-2893.
- Cook, E.R., Woodhouse, C.A., Eakin, C.M., Meko, D.M., Stahle, D.W., 2008. Long-term aridity changes in the western United States. *Science* 306, 1015-1018.
- Cooke, R.U., Reeves, R.W., 1976. *Arroyos and Environmental Change in the American Southwest*. Clarendon Press, Oxford.
- Conroy, J.L., Overpeck, J.T., Cole, J.E., Shanahan, T.M., Stinitz-Kannan, M., 2008. Holocene changes in eastern tropical Pacific climate inferred from a Galápagos lake sediment record. *Quaternary Science Reviews* 27, 1166-1180.
- Daniels, J.M., 2008. Distinguishing allogenic from autogenic causes of bed elevation change in late Quaternary alluvial stratigraphic records. *Geomorphology* 101, 159-171.
- Delong, S.B., Pelletier, J.D., Arnold, L.J., Late Holocene alluvial history of the Cuyama River, California, USA. *Geological Society of America Bulletin* 123, 2160-2176.

- Denton, G.H., Karlen, W., 1973. Holocene climatic variations: their pattern and possible cause. *Quaternary Research* 3, 155-205.
- Doelling, H.H., Blackett, R.E., Hamblin, A.H., Powell, J.D., Pollock, G.L., 200. Geology of Grand Staircase-Escalante National Monument, Utah. In: Sprinkel, D.A., Chidsey, Jr., T.C., and Anderson, P.B. (Eds.), *Geology of Utah's Parks and Monuments*, Utah Geological Association Publication 28, 198-231.
- Duller, G.A.T., 2008. Single-grain optical dating of Quaternary sediments: recent advances. *Journal of Quaternary Science* 19 (2), 183-192.
- Ely, L.L., 1997. Response of extreme floods in the south-western United States to climatic variations in the late Holocene. *Geomorphology* 19, 175-201.
- Euler, R.C., Gumerman, G.J., Karlstrom, T.N.V., Dean, J.S., Hevly, R.H., 1979. The Colorado Plateaus: Cultural dynamics and paleoenvironment. *Science* 205, 1089-1101.
- Fall, P.L., 1997. Timberline fluctuation and late Quaternary paleoclimates in the southern Rocky Mountains, Colorado. *Geological Society of America Bulletin* 109, 1306-1320.
- Ford, R.L., Gillman, S.L., Wilkins, D.E., Clement, W.P., Nicoll, K., 2010. Geology and geomorphology of Coral Pink Sand Dunes State Park, Utah. In: Sprinkel, D.A., Chidsey, T.C., Anderson, P.B. (Eds.), *Geology of Utah's Parks and Monuments*. Utah Geological Association Publication 28 (third ed.).
- Galbraith, R.F., Roberts, R.G., Laslett, G.M., Yoshida, H., Olley, J.M., 1999. Optical dating of single and multiple grains of quartz from Jinmium rock shelter, northern Australia. Part I. *Archaeometry* 41 (2), 339-364.
- Gellis, A.C., and Elliott, J.G., 2001. Arroyo changes in selected watersheds of New Mexico, Unites States. In Harvey, M., Anthony, D. (Eds.), *Applying geomorphology to environmental management, a special publication honory Stanley A. Schumm*, Water Resrouces Publications, LLC Press, pp. 225-240.
- Graf, W.L., 1983. The arroyo problem – Paleohydrology and paleohydraulics in the short term. In: Gregory, K.G. (Ed.), *Background to Paleohydrology*. John Wiley and Sons, New York, 297-302.
- Griffin, D., Woodhouse, C.A., Meko, D.M., Stahle, D.W., Faulstich, H.L., Carrillo, C., Touchan, R., Castro, C.L., Leavitt, S.W., 2013. North American monsoon precipitation reconstructed from tree-ring latedwood. *Geophysical Research Letter* 40, 1-5.
- Hack, J.T., 1942. Erosion and sedimentation in the Jeddito Valley and other valleys of the western Navaho country. *Papers of the Peabody Museum of American Archeology and Ethnology*, Cambridge 35, pp. 45-69.
- Hall, S.A., 1977. Late Quaternary sedimentation and paleoecologic history of Chaco Canyon, New Mexico. In: *Geological Society of America Bulletin* 88, 1593-1618.

- Harvey, J.E., 2009. Reconciling Holocene alluvial records in Buckskin Wash, southern Utah. M.S., Thesis Utah State University, unpublished.
- Harvey, J.E., Pederson, J.L., 2011. Reconciling arroyo cycle and paleoflood approaches to late Holocene alluvial records in dryland streams. *Quaternary Science Reviews* 30, 855-866.
- Harvey, J.E., Pederson, J.L., Rittenour, T.M., 2011. Exploring relations between arroyo cycles and canyon paleoflood records in Buckskin Wash, Utah: Reconciling scientific paradigms. *Geological Society of America Bulletin* 123, 2266-2276.
- Hayden, A.E., 2011. Reconstructing the Holocene arroyo history of the upper Ecsalanate River, southern Utah, using optically stimulated luminescence (OSL) and radiocarbon dating. M.S. Thesis, Utah State University. unpublished.
- Hereford, R., 1986. Modern alluvial history of the Paria River drainage basin. *Quaternary Research* 25, 293-311.
- Hereford, R., 2002. Valley-fill alluviation during the Little Ice Age (ca. A.D. 1400-1880), Paria River basin and southern Colorado Plateau, United States. *Geological Society of America Bulletin* 114 (12), 1550-1563.
- Hereford, R., Webb, R.H., 1992. Historic variation of warm-season rainfall, southern Colorado Plateau, southwest United States. *Climatic Change* 22, 239-256.
- Hereford, R., Jacoby, G.C., and McCord, V.A.S., 1996. Late Holocene alluvial geomorphology of the Virgin River in the Zion National Park area, southwest Utah. *Geological Society of America Special Paper* 310, 41 p.
- Huckleberry, G.A., Billman, B.R., 1998. Floodwater Farming, Discontinuous Ephemeral Streams, and Puebloan Abandonment in Southwestern Colorado. *American Antiquity* 63, 595-616.
- Huckleberry, G.A., Duff, A.I., 2008. Alluvial cycles, climate, and Puebloan settlement shifts near Zuni Salt Lake, New Mexico, USA. *Geoarchaeology* 23, 107-130.
- Huntington, E., 1914. *The Climatic Factor as Illustrated in Arid America*. Carnegie Institute Washington Pub.
- Huntley, D.J., Godfrey-Smith, D.I., Thewalt, M.L.W., 1985. Optical dating of sediments. *Nature* 313, 105-107.
- Jones, L.S., Ronseburg, M., del Mar Figueroa, M., McKee, K., Haravitch, B., Hunter, J., 2010. Holocene valley-floor deposition and incision in a small drainage basin in western Colorado, USA. *Quaternary Research* 74, 199-206.
- Karlstrom, T.N.V., 1988. Alluvial chronology and hydrologic change of Black Mesa and nearby regions. In: Bumerman, G.J. (Eds.), *The Anasazi in a Changing Environment*. Cambridge University Press, pp. 45-91.

- Knox, J.C., 1983. Responses of river systems to Holocene climates. In: Wright, Jr., H.E. (Ed.), Late Quaternary Environments of the United States. The Holocene, vol. 2. University of Minnesota Press, Minneapolis, pp. 26-41.
- Leopold, L.B., 1951. Rainfall frequency: An aspect of climatic variation. Transactions of the American Geophysical Union 32, 347-357.
- Liu, Zhengyu, Kutzbach, J., Wu, Lixin, 2000. Modeling climate shift of El Niño variability in the Holocene. Geophysical Research Letters 27, 2265-2268.
- Mann, D.H., Meltzer, D.J., 2007. Millennial-scale dynamics of valley fills over the past 12,000  $^{14}\text{C}$  in northeastern New Mexico, USA. Geological Society of America Bulletin 119, 1433-1448.
- McFadden, L.F., McAuliffe, J.R., 1997. Lithologically influenced geomorphic responses to Holocene climatic changes in the southern Colorado Plateau, Arizona: A soil-geomorphic perspective. Geomorphology 19, 303-332.
- McFadgen, B.G., 1982. Dating New Zealand archaeology by radiocarbon. New Zealand Journal of Science 25, 379-392.
- Meltzer, D.J., 2006. Folsom: New archaeological investigations of a classic Paleoindian bison kill. University of California Press. Berkeley.
- Menking, K.M., Anderson, R.Y., 2003. Contributions of La Niña and El Niño to middle Holocene drought and Holocene moisture in the American southwest. Geology 31, 937-940.
- Miall, A.D., 2000, Principles of Sedimentary Basin Analysis, 3<sup>rd</sup> ed. Springer, New York.
- Miller, J.R., Kochel, R.C., 1999. Review of Holocene hillslope, piedmont, and arroyo system evolution in Southwestern United States: Implications to climate-induced landscape modifications in southern California. In Rose, M.R., Wigand, P.G. (Eds.), Trends and Extremes of the Past 2000 Years, pp. 139-192. Proceedings of the southern California climate symposium, October 25, 1991, Technical report No. 11. Los Angeles: Natural History Museum of Los Angeles County.
- Moy, C.M., Seltzer, G.O., Rodbell, D.T., Anderson, D.M., 2002. Variability of El Niño/Southern Oscillation activity at millennial timescales during the Holocene epoch. Nature 20, 162-165.
- Munroe, J.S., Klem, C.M., Bigl, M.F., 2013. A lacustrine sedimentary record of Holocene periglacial activity from the Uinta Mountains, Utah, U.S.A. Quaternary Research 79, 101-109.
- Murray, A.S., Olley, J.M., 2002, Precision and accuracy in the optically stimulated luminescence dating of sedimentary quartz: A status review. Geochronometria 21, 1-16.

- Murray, A.S., Wintle, A.G., 2000. Luminescence dating of quartz using an improved single-aliquot regenerative-dose protocol. *Radiation Measurements* 32, 57-73.
- Okin, G.S., Reheis, M.C., 2002. An ENSO predictor of dust emission in the southwestern United States. *Geophysical Research Letters* 29, 46.1-46.3.
- Patton, P.C., Schumm, S.A., 1981. Ephemeral-stream processes: Implications for studies of Quaternary valley fills. *Quaternary Research* 15, 24-43.
- Patton, P.C., Boison, P.J., 1986. Processes and rates of formation of Holocene alluvial terraces in Harris Wash, Escalante River basin, south-central Utah. *GSA Bulletin* 97, 369-378.
- Poore, R.Z., Pavich, M.J., Grissino-Mayer, H.D., 2005. Records of the North American southwest monsoon from Gulf of Mexico sediment cores. *Geology* 33, 209-212.
- Redmond, K.T., Koch, R.W., 1991. Surface climate and streamflow variability in the western United States and their relationship to large-scale circulation indices: *Water Resources Research* 27, 2381-2399.
- Reheis, M.C., 2006. 16-year record of dust deposition in southern Nevada and California, USA. *Journal of Arid Environments* 67, 487-520.
- Reheis, M.C., Reynolds, R.L., Goldstein, H., Roberts, H.M., Yount, J.C., Axford, Y., Cummings, L.S., Shearin, N., 2005. Late Quaternary eolian and alluvial response to Paleoclimate, Canyonlands, southeastern Utah. *GSA Bulletin* 117, 1051-1069.
- Reimer, P.J., M G L Baillie, M.G.L., Bard, E., Bayliss, A., Beck, J.W., Blackwell, P.G., Bronk Ramsey, C., Buck, C.E., Burr, G.S., Edwards, R.L., Friedrich, M., Grootes, P.M., Guilderson, T.P., Hajdas, I., Heaton, T.J., Hogg, A.G., Hughen, K.A., Kaiser, K.F., Kromer, B., McCormac, F.G., Manning, S.W., Reimer, R.W., Richards, D.A., Southon, J.R., Talamo, S., Turney, C.S.M., van der Plicht, J., Weyhenmeyer, C.E., 2009. Intcal09 and Marine09 radiocarbon age calibration curves, 0-50,000 years cal BP. *Radiocarbon* 51 (4), 1111-1150.
- Rittenour, T.M., 2008. Luminescence dating of fluvial deposits: applications to geomorphic, palaeoseismic, and archaeological research. *Boreas* 37, 613-635.
- Schumm, S.A., Hadley, R.F., 1957. Arroyos and the semiarid cycle of erosion. *American Journal of Science* 255, 161-172.
- Schumm, S.A., 1973. Geomorphic thresholds and complex response of drainage systems. In: Morisawa, M. (Ed.), *Fluvial Geomorphology*. SUNY Binghamton, New York, pp. 299-310.
- Shafer, D.S., 1989. Holocene climatic patterns inferred from pollen and macrofossil records of Holocene lakes of the northern Colorado Plateau, Utah and Arizona. *GSA Abstracts with Programs* 21 (5), 142.

- Sheppard, P.R., Comrie, A.C., Packin, G.D., Angersbach, K., Hughers, M.K., 2002. The climate of the US southwest. *Climate Research* 21, 219-238.
- Smith, S.S., 1990. Relationship of large floods and rapid entrenchment of Kanab Creek, southern Utah. M.S. Thesis, University of Arizona.
- Stahle, D.W., D'Arrigo, R., Krusic, J., Cleaveland, M., Cook, E., Allan, R., Cole, J., Dunbar, R.G., Therrell, M.D., Gay, D.A., Moore, M.D., Stokes, M.A., Burns, B.T., Thompson, L.G., 1998. Experimental dendroclimatic reconstruction of the Southern Oscillation. *Bulletin of the American Meteorological Society* 79, 2137-2152.
- Summa, M. C., 2009. Geologic mapping, alluvial stratigraphy, and optically stimulated luminescence dating of the Kanab Creek area, southern Utah. M.S. Thesis, Utah State University, unpublished
- Summa-Nelson, M.C., Rittenour, T.M., 2012. Application of OSL dating to middle to late Holocene arroyo sediments in Kanab Creek, southern Utah, USA. *Quaternary Geochronology* 10, 167-174.
- Thompson, R.S., Whitlock, C.B., Patrick, J., Harrison, S.P., and Spaulding, W.G., 1993. Climatic changes in the Western United States since 18,000 yr B.P., In: Wright, H.E. Jr., (Ed.), *Global Climates Since the Last Glacial Maximum*: Minneapolis, University of Minnesota Press, 468-513.
- Thorntwaite, C.W., Sharpe, C.F.S, Dosch, E.F., 1942. Climate and accelerated erosion in the arid and semi-arid Southwest with special reference to the Polacca Wash drainage basin, Arizona. U.S. Dep. Agric. Tech. Bull. 808, 134 pp.
- Tucker, G.E., Arnold, L., Bras, R.L., Flores, H., Istanbuloglu, E., Solyon, P., 2006. Headwater channel dynamics in semiarid rangelands, Colorado high plains, USA. *Geological Society of America Bulletin* 118, 959-974.
- Wallinga, J., Murray, A.S., Duller, G.A.T., Törnqvist, T.E., 2001. Testing optically stimulated luminescence dating of sand-sized quartz and feldspar from fluvial deposits. *Earth and Planetary Science Letters* 193, 617-630.
- Wallinga, J., 2002. Optically stimulated luminescence dating of fluvial sediments: a review. *Boreas*, v. 31. 302-322.
- Webb, R.H., Baker, V.R., 1987. Change in hydrologic condition related to large floods on the Escalante River, south-central Utah. In: Singh, V.D. (Ed.), *Regional Flood-frequency Analysis*. D. Reidel Publishers, The Netherlands, 306-320.
- Webb, R.H., Smith, S.S., McCord, V.A., 1991. Historic channel change of Kanab Creek, southern Utah and Northern Arizona. *Grand Canyon Natural History Association Monograph*.
- Webb, R.H., Hasbargen, J., 1997. Floods, ground-water levels, and arroyo formation on the Escalante River, south-central Utah. In: Hill, L.M. (Ed.), *Learning from the Land: Grand*

Staircase-Escalante National Monument Science Symposium Proceedings. U.S. Department of the Interior, pp. 335-345.

Webb, R.H., Leake, S.A., 2006, Ground-water surface-water interactions and long-term change in riverine riparian vegetation in the southwestern United States. *Journal of Hydrology* 320, 302-323.

Wilkins, D., Ford, R.L., Clement, W., Nicoll, K, 2005. Little Ice Age behavior of the Coral Pink Sand Dunes, Kane County, Utah. *GSA Abstracts with Programs* 37, p. 426.

## . CHAPTER 4

## FINAL CONCLUSIONS AND RECOMMENDATIONS FOR FUTURE WORK

Research for this thesis investigated the alluvial chronology of Kitchen Corral Wash, southern Utah. Chapter 2 tested the applicability of combining AMS radiocarbon and OSL dating to date alluvial sediments in order to construct a reach-wide alluvial chronology in a dryland fluvial system. Both AMS radiocarbon and OSL dating have been previously reported to have both limitations and successes in semiarid systems. In Chapter 3, the reconstructed alluvial chronology from KCW was combined with detailed stratigraphic descriptions to create a robust mid to late Holocene chronostratigraphy of past arroyo cut-fill events. Results from this chronostratigraphy were compared to regional alluvial records from Kanab Creek and the upper Escalante River and regional paleoclimate records in order to test for an allogenic (climate-related) or autogenic (internal geomorphic threshold) forcing of arroyo cut-fill dynamics.

Chapter 2 discusses the benefits of using a combination of AMS radiocarbon and OSL dating to build alluvial chronologies in dryland alluvial systems. Benefits included increased sampling opportunities and a greater ability to cross-check results to identify age inaccuracies. Results highlighted potential problems with both dating techniques, but suggested these problems can generally be mitigated by sampling recommendations.

Past studies have suggested that problems involving redeposition of organic material and sampling of Cretaceous coal would be encountered when using radiocarbon as a dating tool, and this was also the case in KCW. Despite using measures to avoid these and other problems associated with radiocarbon dating in dryland fluvial systems, most notably sampling of angular charcoal fragments from charcoal-rich lenses, ten of the 37 radiocarbon samples analyzed for this study still returned significant age overestimations or age inversions. Hence, in the absence of annual plant litter, it may not be enough to sample from a charcoal-rich lens to get a consistent

radiocarbon age. Rather, Chapter 2 suggests additional recommendations to mitigate problems with this dating method.

The first recommendation is to use alternative means beyond microscopic analysis to discern charcoal from coal. In especially small samples, it can be difficult distinguish the characteristic carbonized rings of charcoal from the heterogeneous structure of coal. Instead, density and specific gravity differences between these two organic materials may be a more useful identification tool and can be tested byfield or lab analysis of the presence of suspended or floating charcoal. The second recommendation is to avoid redeposited organic material by sampling for radiocarbon material several meters away from a colluvial deposit. In this study, radiocarbon samples collected less than a meter from a colluvial wedge returned inverted ages because of the likliehood that they were originally source from an older deposit and subsequently redeposited following slope failure of the incised arroyo wall. The final recommendation is to collect relatively large pieces of angular charcoal, or organic material, so that only a single piece meets the weight and volume requirements for AMS analysis, effectively avoiding contamination by mixing differently aged material.

The alluvial stratigraphy and sedimentology in KCW suggests the system has experienced multiple flashy-flow and high-sediment discharge events. These conditions have often been noted to be problematic for OSL dating because sediments tend to be deposited rapidly and with little solar exposure, which ultimately results in partial resetting of the luminescence signal and age overestimation. The representative bedding characteristics in the KCW arroyo wall stratigraphy, including bedding facies, bedding thickness, and original sediment source, of each alluvial deposit were primarily used in Chapter 2 to discuss optimal sample strategies for OSL dating. Preliminary single-grain age results and statistical analysis of  $D_e$  distributions suggest that previous OSL sampling strategies proposed by Summa-Nelson and Rittenour (2012) from a study in the Kanab Creek arroyo (e.g. Summa-Nelson and Rittenour, 2012) may not always be applicable to KCW, and additional strategies for OSL sampling based on bedding

characteristics may be more favorable. In addition to sampling deposits less than 40 cm thick, this study suggests that targeting alluvial deposits based on their original sediment source could result in OSL samples that have been more adequately bleached, as evidenced in overdispersion values of the De and CAM to MAM ratios. In general, this study found that grains were more adequately bleached when the majority of sediments in a sampled deposit contained very pale brown, fine- to medium-grained, well sorted frosted quartz sand grains from upstream sources (e.g. Navajo Sandstone). Poorly bleached sediments were red, very fine- to fine-grained, moderately to poorly sorted sands with variable amounts of clays and silts and were derived from local bedrock, hillslope, and tributary sources. Locally sourced sediments likely had a shorter transportation distance and were deposited more rapidly, effectively limiting the amount of solar exposure prior to burial.

It should be noted that these advised sampling strategies will not necessarily result in an increased number of accepted grains for single-grain dating because the majority of grains analyzed commonly do not produce a natural luminescent signal. Additionally, it is still likely that sediments attained from optimally targeted deposits will still show considerable signs of partial bleaching. For example, age overestimations would still be produced if the natural luminescence signals are averaged or if the most appropriate De values are not correctly chosen. Consequently, this study also advises using a combination of single-grain dating and use of a statistical age model (CAM, MAM-3, or MAM-4) to help measure and select De values and objectively calculate the most accurate age of a sample.

In addition to the recommendations highlighted in Chapter 2, it would be valuable for future research to validate recommendations of strategic sampling based on sediment source for OSL dating. Originally, the separation of OSL samples into upstream, local, and mixed was subjectively based on field and lab observations. These observations could be validated for KCW sediments by measuring the particle size distribution of a sample using a Malvern particle size analyzer to objectively determine whether samples are more homogenous, as expected of

upstream sediments derived from the well-sorted Navajo Sandstone, or heterogeneous, as expected of local sediments derived from poorly sorted siltstones and sandstones. If an upstream sample did not return the homogeneity expected, there could be some additional factor controlling the bleaching characteristics of KCW samples. Additionally, the sediment source strategy could be tested in other arroyos throughout the southwest where upstream and local alluvium sources can be differentiated.

Chapter 3 indentified at least six episodes of aggradation and incision in the KCW arroyo walls by combining stratigraphic relationships with the age control from AMS radiocarbon and OSL dating. These aggradation events comprise the alluvial packages from 12 study sites, which can be identified from oldest to youngest as: ~7.3-4.85 ka older fill of Hereford (2002), ~4.35 – 3.4 ka (Qf1), ~3.2 – 2.25 ka (Qf2), ~2.15 – 1.45 ka (Qf3), ~1.3 – 0.8 ka (Qf4), and ~0.7– 0.12 ka (Qf5). The chronostratigraphy of KCW was initially compared with the location of alluvial fill preserved arroyo-wall heights along the modern stream profile to help reconstruct the cut-fill alluvial history of KCW. While field observations and the stream profile revealed the presence of >6 m tall bedrock knickpoints in the channel, the preservation of alluvial fills and preservation of paleosurface along the knickpoints suggest these topographic anomalies have not affected headward migration of the channel cut. Rather, arroyo cut-fill events in KCW appear to have been influenced by the transition of an irregular profile following entrenchment to a more convex and critically unstable profile during aggradation, which likely induced incision during high-magnitude flood events. Additionally, the identification of Qf5' sheetflood deposit that cap several alluvial fills may have been deposited concurrent with arroyo entrenchment, as described by DeLong et al. (2011), or may have been deposited due to a change in channel paleohydrology immediately before channel incision.

In addition to reconstructing the fluvial history of KCW, results from the chronostratigraphy were also compared with alluvial chronologies from regional drainages and to paleoclimate records to test if the hypotheses related to arroyo formation and evolution. Hereford

(2002) originally suggested that the nearly synchronous nature of arroyo cut-fill events over the last ~1 ka could be tied to regional climate pattern, and so a primary goal of this study was to test alluvial chronologies from similarly sized catchments in southern Utah shared a near-synchronous or asynchronous relationship. A comparison of the alluvial chronostratigraphy from KCW and alluvial chronologies from the canyon reach of Kanab Creek and the upper Escalante River reveals that a number of arroyo aggradation and incision episodes appear to be near-synchronous, but some are asynchronous. Reasons for this variability can partly be attributed to a combination of uncertainties in the preservation of regional alluvial fills and an inaccurate interpretation of stratigraphic relationships. Nonetheless, it is also possible the temporal relationships of regional arroyo cutting and filling can be correlated with both climate and geomorphic conditions. Paleoclimate records suggest that the frequency of arroyo cutting and filling respond to changes in the variability of climate perturbations, potentially contributing the near-synchronous timing. However, even when uncertainties are accounted for, it appears catchment-specific geomorphic (and biologic) thresholds may also play a role because asynchronous cut-fill relationships do exist in the regional alluvial chronologies.

Additional work should begin by focusing on building a tighter chronology of the valley surface sheet-flow alluvium (Qf5') to support or reject the hypothesis that this unit was deposited concurrent with the historic arroyo cutting event, as suggested by DeLong et al. (2011). Constraining the age of these deposits might shed additional light on the fluvial processes specific of KCW that are occurring during or just prior to arroyo incision. Preliminary results indicate that single-grain OSL and radiocarbon dating using the recommendations of Chapter 2 may not be sufficient. Rather, for alluvial deposits this young, ring counting of buried Juniper trees may be best for dating. For this, alluvial deposits would be dated by locating the base of a buried Juniper trees and counting the number of annual tree-rings at that level. Ring counts on a buried tree would provide a maximum age of the surrounding deposit, and this dating technique has already been successfully used in KCW by Hereford (2002) and Harvey (2009).

An interesting observation is the relatively strong correlation of arroyo cut-fill events over the past ~1 ka between regional drainages not only discussed in this study but also between the proximal Virgin River (Hereford et al., 1996), Black Mesa region (Hall, 1977), and Chaco Canyon (Karlstrom, 1988). Historic arroyo cutting was initially tied to poor land practices by early pioneer settlers, and so it could be possible that the most recent prehistoric (~0.7-0.8 ka) arroyo cutting event was also partly related to anthropogenic practices. Setting aside potential climatic and geomorphologic influences, it would be interesting to investigate the population densities and agricultural practices of Puebloan cultures surrounding KCW and regional drainage, and their potential effect on prehistoric arroyo cutting and filling. Archaeologists suggest that the presence of the Pueblo II and Pueblo III Anasazi cultures increased proximal to drainages in southern Utah around ~1.1 ka as precipitation and rising water tables gave rise to the cultivation of maize (Cuchs, 2000). Maize remained a large component of the Basketmaker II to Puebloan III and Fremont cultures, and its cultivation necessitated irrigation canals and flood-water farming (Barlow, 2002; Huckleberry and Billman, 2008) which could have channelized run-off and promoted incision during periods of intense precipitation. Archaeological artifacts found in a pithouse excavation in Park Wash suggested evidence for Basketmaker III or Puebloan I occupation at ~1.0 to 1.3 ka (Ahlstrom, 2000). Additionally, Harvey et al., (2011) reported evidence of a cultural horizon capping the Qf2 alluvial fill at study site KCW-I. Based on potsherds of the "black-and-white" style, he suggested this paleosurface was occupied by the Puebloan II or III Kayenta Anasazi culture ca. 0.8-1.2 ka. Hereford (2002) also provided evidence of Puebloan artifacts that dated to ~1.1-1.3 ka. Although it is evident that occupation of the alluvial valley in this region existed, estimations of the total population and the timing of occupation remains unclear, and evidence of irrigation canals in KCW has yet to be suggested.

Finally, more work is needed to bridge the gap that exists with the correlation uncertainties between the chronostratigraphy of KCW and the regional alluvial chronologies or paleoclimate records used in this study. Accordingly, future work could focus on obtaining

alluvial chronologies from characteristically similar drainages proximal and distal to KCW. For example, Johnson Wash is an arroyo system located ~25 km to the west KCW that shares similar reach elevations (2800 – 1500 m asl) and arroyo wall heights (< 15 m), but does not currently contain an alluvial chronology. Hence, creating a chronostratigraphy for Johnson Wash alluvial and correlating it with KCW may be meaningful, and could help reconcile correlation uncertainties that could strengthen arguments for an autogenic or allogenic forcing.

While a number of the paleoclimate records examined in this study were obtained from databases surrounding the Colorado Plateau, a few were also obtained from more distal locations (i.e. the El Juno sand record from the Galapagos Islands) and may not have significantly correlated with the KCW chronostratigraphy. Accordingly, it would also be more meaningful to compare the alluvial chronology of KCW to locally derived paleoclimate records to more accurately resolve a cut-fill relationship to climate. In this case, a dendroclimatological reconstruction for the KCW catchment or an expansion of existing tree-ring databases for the surrounding region might help resolve potential problems that are caused by correlating arroyo responses to regional and distal climate signals or to orographic effects.

## REFERENCES

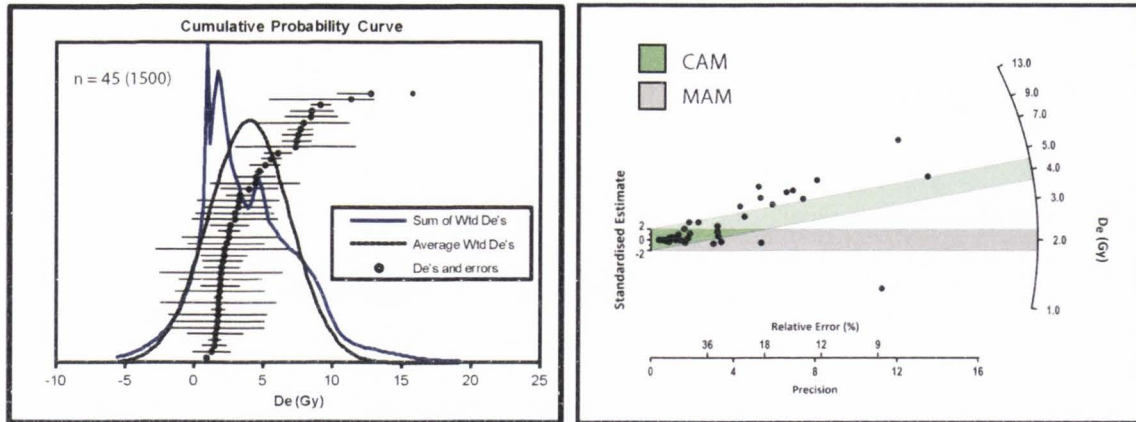
- Ahlstrom, R.V.N. (Ed), 2000. Pithouse excavations at the Park Wash Site (42KA4280) Grand Staircase-Escalante National Monument Southcentral Utah. HRA Papers in Archaeology No. 1. Prepared for Bureau of Land Management. Las Vegas: HRA, Inc.
- Barlow, R.K., 2002. Predicting maize agriculture among the Fremont: An economic comparison of farming and foraging in the American Southwest. *American Antiquity* 67, 65-88.
- Delong, S.B., Pelletier, J.D., Arnold, L.J., Late Holocene alluvial history of the Cuyama River, California, USA. *Geological Society of America Bulletin* 123, 2160-2176.
- Cuch, F.S. (Ed), 2000. A History of Utah's American Indians. Salt Lake City: Utah Division of Indian Affairs/Utah Division of History.
- Hall, S.A., 1977. Late Quaternary sedimentation and paleoecologic history of Chaco Canyon, New Mexico. In: *Geological Society of America Bulletin*, vol. 88, pp. 1593-1618.

- Harvey, J.L., 2009. Reconciling Holocene Alluvial Records in Buckskin Wash, Southern Utah.. M.S. Thesis, Utah State University, unpublished.
- Hereford, R., Jacoby, G.C., and McCord, V.A.S., 1996. Late Holocene alluvial geomorphology of the Virgin River in the Zion National Park area, southwest Utah. Geological Society of America Special Paper 310, 41 p.
- Hereford, R., 2002. Valley-fill alluviation during the Little Ice Age (ca. A.D. 1400–1880), Paria River basin and southern Colorado Plateau, United States. Geological Society of America Bulletin 114 (12), 1550-1563.
- Huckleberry, G.A., Billman, B.R., 1998. Floodwater Farming, Discontinuous Ephemeral Streams, and Pueblan Abandonment in Southwestern Colorado. American Antiquity 63, 595-616.
- Karlstrom, T.N.V, 1988. Alluvial chronology and hydrologic change of Black Mesa and nearby regions. In: Bumerman, G.J. (Ed), The Anasazi in a Changing Environment. Cambridge University Press, pp. 45-91.
- Summa-Nelson, M.C., Rittenour, T.M., 2012. Application of OSL dating to middle to late Holocene arroyo sediments in Kanab Creek, southern Utah, USA. Quaternary Geochronology 10, 167-174.

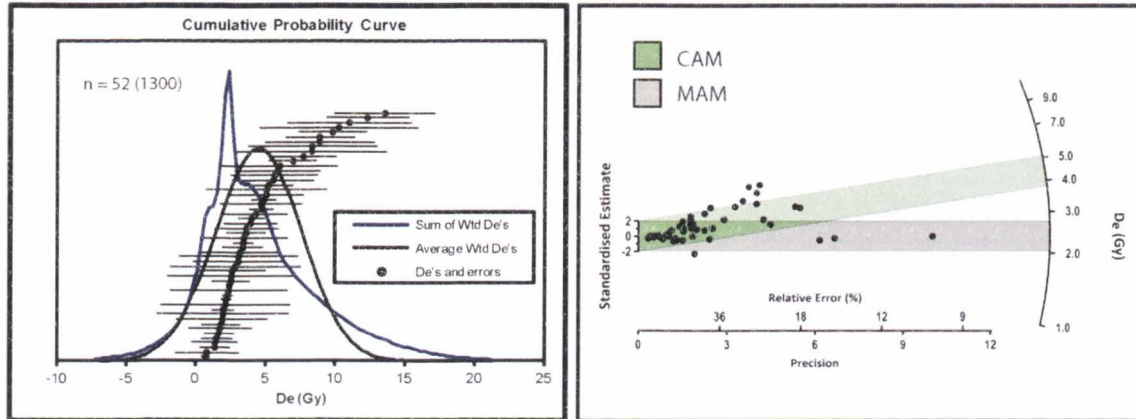
APPENDICES

## APPENDIX A. OPTICALLY STIMULATED LUMINESCENCE DATA

USU-1026



USU-1027



USU-1028

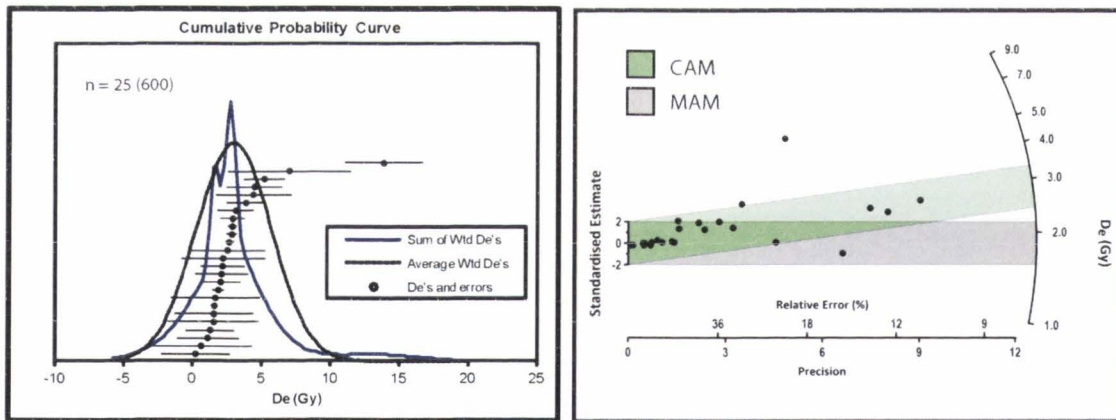


Fig. A-1. Single-grain De distribution for select OSL samples (USU-1026, USU-1027, USU-1028) as indicated on probability density functions (left) and radial plots (right).

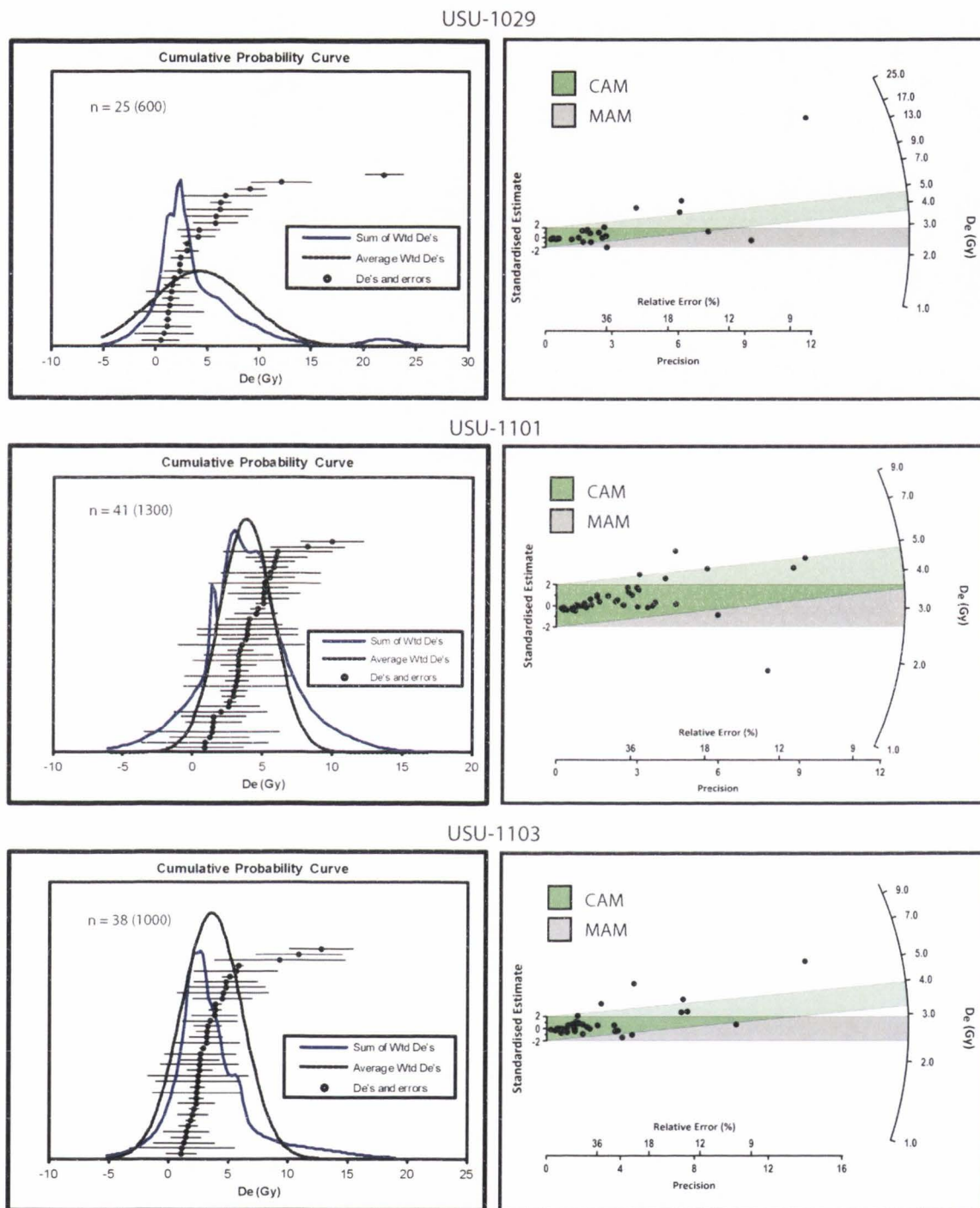
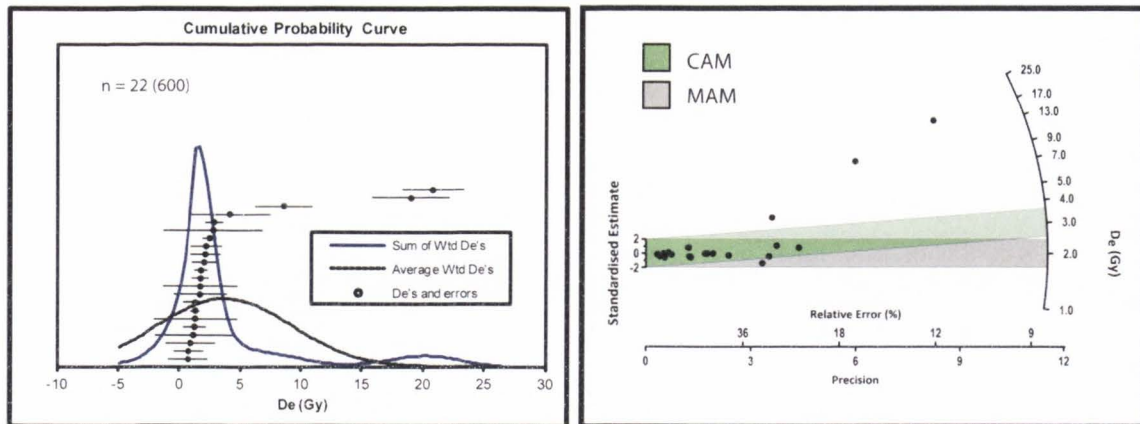
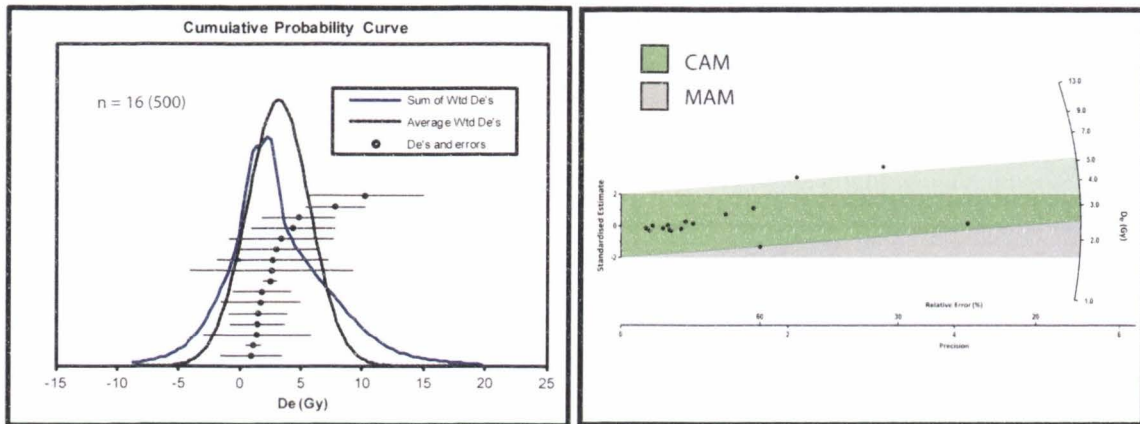


Fig. A-2. Single-grain De distribution for select OSL samples (USU-1029, USU-1101, USU-1103) as indicated on probability density functions (left) and radial plots (right)

USU-1176



USU-1177



USU-1178

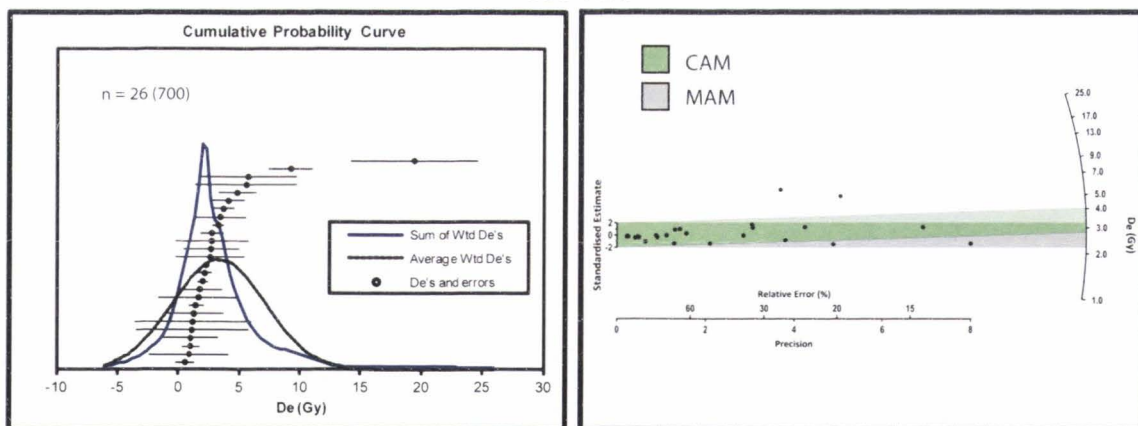


Fig. A-3. Single-grain De distribution for select OSL samples (USU-11176, USU-1177, USU-1178) as indicated on probability density functions (left) and radial plots (right).

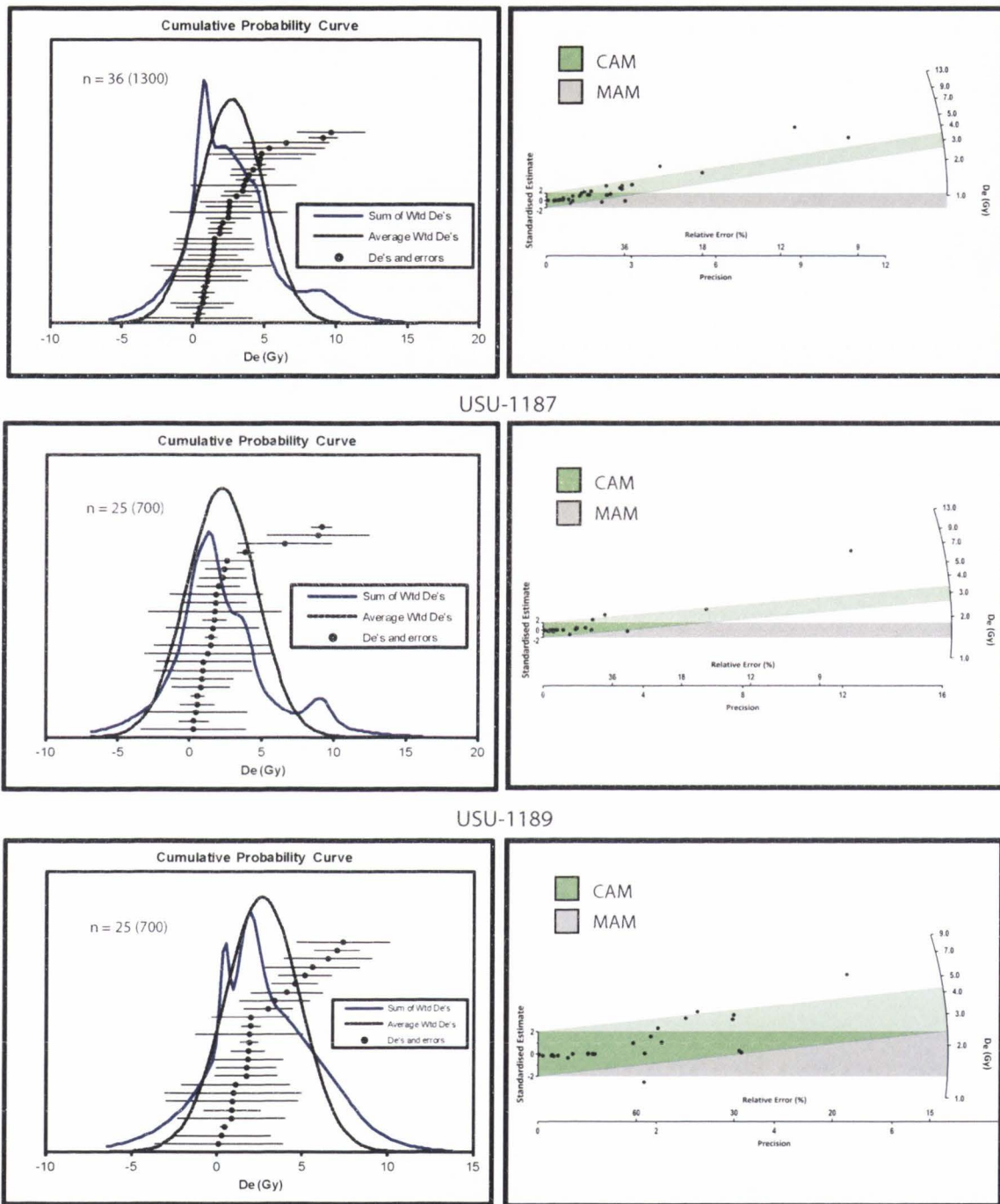
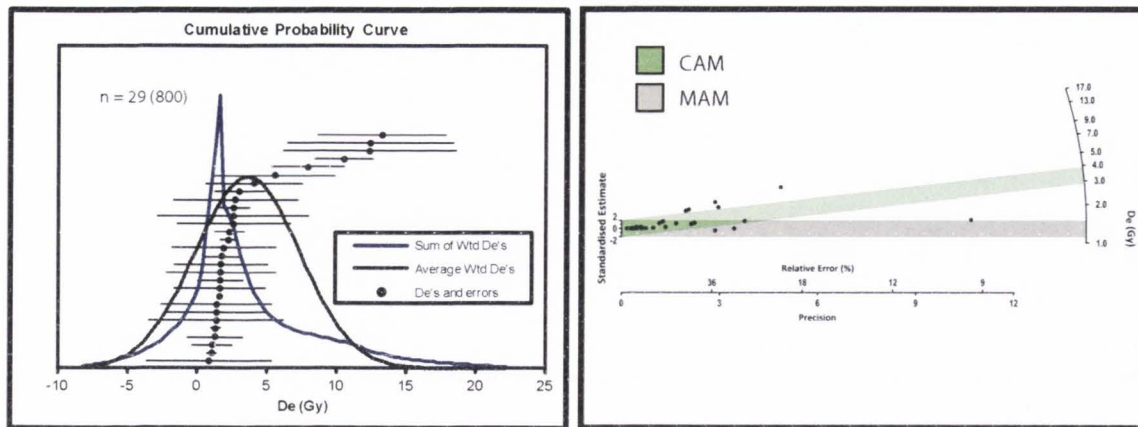


Fig. A-4. Single-grain De distribution for select OSL samples (USU-1181, USU-1187, USU-1189) as indicated on probability density functions (left) and radial plots (right).

## USU-1192



## USU-1194

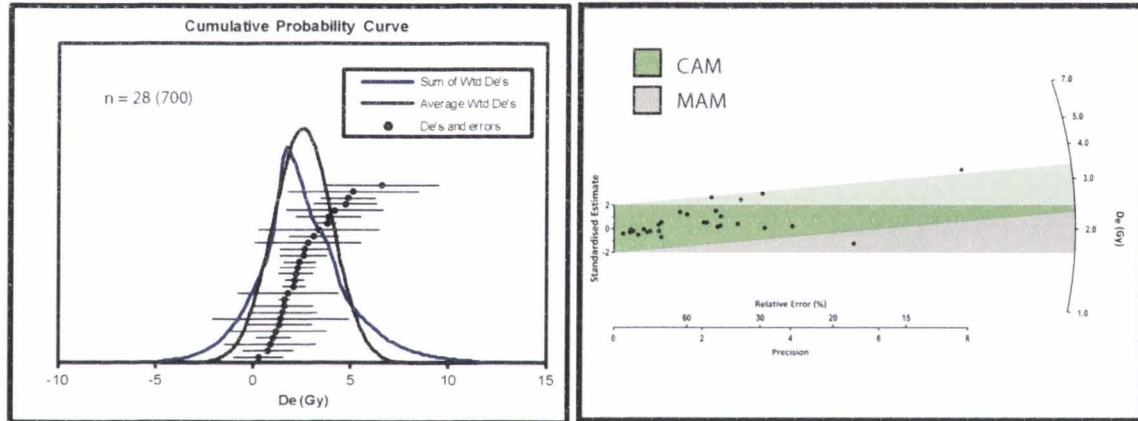


Fig. A-5. Single-grain De distribution for select OSL samples (USU-1192, USU-1194) indicated on probability density functions (left) and radial plots (right).

## APPENDIX B. STRATIGRAPHIC COLUMNS AND SEDIMENTOLOGIC DESCRIPTIONS

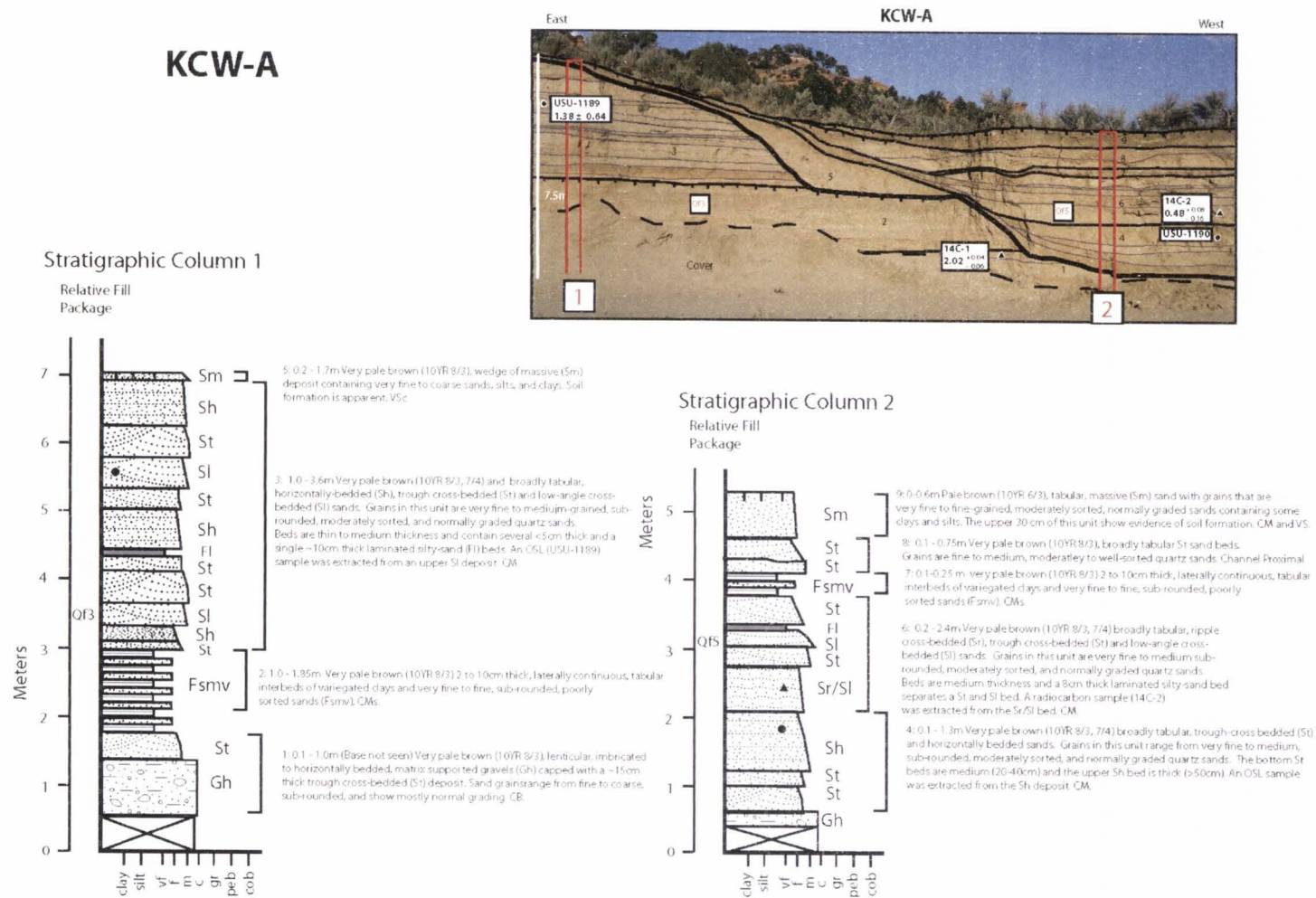
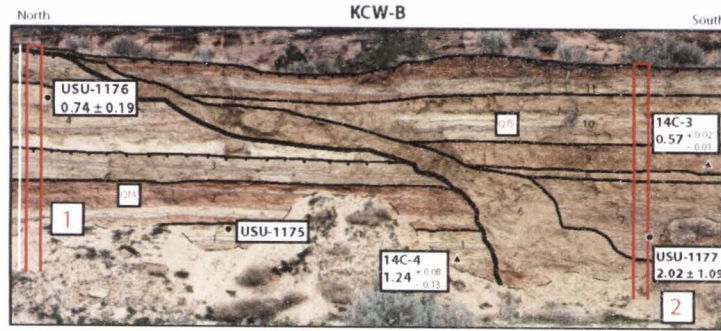
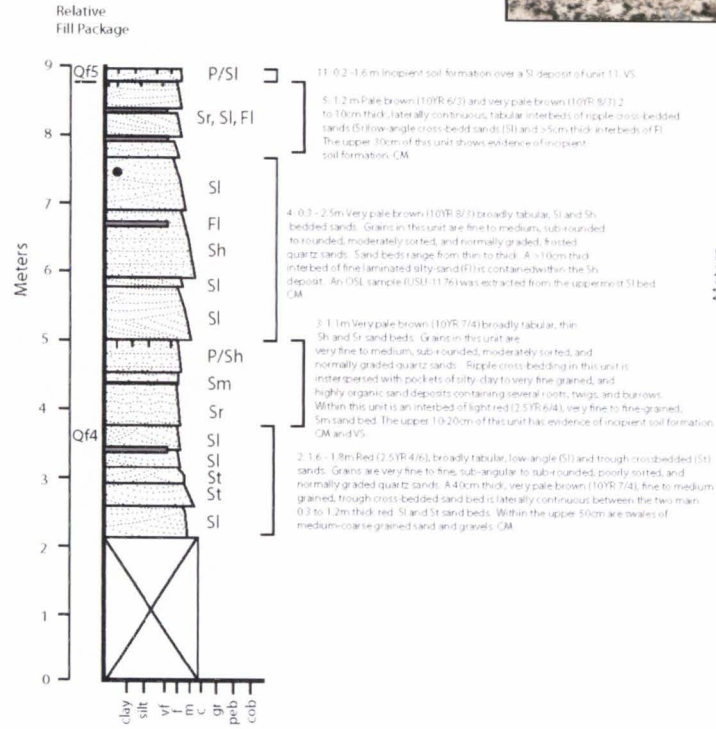


Fig B-1. Stratigraphic columns and sedimentologic descriptions of KCW-A.

# KCW-B



## Stratigraphic Column 1



## Stratigraphic Column 2

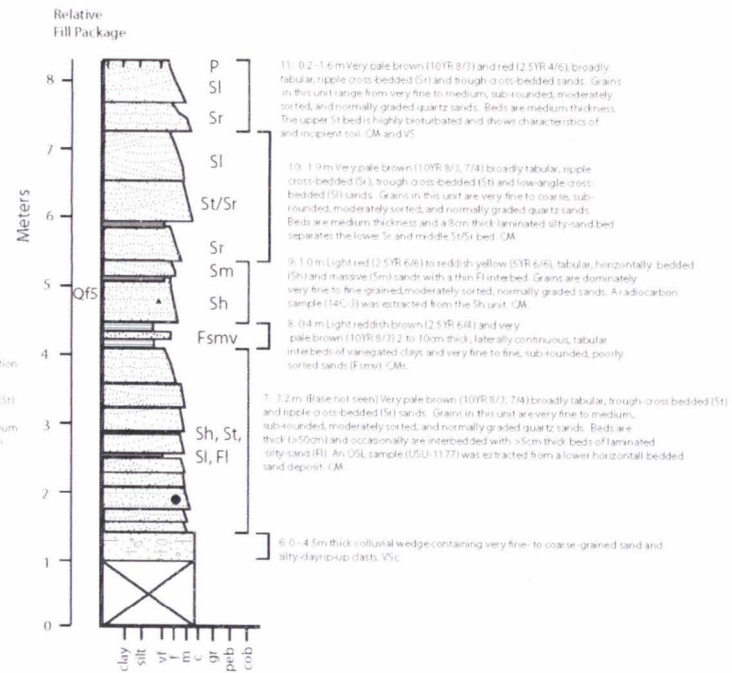
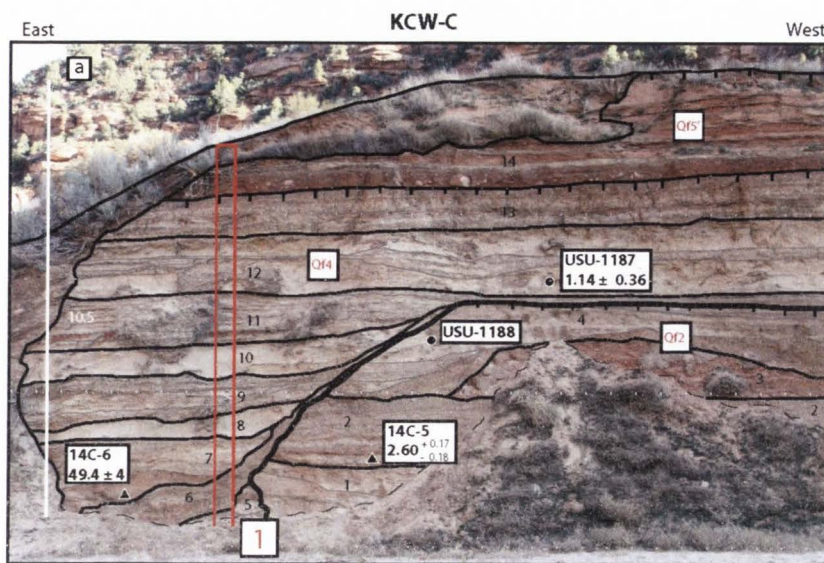


Fig B-2. Stratigraphic columns and sedimentologic descriptions of KCW-B.

KCW-C



Stratigraphic Column 1

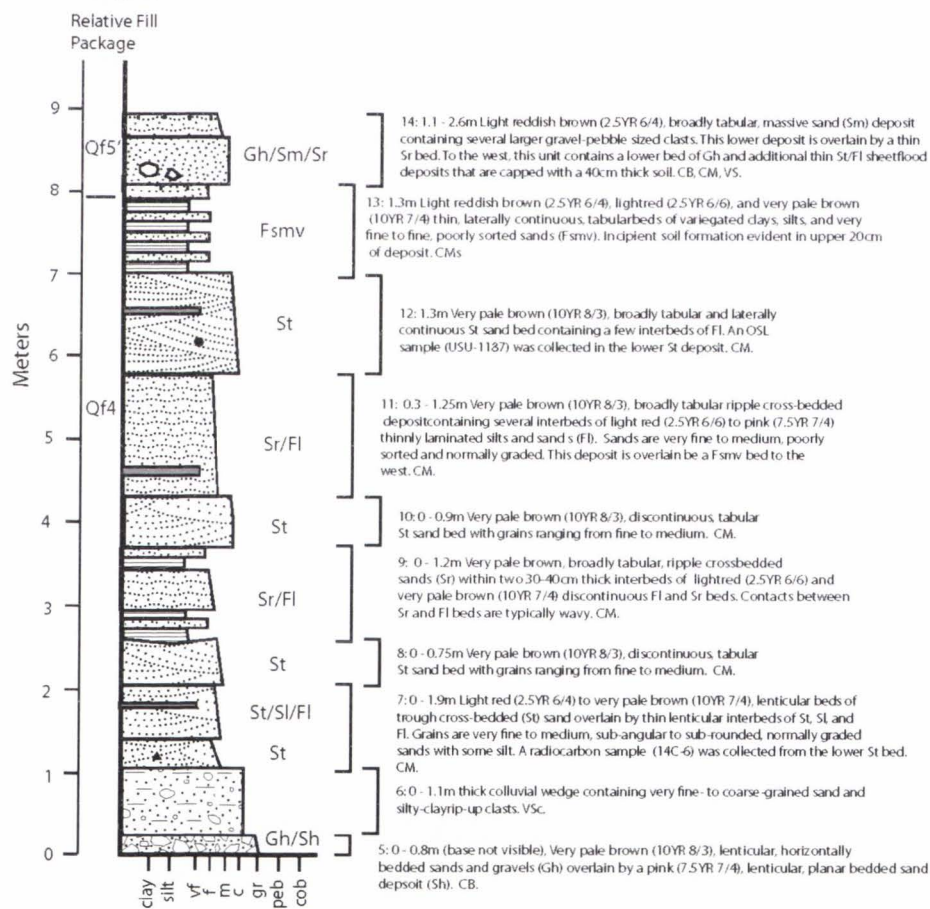
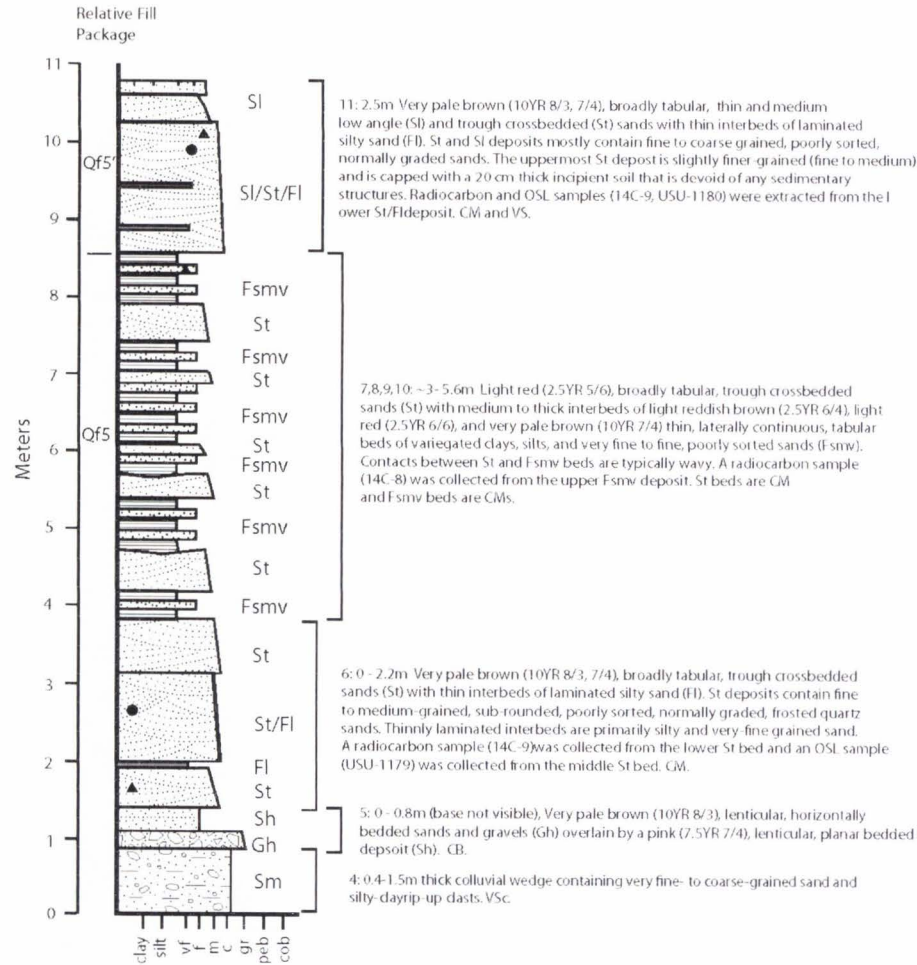
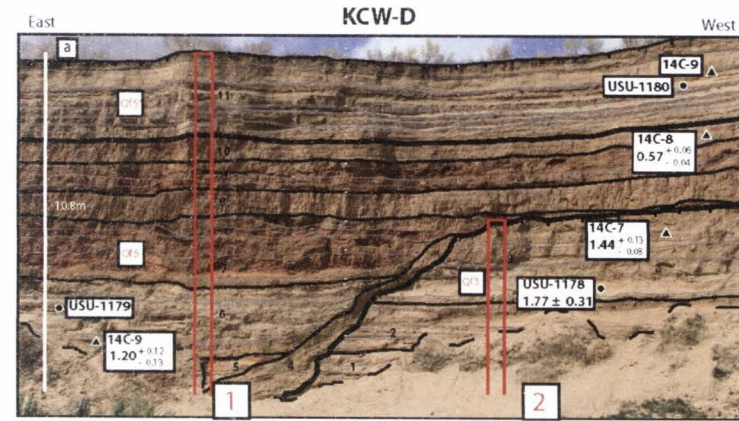


Fig. B-3. Stratigraphic column and sedimentologic descriptions of KCW-C.

### Stratigraphic Column 1



### KCW-D



### Stratigraphic Column 2

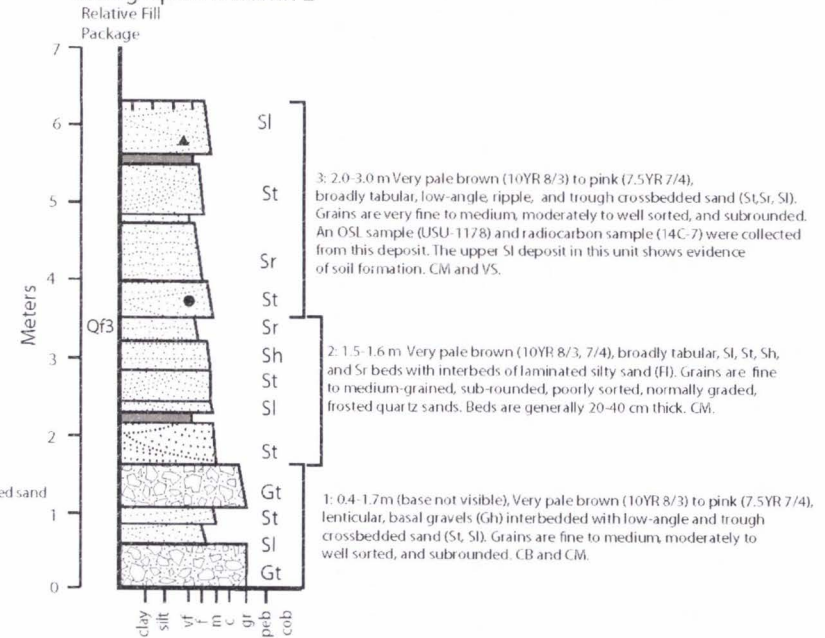
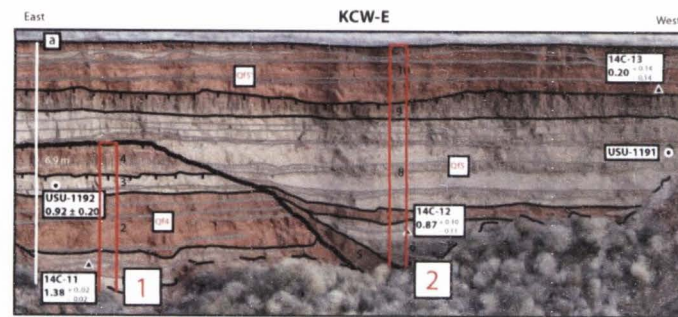
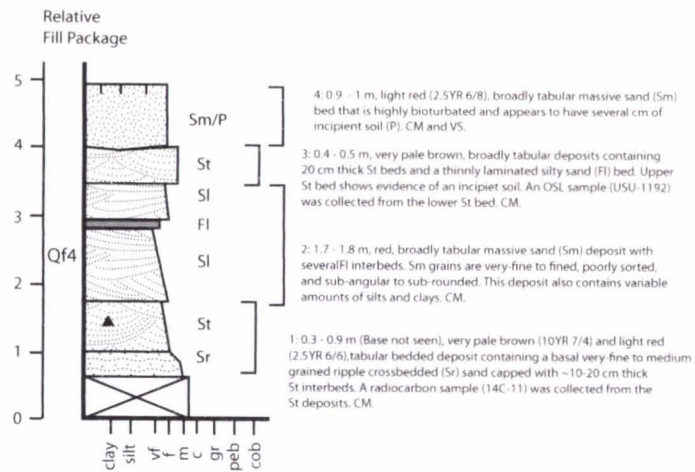


Fig. B-4. Stratigraphic columns and sedimentologic descriptions of KCW-D.



### Stratigraphic Column 1



### KCW-E

### Stratigraphic Column 2

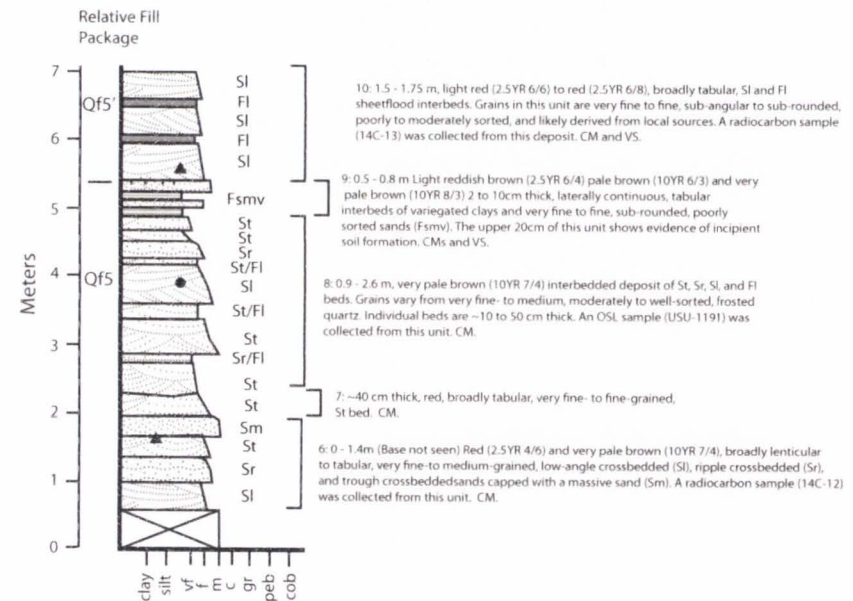
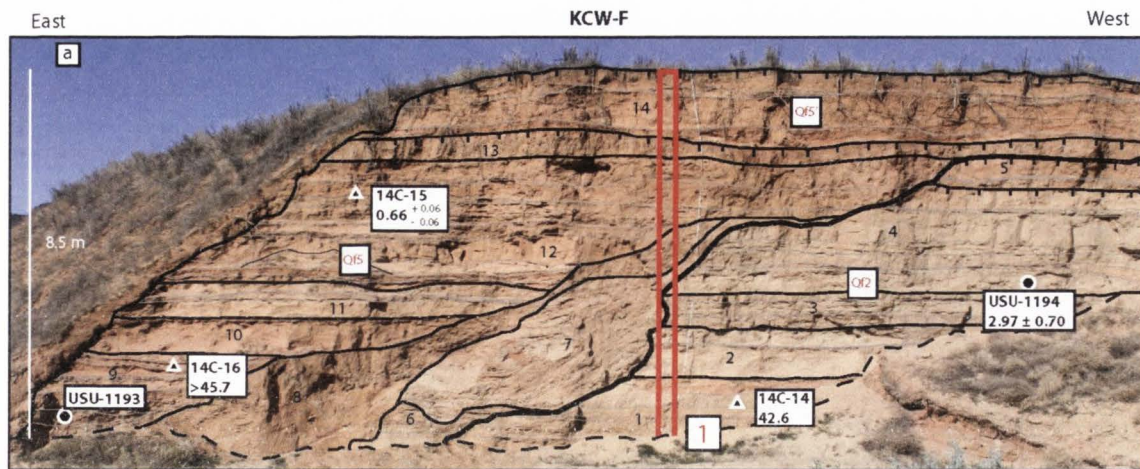


Fig. B-5. Stratigraphic columns and sedimentologic descriptions of KCW-E.



Stratigraphic Column 1

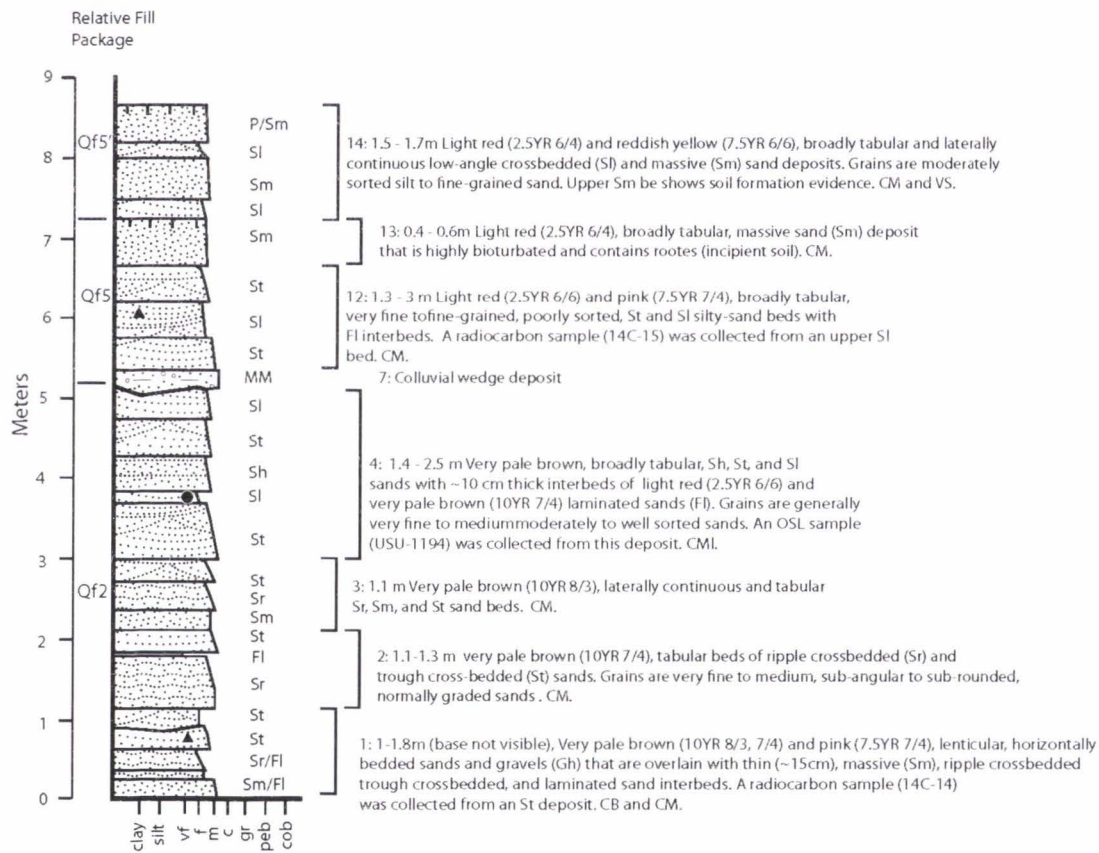
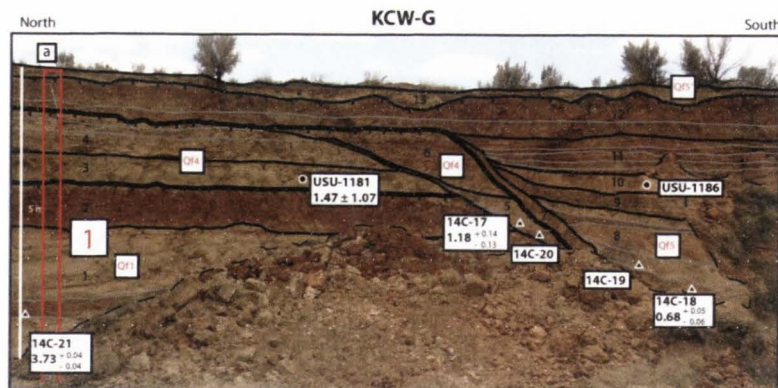


Fig. B-6. Stratigraphic column and sedimentologic descriptions of KCW-F.



### Stratigraphic Column 1

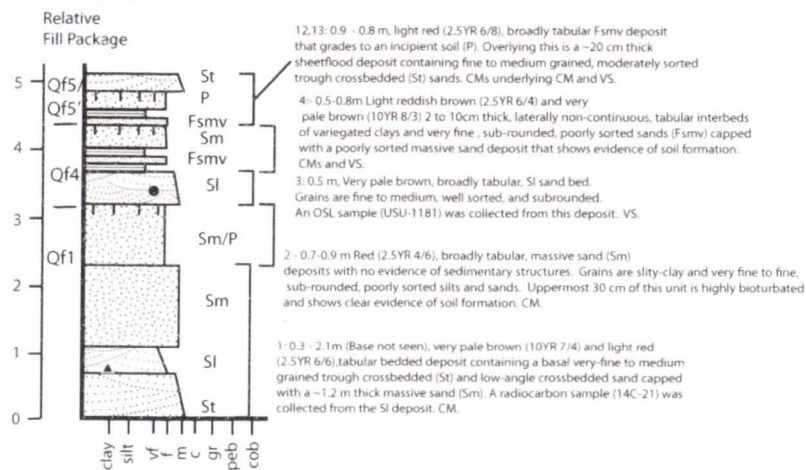
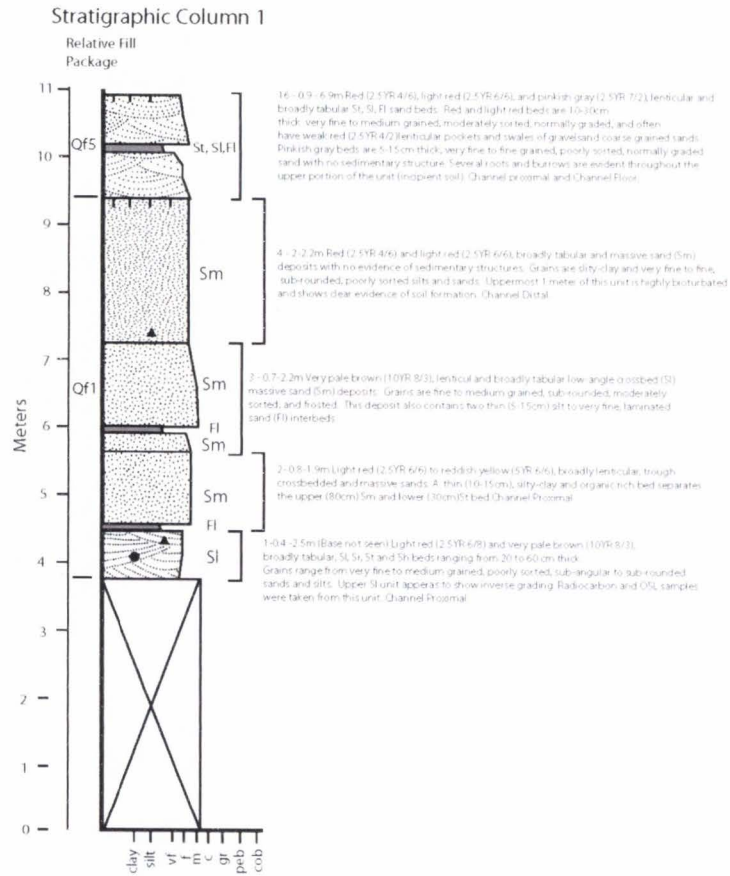


Fig. B-7. Stratigraphic column and sedimentologic descriptions of KCW-G.

KCW-H



Stratigraphic Column 2

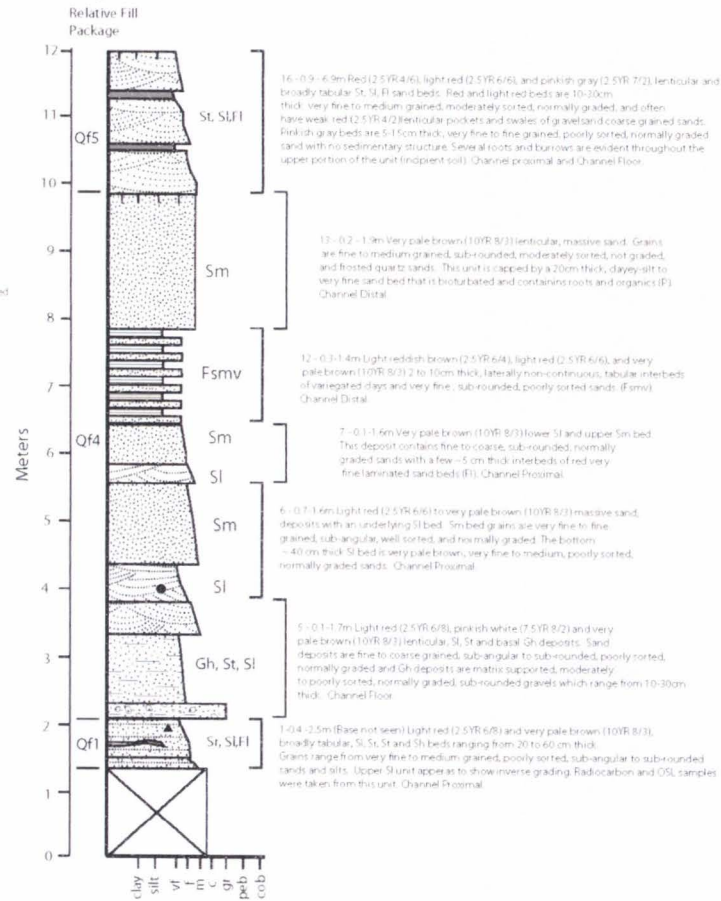
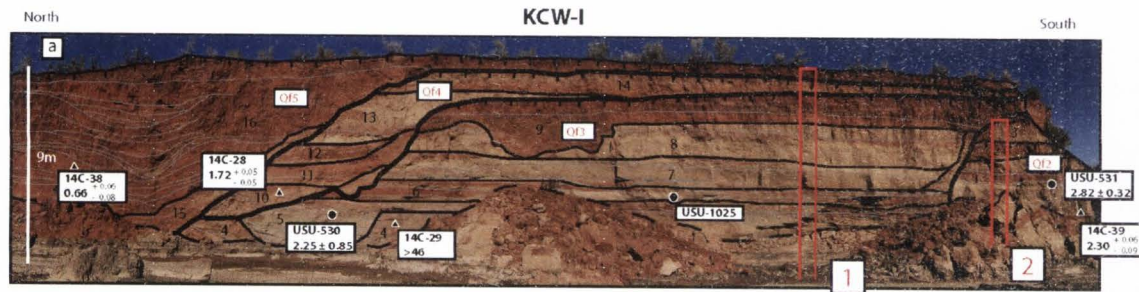
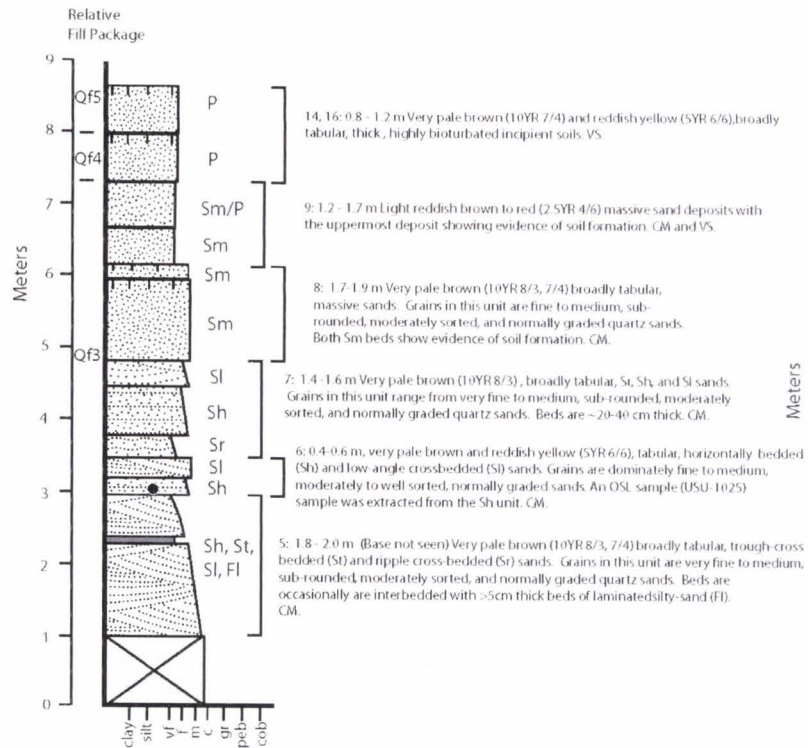


Fig. B-8. Stratigraphic columns and sedimentologic descriptions of KCW-H.



Stratigraphic Column 1



Stratigraphic Column 2

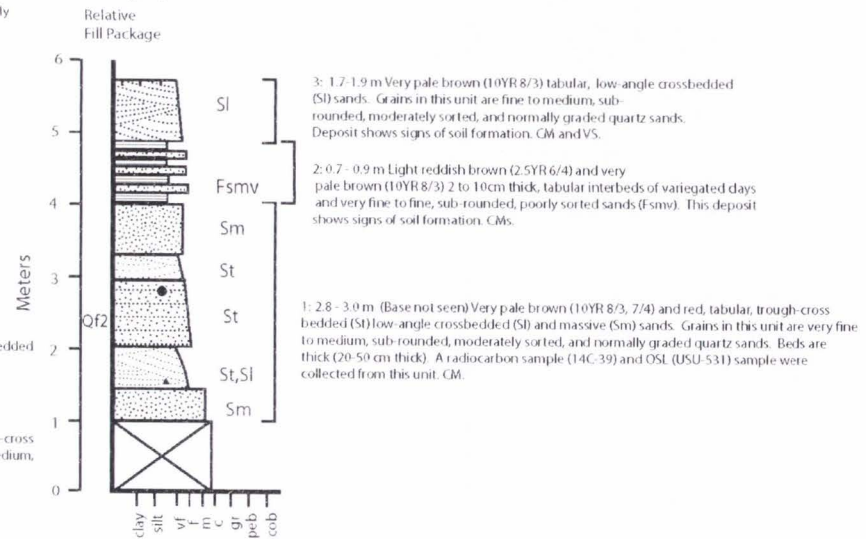


Fig. B-9. Stratigraphic columns and sedimentologic descriptions of KCW-I.

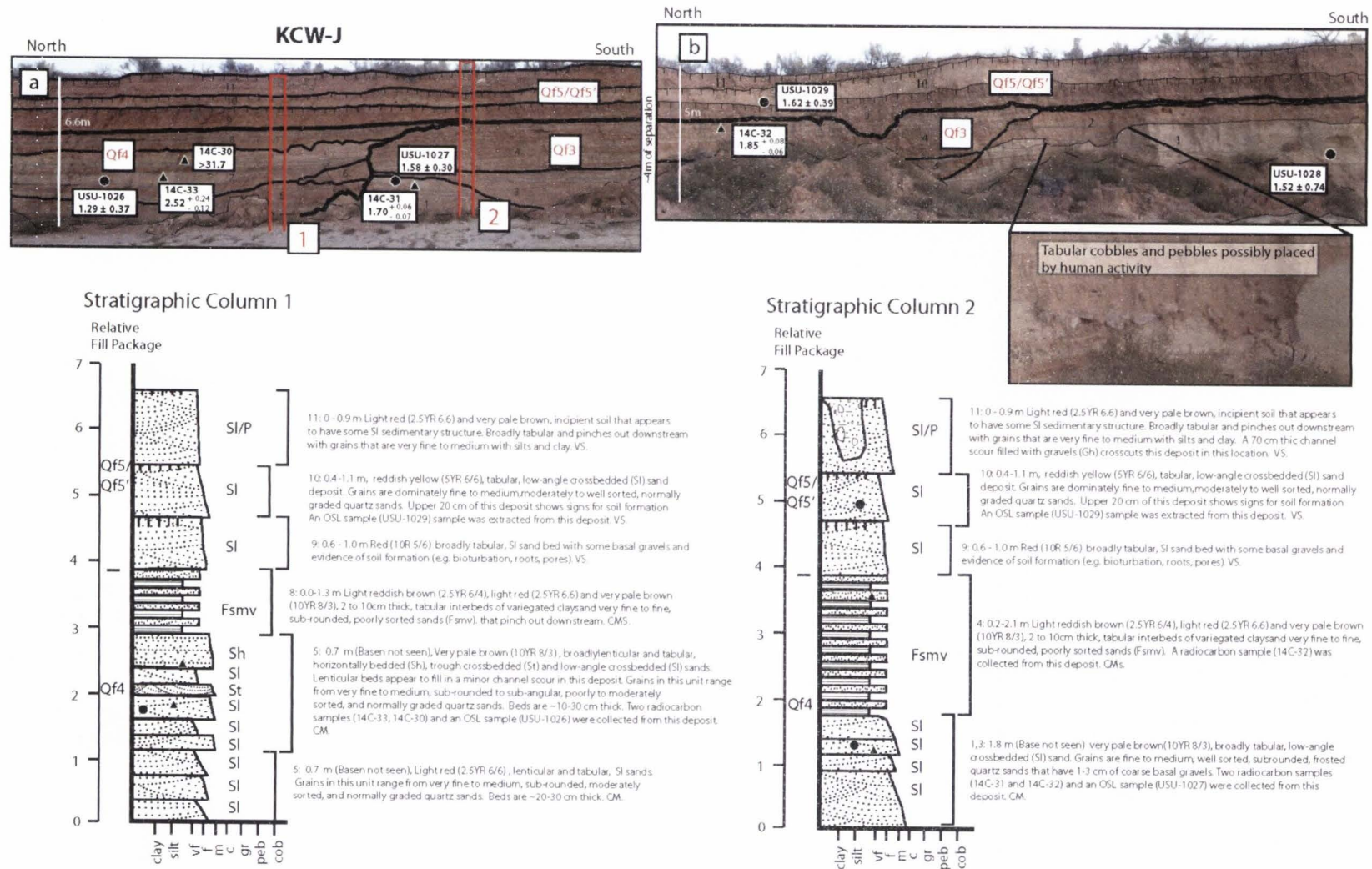
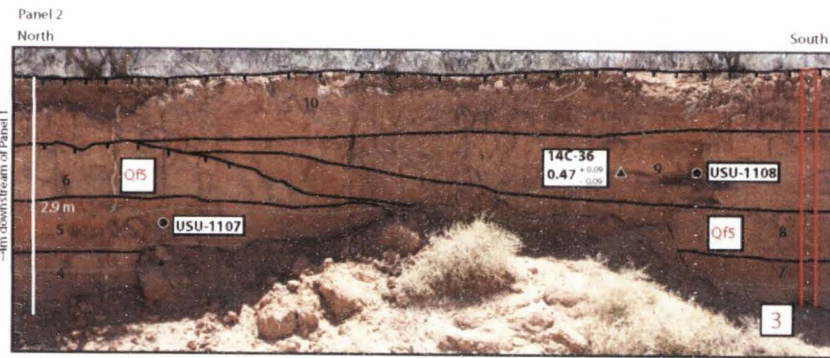
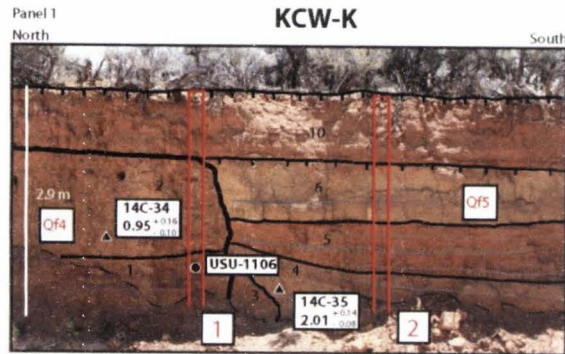
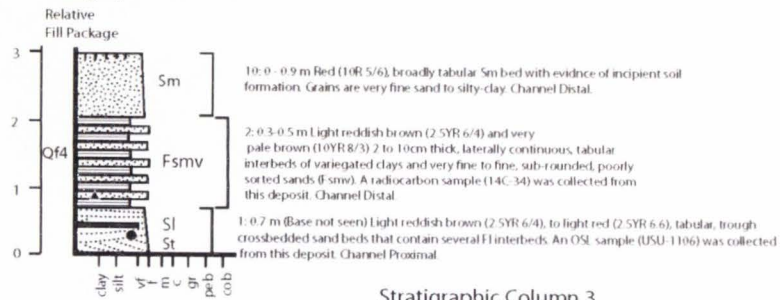


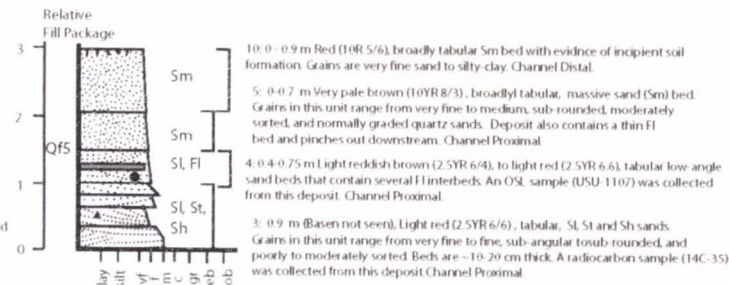
Fig. B-10. Stratigraphic columns and sedimentologic descriptions of KCW-J.



Stratigraphic Column 1



Stratigraphic Column 2



Stratigraphic Column 3

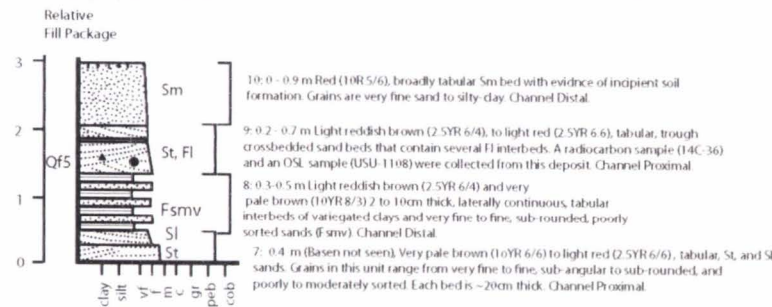


Fig. B-11. Stratigraphic columns and sedimentologic descriptions of KCW-K.